UNIVERSIDADE ESTADUAL DE CAMPINAS
Faculdade de Engenharia Elétrica e de Computação

FELIPE ANTONIO MOURA MIRANDA

STUDY ON THE ENERGY CONSUMPTION IN WIRELESS SENSOR NETWORKS

ESTUDO SOBRE O CONSUMO DE ENERGIA EM REDES DE SENSORES SEM FIO

CAMPINAS
2018

UNIVERSIDADE ESTADUAL DE CAMPINAS
Faculdade de Engenharia Elétrica e de Computação

FELIPE ANTONIO MOURA MIRANDA

STUDY ON THE ENERGY CONSUMPTION IN WIRELESS SENSOR NETWORKS

‘

ESTUDO SOBRE O CONSUMO DE ENERGIA EM REDES DE SENSORES SEM FIO

Doctoral thesis presented to the School of Electrical and Computer Engineering (FEEC) of the University of Campinas in partial fulfillment of the requirements for the degree of Doctor in Electrical Engineering, in the area of Telecommunications and Telematics

Tese de Doutorado apresentada à Faculdade de Engenharia Elétrica e de Computação (FEEC) da Universidade Estadual de Campinas como parte dos requisitos exigidos para a obtenção do título de Doutor em Engenharia Elétrica, na Área de Telecomunicações e Telemática

Orientador: Prof. Dr. Paulo Cardieri

ESTE EXEMPLAR CORRESPONDE À VERSÃO FINAL TESE DEFENDIDA PELO ALUNO FELIPE ANTONIO MOURA MIRANDA, E ORIENTADA PELO PROF. DR. PAULO CARDIERI

CAMPINAS
2018

Agência(s) de fomento e nº(s) de processo(s): CAPES
ORCID: https://orcid.org/0000-0002-0132-6884

Ficha catalográfica
Universidade Estadual de Campinas
Biblioteca da Área de Engenharia e Arquitetura
Rose Meire da Silva - CRB 8/5974

M672s	Miranda, Felipe Antonio Moura, 1987- Study on the energy consumption in wireless sensor networks / Felipe Antonio Moura Miranda. – Campinas, SP : [s.n.], 2018. Orientador: Paulo Cardieri. Tese (doutorado) – Universidade Estadual de Campinas, Faculdade de Engenharia Elétrica e de Computação.

Informações para Biblioteca Digital

Título em outro idioma: Estudo sobre o consumo de energia em redes de sensores sem fio
Palavras-chave em inglês:
Wireless sensor networks
Energy
Área de concentração: Telecomunicações e Telemática
Titulação: Doutor em Engenharia Elétrica
Banca examinadora:
Paulo Cardieri [Orientador]
José Antonio Martins
Omar Carvalho Branquinho
Leandro Tiago Manera
João Furtado de Souza
Data de defesa: 03-12-2018
Programa de Pós-Graduação: Engenharia Elétrica

COMISSÃO JULGADORA – TESE DE DOUTORADO

Candidato: Felipe Antonio Moura Miranda **RA**:089182

Data da Defesa: 03/12/2018
Título da Tese: "STUDY ON THE ENERGY CONSUMPTION IN WIRELESS SENSOR NETWORKS" / "ESTUDO SOBRE O CONSUMO DE ENERGIA EM REDES DE SENSORES SEM FIO"

Prof. Dr. Paulo Cardieri (Orientador e Presidente da Banca)
Prof. Dr. José Antonio Martins
Prof. Dr. Omar Carvalho Branquinho
Prof. Dr. Leandro Tiago Manera
Prof. Dr. João Furtado de Souza

A ata de defesa, com as respectivas assinaturas dos membros da Comissão Julgadora, encontra-se no SIGA (Sistema de Fluxo de Dissertação/Tese) e na secretaria de Pós-Graduação da Faculdade de Engenharia Elétrica e de Computação.

Dedico este trabalho a Deus e à minha família.

AGRADECIMENTOS

O presente trabalho foi realizado com apoio da Coordenação de Aperfeiçoamento de Pessoal de Nível Superior - Brasil (CAPES) – Código de Financiamento 001.

Ao Prof. Paulo Cardieri por ter me orientado neste trabalho, ao Prof. Carlos Reis por ter me orientado durante meu Mestrado, ao Prof. Luiz Cesar Martini pelos conselhos extremamente positivos de como tornar este trabalho mais acessível.

A Universidade Estadual de Campinas, a Faculdade de Engenharia Elétrica e de Computação e em especial a equipe do SATE, Nestor, João Paulo, Juliana e Bruno.

A minha família, em especial meus pais, Irene e Antônio Miranda, e minha esposa, Jessica Miranda, e aos meus estimados Formigão e Margareth, por terem me apoiado em todos os momentos.

A Deus, por ter concedido tudo que me trouxe até aqui.

RESUMO

É amplamente aceito que o consumo de energia é um dos principais problemas que afetam o desempenho das redes de sensores sem fio. Os nós, que são as principais unidades de aquisição, processamento e transmissão de dados nesse tipo de rede, são tipicamente alimentados por baterias, e o processo de substituição ou recarga de suas baterias pode ser uma tarefa extremamente difícil, cara ou até mesmo proibida, dependendo do local de instalação. Isso tem motivado diversos trabalhos focados tanto em entender como se dá o consumo de energia quanto em técnicas e estratégias para utilizar cada vez menos energia e de forma mais eficiente. Neste trabalho, apresentamos um estudo que analisa de diversas formas o consumo de energia em redes de sensores sem fio, oferecendo como suas principais contribuições formas de tornar suas operações energeticamente mais eficientes. Inicialmente, apresentamos uma análise exploratória feita em componentes comumente utilizados nos nós de redes de sensores sem fio, mostrando seus respectivos perfis de consumo em diversos estados de operação, utilizando uma metodologia especialmente concebida para proporcionar uma apresentação com grande fidelidade à realidade. No prosseguimento deste trabalho, esses perfis de consumo são utilizados para uma análise mais acurada de duas propostas visando uma utilização mais eficiente de energia: (*i*) utilização de múltiplos níveis de potência de transmissão; (*ii*) modelo matemático de cálculo do consumo individual e distribuição proporcional de energia. A utilização de múltiplos níveis de potência de transmissão é analisada em diversos cenários distintos e com diferentes métricas, proporcionando uma visão de seus aspectos positivos e negativos, dependendo do cenário. Ainda neste trabalho, apresentamos e analisamos um modelo para estimar a energia consumida pelos nós em vários cenários distintos. O modelo considera os estados primários dos nós, como transmissão e recepção de mensagens, bem como estados secundários, como o modo *sleep* ou *idle*. Além disso, o modelo é capaz de estimar os efeitos da cooperação entre os nós no processo de roteamento de mensagens. Utilizando o modelo proposto, avaliamos seu desempenho analisando a estratégia de distribuição proporcional de energia, feita de acordo com o consumo individual calculado. Os resultados da análise revelaram claramente não apenas que a estratégia de atribuir energia inicial aos nós proporcionalmente aos seus gastos calculados é um meio de aumentar significativamente o tempo de vida da rede, também como mostraram o quanto parâmetros como intensidade de tráfego e localização dos nós afetam o tempo de vida da rede. Visando um trabalho acessível para todos os leitores, o mesmo foi escrito utilizando princípios do Desenho Universal (*Universal Design*), evitando a utilização de siglas, colocando imagens em dimensões maiores e descrevendo elementos gráficos em texto para utilização de software de leitura de tela.

Palavras-Chave: Redes de Sensores Sem Fio; Energia; Potência de Transmissão; Redistribuição; Tempo de vida.

ABSTRACT

It is widely accepted that power consumption is one of the major issues affecting the performance of wireless sensor networks. Motes in such networks are typically battery powered, and the process of replacing or recharging their batteries can be an extremely difficult, expensive or even a forbidden task, depending on where they are deployed. This issue has motivated several works focused on both understanding how the energy is consumed as well as techniques and strategies to demand less energy and to use it more efficiently. In this work, we present a study that analyzes in different ways the energy consumption in wireless sensor networks, offering as its main contributions, forms to make their operation more energy efficient. Initially, we present an exploratory analysis of components commonly used in wireless sensor network motes, showing their respective energy consumption profiles in different states of operation, using a methodology specially designed show all details of the measurements. Next, these consumption profiles are used for providing a more accurate analysis of two proposals aimed at a more efficient energy usage: (*i*) use of multiple transmission power levels; (*ii*) mathematical model to calculate the individual energy consumption and proportional distribution of energy. The use of multiple transmission power levels is analyzed in several different scenarios and with different metrics, providing an analysis of its positive and negative aspects, depending on the scenario. Also, we propose a model for estimating the energy consumed by motes in an arbitrary network based on the tasks performed by motes. The model considers the primary states of the mote, such as message transmission and reception, as well as secondary states, such as the sleep mode. Also, the model is capable of capturing the effects of cooperation among motes in the message forwarding process. Using the proposed model, we then evaluate its performance in the study of strategies of energy distribution among motes. The results of the analysis have clearly revealed not only that the strategy of assigning initial energy to the motes in proportion to their expenditures is a means of increasing significantly the network lifetime, but in special have shown how parameters like traffic intensity and sink mote location affect the network lifetime. In order to provide a work accessible to all readers, it was written using principles of Universal Design, avoiding the use of acronyms, using images in larger dimensions and describing graphic elements in text for use of screen reader software.

Keywords: Wireless Sensor Networks; Energy; Transmission Power; Lifetime.

FIGURE INDEX

TABLE INDEX

SYMBOLS

α_m	Energy consumed by a mote m to read its sensors and assemble a new message.
$\boldsymbol{\alpha}$	Vector with all α_m of the network.
β_m	Energy consumed by a mote m to transmit a message.
$\boldsymbol{\beta}$	Vector with all β_m of the network.
γ_m	Energy consumed by a mote m to receive and process a message.
$\boldsymbol{\gamma}$	Vector with all γ_m of the network.
P_ω	Power consumed by secondary states.
ω_m	Energy consumed by a mote m when it is in the secondary state.
$\boldsymbol{\omega}$	Vector with all ω_m of the network.
e_m	Total energy consumption of a mote m per network cycle.
$\boldsymbol{e}$	Vector with all e_m of each mote in the network.
b_m	Absolute burden of a mote m.
$\boldsymbol{b}$	Vector with all b_m of the network.
$w_{m,n}$	Number of messages transmitted by mote m and received by mote n.
ρ_m	Generation rate of new messages of a mote m.
$\boldsymbol{\rho}$	Vector with all ρ_m of the network.
μ_m	Quantity of all messages received/listened by a mote m.
$\boldsymbol{\mu}$	Vector with all μ_m in the network.
$f_{m,n}$	Fraction of messages that will be routed through a link connecting mote m to n.
$\boldsymbol{F}$	Adjacency matrix with all $f_{m,n}$ of each link in the network.
$q_{m,n}$	Quantity of all messages transmitted through a link connecting mote m to n.
$\boldsymbol{Q}$	Matrix with all $q_{m,n}$.
T	Network cycle.
T_α	Time spent by a mote to read all its sensors and assemble a new message.
T_p	Time spent by a mote in primary states.
T_{tx}	Time spent by a mote to transmit a message.
T_{rx}	Time spent by a mote to receive and process a message.
$\boldsymbol{N}$	Adjacency matrix representing the network.
Ξ_m	Set of all neighbors of a mote m.
Π_m	Set of all predecessor neighbors of a mote m.
Γ_m	Set of all successor of a mote m.
l, m, n	Mote identifiers.

INDEX

Chapter I

INTRODUCTION

This chapter introduces the subject, the scope, the methodology and the structure of this work. It intends to present and summarize the main topics of the whole work and its chapters.

1.1 Research Subject and Motivation

Wireless Sensor Networks (WSNs) [1]–[9] are important and valuable systems that emerged recently and, more and more, are reaching a substantial role in many types of applications. The prediction made by Moore in 1965 [10] is still valid for equipment that uses integrated electronic circuits, turning computational limitations, for both hardware and software, just transient topics. However, all electronic devices need electrical energy to work, making the energy consumption issue a serious problem.

The operation of Wireless Sensor Networks is based on the cooperative behavior of many motes spread over a given area, generally relying solely on their supplied batteries. Since motes have no other energy source and replacing the batteries of each mote spread over a wide area is such a challenging task [2], [6], strategies for reducing energy consumption have recently received a great deal of attention.

It would be reasonable to imagine that the best solution to increase network lifetime would just give the largest amount of energy possible to each mote. Nevertheless, as pointed out in [1], [11], in some cases, almost 90% of the energy of a network is not used even when the network is inoperative. Therefore, it is essential to understand and quantify the amount of energy consumed by each task performed by motes in a network and hence make the best use of the energy available.

1.2 Research Scope

In this work, we analyze and present strategies to make efficient usage of the batteries and to increase the lifetime of Wireless Sensor Networks while maintaining the same energy budget, i.e., using the same amount of energy and making a Wireless Sensor Network operational for a longer period of time.

Our work first focused on measuring and understanding how is the current consumption profile of the components of a mote. After determining the form that each part and, consequently, the whole mote consumes its battery, our analysis investigated the impact of using multiple transmission power levels and proposed a strategy to calculate the individual energy consumption of a mote and a heuristic to assign a battery set proportional to the energy demand of each mote.

In addition to the main scope of each analysis, different metrics were employed to provide an extensive analysis of the impact of each of our approaches in distinct parameters.

1.3 Methodology

This work was made using data acquired from both direct measurements (detailed in Chapter II), Matlab simulations [12]–[17] and the respective datasheets of each part, and, Mathematical models used in related academic literature (all referenced along the text). The results were also confronted with some previous academic works in order to ascertain their validity and were presented at both national and international scientific events.

Each chapter uses a specific set of metrics for presenting a clearer and consistent analysis about the performed investigation.

1.4 Chapters

This work is divided into six chapters, counting with this current section. The next subsections present a brief resume of each chapter.

1.4.1 Chapter II: Current Consumption in Radio Modules for Wireless Sensor Networks

This chapter presents an expanded version of an experimental work, presented at the XXXV Brazilian Symposium on Telecommunications and Signal Processing–SBrT, entitled "Current Consumption in Radio Modules for Wireless Sensor Networks" [18]. The aforementioned work was designed to investigate current consumption in electronic parts, especially radio modules, commonly used in Wireless Sensor Networks. After designing a high-speed measurement setup, we collected current consumption profiles (waveforms) of several radio modules in different states, including transmitting, receiving and idle states. Results show a much more detailed current consumption profile when compared with the information provided in datasheets. As radio modules used in Wireless Sensor Networks usually operate under energy-limited conditions, detailed current consumption profiles, such as those presented in this chapter, can be useful when designing energy-aware protocols or subsystems.

1.4.2 Chapter III: The Impact of Multiple Transmission Power Levels on Wireless Sensor Networks

This chapter presents an expanded version of the works "The Impact of Multiple Power Levels on the Lifetime of Wireless Sensor Networks," [19] presented at the 20th IEEE International Symposium on Consumer Electronics–IEEE/ISCE and "An Analysis of the Use of Multiple Transmission Power Levels on Wireless Sensor Networks," [20] presented at the 5th International Electronic Conference on Sensors and Applications - 5th ECSA. The aforementioned work presents an extensive analysis of how Wireless Sensor Networks are impacted by the use of different transmission power levels.

The analysis of different transmission power, which is a novel feature available on some radio modules used in some Wireless Sensor Networks motes, was motivated by its current application on both academic works and commercial solutions.

1.4.3 Chapter IV: Lifetime Maximization with Multiple Battery Levels in Irregular Topology Wireless Sensor Networks

This chapter presents an expanded version of the works "Lifetime Maximization With Multiple Battery Levels in Irregularly Distributed Wireless Sensor Networks," presented at the 10th International Symposium on Ambient Intelligence and Embedded Systems–AMIES and "Lifetime Maximization with Multiple Battery Levels in Irregular Topology Wireless Sensor Networks," sent to Sensors – Open Access Journal (ISSN 1424-8220; CODEN: SENSC9). The aforementioned works present a novel heuristic method to increment the lifetime of Wireless Sensor Networks is proposed. The main difference between the proposed strategy and the others is that it can be used in networks with no topology restrictions. A model for energy consumption estimation of each mote in a time-driven network is also presented. The heuristic validation was carried out by means of simulations using motes with realistic parameter values. Three different network topologies were evaluated and the results show that the proposed heuristic can be a feasible mean to increase the lifetime of Wireless Sensor Networks, extending the lifetime of some simulated networks more than 200%.

1.4.4 Chapter V: Impact of Multiple Battery Levels and Multiple Transmission Power Levels on Wireless Sensor Networks

This chapter, the use of multiple transmission levels, analyzed in Chapter III and in [19], [20], and the strategies for calculating the individual energy consumption and the battery distribution heuristic, presented in Chapter IV, are examined on three different network topologies in 54 distinct scenarios. The simulated networks were designed to have different levels of topology irregularity, from a well-organized network, with its base station exactly in its center to a network with its base station isolated from the network cluster.

1.4.5 Chapter VI: Work Summary and Concluding Remarks

This chapter presents the summary of all results shown in this work along with remarks of its authors.

1.5 Writing Style

This work was written under the principles of Universal Design [21]–[26], aiming a more comfortable and accessible text for all readers. For supporting an easier usage of screen reader software, this work repeats some discussion and definitions in every chapter that needs them. All graphics elements, viz.: tables, figures, algorithms, flowcharts, graphics/charts are described in text form for the use of screen reader software. For low vision readers, all graphic elements are as magnified as possible in order to make it easier to interpret and some words are in bold style to facilitate the text navigation.

1.6 Published Works

The published works related to this research are listed below:

- MIRANDA, F. A. M.; REIS FILHO, Carlos Alberto dos; Lifetime Maximization With Multiple Battery Levels in Irregularly Distributed Wireless Sensor Networks, 09/2011, 10th International Symposium on Ambient Intelligence and Embedded Systems - AmiEs 2011,Vol. 1, pp.1-1, Chania, Greece, 2011.

- MIRANDA, F. A. M.; CARDIERI, P.; The Impact of Multiple Power Levels on the Lifetime of Wireless Sensor Networks, 09/2016, 20th IEEE International Symposium on Consumer Electronics - 20th ISCE, São Paulo, Brazil, 2016.
- MIRANDA, F. A. M.; CARDIERI, P.; Current Consumption in Radio Modules for Wireless Sensor Networks, 2017, XXXV Brazilian Symposium on Telecommunications and Signal Processing - XXXV SBrT, Sao Pedro, Brazil, 2017.
- MIRANDA, F. A. M.; CARDIERI, P.; An Analysis of the Use of Multiple Transmission Power Levels on Wireless Sensor Networks, 2018, 5th International Electronic Conference on Sensors and Applications - 5th ECSA, *online*, 2018.
- MIRANDA, F. A. M.; REIS FILHO, Carlos Alberto dos; Lifetime Maximization with Multiple Battery Levels in Irregular Topology Wireless Sensor Networks, 2018, Sensors – Open Access Journal (ISSN 1424-8220; CODEN: SENSC9) – *under review*.

Chapter II

CURRENT CONSUMPTION IN RADIO MODULES FOR WIRELESS SENSOR NETWORKS

This chapter presents an expanded version of an experimental work, presented at the XXXV Brazilian Symposium on Telecommunications and Signal Processing, entitled "Current Consumption in Radio Modules for Wireless Sensor Networks." [18] The aforementioned work was designed to investigate current consumption in electronic parts, especially radio modules, commonly used in Wireless Sensor Networks. Using high-speed measurement setup, we collected current consumption profiles (waveforms) of several radio modules in different states, including transmitting, receiving and idle states. Results show a much more detailed current consumption when compared with the information provided in datasheets. As radio modules used in Wireless Sensor Networks usually operate under energy-limited conditions, detailed current consumption profiles, such as those presented in this chapter, can be useful when designing energy-aware protocols or subsystems.

2.1 Introduction

The energy constraint is an issue that affects any study or implementation of Wireless Sensor Networks, because those terminals in these networks, usually called motes, typically have limited energy available and battery replacement is either impossible or expensive [2].

Among all the subsystems that compose a mote, the radio module alone represents a substantial share of their energy consumption [27]. As the energy constraint is a critical issue when using Wireless Sensor Networks, analyzing and understanding the way radio modules use the energy available is an important topic.

The primary documentation about technical characteristics of an electronic part is always its respective datasheet. Manufacturers gather mechanical and electrical characteristics, sometimes in many different scenarios, and compile them in datasheets. The problem is that, sometimes, even when a static value presented in a datasheet is precise, that information is just a small portion of a much bigger and more complex characterization of that part.

As there is no standard radio technology used by Wireless Sensor Networks, different transmission schemes have been adopted by radio modules manufacturers. There are radio modules employing analog, digital or even spread spectrum modulation [28] and because each modulation needs a specific circuitry, it is reasonable to expect different consumption profiles for different radio technologies. With the emerging technology of energy harvesting [29], [30], based on collecting small amounts of energy from the surrounding environment, understanding how an electronic part uses the available energy can be a valuable information when designing energy harvesting systems.

This chapter presents an exploratory work, aiming at bringing forward a detailed analysis of the current consumption of several different radio modules commonly used in Wireless Sensor Networks. We present fairly detailed waveforms of current consumption, showing how a single task can delineate distinct and complex consumption profiles, which may impact the design of other components and subsystems of the whole network.

2.2 Related Works

Accurate current consumption profiles are quite helpful information for designing energy-constraint motes [31] or for designing efficient power supplies, especially the sensible energy harvesting power supplies [32].

Embedded systems usually require constant voltage to operate, simplifying the process of estimating their energy consumption by just measuring their current consumption [33]. Techniques for measuring current consumption in Wireless Sensor Networks motes/parts can be divided into two categories: benchtop measurements and embedded measurements.

Benchtop measurements, which is the adopted approach in this work, tend to have the most accurate and precise results, due to the possibility of using high-precision equipment, hardware and others resources. Works like [33]–[38] use very specific circuitry, usually current mirrors or a single shunt resistor, together with high-grade measuring instruments, such as oscilloscopes, proprietary data acquisition devices or even microprocessors.

On the other hand, embedded measurements have more hardware, space and energy constraints when compared to the benchtop approach. However, embedded measurements have the advantage of being part of a mote, allowing for real-time data acquisition, even when the mote is deployed in the field. Works like [39]–[42] show how add-on boards or specific testbeds can provide in-field real-time data acquisition with fairly reliable results.

In this present exploratory work, the benchtop approach was selected in order to retrieve more detailed current consumption profiles of various motes commonly used in Wireless Sensor Networks. Details about the hardware setup and measurements approaches are described in the next section.

2.3 Methodology

In order to perform the current consumption measurements presented in this work, we designed a methodology considering the following primary objectives:

- Enough measurement resolution,
- Noise and interference avoidance,
- Measurement of different states of consumption.

The following subsections describe the methodology used to meet the aforementioned objectives and other topics related to this work, like the circuitry and radio modules specifications.

2.3.1 Measurement Resolution

As presented in [43], [44], the consumption profile of a mote is made of long periods of low-current, usually few microamperes or milliamperes, interrupted by some narrow high-current bursts, from dozens to hundreds of milliamperes. Therefore, there is a need for a specific methodology for measuring the energy consumption of the electronic parts used in Wireless Sensor Network motes.

Many types of equipment, like voltmeters, ammeters and multimeters are capable of measuring physical quantities with excellent precision and accuracy, however, due to the consumption characteristics of Wireless Sensor Networks motes, there is a need of high-rate sample acquisition equipment. The fast variation of some measured signals could cause some errors on the measurements performed by low-rate sample acquisition equipment, consequently, we needed faster equipment to perform these measurements.

Considering the need of high-rate samples, an oscilloscope was the most suitable equipment for these measurements of this work. On most cases, the sampling rate of oscilloscopes is expressively higher than the sampling rate of multimeters, even when compared to bench ones. Table I and Table II present the sampling rate of some multimeters and oscilloscopes.

Sampling rate of some commercial multimeters (also shown in Table I):

- 34405A (Agilent) [45] – 19 samples per second.
- 34401A (Agilent) [46] – 1 kilosamples per second.
- Fluke 45 (Fluke) [47] – 30 kilosamples per second.
- 34411A (Agilent) [48] – 50 kilosamples per second.

Sampling rate of some commercial oscilloscopes (also shown in Table II):

- DSO-X 2002A (Agilent) [49] – 2 gigasamples per second.
- MO-2200 (Minipa) [50] – 1 gigasamples per second.
- TDS 460A (Tektronix) [51] – 100 megasamples per second.
- HDO4022 (LeCroy) [52] – 2.5 gigasamples per second.

Table I – Sampling rate of some commercial multimeters.

Model (Manufacturer)	**Sample Rate**
34405A (Agilent) [45]	19 samples/s
34401A (Agilent) [46]	1 ksamples/s
Fluke 45 (Fluke) [47]	30 ksamples/s
34411A (Agilent) [48]	50 ksamples/s

Table II – Sampling rate of some commercial oscilloscopes.

Model (Manufacturer)	**Sample Rate**
DSO-X 2002A (Agilent) [49]	**2 Gsample/s**
MO-2200 (Minipa) [50]	1 Gsample/s
TDS 460A (Tektronix) [51]	100 Msample/s
HDO4022 (LeCroy) [52]	2.5 Gsample/s

The use of an oscilloscope (in this work, we used a model DSO-X 2002A) for measuring current consumption has some differences when compared to the utilization of an ammeter. The main when an oscilloscope is used, a shunt resistor is necessary, as in [43]. The connection of this shunt, in series, between the radio modules and the power supply assures that all current consumed by these radio modules passes through this shunt resistor and, consequently, causes an electrical potential difference, i.e., an electric tension/voltage, between the terminals of the shunt resistor directly proportional to the current consumption of the radio module [53], [54]. The simplified schematic of the measurement setup is shown in Fig. 1.

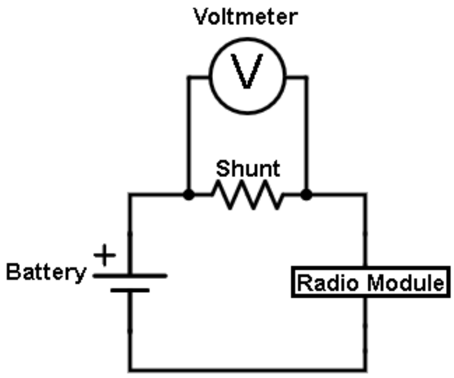

Fig. 1 – Schematic of the measurement circuit used in this work.

As the shunt resistor, instead of using a simple passive shunt resistor, we used a Valhalla 2575A Active Shunt [55]. We decided to use this active shunt because it has a very precise amplifier, which allows the use of low-resistance shunts without having problems while measuring their terminals. Valhalla 2575A Active Shunt characteristics are (also shown in Table III):

- **Range**: 100 amperes; **Shunt value**: 0.001 ohm; **DC Accuracy**: ±0.05%.
- **Range**: 20 amperes; **Shunt value**: 0.0 1 ohm; **DC Accuracy**: ±0.02%.
- **Range**: 2 amperes; **Shunt value**: 0. 1 ohms **DC Accuracy**: ±0.02%.
- **Range**: 200 milliamperes; **Shunt value**: 1 ohm; **DC Accuracy**: ±0.01%.
- **Range**: 20 milliamperes; **Shunt value**: 10 ohms; **DC Accuracy**: ±0.01%.
- **Range**: 2 milliamperes; **Shunt value**: 100 ohms; **DC Accuracy**: ±0.01%.

Table III – Valhalla 2575A Active Shunt Characteristics.

Range	Shunt Value	DC Accuracy	AC Accuracy	Frequency Response
100A	0.001Ω	±0.05%	±0.1%	DC to 1kHz
20A	0.01Ω	±0.02%	±0.1%	DC to 10kHz
2A	0.1Ω	±0.02%	±0.1%	DC to 10kHz
200mA	1Ω	±0.01%	±0.1%	DC to 10kHz
20mA	10Ω	±0.01%	±0.1%	DC to 10kHz
2mA	100Ω	±0.01%	±0.1%	DC to 10kHz

The scheme of our test setup is shown in Fig. 2. Our setup uses a regulated and filtered power supply, shown in Fig. 4, together with the oscilloscope for measuring the voltage across the shunt resistor in order to measure the current consumed by the radio module. For more accurate measurements, each waveform is an average of 64 acquisitions.

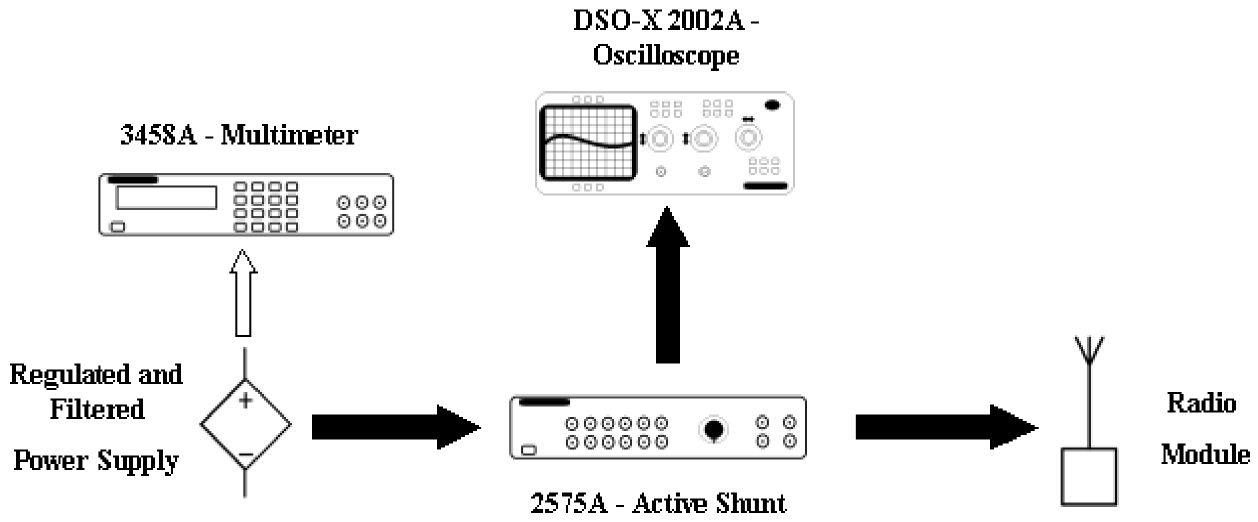

Fig. 2 – Measurement setup.

2.3.2 Noise Avoidance

During measurements, noise and other interference signals were avoided as discussed below.

In order to prevent external electromagnetic interference (EMI), both in the communication link between the radio modules and in the measured waveforms, we performed all measurements inside an EMI double-shielded room, as shown in Fig. 3. Transmitters and receivers were placed at the same height and the distance between their antennas was adjusted to 1 m.

The power supplies for the instruments were filtered by an external unity, protecting the measurement setup from interference coming from the power line. Additionally, we used batteries and voltage regulators as power supplies for the radio modules, in order to minimize the noise effect in these modules. The schematic of our power supply is shown in Fig. 4.

Fig. 3 – Measurement setup inside the EMI shielded room.

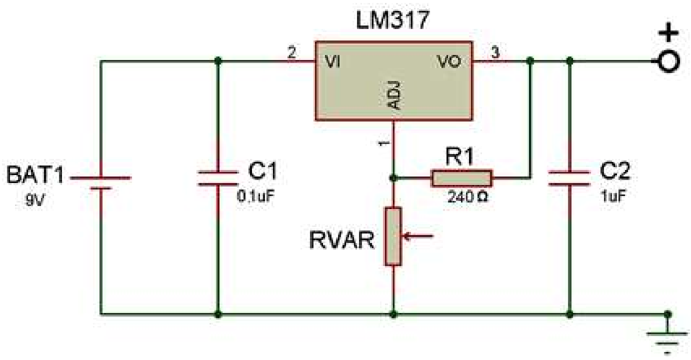

Fig. 4 – Power supply used in measurements.

2.3.3 Transmitted Signal and Measurement of Different States

The measurement of the current consumption profile in both transmission and reception modes was made while the radio module was transmitting or receiving a single-byte message, consisting of the "U" character. In ASCII code, this character corresponds to a perfect square waveform of four cycles, i.e., the bit array "01010101".

The UART (Universal Asynchronous Receiver/Transmitter), which was used to generate the messages, adds one extra bit, the start bit "1", and uses high-voltage for no data state. For a better visualization of the measurements, the signal was inverted before transmission, as shown in Fig. 5. The only exception to the signal inversion was in the case of the radio module XBee PRO, which needs standard UART signals as input signal, shown in Fig. 6.

The transmission data rate of all modules, excluding the XBee PRO module, was the same as the data rate of the generated signal, i.e., 1.2 kbit/s. The XBee PRO module has a fixed transmission data rate of 250 kbit/s.

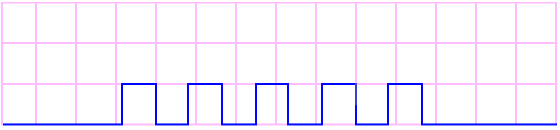

Fig. 5 – "U" in inverted UART levels.

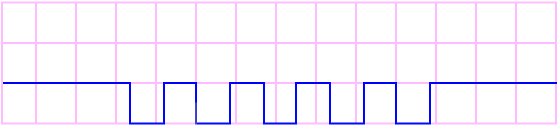

Fig. 6 – "U" in standard UART levels.

We used the bit rate of 1200 bps in all cases.

2.3.4 Radio Modules

Six different radio modules, listed below and in Table IV, were used in this work.

- **DR3000 – modulation**: OOK/ASK; **function**: transceiver; **frequency**: 916 MHz.
- **TRM 315 LT – modulation**: OOK; **function**: transceiver; **frequency**: 315 MHz.
- **TRM 433 LT – modulation**: OOK; **function**: transceiver; **frequency**: 433.92 MHz.
- **RT4 433 – modulation**: ASK; **function**: transmitter; **frequency**: 433.92 MHz.
- **RR3 433 – modulation**: ASK; **function**: receiver; **frequency**: 433.92 MHz.
- **XBee PRO – modulation**: DSSS; **function**: transceiver; **frequency**: 2.4 GHz.

Table IV – Radio modules basic specifications.

Radio	**Modulation**	**Function**	**Frequency**	**Vdc**	**Max. Output Power**
DR3000	OOK/ASK	Tx/Rx	916 MHz	3.3 V	>0.75mW

TRM 315 LT	OOK	Tx/Rx	315 MHz	3.3 V	12.5 mW
TRM 433 LT	OOK	Tx/Rx	433.92 MHz	3.3 V	12.5 mW
RT4 433	ASK	Tx	433.92 MHz	3.3 V	10 mW
RR3 433	ASK	Rx	433.92 MHz	5 V	-
XBee PRO	DSSS	Tx/Rx	2.4 GHz	3.3 V	63 mW

The output power of all modules, excluding the XBee PRO module, is directly related to its power supply voltage (Vdc column in Table IV). For the case of XBee PRO, the output power can be configured by software. In the cases reported here, the output power of the XBee PRO module was set to its maximum value, 63 mW.

2.3.5 Measurement Scales

As the current consumption of the radio modules used in this chapter was very different when compared to each other and our active shunt had maximum input currents for each shunt resistor, we had to use different shunt resistors according to the current consumption of each radio module. Table V shows the value of the shunt resistor used with each radio module.

Shunt resistor values and resultant scale of all measurements (also shown in Table V):

- **DR3000** – 1 ohm.
- **TRM 315 LT** – 1 ohm.
- **TRM 433 LT** – 1 ohm.
- **RT4 433** – 1 ohm.
- **RR3 433** – 1 ohm.
- **XBee PRO** – 0.1 ohm.

Table V – Shunt resistor values.

Radio Module	Shunt Value
Xbee Pro	0.1 Ω
DR3000	1 Ω
TRM 315	1 Ω
TRM 433	1 Ω
RT4	1 Ω
RR3	1 Ω

2.4 Measurements

The measurements show that, in most of the cases reported here, the current waveforms of active states (transmission and reception) were not time-invariant and, in some cases, the resulting waveforms of current consumption are different from the message sent.

2.4.1 Idle and Sleep States

All measurements for both idle and sleep states (also called "power down" or "power saving" states) show time-invariant current consumption. The results of our measurements presented no significant difference when compared with results presented in datasheets. The current consumption for idle and sleep states are shown in Table VI.

Power-Down consumption (also shown in Table VI):

- **DR3000 – idle state**: 2 mA (ASK)/ 0 mA (OOK); **sleep state**: 0.7 microamperes.
- **TRM 315 LT – idle state**: 4 mA; **sleep state**: 11.5 microamperes.
- **TRM 433 LT – idle state**: 4 mA; **sleep state**: 11.5 microamperes.
- **RT4 433 – idle state**: 0 mA; **sleep state**: not available.
- **RR3 433 – idle state**: 3 mA; **sleep state**: not available.
- **XBee PRO – idle state**: 58 mA; **sleep state**: less than 10 microamperes.

Table VI – Power-Down consumption.

Radio Module	**Idle State**	**Sleep State**[1]
DR3000	2 mA (ASK)/ 0 mA (OOK)	0.7 μA
TRM 315 LT	4 mA	11.5 μA
TRM 433 LT	4 mA	11.5 μA
RT4–433	0 mA	Not Applicable
RR3–433	3 mA	Not Applicable
Xbee Pro	58 mA	≤10 μA

[1] Values retrieved from the datasheets.

2.4.2 Murata DR3000

DR3000 is a radio transceiver manufactured by Murata Manufacturing Co. [56]. It operates at 916.5 MHz and offers two options of modulation scheme: Amplitude Shift Keying (ASK) and On-Off Keying (OOK).

Murata DR3000 characteristics:

- **Frequency** – 916.5 MHz.
- **Modulation** – OOK/ASK.
- **Supply Voltage** – 2.7 – 3.5V.
- **Data Rate** – 2.4 kbps.
- **Output Power** – 0.75 mW.

2.4.2.1 Current Consumption: Transmission – ASK Modulation

The current consumption measurement of DR3000 is presented in Fig. 7, and shows a close resemblance to the transmitted signal (shown in Fig. 5), switching between approximately 2 mA and 7 mA. One distinction between the transmitted signal and the current consumption is a small bias on the current consumption (~2 mA), indicating a non-zero current consumption when no signal is being transmitted. The DR3000 datasheet [56] does not report any data about the current consumption for ASK modulation in transmitting mode, but the current measured in our experiment was below the maximum current consumption indicated in the datasheet, which is equal to 12 mA at 3 V when using OOK modulation.

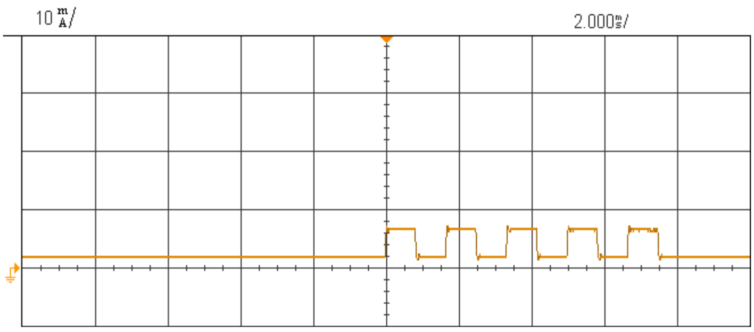

Fig. 7 – DR3000 consumption @ 3.3 V (ASK transmission).

2.4.2.2 Current Consumption: Transmission – OOK Modulation

As in the ASK transmission case, OOK transmission resulted in a current consumption profile very similar to the transmitted signal waveform. As can be observed in Fig. 8, both the amplitude and the width are close to the measured in the ASK transmission case. The measured current switched between 0 and approximately 7 mA. A key difference is that with OOK modulation there is no current consumption when no signal (or a “0” bit) is transmitted. The measured values are below the maximum current consumption of 12 mA at 3 V reported in the DR3000 datasheet [56].

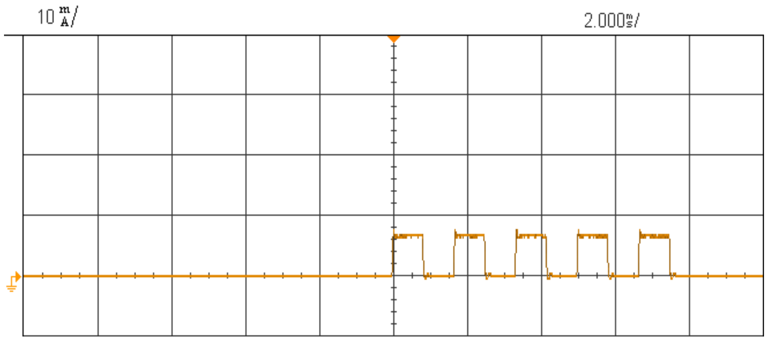

Fig. 8 – DR3000 consumption @ 3.3 V (OOK transmission).

2.4.2.3 Current Consumption: Reception – ASK and OOK Modulation

The DR3000 module employs the same reception mode for both OOK and ASK modulation schemes. For both modulation schemes, the measured current was the same constant value, as shown in Fig. 9. It should be noted that the consumed current remains constant, even when no message is received.

The measured value, approximately 4 mA at 3.3 V, is slightly above the maximum current consumption of 3.1 mA at 3 V, reported in the DR3000 datasheet [56].

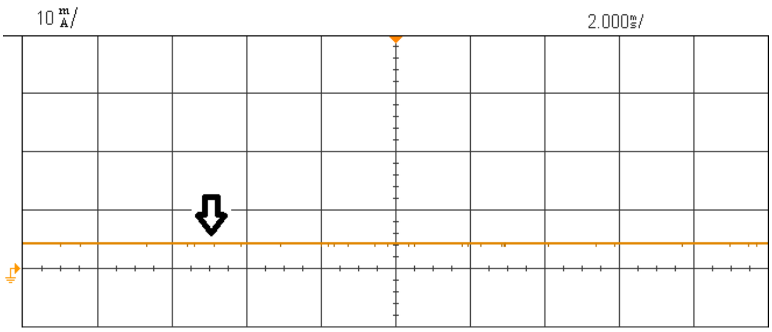

Fig. 9 – DR3000 consumption @ 3.3 V (reception).

2.4.3 Linx TRM 315 LT

The TRM 315 LT is a radio transceiver manufactured by Linx Technologies [57], and operates at 315 MHz, using OOK modulation.

Linx TRM 315 LT characteristics:

- **Frequency** – 315 MHz.
- **Modulation** – OOK.

- **Supply Voltage** – 2.1 – 3.6V.
- **Data Rate** – 10 kbps.
- **Output Power** – 10 mW.

2.4.3.1 Current Consumption: Transmission

The measurements are presented in Fig. 10, and show a close resemblance to the transmitted signal (see Fig. 5).

Like the current consumption of DR3000 using ASK modulation, the consumption of TRM 315 is also biased, switching between 4 mA and 17 mA. The high level (~17 mA) is above the maximum current consumption of 14 mA specified in the TRM 315 datasheet [57]. This discrepancy may be explained by the fact that in the measurements the TRM 315 module was powered with a 3.3V power supply, while the maximum current consumption reported in the datasheet corresponds to a 3V power supply.

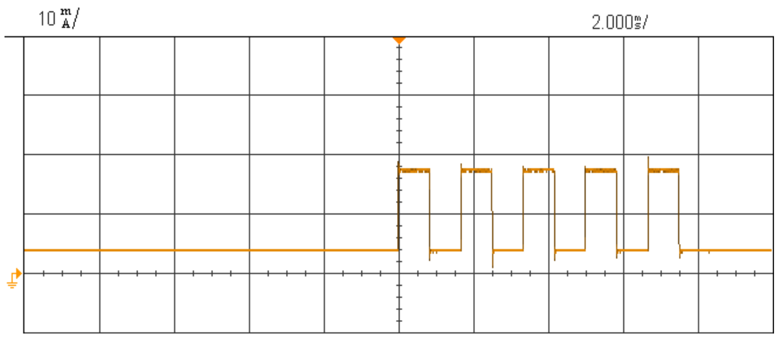

Fig. 10 – TRM 315 consumption @ 3.3 V (transmission).

2.4.3.2 Current Consumption: Reception

The results for the TRM 315 LT module in reception mode is shown Fig. 11. Differently from the case of the DR3000 module (see Fig. 9), the current consumption of TRM 315 LT is not constant. In fact, the waveform has almost the same shape of the transmitted message (see Fig. 5), switching from approximately 6 mA to 8 mA. These measured values are under the maximum current consumption of 7.9 mA at 3 V, reported in the TRM 315 datasheet [57].

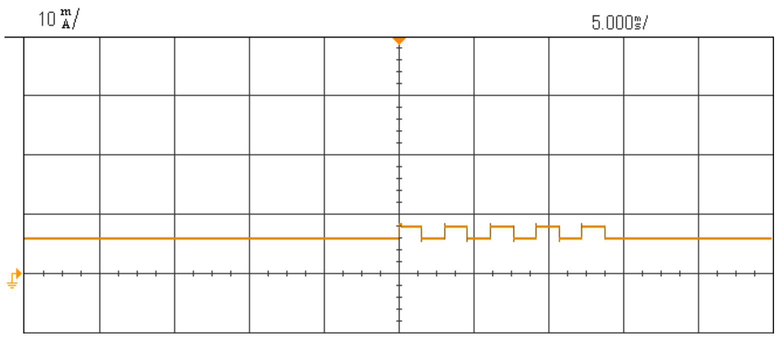

Fig. 11 – TRM 315 consumption @ 3.3 V (reception).

2.4.4 Linx TRM 433 LT

The TRM 433 LT is a radio transceiver manufactured by Linx Technologies [57], and operates at 433.92 MHz, using OOK modulation.

Linx TRM 315 LT characteristics:

- **Frequency** – 433.92 MHz.
- **Modulation** – OOK.
- **Supply Voltage** – 2.1 – 3.6V.
- **Data Rate** – 10 kbps.
- **Output Power** – 10 mW.

2.4.4.1 Current Consumption: Transmission

The measurements are presented in Fig. 12, and show a close resemblance to the transmitted signal (see Fig. 5).

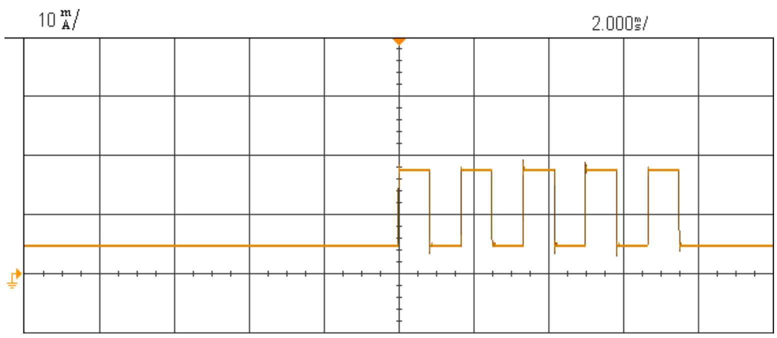

Fig. 12 – TRM 433 consumption @ 3.3 V (transmission).

Like the current consumption of DR3000 using ASK modulation, the consumption of TRM 433 is also biased, switching between 4 mA and 17 mA. The high level (~17 mA) is above the maximum current consumption of 14 mA specified in the TRM 433 datasheet [57]. This discrepancy may be explained by the fact that in the measurements the TRM 433 module was powered with a

3.3V power supply, while the maximum current consumption reported in the datasheet corresponds to a 3V power supply.

2.4.4.2 Current Consumption: Reception

The results for the TRM 433 LT module in reception mode is shown Fig. 13. Differently from the case of the DR3000 module (see Fig. 9), the current consumption of TRM 433 LT is not constant. In fact, the waveform has almost the same shape of the transmitted message (see Fig. 5), switching from approximately 6 mA to 8 mA. These measured values are under the maximum current consumption of 7.9 mA at 3 V, reported in the TRM 433 datasheet [57].

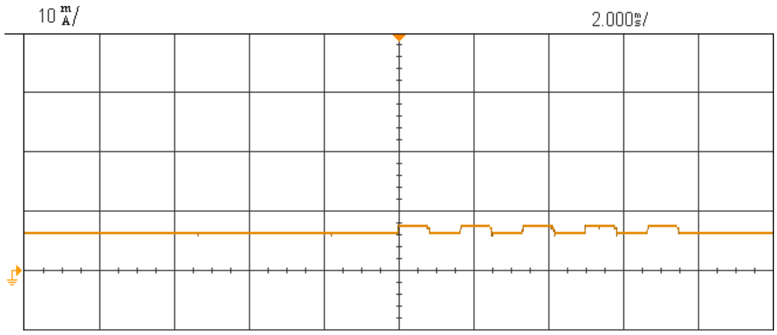

Fig. 13 – TRM 433 consumption @ 3.3 V (reception).

2.4.5 Telecontrolli RT4–433

The RT4–433 module is a radio transmitter manufactured by Telecontrolli SRL [58]. It operates at 433.92 MHz and uses ASK modulation.

Telecontrolli RT4–433 characteristics:

- **Frequency** – 433.92 MHz.
- **Modulation** – OOK.
- **Supply Voltage** – 2 – 14V.
- **Data Rate** – 9.6 kbps.
- **Output Power** – 10 mW.

2.4.5.1 Current Consumption: Transmission

The measured current consumption is presented in Fig. 14, and shows that consumption profile of the RT4–433 has a close resemblance to the transmitted signal (see Fig. 5). As in the case of OOK transmission of the DR3000 module, shown in Fig. 6, the consumption of RT4–433 in the transmission mode has no bias. The measurements present peak values near the typical current consumption of 4 mA at 5 V, reported in the RT4 datasheet [58].

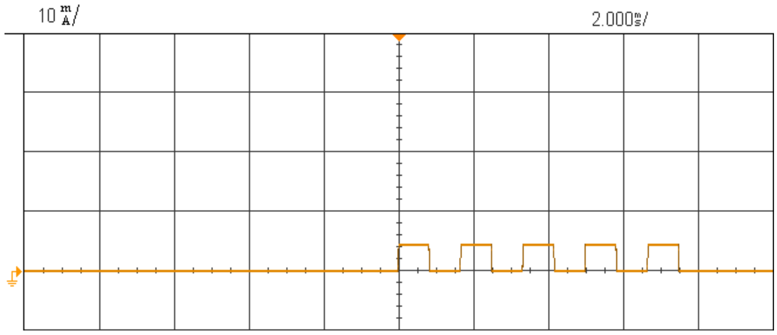

Fig. 14 – RT4 consumption @ 3.3 V (transmission).

2.4.6 Telecontrolli RR3–433

The RR3–433 module is a radio receiver manufactured by Telecontrolli SRL [59]. It operates at 433.92 MHz and uses Amplitude Modulation (AM).

Telecontrolli RR3–433 characteristics:

- **Frequency** – 433.92 MHz.
- **Modulation** – OOK.
- **Supply Voltage** – 4.5 – 5.5V.
- **Data Rate** – 4.8 kbps.
- **Sensibility** – -100 dBm.

2.4.6.1 Current Consumption: Reception

The result is shown in Fig. 15 and we can see that the current consumption profile is similar to that for the DR3000 module (see Fig. 9).

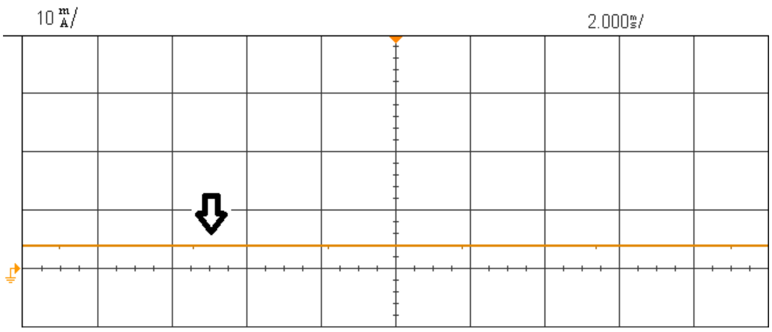

Fig. 15 – RR3 consumption @ 5 V (reception).

We can also see that, even when the RR3-433 module is receiving a message, no variation in its current consumption is observed. The measured values are close to the maximum current consumption of 3 mA at 5 V, specified in the RR3 datasheet [59].

2.4.7 Digi XBee Pro 2.4 GHz 802.15.4

The XBee Pro 2.4 GHz 802.15.4 module is a radio transceiver manufactured by Digi International Inc. [60]. It operates at 2.4 GHz and uses Direct-Sequence Spread Spectrum (DSSS) modulation.

Among the radio modules investigated in this work, the XBee Pro module is the most complex device, having many embedded functionalities, like carrier sensing, routing protocols, multi-channel operation and encryption.

Digi XBee Pro 2.4 GHz 802.15.4 characteristics:

- **Frequency** – 2.4 GHz.
- **Modulation** – QPSK.
- **Supply Voltage** – 2.8 – 3.4V.
- **Data Rate** – 250 kbps.
- **Output Power** – 10-60mW.

2.4.7.1 Current Consumption: Transmission – Non-Encrypted

Differently from all measurements shown before, the current consumption profile of the XBee Pro module, shown in Fig. 16, has no resemblance to the transmitted signal (see Fig. 6). As the XBee Pro module is a complex radio device, it is reasonable to associate this current profile to internal routines related to message transmission processing. The measured peak current (~230 mA) is below the maximum current consumption of 250 mA at 3.3 V, reported in the XBee PRO datasheet [60].

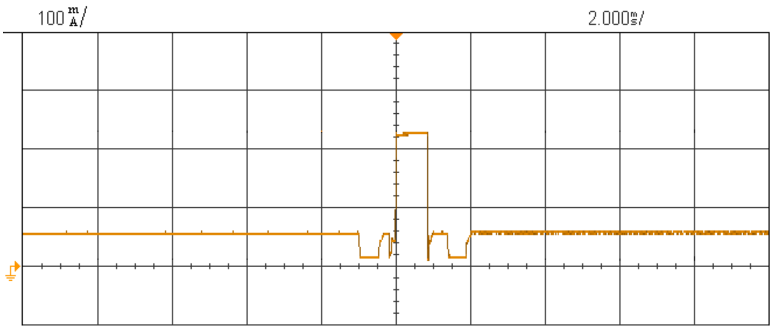

Fig. 16 – XBee consumption @ 3.3 V (non-encrypted transmission).

2.4.7.2 Current Consumption: Transmission – Encrypted

This measurement, shown in Fig. 17, was made when the XBee module was transmitting a message (see Fig. 6) using the encryption offered by the module. Again, the measured peak current (~230 mA) is below the maximum current consumption of 250 mA at 3.3 V, reported in the XBee PRO datasheet [60]. The main difference is that the encrypted transmission is approximately 0.5 ms longer than the non-encrypted.

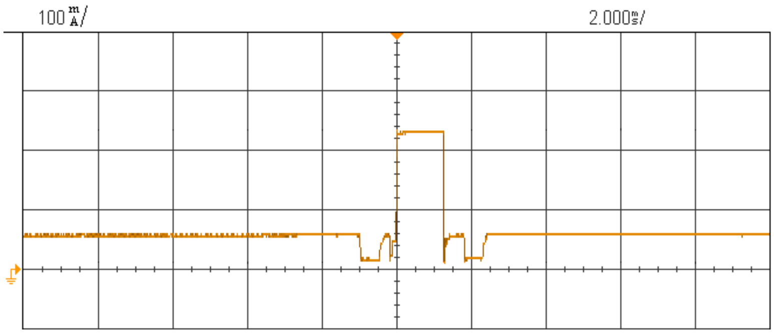

Fig. 17 – XBee consumption @ 3.3 V (encrypted transmission).

2.4.7.3 Current Consumption: Reception – Non-Encrypted

Again, the XBee Pro module in reception mode presented a current consumption profile, shown in Fig. 18, with no resemblance to the transmitted signal. The shape of the resulting waveform is similar to the waveform observed in the transmitting case. The waveform presented a narrow pulse, less than 0.5 ms long, with high amplitude, reaching approximately 260 mA.

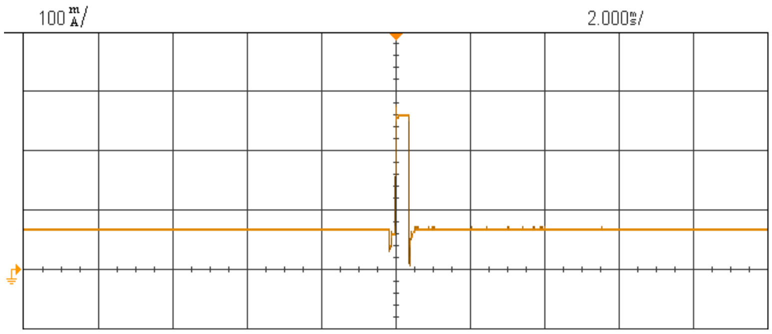

Fig. 18 – XBee consumption @ 3.3 V (non-encrypted reception).

We can also see that, in the idle state, the measurements show a constant current consumption close to the typical current consumption of the idle state, 55 mA at 3.3 V, reported in the XBee PRO datasheet [60]. However, the datasheet does not report any difference between the current consumption of "idle" and "reception" states, and no further information about the reception current consumption is provided.

2.4.7.4 Current Consumption: Reception – Encrypted

The current consumption profile of the XBee PRO receiving an encrypted message, shown in Fig. 19 is almost the same of the non-encrypted scenario (see Fig. 18). Therefore, the same comments and analysis made for the non-encrypted scenario are valid for the encrypted scenario as well.

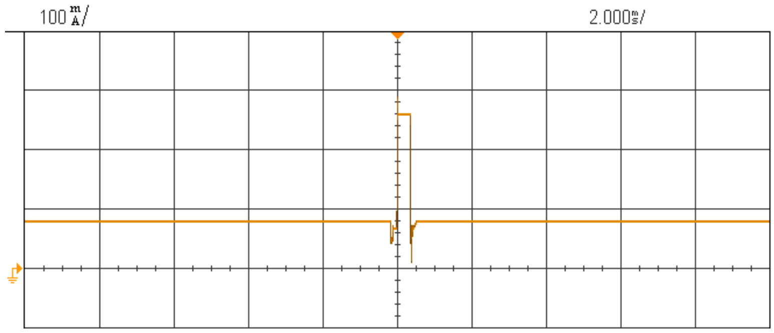

Fig. 19 – XBee consumption @ 3.3 V (encrypted reception).

2.5 Concluding Remarks

The measurements presented in this chapter show how the current consumptions of radio modules typically employed in Wireless Sensor Networks can be more complex and intricate than the constant values presented in their respective datasheets. The complexity of the observed waveforms is closely related to the complexity of the radio module.

All measurements show, as expected, that the datasheets present reliable information about an electronic device. However, when precise information about current consumption is required, the information available in datasheet may not be enough, and a more detailed analysis of the current consumption profile of the involved devices may be necessary. The use of detailed energy consumption profiles is very needed when designing energy-aware techniques for Wireless Sensor Networks, or when motes in a Wireless Sensor Networks are powered by alternative power supplies, such as energy harvesting power supplies.

The measurement setup employed in this work provided both sufficient resolution and clear waveforms, being suitable for the future steps of this work, namely, analysis of other radio modules and evaluation of external factors that affect current consumption in Wireless Sensor Networks.

Chapter III

THE IMPACT OF MULTIPLE TRANSMISSION POWER LEVELS ON WIRELESS SENSOR NETWORKS

Energy consumption in Wireless Sensor Networks is an important issue, as in many applications replacing batteries is not a viable task. Therefore, it is essential to understand and quantify the amount of energy consumed by each task performed by motes in a network and hence make the best use of the energy available. In this chapter, we present an extensive analysis of how Wireless Sensor Networks are impacted by the use of different transmission power levels. The analysis of different transmission power, which is a novel feature available on some radio modules used in some Wireless Sensor Network motes, was motivated by its current application on both academic works and commercial solutions.

This chapter presents an expanded version of the works "The Impact of Multiple Power Levels on the Lifetime of Wireless Sensor Networks," [19] presented at the 20th IEEE International Symposium on Consumer Electronics–IEEE/ISCE and "An Analysis of the Use of Multiple Transmission Power Levels on Wireless Sensor Networks," [20] presented at the 5th International Electronic Conference on Sensors and Applications - 5th ECSA.

For supporting an easier usage of screen reader software, this chapter repeats some discussion and definitions already made in previous chapters.

3.1 Introduction

As pointed in [61], the energy consumption of a Wireless Sensor Network mote is the summation of the individual consumption of all its parts. Each one of these components, generally, has multiple states and different consumptions levels related to them. Manufacturers are increasingly achieving low power consumption [62] but, when performing a long-term analysis, even the few microamperes consumed by idle and sleep states are not negligible for a Wireless Sensor Network mote.

The energy amount consumed by inactive states has a direct proportionality to the time spent in these states. Therefore, a Wireless Sensor Network that generates and sends more messages spends less energy on these unimportant states than a low-activity WSN. Among the main active tasks of a WSN mote, transmitting is one that requires more power for being performed [1].

3.2 Multiple Transmission Power Levels

The use of multiple/dynamic transmission power levels is employed in both in academic works [63]–[67] and commercial products [60], [68]–[70], having the potential to be employed in Wireless Sensor Networks motes. A common and widespread technology that uses multiple/dynamic transmission power levels is the Bluetooth [71], [72], specifically, the Class 1 devices [73], [74].

3.3 The Cost of a Wireless Sensor Network

Besides the Wireless Sensor Networks paradigm states that they are made of inexpensive motes, the price of many parts used in these motes still not insignificant. Some commercial motes have even higher prices, over US$60 [75]–[79], due to their integrated and assembled equipment. As Wireless Sensor Network motes are high technology tools, it is feasible that they are not very cheap when they are produced.

As a Wireless Sensor Network can be constituted by thousands of motes, its total cost has a direct proportionality with both the price of its motes and its dimension. Another issue, which can cause both monetary and environmental damages, is the deployment of potentially harmful parts, especially batteries, in a sensible environment [80]–[84].

3.4 Methodology

This chapter was made using Matlab simulations [12]–[17], data acquired from both direct measurements (detailed in Chapter II and in [18]) and the respective datasheets of each component, and, Mathematical models used in related academic literature (referenced along the text). The results were also confronted with some previous academic works in order to ascertain their validity.

3.4.1 Mote Architecture

The motes considered in the analysis presented in this chapter follow a basic architecture, having one battery, one microcontroller, one radio transceiver and one sensor [85], as shown in Fig. 20. Each mote used Digi XBee PRO [60] as its radio transceiver, Texas Instruments LM75 [86] as its sensor, Atmel Atmega8L [87] as its microcontroller and COMP-18-3-NMH as its battery (150 mAh; one per mote).

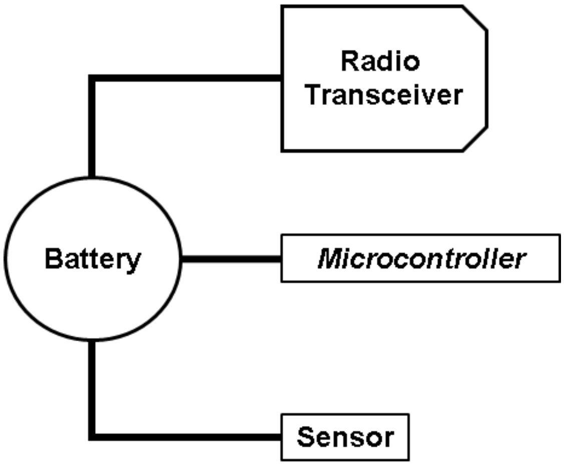

Fig. 20 – Mote architecture.

3.4.2 Energy Consumption

The motes considered in the analysis presented in this chapter follow a simple architecture, having a battery, a microcontroller, a radio transceiver and a sensor [19], [20], [85]. The energy consumption model used in this chapter is shown in Equation (1) and described below:

- The total energy consumption of a mote at a given time is equals to the summation of the energy consumption of its radio module, its sensor, and its microcontroller.

$$c_m(t) = c_r(t) + c_s(t) + c_\mu(t), \tag{1}$$

where c_m is the total consumption of a mote and c_r, c_s and c_μ are, respectively, the consumption of its radio module, sensor and microcontroller. In order to achieve accurate results, we followed the current consumption of each component given by direct measurements [18] (Xbee active states) and their respective datasheets. As shown in their datasheets [60], [86], [87], all parts have different consumption levels according to their current states, consequently, these different levels were computed in our simulations. The sleep state was the standard state of all parts, thus, all parts just changed to active states when a new message had to be generated or only the radio module and the microcontroller when a mote had to receive a message.

3.4.2.1 Primary and Secondary Energy Consumption

We divide the energy consumption into two categories: *Primary* and *Secondary*. Primary energy consumption refers to the energy consumed by active states, like reading sensors, processing data, transmitting or receiving messages etc. Secondary energy consumption refers to the energy consumed by inactive states, like idle and power-down/sleep states [60], [86]–[88].

It is important to note that every electronic part used in a mote consumes energy, including when they are in secondary states, like idle and sleep and that the energy consumption of secondary states is usually very low when compared to the primary states [18].

3.4.3 Transmission Power Levels

In order to calculate the power of the received signal, denoted by P_{rx}, by motes at a given distance, we assumed the Plane Earth Propagation Model [89], which is shown in Equation (2) and described below:

- The reception power is equals to the multiplication of the transmission power, the antenna gain of the transmitter, the antenna gain of the receiver, the square of the antenna height of the transmitter and the square of the antenna height of the receiver, all them divided by the distance between the antennas raised to the power of the path loss exponent of the medium which, in this chapter, is set to **3.5** in all scenarios.

$$P_{rx} = \frac{P_{tx} G_{tx} G_{rx} {h_{tx}}^2 {h_{rx}}^2}{d^{\gamma}}, \tag{2}$$

where P_{tx} is the transmission power which, in this chapter, is the Xbee PRO [60] maximum transmission power; G_{tx} and G_{rx} are the antenna gains of the transmitter and the receiver, respectively; h_{tx} and h_{rx} are, respectively, the heights of the transmitter and receiver antennas; d is the distance between transmitter and receiver antennas, and γ is the path loss exponent, which, in this chapter, is set to **3.5** [90]–[92].

As all motes have the same antenna gains and heights, in order to keep the same P_{rx} at different distances, the transmission power P_{tx} was the only adjustable parameter. Letting d be denoted by the maximum distance that two motes can communicate with the standard transmission power P_{tx}, the transmission power levels used in this chapter are:

- **Path loss exponent set to 3.5** (also shown in Table VII**)**:
  - P_{tx} reaching 1 hop (d); $11.31P_{tx}$ reaching 2 hops ($2d$); $46.76P_{tx}$ reaching 3 hops ($3d$) ; $128P_{tx}$ reaching 4 hops ($4d$) ; $279.50P_{tx}$ reaching 5 hops ($5d$) ;

$529.08P_{tx}$ reaching 6 hops ($6d$) ; $907.49P_{tx}$ reaching 7 hops ($7d$) ; $1448.15P_{tx}$ reaching 8 hops ($8d$) ; $2187P_{tx}$ reaching 9 hops ($9d$) ; $3162.27P_{tx}$ reaching 10 hops ($10d$).

Table VII – Transmission power levels used for a path loss exponent set to **3.5**.

Distance	Transmission Power
d	P_{tx}
$2d$	$11.31P_{tx}$
$3d$	$46.76P_{tx}$
$4d$	$128P_{tx}$
$5d$	$279.50P_{tx}$
$6d$	$529.08P_{tx}$
$7d$	$907.49P_{tx}$
$8d$	$1448.15P_{tx}$
$9d$	$2187P_{tx}$
$10d$	$3162.27P_{tx}$

In the simulations of this chapter, we analyzed six different situations (also shown in Fig. 21):

- All motes transmitting for reaching one hop.
- Motes transmitting for reaching two hops.
- Motes transmitting for reaching three hops.
- Motes transmitting for reaching four hops.
- Motes transmitting for reaching five hops.
- All motes transmitting for reaching, directly, the base station.

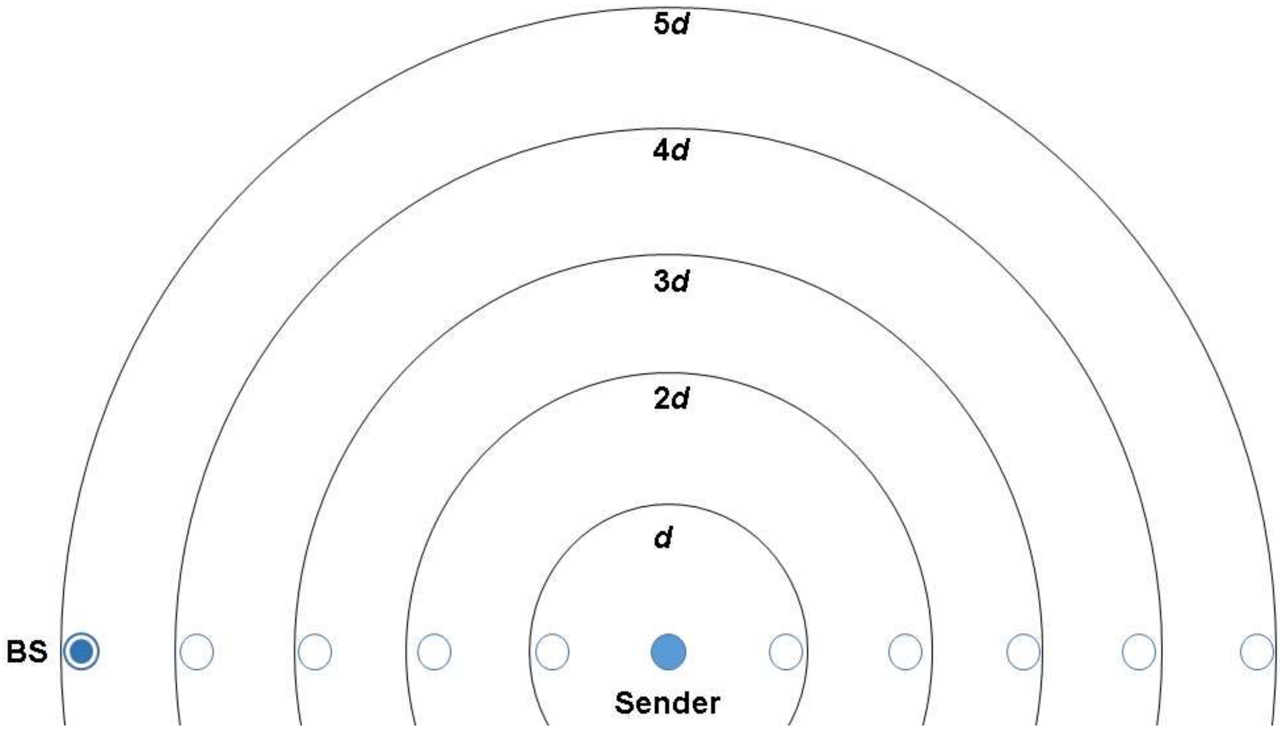

Fig. 21 – Transmission radius with different power levels.

As all motes transmit their messages towards a single base station, their maximum P_{tx} did not exceed the power needed to reach the base station in any situation.

3.4.4 Network Lifetime

The network lifetime [93]–[96] of a Wireless Sensor Network can have different definitions: the time until the network communication backbone ceases to exist; the time until the message delivery rate is bellow a threshold or when one or more motes have their battery depleted. Since this work focuses on energy consumption, the adopted definition of network lifetime does not account for other factors but tasks that consumes the battery charge of the Wireless Sensor Network motes.

In this chapter, we defined the lifetime of a Wireless Sensor Network as the period of time from the moment the network operation begins until the first mote runs out of battery, as considered in [19], [20], [93]–[97]. Assuming our simulated mote model, a 150 mAh battery provides the maximum lifetime, i.e., when the mote neither sends nor receives messages, of 7142.85 hours.

3.4.5 Network Cost

We defined the network cost as the summation of the price of all parts used in the simulated networks. The quotation of all components was made on Mouser and Farnell [77], [78] during 2017, and their average prices are shown in Table VIII.

- **Average prices of all components** (also shown in Table VIII**)**:
  - **Battery** – model: COPM-18-3-NMH, price: US$4.99.
  - **Radio Module** – model: Xbee PRO 2.4 GHz, price: US$34.00.
  - **Microcontroller** – model: Atmega8L, price: US$3.66.
  - **Sensor** – model: LM75, price: US$1.86.

Table VIII – Average prices of all components.

Part	**Model**	**Price**
Battery	COMP-18-3-NMH	US$4.99
Radio Module	Xbee PRO 2.4 GHz	US$34.00
Microcontroller	Atmega8L	US$3.66
Sensor	LM75	US$1.86

The total network cost of the simulated network, with 60 motes, was US$2,670.60.

Facing the waste of its remaining parts, it is feasible to relate the cost a Wireless Sensor Networks with its lifetime. In this chapter, we also use the metric cost per hour relating the total cost of a network with its lifetime, as shown in Equation (3) and described below:

- Network Cost per hour is equals to the total cost of the network divided by its lifetime in hours.

$$h = \frac{c}{l}, \tag{3}$$

where h is the cost per hour of the network, c is the total cost of the network and l is its lifetime (in hours).

3.4.5.1 The Nonlinearity of the Energy Price

Due to the different charges and nonlinear prices, the assortment of battery sets under cost constraints is quite a complex problem. This problem is well addressed in [98], [99].

3.4.6 Messages per Hour

As the simulations have different generation periods, when each mote generates a new message, there is also a need to analyze how many messages a network generates throughout its lifetime. We decided to associate the number of generated messages with the network lifetime, as shown in Equation (4) and described below:

- Messages generated per hour is equals to the total number of messages generated by a network divided by its lifetime.

$$M = \frac{m}{l}, \tag{4}$$

where M is the quantity of messages per hour of the network, m is the summation of all messages generated by the network and l is its lifetime (in hours).

3.4.7 Message Log

After the end of each simulation, all messages were accounted and divided into four categories:

- **Listened Messages**: All messages **received** by a mote, regardless the addressee of them.
- **Rerouted Messages**: All messages that a mote had to **reroute** in order to reach the base station, in other words, all messages addressed to others motes that had to perform multiple hops towards the base station.

- **Overheard Messages**: Only the messages that a mote received but were **not** addressed to it, in other words, the messages that were **unnecessarily** received/listened by a mote.
- **Generated Messages**: All messages **created** and **sent** by a mote. These messages have the data that a mote wants to transmit to the base station and are created at each network cycle.

The occurrence of overheard messages is a problem that has multiple strategies to be avoided, like using different channels, synchronized sleep cycles or letting the radio module discarding messages not addressed to them [60], [100]–[103]. Xbee PRO, the radio module used as basis of the simulations, can discard messages not addressed to them without using the microcontroller but, as not all radio modules have this feature of discarding messages, the simulations were made with all messages being processed by the microcontroller of each mote, and just after that they were discarded or rerouted.

3.4.8 Implemented Protocols

There are two different protocols considered to make the simulations presented in this chapter: the first is the media access control protocol, which is a built-in software of the Xbee radio module [60] and second is the protocol for sensing the environment, transmitting, receiving and processing messages. The aforementioned protocols are described in the next subsections.

3.4.8.1 Protocol for Sensing, Transmitting, Receiving and Processing Messages

This protocol was implemented on all network motes and it is responsible for all basic tasks performed by them. All motes have same functions, parts and settings and the equal roles, and tasks on the network.

3.4.8.1.1 Network Cycle

Similar to [19], [20], this work employed simulations using energy consumption data acquired from both direct measurements [18], [19] and the datasheets of the electronic components. The simulations followed the rules of a time-driven network [104]–[108], therefore, all motes performed their tasks following a network cycle, similarly to [108]–[116]. All motes kept their microcontrollers, sensors and radio transceivers on the power-down/sleep states [60], [86]–[88] until the moment when they had to sense the environment and send their messages or to reroute messages of other motes. The algorithm presented in Algorithm 1 and its resulting flowchart presented in Fig. 22 shows the routine abide by a mote at each network cycle.

Algorithm 1 – Algorithm abide by a mote at each network cycle.

1. Activate microcontroller
2. Read sensor
3. Assembly message
4. Send message
5. Put transceiver, sensor and microcontroller in sleep state
6. Wait a network cycle

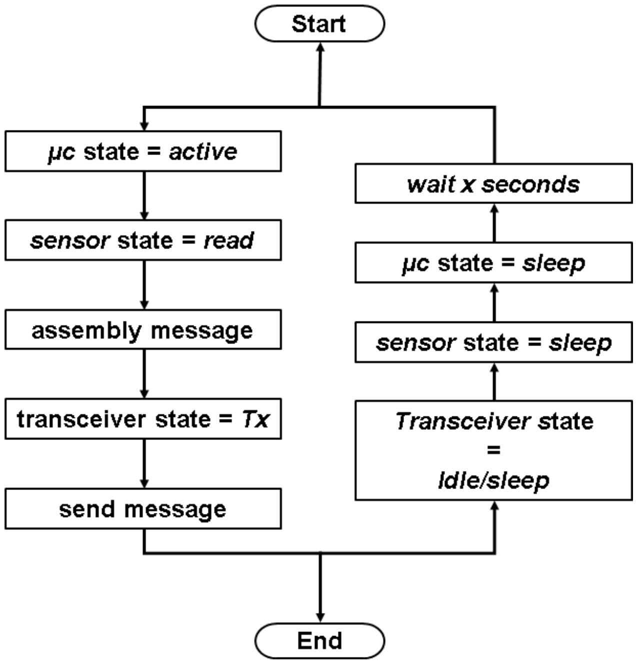

Fig. 22 – Algorithm abide by a mote at each network cycle.

Each network cycle *T* starts over after a settled period of time, it is when all motes generate a new message and send it, directly or with the help of other motes, to the base station. In this chapter, we used six different periods of time (also shown in Table IX): 1 second; 10 seconds; 60 seconds (one minute); 600 seconds (10 minutes); 3600 seconds (one hour) and 86400 seconds (one day).

Table IX – Network cycles used in this chapter.

Network Cycle/Generation Period (in seconds)	**Traffic Load (msg/s)**
86400	1.16E-05
3600	2.78E-04
600	0.00166
60	0.166
10	0.1
1	1

3.4.8.1.2 Receiving and Processing Messages

The situation of receiving messages was modeled after interruptions [117], [118], when the radio transceiver calls an interruption at the microcontroller, waking it, and passing the message to the microcontroller every time a new one is received. This routine is also referred as Wake-up Radio [119]–[123]. In our simulations, to keep the simulations closer to real situations, every message had to be processed, obligatorily, by the microcontroller of the receiver mote.

Xbee transceiver offers the option of filtering received packages which were not addressed to the receiver, but, on our simulations, the identification of the addressee was not made in the same layer [124], [125] of the receiver, thus, always having to be processed by the microcontroller of the receiver [126]. This promiscuous reception [127], which is common when using simpler radio modules [57], [59], was kept to perform more embracing simulations.

After receiving and processing a message, two actions can be performed by a mote (also shown in Fig. 23):

- **Rerouting** the message to a successor mote, **IF** the received message was addressed to the receiver.
- **Discarding** the message, **IF** the received message was **NOT** addressed to the receiver.

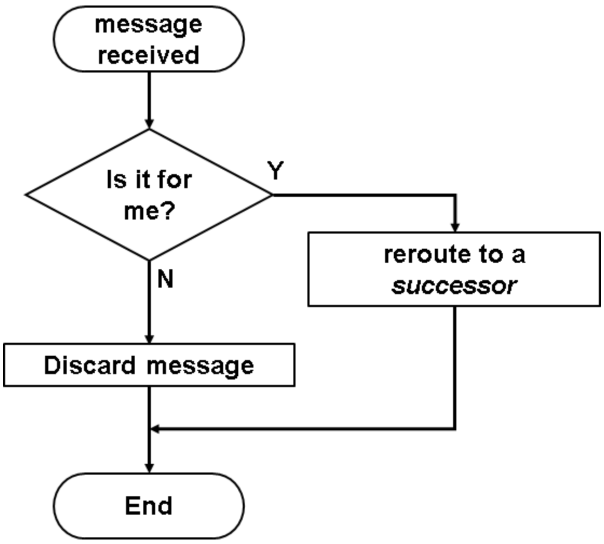

Fig. 23 – Algorithm abide by a mote after receiving a message.

3.4.8.2 Medium/Media Access Control

Xbee PRO radio module has built-in functions and protocols for Medium/Media Access Control (MAC) [124], [125], [128] in order to allow multiple modules to use the shared medium. The Carrier Sense Multiple Access with Collision Avoidance (CSMA/CA) [124], [125], [128]–[131], used in Xbee PRO modules, provides a reliable way to send and receive messages without major problems caused by collisions [132]–[135].

The additional reliability of RTS/CTS handshake (**R**equest **T**o **S**end and **C**lear **T**o **S**end) [89], [124], [125], [128] and the possible retransmissions of corrupted packages are also already implemented on Xbee modules, but, in order to keep the analysis focused just on energy consumption issues, neither RTS/CTS handshake nor collisions/retransmissions were considered on our simulations.

3.5 Simulations and Results

In this chapter we adopted the path loss exponent set to **3.5** [90]–[92]. All simulations used identical parts/motes and network topology, with **60** motes, organized in rows of 10, with the base station allocated in its center (pointed as the best topology in [136]), as shown in Fig. 24. As the motes used 540 Coulomb batteries, the maximum lifetime of the simulated motes (i.e., when the mote neither sends nor receives messages) would be 7142.85 hours.

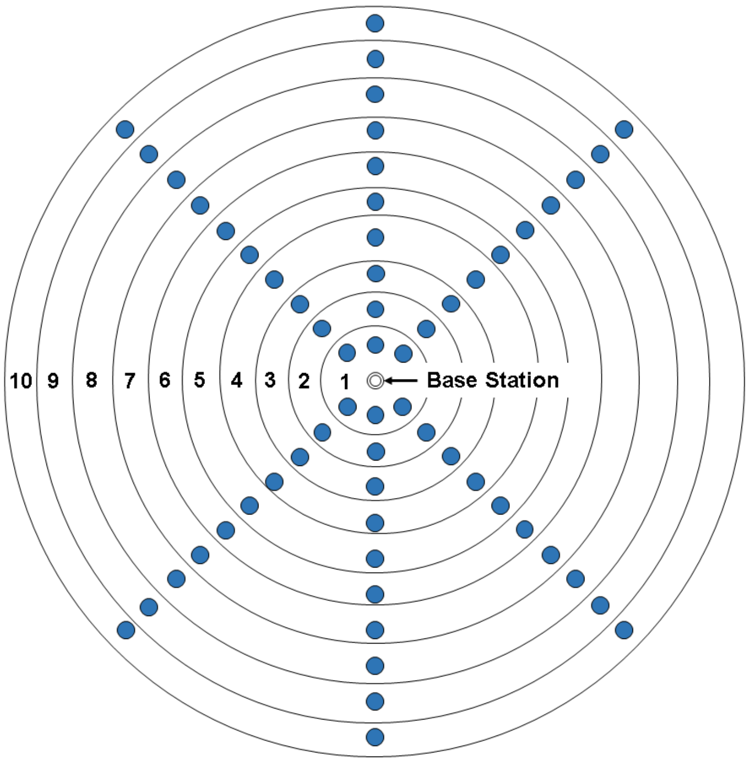

Fig. 24 – Network simulated in this chapter.

3.5.1 Results

For a better organization, the simulations results are presented and commented in the next subsections.

3.5.1.1 Primary and Secondary Consumption

As can be observed in Fig. 25 and Table X, the average primary consumption, which is the consumption for reading sensors, transmitting/receiving and processing messages, has a descendant share on the total consumption of the network when the message generation is lower. This trend was maintained with all power levels.

The average primary consumptions were:

- P_{tx} – 1 hop
    - 1 message per second: **99.58%**; 1 message at each 10 seconds: **95.83%**;

      1 message at each 60 seconds: **79.25%**; 1 message at each 600 seconds: **27.62%**;

      1 message at each 3600 seconds: **5.98%**; 1 message at each 86400 seconds: **0.26%**.

- $11.31P_{tx}$ – 2 hops
    - 1 message per second: **99.81%**; 1 message at each 10 seconds: **98.03%**;

      1 message at each 60 seconds: **89.20%**; 1 message at each 600 seconds: **45.22%**;

      1 message at each 3600 seconds: **12.09%**; 1 message at each 86400 seconds: **0.57%**.

- $46.76P_{tx}$ – 3 hops
    - 1 message per second: **99.91%**; 1 message at each 10 seconds: **99.09%**;

      1 message at each 60 seconds: **94.75%**; 1 message at each 600 seconds: **64.33%**;

      1 message at each 3600 seconds: **23.11%**; 1 message at each 86400 seconds: **1.23%**.

- $128P_{tx}$ – 4 hops
    - 1 message per second: **99.95%**; 1 message at each 10 seconds: **99.49%**;

      1 message at each 60 seconds: **97.04%**; 1 message at each 600 seconds: **76.63%**;

1 message at each 3600 seconds: **35.34%**; 1 message at each 86400 seconds: **2.22%**.

- $279.50P_{tx}$ – 5 hops
  - 1 message per second: **99.97%**; 1 message at each 10 seconds: **99.68%**;

    1 message at each 60 seconds: **98.15%**; 1 message at each 600 seconds: **84.16%**;

    1 message at each 3600 seconds: **46.96%**; 1 message at each 86400 seconds: **3.56%**.
- Maximum P_{tx} – directly to base station
  - 1 message per second: **99.99%**; 1 message at each 10 seconds: **99.91%**;

    1 message at each 60 seconds: **99.49%**; 1 message at each 600 seconds: **95.11%**;

    1 message at each 3600 seconds: **76.44%**; 1 message at each 86400 seconds: **11.89%**.

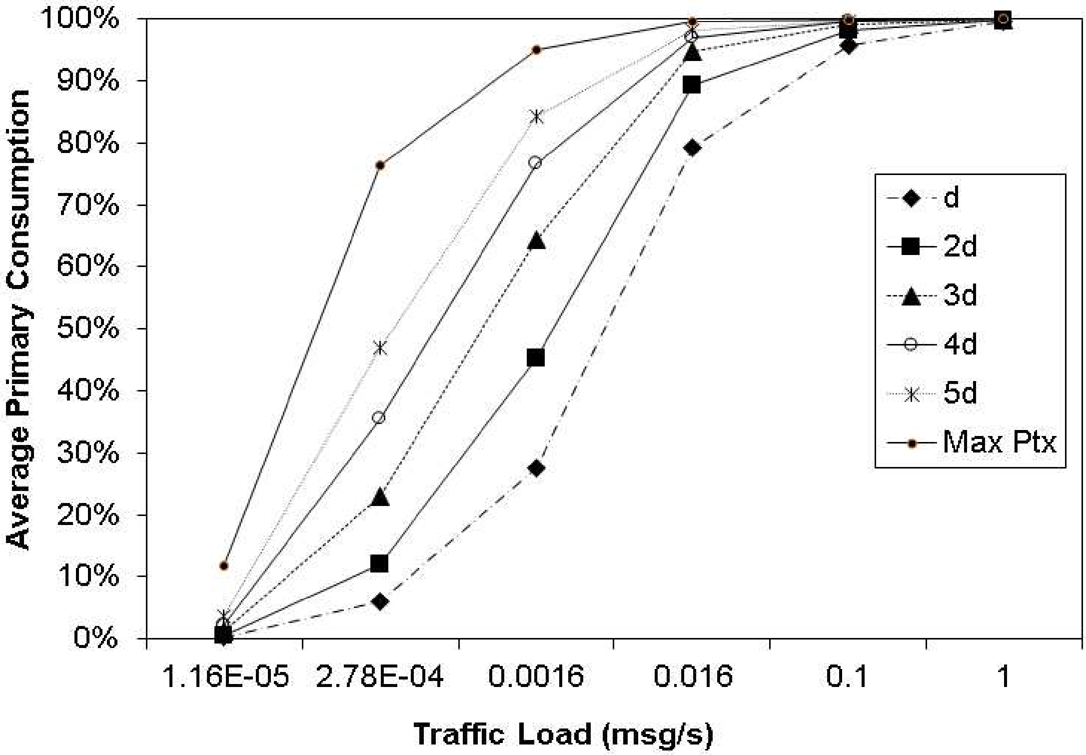

Fig. 25 – Average primary/secondary energy consumption of the simulated networks.

Table X – Average primary energy consumption of the simulated networks.

Traffic Load (msg/s)	Average Primary Consumption – $1d$	Average Primary Consumption – $2d$	Average Primary Consumption – $3d$	Average Primary Consumption – $4d$	Average Primary Consumption – $5d$	Average Primary Consumption – Max Power
1.16E-05	0.26%	0.57%	1.23%	2.22%	3.56%	11.89%
2.78E-04	5.98%	12.09%	23.11%	35.34%	46.96%	76.44%
0.00166	27.62%	45.22%	64.33%	76.63%	84.16%	95.11%
0.166	79.25%	89.20%	94.75%	97.04%	98.15%	99.49%
0.1	95.83%	98.03%	99.09%	99.49%	99.68%	99.91%
1	99.58%	99.81%	99.91%	99.95%	99.97%	99.99%

3.5.1.2 Lifetime

Fig. 26 and Table XI show that the lifetimes of the simulated networks with higher transmission power were shorter when compared to standard transmission power. Fig. 26 and

Table XI also show that the difference between the lifetime of the simulated networks decreased when the traffic load got lower. As the traffic load was being reduced, networks using higher transmission power almost attained the same lifetime of the standard transmission power network, with an exception on the network using the maximum transmission power.

The lifetimes of the simulations were:

- $P_{tx} - 1d$
  - 1 message per second: **18.65 hours**; 1 message at each 10 seconds: **182.28 hours**;

    1 message at each 60 seconds: **969.93 hours**; 1 message at each 600 seconds: **4364.89 hours**; 1 message at each 3600 seconds: **6457.86 hours**; 1 message at each 86400 seconds: **7111.35 hours**.
- $11.31P_{tx} - 2d$
  - 1 message per second: **7.76 hours**; 1 message at each 10 seconds: **76.89 hours**;

    1 message at each 60 seconds: **437.78 hours**; 1 message at each 600 seconds: **2821.47 hours**; 1 message at each 3600 seconds: **5690.14 hours**; 1 message at each 86400 seconds: **7067.55 hours**.
- $46.76P_{tx} - 3d$

  - 1 message per second: **3.57 hours**; 1 message at each 10 seconds: **35.62 hours**; 1 message at each 60 seconds: **208.51 hours**; 1 message at each 600 seconds: **1651.28 hours**; 1 message at each 3600 seconds: **4595.49 hours**; 1 message at each 86400 seconds: **6981.56 hours**.

- $128P_{tx} - 4d$
  - 1 message per second: **2.10 hours**; 1 message at each 10 seconds: **20.26 hours**; 1 message at each 60 seconds: **119.86 hours**; 1 message at each 600 seconds: **1041.33 hours**; 1 message at each 3600 seconds: **3614.01 hours**; 1 message at each 86400 seconds: **6863.59 hours**.

- $279.50P_{tx} - 5d$
  - 1 message per second: **0.94 hours**; 1 message at each 10 seconds: **9.45 hours**; 1 message at each 60 seconds: **56.35 hours**; 1 message at each 600 seconds: **526.16 hours**; 1 message at each 3600 seconds: **2307.02 hours**; 1 message at each 86400 seconds: **6568.67 hours**.

- Maximum P_{tx} – directly to base station
  - 1 message per second: **0.17 hours**; 1 message at each 10 seconds: **1.69 hours**; 1 message at each 60 seconds: **10.13 hours**; 1 message at each 600 seconds: **100.01 hours**; 1 message at each 3600 seconds: **561.01 hours**; 1 message at each 86400 seconds: **4797.62 hours**.

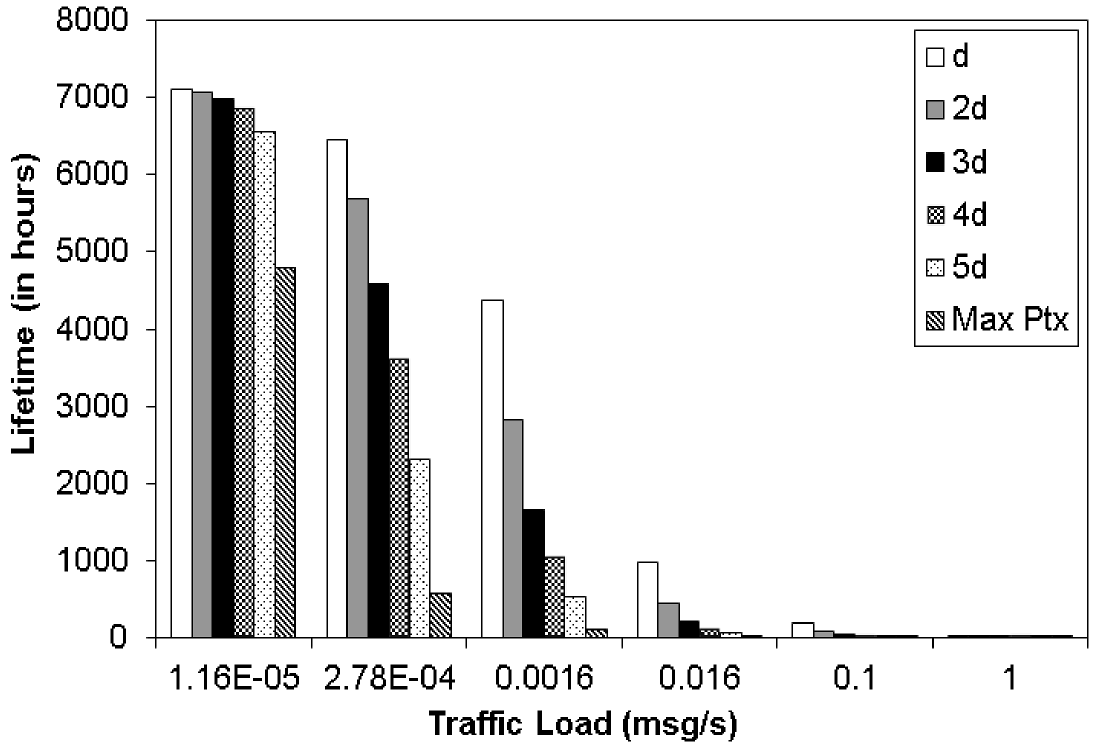

Fig. 26 – Lifetime of the simulated networks with different transmission powers.

Table XI – Lifetime of the simulated networks with different transmission powers.

Traffic Load (msg/s)	**Lifetime (in hours) – 1*d***	**Lifetime (in hours) – 2*d***	**Lifetime (in hours) – 3*d***	**Lifetime (in hours) – 4*d***	**Lifetime (in hours) – 5*d***	**Lifetime (in hours) – Max Power**
1.16E-05	7111.35	7067.55	6981.56	6863.59	6568.67	4797.62
2.78E-04	6457.86	5690.14	4595.49	3614.01	2307.02	561.01
0.00166	4364.89	2821.47	1651.28	1041.33	526.16	100.01
0.166	969.93	437.78	208.51	119.86	56.35	10.13
0.1	182.28	76.89	35.62	20.26	9.45	1.69
1	18.65	7.76	3.57	2.10	0.94	0.17

3.5.1.2.1 Lifetime Comparison

Fig. 27 and Table XII show the comparison between the lifetimes of the networks with higher transmission powers (2*d*, 3*d*, 4*d*, 5*d* and directly to the base station) and the standard transmission power (P_{tx} /1*d*). Both Fig. 27 and Table XII show that, again, both higher transmission powers and traffic loads compounded the difference between lifetimes.

The lifetime comparisons of the simulations were:

- $11.31P_{tx} - 2d$
    - 1 message per second: **-58.39%**; 1 message at each 10 seconds: **-57.82%**;

      1 message at each 60 seconds: **-54.86%**; 1 message at each 600 seconds: **-35.36%**;

      1 message at each 3600 seconds: **-11.89%**; 1 message at each 86400 seconds: **-0.62%**.
- $46.76P_{tx} - 3d$
    - 1 message per second: **-80.86%**; 1 message at each 10 seconds: **-80.46%**;

      1 message at each 60 seconds: **-78.50%**; 1 message at each 600 seconds: **-62.17%**;

      1 message at each 3600 seconds: **-28.84%**; 1 message at each 86400 seconds: **-1.83%**.
- $128P_{tx} - 4d$
    - 1 message per second: **-88.74%**; 1 message at each 10 seconds: **-88.89%**;

      1 message at each 60 seconds: **-87.64%**; 1 message at each 600 seconds: **-76.14%**;

      1 message at each 3600 seconds: **-44.04%**; 1 message at each 86400 seconds: **-3.48%**.
- $279.50P_{tx} - 5d$
    - 1 message per second: **-94.96%**; 1 message at each 10 seconds: **-94.82%**;

      1 message at each 60 seconds: **-94.19%**; 1 message at each 600 seconds: **-87.95%**;

      1 message at each 3600 seconds: **-64.28%**; 1 message at each 86400 seconds: **-7.63%**.
- Maximum P_{tx} – directly to base station
    - 1 message per second: **-99.09%**; 1 message at each 10 seconds: **-99.07%**;

      1 message at each 60 seconds: **-98.96%**; 1 message at each 600 seconds: **-97.71%**;

1 message at each 3600 seconds: **-91.31%**; 1 message at each 86400 seconds: **-32.54%**.

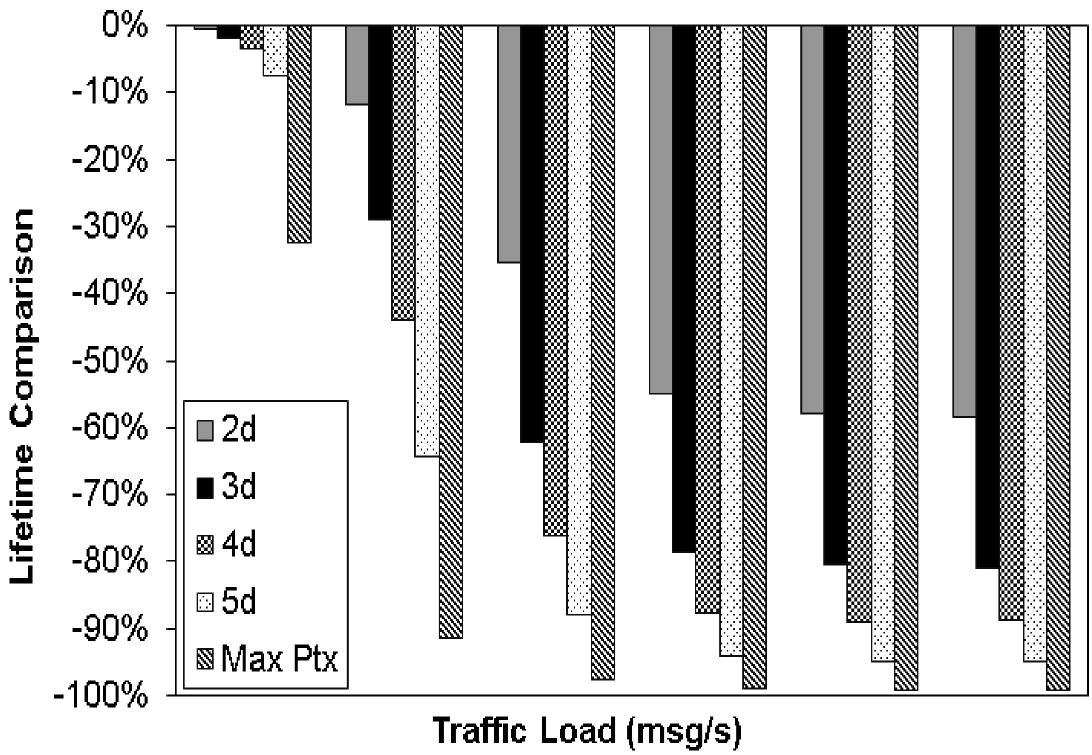

Fig. 27 – Lifetime comparison of the simulated networks.

Table XII – Lifetime comparison of the simulated networks.

Traffic Load (msg/s)	Lifetime Increase – 2*d*	Lifetime Increase – 3*d*	Lifetime Increase – 4*d*	Lifetime Increase – 5*d*	Lifetime Increase – Max Power
1.16E-05	-0.62%	-1.83%	-3.48%	-7.63%	-32.54%
2.78E-04	-11.89%	-28.84%	-44.04%	-64.28%	-91.31%
0.00166	-35.36%	-62.17%	-76.14%	-87.95%	-97.71%
0.166	-54.86%	-78.50%	-87.64%	-94.19%	-98.96%
0.1	-57.82%	-80.46%	-88.89%	-94.82%	-99.07%
1	-58.39%	-80.86%	-88.74%	-94.96%	-99.09%

3.5.1.3 Network Cost per Working Hour

Fig. 28 and Table XIII show the cost of each network per hour of their lifetime. As the network cost is the same on all simulated networks (US$2,670.60), the lifetime was the critical, making the cost of each network cheaper according to the traffic generation got lower. In this scenario, all network costs got lower when the traffic generation was reduced.

The network costs of the simulations were:

- $P_{tx} - 1d$
  - 1 message per second: **US$ 143.14**; 1 message at each 10 seconds: **US$14.65**;

    1 message at each 60 seconds: **US$2.75**; 1 message at each 600 seconds: **US$0.61**; 1 message at each 3600 seconds: **US$0.41**; 1 message at each 86400 seconds: **US$0.37**.
- $11.31P_{tx} - 2d$
  - 1 message per second: **US$343.95**; 1 message at each 10 seconds: **US$34.73**;

    1 message at each 60 seconds: **US$6.10**; 1 message at each 600 seconds: **US$0.94**; 1 message at each 3600 seconds: **US$0.47**; 1 message at each 86400 seconds: **US$0.37**.
- $46.76P_{tx} - 3d$
  - 1 message per second: **US$746.38**; 1 message at each 10 seconds: **US$74.97**;

    1 message at each 60 seconds: **US$12.80**; 1 message at each 600 seconds: **US$1.61**; 1 message at each 3600 seconds: **US$0.58**; 1 message at each 86400 seconds: **US$0.38**.
- $128P_{tx} - 4d$
  - 1 message per second:**US$1,314.48**; 1 message at each 10 seconds:**US$131.80**;

    1 message at each 60 seconds: **US$22.28**; 1 message at each 600 seconds: **US$2.56**; 1 message at each 3600 seconds: **US$0.73**; 1 message at each 86400 seconds: **US$0.39**.
- $279.50P_{tx} - 5d$
  - 1 message per second:**US$2,820.22**; 1 message at each 10 seconds:**US$282.42**;

    1 message at each 60 seconds: **US$47.40**; 1 message at each 600 seconds: **US$5.07**; 1 message at each 3600 seconds: **US$1.15**; 1 message at each 86400 seconds: **US$0.40**.

- Maximum P_{tx} – directly to base station

- 1 message per second:**US$15,760.91**; 1 message at each 10 seconds: **US$1,581.01**; 1 message at each 60 seconds: **US$263.53**; 1 message at each 600 seconds: **US$26.70**; 1 message at each 3600 seconds: **US$4.76**; 1 message at each 86400 seconds: **US$0.55**.

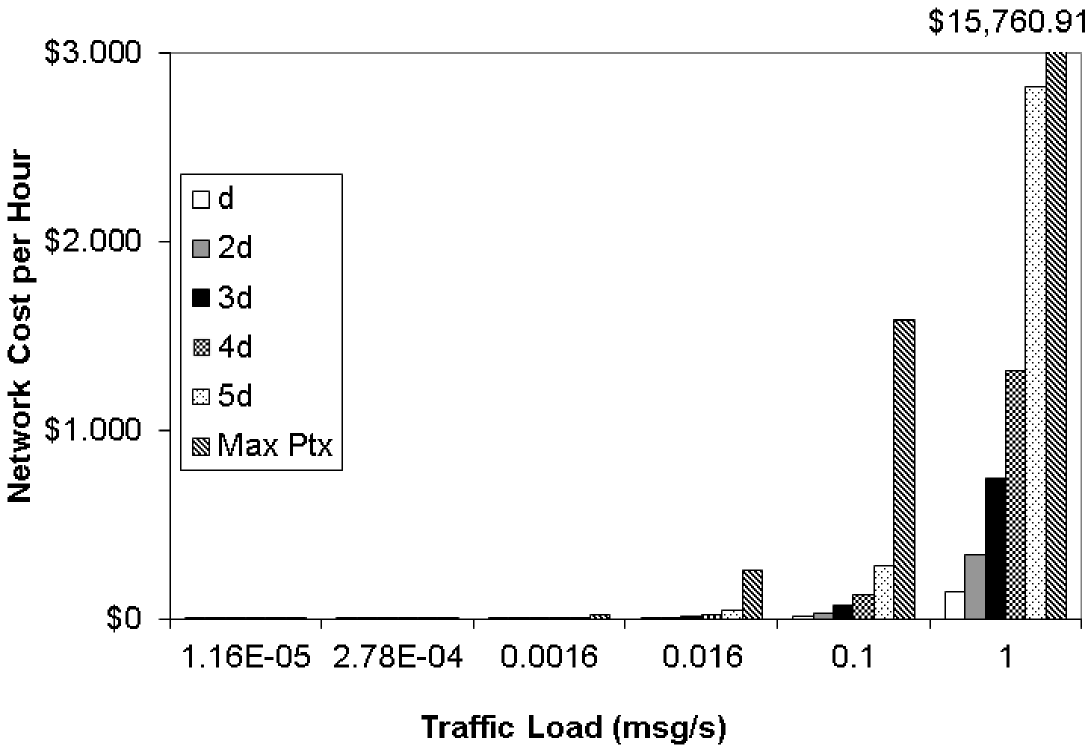

Fig. 28 – Network cost of the simulated networks.

Table XIII – Network cost of the simulated networks.

Traffic Load (msg/s)	Network Cost – 1*d*	Network Cost – 2*d*	Network Cost – 3*d*	Network Cost – 4*d*	Network Cost – 5*d*	Network Cost – Max Power
1.16E-05	US$0.37	US$0.37	US$0.38	US$0.39	US$0.40	US$0.55
2.78E-04	US$0.41	US$0.47	US$0.58	US$0.73	US$1.15	US$4.76
0.00166	US$0.61	US$0.94	US$1.61	US$2.56	US$5.07	US$26.70
0.166	US$2.75	US$6.10	US$12.80	US$22.28	US$47.40	US$263.53
0.1	US$14.65	US$34.73	US$74.97	US$131.80	US$282.42	US$1,581.01
1	US$143.14	US$343.95	US$746.38	US$1,314.48	US$2,820.22	US$15,760.91

3.5.1.3.1 Network Cost Comparison

Fig. 29 and Table XIV show the comparison between the with higher transmission powers (2d, 3d, 4d, 5d and directly to the base station) and the standard transmission power (P_{tx}/1d).

The network costs comparisons of the simulations were:

- $11.31P_{tx} - 2d$
  - 1 message per second: **0.00%**; 1 message at each 10 seconds: **14.63%**;

    1 message at each 60 seconds: **54.10%**; 1 message at each 600 seconds: **121.82%**;

    1 message at each 3600 seconds: **137.06%**; 1 message at each 86400 seconds: **140.29%**.
- $46.76P_{tx} - 3d$
  - 1 message per second: **2.70%**; 1 message at each 10 seconds: **41.46%**;

    1 message at each 60 seconds: **163.93%**; 1 message at each 600 seconds: **365.45%**; 1 message at each 3600 seconds: **411.74%**; 1 message at each 86400 seconds: **421.43%**.
- $128P_{tx} - 4d$
  - 1 message per second: **5.41%**; 1 message at each 10 seconds: **78.05%**;

    1 message at each 60 seconds: **319.67%**; 1 message at each 600 seconds: **710.18%**; 1 message at each 3600 seconds: **799.66%**; 1 message at each 86400 seconds: **818.32%**.
- $279.50P_{tx} - 5d$
  - 1 message per second: **8.11%**; 1 message at each 10 seconds: **180.49%**;

    1 message at each 60 seconds: **731.15%**; 1 message at each 600 seconds: **1,623.64%**; 1 message at each 3600 seconds: **1,827.78%**; 1 message at each 86400 seconds: **1,870.25%**.

- Maximum P_{tx} – directly to base station
    - 1 message per second: **48.65%**; 1 message at each 10 seconds: **1,060.98%**; 1 message at each 60 seconds: **4,277.05%**; 1 message at each 600 seconds: **9,482.91%**; 1 message at each 3600 seconds: **10,691.88%**; 1 message at each 86400 seconds: **10,910.84%**.

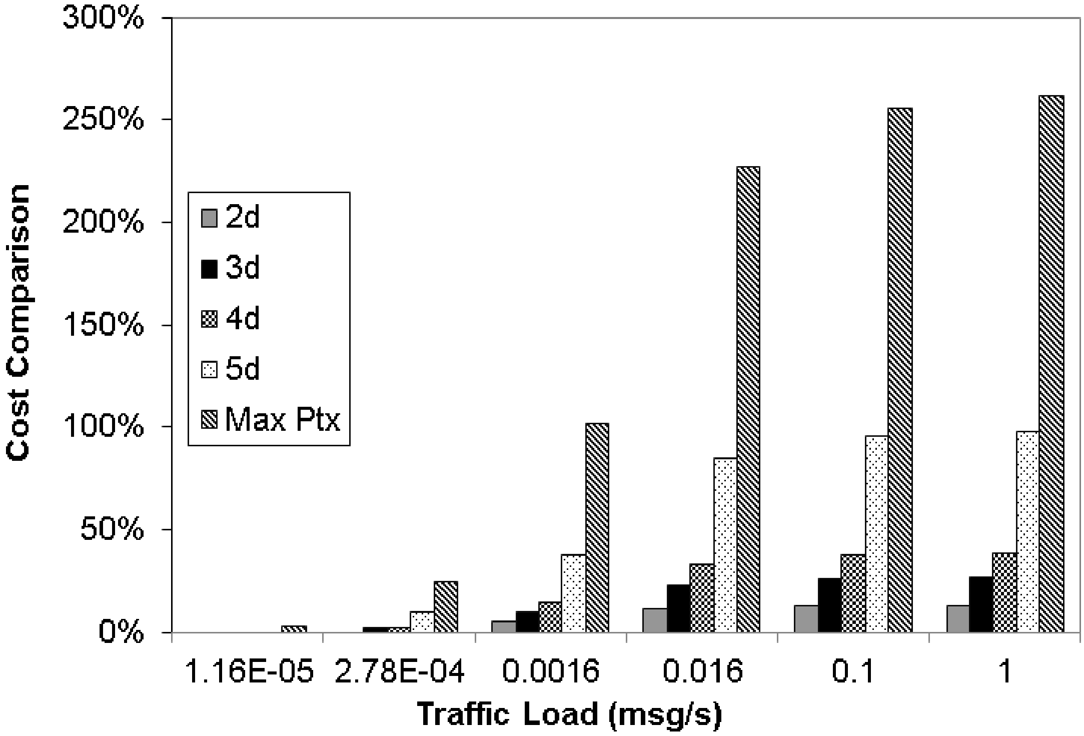

Fig. 29 – Network cost comparison of the simulated networks.

Table XIV – Network cost comparison of the simulated networks.

Traffic Load (msg/s)	Network Cost Comparison – 2*d*	Network Cost Comparison – 3*d*	Network Cost Comparison – 4*d*	Network Cost Comparison – 5*d*	Network Cost Comparison – Max Power
1.16E-05	0.00%	2.70%	5.41%	8.11%	48.65%
2.78E-04	14.63%	41.46%	78.05%	180.49%	1,060.98%
0.00166	54.10%	163.93%	319.67%	731.15%	4,277.05%
0.166	121.82%	365.45%	710.18%	1,623.64%	9,482.91%
0.1	137.06%	411.74%	799.66%	1,827.78%	10,691.88%
1	140.29%	421.43%	818.32%	1,870.25%	10,910.84%

3.5.1.4 Remaining Energy

Fig. 30 and Table XV show the average remaining energy of the simulated networks. The average remaining energy was higher when the traffic load was higher or when the transmission power was also higher, indicating a higher energy waste. When using maximum P_{tx}, the average remaining energy was considerably higher than the others in all cases.

The average remaining energy of the simulations was:

- $P_{tx} - 1d$
    - 1 message per second: **39.95%**; 1 message at each 10 seconds: **39.03%**;
      1 message at each 60 seconds: **34.61%**; 1 message at each 600 seconds: **15.57%**;
      1 message at each 3600 seconds: **3.84%**; 1 message at each 86400 seconds: **0.17%**.
- $11.31P_{tx} - 2d$
    - 1 message per second: **46.04%**; 1 message at each 10 seconds: **45.60%**;
      1 message at each 60 seconds: **43.26%**; 1 message at each 600 seconds: **27.88%**;
      1 message at each 3600 seconds: **9.37%**; 1 message at each 86400 seconds: **0.48%**.
- $46.76P_{tx} - 3d$
    - 1 message per second: **45.74%**; 1 message at each 10 seconds: **45.54%**;
      1 message at each 60 seconds: **44.43%**; 1 message at each 600 seconds: **35.19%**;
      1 message at each 3600 seconds: **16.32%**; 1 message at each 86400 seconds: **1.03%**.
- $128P_{tx} - 4d$
    - 1 message per second: **44.00%**; 1 message at each 10 seconds: **43.90%**;
      1 message at each 60 seconds: **43.28%**; 1 message at each 600 seconds: **37.60%**;
      1 message at each 3600 seconds: **21.74%**; 1 message at each 86400 seconds: **1.72%**.
- $279.50P_{tx} - 5d$
    - 1 message per second: **57.74%**; 1 message at each 10 seconds: **57.67%**;
      1 message at each 60 seconds: **57.30%**; 1 message at each 600 seconds: **53.49%**;
      1 message at each 3600 seconds: **39.10%**; 1 message at each 86400 seconds: **4.64%**.

- Maximum P_{tx} – directly to base station
    - 1 message per second: **72.33%**; 1 message at each 10 seconds: **72.35%**; 1 message at each 60 seconds: **72.23%**; 1 message at each 600 seconds: **71.34%**; 1 message at each 3600 seconds: **66.65%**; 1 message at each 86400 seconds: **23.76%**.

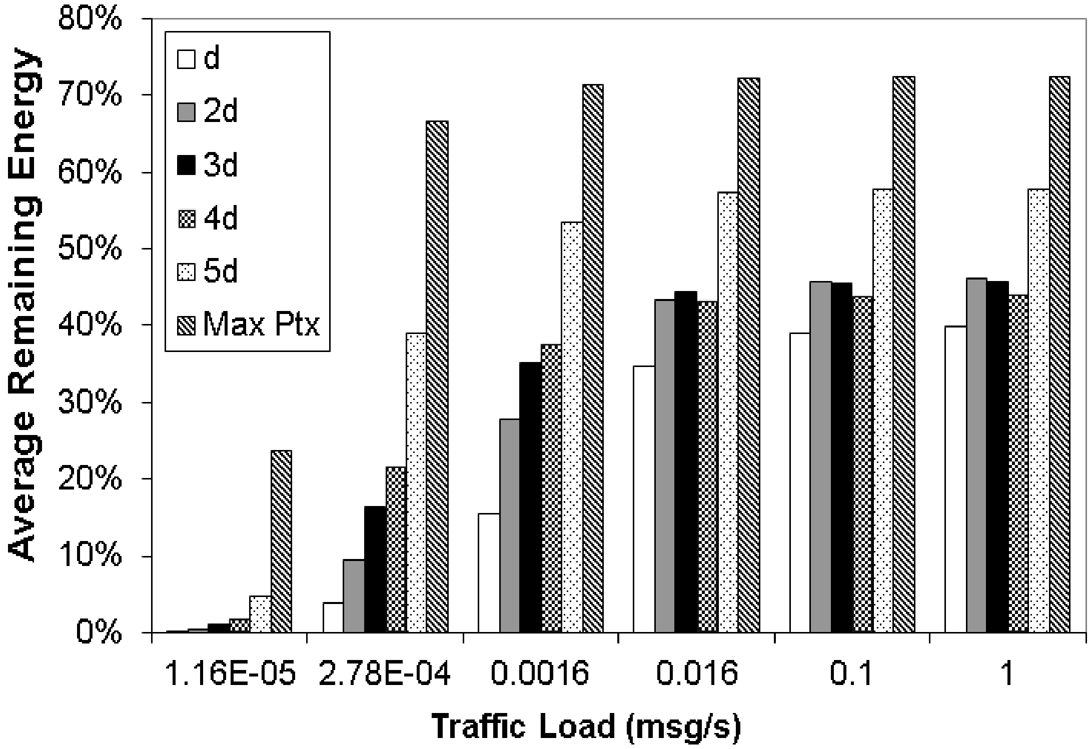

Fig. 30 – Average remaining energy of each simulated network.

Table XV – Average remaining energy of each simulated network.

Traffic Load (msg/s)	Average Remaining Energy – 1*d*	Average Remaining Energy – 2*d*	Average Remaining Energy – 3*d*	Average Remaining Energy – 4*d*	Average Remaining Energy – 5*d*	Average Remaining Energy – Max Power
1.16E-05	0.17%	0.48%	1.03%	1.72%	4.64%	23.76%
2.78E-04	3.84%	9.37%	16.32%	21.74%	39.10%	66.65%
0.00166	15.57%	27.88%	35.19%	37.60%	53.49%	71.34%
0.166	34.61%	43.26%	44.43%	43.28%	57.30%	72.23%
0.1	39.03%	45.60%	45.54%	43.90%	57.67%	72.35%
1	39.95%	46.04%	45.74%	44.00%	57.74%	72.33%

3.5.1.4.1 Average Remaining Energy per Layer – P_{tx} (1*d*)

Fig. 31 and Table XVI show the average remaining energy per layer of the networks using P_{tx} (1 hop). In these simulations, layer 2 was the first to have its energy depleted.

The average remaining energy per layer of the simulations in this scenario were:

- Layer 1
    - 1 message per second: **5.47%**; 1 message at each 10 seconds: **5.34%**;

      1 message at each 60 seconds: **4.74%**; 1 message at each 600 seconds: **2.13%**;

      1 message at each 3600 seconds: **0.52%**; 1 message at each 86400 seconds: **0.02%**.
- Layer 2
    - 1 message per second: **depleted**; 1 message at each 10 seconds: **depleted**;

      1 message at each 60 seconds: **depleted**; 1 message at each 600 seconds: **depleted**; 1 message at each 3600 seconds: **depleted**; 1 message at each 86400 seconds: **depleted**.
- Layer 3
    - 1 message per second: **10.94%**; 1 message at each 10 seconds: **10.69%**;

      1 message at each 60 seconds: **9.48%**; 1 message at each 600 seconds: **4.26%**;

      1 message at each 3600 seconds: **1.05%**; 1 message at each 86400 seconds: **0.04%**.
- Layer 4
    - 1 message per second: **21.89%**; 1 message at each 10 seconds: **21.38%**;

      1 message at each 60 seconds: **18.96%**; 1 message at each 600 seconds: **8.53%**;

      1 message at each 3600 seconds: **2.10%**; 1 message at each 86400 seconds: **0.09%**.
- Layer 5
    - 1 message per second: **32.83%**; 1 message at each 10 seconds: **32.08%**;

      1 message at each 60 seconds: **28.45%**; 1 message at each 600 seconds: **12.80%**;

      1 message at each 3600 seconds: **3.15%**; 1 message at each 86400 seconds: **0.14%**.

- Layer 6
  - 1 message per second: **43.78%**; 1 message at each 10 seconds: **42.77%**; 1 message at each 60 seconds: **37.93%**; 1 message at each 600 seconds: **17.07%**; 1 message at each 3600 seconds: **4.21%**; 1 message at each 86400 seconds: **0.19%**.
- Layer 7
  - 1 message per second: **54.72%**; 1 message at each 10 seconds: **53.47%**; 1 message at each 60 seconds: **47.41%**; 1 message at each 600 seconds: **21.33%**; 1 message at each 3600 seconds: **5.26%**; 1 message at each 86400 seconds: **0.24%**.
- Layer 8
  - 1 message per second: **65.67%**; 1 message at each 10 seconds: **64.16%**; 1 message at each 60 seconds: **56.90%**; 1 message at each 600 seconds: **25.60%**; 1 message at each 3600 seconds: **6.31%**; 1 message at each 86400 seconds: **0.29%**.
- Layer 9
  - 1 message per second: **76.61%**; 1 message at each 10 seconds: **74.85%**; 1 message at each 60 seconds: **66.38%**; 1 message at each 600 seconds: **29.87%**; 1 message at each 3600 seconds: **7.36%**; 1 message at each 86400 seconds: **0.33%**.
- Layer 10
  - 1 message per second: **87.56%**; 1 message at each 10 seconds: **85.55%**; 1 message at each 60 seconds: **75.87%**; 1 message at each 600 seconds: **34.14%**; 1 message at each 3600 seconds: **8.41%**; 1 message at each 86400 seconds: **0.38%**.

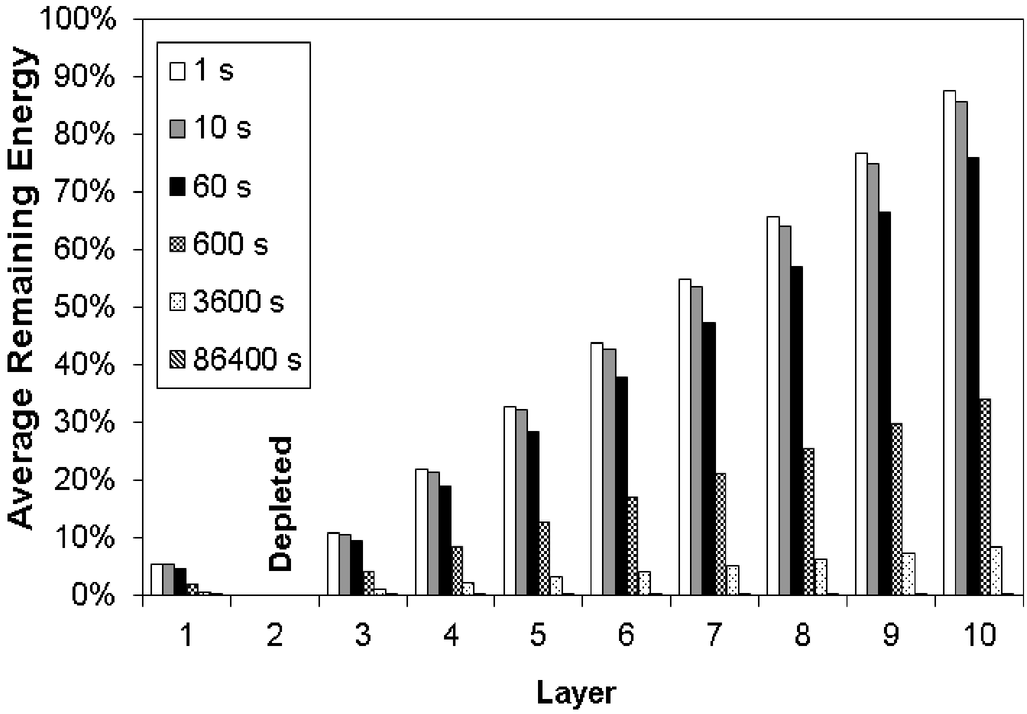

Fig. 31 – Average remaining energy of each layer in this scenario (1 hop).

Table XVI – Average remaining energy of each layer in this scenario (1 hop).

Traffic Load (msg/s)	Layer 1	Layer 2	Layer 3	Layer 4	Layer 5	Layer 6	Layer 7	Layer 8	Layer 9	Layer 10
1.16E-05	0.02%	Depleted	0.04%	0.09%	0.14%	0.19%	0.24%	0.29%	0.33%	0.38%
2.78E-04	0.52%	Depleted	1.05%	2.10%	3.15%	4.21%	5.26%	6.31%	7.36%	8.41%
0.00166	2.13%	Depleted	4.26%	8.53%	12.80%	17.07%	21.33%	25.60%	29.87%	34.14%
0.166	4.74%	Depleted	9.48%	18.96%	28.45%	37.93%	47.41%	56.90%	66.38%	75.87%
0.1	5.34%	Depleted	10.69%	21.38%	32.08%	42.77%	53.47%	64.16%	74.85%	85.55%
1	5.47%	Depleted	10.94%	21.89%	32.83%	43.78%	54.72%	65.67%	76.61%	87.56%

3.5.1.4.2 Average Remaining Energy per Layer – 11.31P_{tx} (2*d*)

Fig. 32 and Table XVII show the average remaining energy per layer of the networks using 11.31P_{tx} (2d). In these simulations, layer 2 was the first to have its energy depleted.

The average remaining energy per layer of the simulations in this scenario were:

- Layer 1
  - 1 message per second: **77.22%**; 1 message at each 10 seconds: **76.47%**;

    1 message at each 60 seconds: **72.57%**; 1 message at each 600 seconds: **46.77%**;

    1 message at each 3600 seconds: **15.72%**; 1 message at each 86400 seconds: **0.81%**.

- Layer 2

    - 1 message per second: **depleted**; 1 message at each 10 seconds: **depleted**;

      1 message at each 60 seconds: **depleted**; 1 message at each 600 seconds: **depleted**; 1 message at each 3600 seconds: **depleted**; 1 message at each 86400 seconds: **depleted**.

- Layer 3
    - 1 message per second: **18.88%**; 1 message at each 10 seconds: **18.69%**;

      1 message at each 60 seconds: **17.74%**; 1 message at each 600 seconds: **11.43%**;

      1 message at each 3600 seconds: **3.84%**; 1 message at each 86400 seconds: **0.20%**.

- Layer 4
    - 1 message per second: **17.01%**; 1 message at each 10 seconds: **16.85%**;

      1 message at each 60 seconds: **15.99%**; 1 message at each 600 seconds: **10.30%**;

      1 message at each 3600 seconds: **3.46%**; 1 message at each 86400 seconds: **0.17%**.

- Layer 5
    - 1 message per second: **36.52%**; 1 message at each 10 seconds: **36.16%**;

      1 message at each 60 seconds: **34.31%**; 1 message at each 600 seconds: **22.12%**;

      1 message at each 3600 seconds: **7.43%**; 1 message at each 86400 seconds: **0.38%**.

- Layer 6
    - 1 message per second: **37.76%**; 1 message at each 10 seconds: **37.39%**;

      1 message at each 60 seconds: **35.48%**; 1 message at each 600 seconds: **22.87%**;

      1 message at each 3600 seconds: **7.68%**; 1 message at each 86400 seconds: **0.39%**.

- Layer 7
    - 1 message per second: **57.26%**; 1 message at each 10 seconds: **56.71%**;

      1 message at each 60 seconds: **53.81%**; 1 message at each 600 seconds: **34.68%**;

      1 message at each 3600 seconds: **11.66%**; 1 message at each 86400 seconds: **0.60%**.

- Layer 8
    - 1 message per second: **58.51%**; 1 message at each 10 seconds: **57.94%**; 1 message at each 60 seconds: **54.98%**; 1 message at each 600 seconds: **35.43%**; 1 message at each 3600 seconds: **11.91%**; 1 message at each 86400 seconds: **0.61%**.
- Layer 9
    - 1 message per second: **78.01%**; 1 message at each 10 seconds: **77.25%**; 1 message at each 60 seconds: **73.31%**; 1 message at each 600 seconds: **47.24%**; 1 message at each 3600 seconds: **15.88%**; 1 message at each 86400 seconds: **0.82%**.
- Layer 10
    - 1 message per second: **79.25%**; 1 message at each 10 seconds: **78.48%**; 1 message at each 60 seconds: **74.47%**; 1 message at each 600 seconds: **48.00%**; 1 message at each 3600 seconds: **16.13%**; 1 message at each 86400 seconds: **0.83%**.

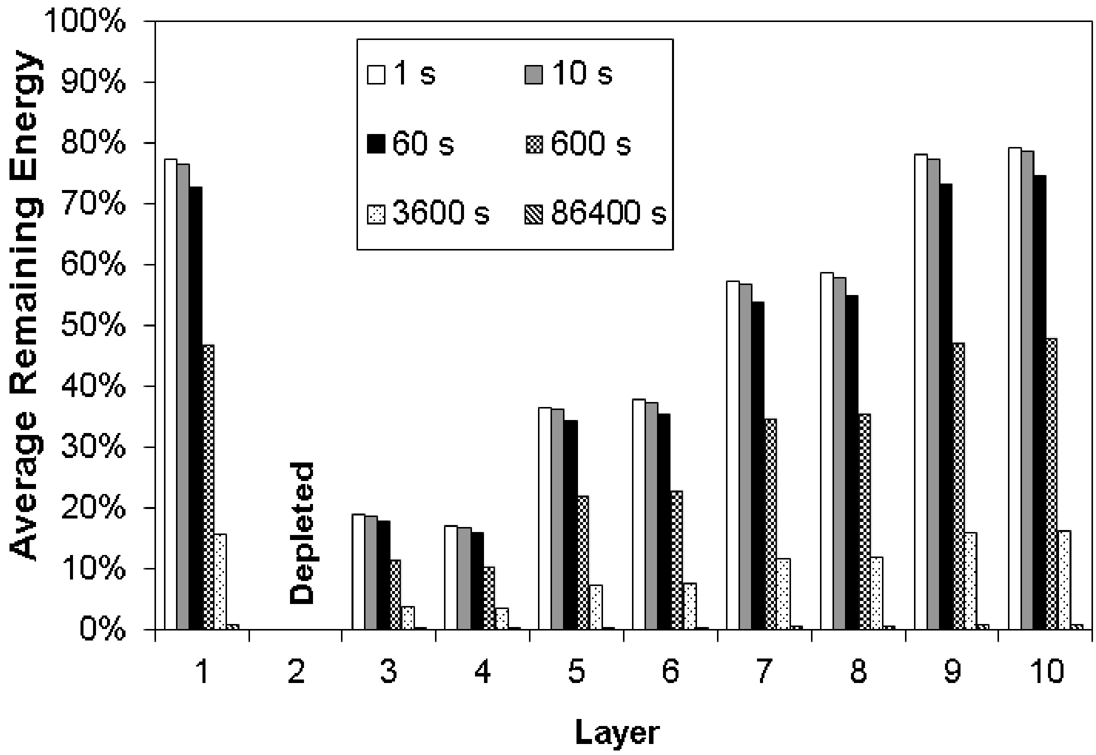

Fig. 32 – Average remaining energy of each layer in this scenario (2 hops).

Table XVII – Average remaining energy of each layer in this scenario (2 hops).

Traffic Load (msg/s)	Layer 1	Layer 2	Layer 3	Layer 4	Layer 5	Layer 6	Layer 7	Layer 8	Layer 9	Layer 10
1.16E-05	0.81%	Depleted	0.20%	0.17%	0.38%	0.39%	0.60%	0.61%	0.82%	0.83%
2.78E-04	15.72%	Depleted	3.84%	3.46%	7.43%	7.68%	11.66%	11.91%	15.88%	16.13%
0.00166	46.77%	Depleted	11.43%	10.30%	22.12%	22.87%	34.68%	35.43%	47.24%	48.00%
0.166	72.57%	Depleted	17.74%	15.99%	34.31%	35.48%	53.81%	54.98%	73.31%	74.47%
0.1	76.47%	Depleted	18.69%	16.85%	36.16%	37.39%	56.71%	57.94%	77.25%	78.48%
1	77.22%	Depleted	18.88%	17.01%	36.52%	37.76%	57.26%	58.51%	78.01%	79.25%

3.5.1.4.3 Average Remaining Energy per Layer – 46.76P_{tx} (3*d*)

Fig. 33 and Table XVIII show the average remaining energy per layer of the networks using $46.76P_{tx}$ (3*d*). In these simulations, layer 4 was the first to have its energy depleted.

The average remaining energy per layer of the simulations was:

- Layer 1
  - 1 message per second: **91.03%**; 1 message at each 10 seconds: **90.62%**;

    1 message at each 60 seconds: **88.41%**; 1 message at each 600 seconds: **70.02%**;

    1 message at each 3600 seconds: **32.48%**; 1 message at each 86400 seconds: **2.05%**.
- Layer 2
  - 1 message per second: **71.03%**; 1 message at each 10 seconds: **70.71%**;

    1 message at each 60 seconds: **68.99%**; 1 message at each 600 seconds: **54.63%**;

    1 message at each 3600 seconds: **25.34%**; 1 message at each 86400 seconds: **1.60%**.
- Layer 3
  - 1 message per second: **0.57%**; 1 message at each 10 seconds: **0.56%**;

    1 message at each 60 seconds: **0.54%**; 1 message at each 600 seconds: **0.44%**;

    1 message at each 3600 seconds: **0.20%**; 1 message at each 86400 seconds: **0.01%**.
- Layer 4
  - 1 message per second: **depleted**; 1 message at each 10 seconds: **depleted**;

1 message at each 60 seconds: **depleted**; 1 message at each 600 seconds: **depleted**; 1 message at each 3600 seconds: **depleted**; 1 message at each 86400 seconds: **depleted**.

- Layer 5
  - 1 message per second: **32.37%**; 1 message at each 10 seconds: **32.22%**; 1 message at each 60 seconds: **31.44%**; 1 message at each 600 seconds: **24.90%**; 1 message at each 3600 seconds: **11.55%**; 1 message at each 86400 seconds: **0.73%**.
- Layer 6
  - 1 message per second: **32.09%**; 1 message at each 10 seconds: **31.94%**; 1 message at each 60 seconds: **31.16%**; 1 message at each 600 seconds: **24.68%**; 1 message at each 3600 seconds: **11.45%**; 1 message at each 86400 seconds: **0.72%**.
- Layer 7
  - 1 message per second: **32.66%**; 1 message at each 10 seconds: **32.51%**; 1 message at each 60 seconds: **31.72%**; 1 message at each 600 seconds: **25.12%**; 1 message at each 3600 seconds: **11.65%**; 1 message at each 86400 seconds: **0.73%**.
- Layer 8
  - 1 message per second: **65.33%**; 1 message at each 10 seconds: **65.03%**; 1 message at each 60 seconds: **63.45%**; 1 message at each 600 seconds: **50.25%**; 1 message at each 3600 seconds: **23.31%**; 1 message at each 86400 seconds: **1.47%**.
- Layer 9
  - 1 message per second: **65.90%**; 1 message at each 10 seconds: **65.60%**; 1 message at each 60 seconds: **64.00%**; 1 message at each 600 seconds: **50.69%**; 1 message at each 3600 seconds: **23.51%**; 1 message at each 86400 seconds: **1.48%**.
- Layer 10
  - 1 message per second: **66.47%**; 1 message at each 10 seconds: **66.17%**;

1 message at each 60 seconds: **64.56%**; 1 message at each 600 seconds: **51.13%**;

1 message at each 3600 seconds: **23.71%**; 1 message at each 86400 seconds: **1.50%**.

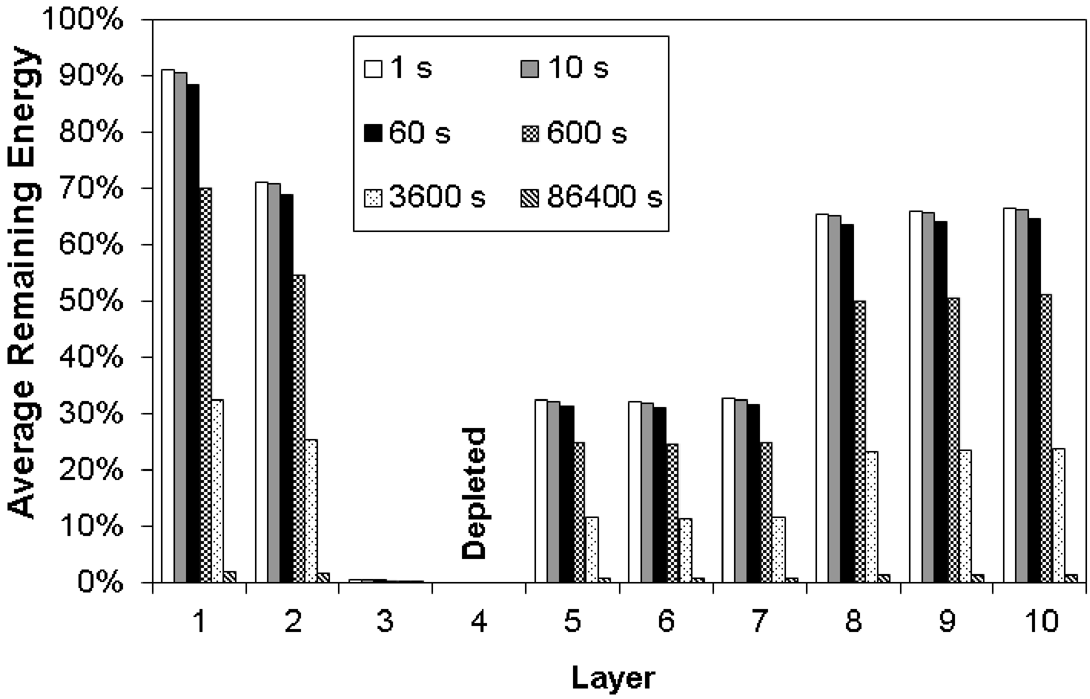

Fig. 33 – Average remaining energy of each layer in this scenario (3*d*).

Table XVIII – Average remaining energy of each layer in this scenario (3*d*).

Traffic Load (msg/s)	Layer 1	Layer 2	Layer 3	Layer 4	Layer 5	Layer 6	Layer 7	Layer 8	Layer 9	Layer 10
1.16E-05	2.05%	1.60%	0.01%	Depleted	0.73%	0.72%	0.73%	1.47%	1.48%	1.50%
2.78E-04	32.48%	25.34%	0.20%	Depleted	11.55%	11.45%	11.65%	23.31%	23.51%	23.71%
0.00166	70.02%	54.63%	0.44%	Depleted	24.90%	24.68%	25.12%	50.25%	50.69%	51.13%
0.166	88.41%	68.99%	0.54%	Depleted	31.44%	31.16%	31.72%	63.45%	64.00%	64.56%
0.1	90.62%	70.71%	0.56%	Depleted	32.22%	31.94%	32.51%	65.03%	65.60%	66.17%
1	91.03%	71.03%	0.57%	Depleted	32.37%	32.09%	32.66%	65.33%	65.90%	66.47%

3.5.1.4.4 Average Remaining Energy per Layer – 128P_{tx} (4*d*)

Fig. 34 and Table XIX show the average remaining energy per layer of the networks using 128P_{tx} (4*d*). In these simulations, layer 4 was the first to have its energy depleted.

The average remaining energy per layer of the simulations was:

- Layer 1
  - 1 message per second: **95.77%**; 1 message at each 10 seconds: **95.53%**;

    1 message at each 60 seconds: **94.19%**; 1 message at each 600 seconds: **81.83%**;

    1 message at each 3600 seconds: **47.32%**; 1 message at each 86400 seconds: **3.74%**.

- Layer 2
  - 1 message per second: **83.71%**; 1 message at each 10 seconds: **83.50%**; 1 message at each 60 seconds: **82.33%**; 1 message at each 600 seconds: **71.53%**; 1 message at each 3600 seconds: **41.36%**; 1 message at each 86400 seconds: **3.27%**.
- Layer 3
  - 1 message per second: **61.76%**; 1 message at each 10 seconds: **61.61%**; 1 message at each 60 seconds: **60.74%**; 1 message at each 600 seconds: **52.77%**; 1 message at each 3600 seconds: **30.52%**; 1 message at each 86400 seconds: **2.41%**.
- Layer 4
  - 1 message per second: **depleted**; 1 message at each 10 seconds: **depleted**; 1 message at each 60 seconds: **depleted**; 1 message at each 600 seconds: **depleted**; 1 message at each 3600 seconds: **depleted**; 1 message at each 86400 seconds: **depleted**.
- Layer 5
  - 1 message per second: **0.31%**; 1 message at each 10 seconds: **0.31%**; 1 message at each 60 seconds: **0.31%**; 1 message at each 600 seconds: **0.27%**; 1 message at each 3600 seconds: **0.14%**; 1 message at each 86400 seconds: **0.01%**.
- Layer 6
  - 1 message per second: **0.15%**; 1 message at each 10 seconds: **0.15%**; 1 message at each 60 seconds: **0.15%**; 1 message at each 600 seconds: **0.13%**; 1 message at each 3600 seconds: **0.06%**; 1 message at each 86400 seconds: **0.00%**.
- Layer 7
  - 1 message per second: **49.34%**; 1 message at each 10 seconds: **49.22%**;

1 message at each 60 seconds: **48.53%**; 1 message at each 600 seconds: **42.16%**; 1 message at each 3600 seconds: **24.38%**; 1 message at each 86400 seconds: **1.92%**.

- Layer 8
    - 1 message per second: **49.34%**; 1 message at each 10 seconds: **49.22%**; 1 message at each 60 seconds: **48.53%**; 1 message at each 600 seconds: **42.16%**; 1 message at each 3600 seconds: **24.38%**; 1 message at each 86400 seconds: **1.92%**.
- Layer 9
    - 1 message per second: **49.66%**; 1 message at each 10 seconds: **49.54%**; 1 message at each 60 seconds: **48.85%**; 1 message at each 600 seconds: **42.44%**; 1 message at each 3600 seconds: **24.54%**; 1 message at each 86400 seconds: **1.94%**.
- Layer 10
    - 1 message per second: **49.99%**; 1 message at each 10 seconds: **49.86%**; 1 message at each 60 seconds: **49.17%**; 1 message at each 600 seconds: **42.72%**; 1 message at each 3600 seconds: **24.70%**; 1 message at each 86400 seconds: **1.95%**.

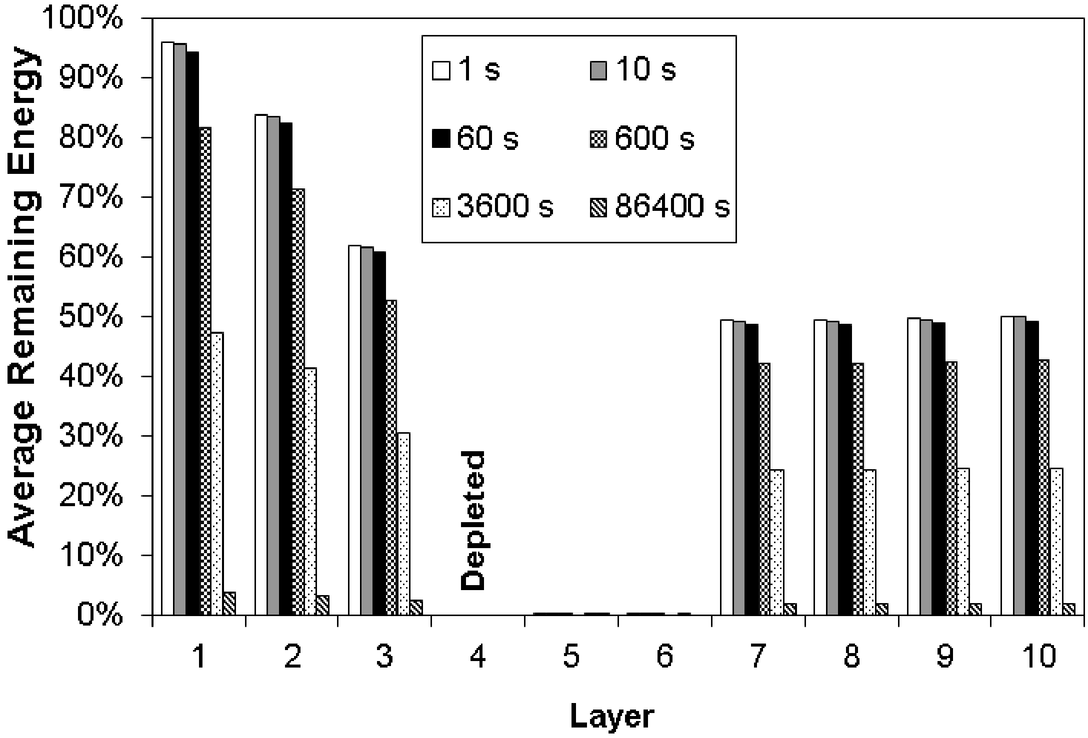

Fig. 34 – Average remaining energy of each layer in this scenario (4*d*).

Table XIX – Average remaining energy of each layer in this scenario (4*d*).

Traffic Load (msg/s)	Layer 1	Layer 2	Layer 3	Layer 4	Layer 5	Layer 6	Layer 7	Layer 8	Layer 9	Layer 10
1.16E-05	3.74%	3.27%	2.41%	Depleted	0.01%	0.00%	1.92%	1.92%	1.94%	1.95%
2.78E-04	47.32%	41.36%	30.52%	Depleted	0.14%	0.06%	24.38%	24.38%	24.54%	24.70%
0.00166	81.83%	71.53%	52.77%	Depleted	0.27%	0.13%	42.16%	42.16%	42.44%	42.72%
0.166	94.19%	82.33%	60.74%	Depleted	0.31%	0.15%	48.53%	48.53%	48.85%	49.17%
0.1	95.53%	83.50%	61.61%	Depleted	0.31%	0.15%	49.22%	49.22%	49.54%	49.86%
1	95.77%	83.71%	61.76%	Depleted	0.31%	0.15%	49.34%	49.34%	49.66%	49.99%

3.5.1.4.5 Average Remaining Energy per Layer – 279.50P_{tx} (5*d*)

Fig. 35 and Table XX show the average remaining energy per layer of the networks using 279.50P_{tx} (5*d*). In these simulations, layer 5 was the first to have its energy depleted.

The average remaining energy per layer of the simulations was:

- Layer 1
    - 1 message per second: **98.43%**; 1 message at each 10 seconds: **98.31%**;

      1 message at each 60 seconds: **97.67%**; 1 message at each 600 seconds: **91.19%**;

      1 message at each 3600 seconds: **66.65%**; 1 message at each 86400 seconds: **7.91%**.

- Layer 2
  - 1 message per second: **94.71%**; 1 message at each 10 seconds: **94.60%**; 1 message at each 60 seconds: **93.97%**; 1 message at each 600 seconds: **87.74%**; 1 message at each 3600 seconds: **64.13%**; 1 message at each 86400 seconds: **7.61%**.
- Layer 3
  - 1 message per second: **82.25%**; 1 message at each 10 seconds: **82.15%**; 1 message at each 60 seconds: **81.62%**; 1 message at each 600 seconds: **76.20%**; 1 message at each 3600 seconds: **55.69%**; 1 message at each 86400 seconds: **6.61%**.
- Layer 4
  - 1 message per second: **53.46%**; 1 message at each 10 seconds: **53.39%**; 1 message at each 60 seconds: **53.05%**; 1 message at each 600 seconds: **49.53%**; 1 message at each 3600 seconds: **36.20%**; 1 message at each 86400 seconds: **4.29%**.
- Layer 5
  - 1 message per second: **depleted**; 1 message at each 10 seconds: **depleted**; 1 message at each 60 seconds: **depleted**; 1 message at each 600 seconds: **depleted**; 1 message at each 3600 seconds: **depleted**; 1 message at each 86400 seconds: **depleted**.
- Layer 6
  - 1 message per second: **49.53%**; 1 message at each 10 seconds: **49.47%**; 1 message at each 60 seconds: **49.15%**; 1 message at each 600 seconds: **45.89%**; 1 message at each 3600 seconds: **33.54%**; 1 message at each 86400 seconds: **3.98%**.
- Layer 7
  - 1 message per second: **49.68%**; 1 message at each 10 seconds: **49.62%**; 1 message at each 60 seconds: **49.30%**; 1 message at each 600 seconds: **46.03%**;

1 message at each 3600 seconds: **33.64%**; 1 message at each 86400 seconds: **3.99%**.

- Layer 8
    - 1 message per second: **49.68%**; 1 message at each 10 seconds: **49.62%**;

      1 message at each 60 seconds: **49.30%**; 1 message at each 600 seconds: **46.03%**;

      1 message at each 3600 seconds: **33.64%**; 1 message at each 86400 seconds: **3.99%**.
- Layer 9
    - 1 message per second: **49.83%**; 1 message at each 10 seconds: **49.77%**;

      1 message at each 60 seconds: **49.45%**; 1 message at each 600 seconds: **46.17%**;

      1 message at each 3600 seconds: **33.74%**; 1 message at each 86400 seconds: **4.00%**.
- Layer 10
    - 1 message per second: **49.83%**; 1 message at each 10 seconds: **49.77%**;

      1 message at each 60 seconds: **49.45%**; 1 message at each 600 seconds: **46.17%**;

      1 message at each 3600 seconds: **33.74%**; 1 message at each 86400 seconds: **4.00%**.

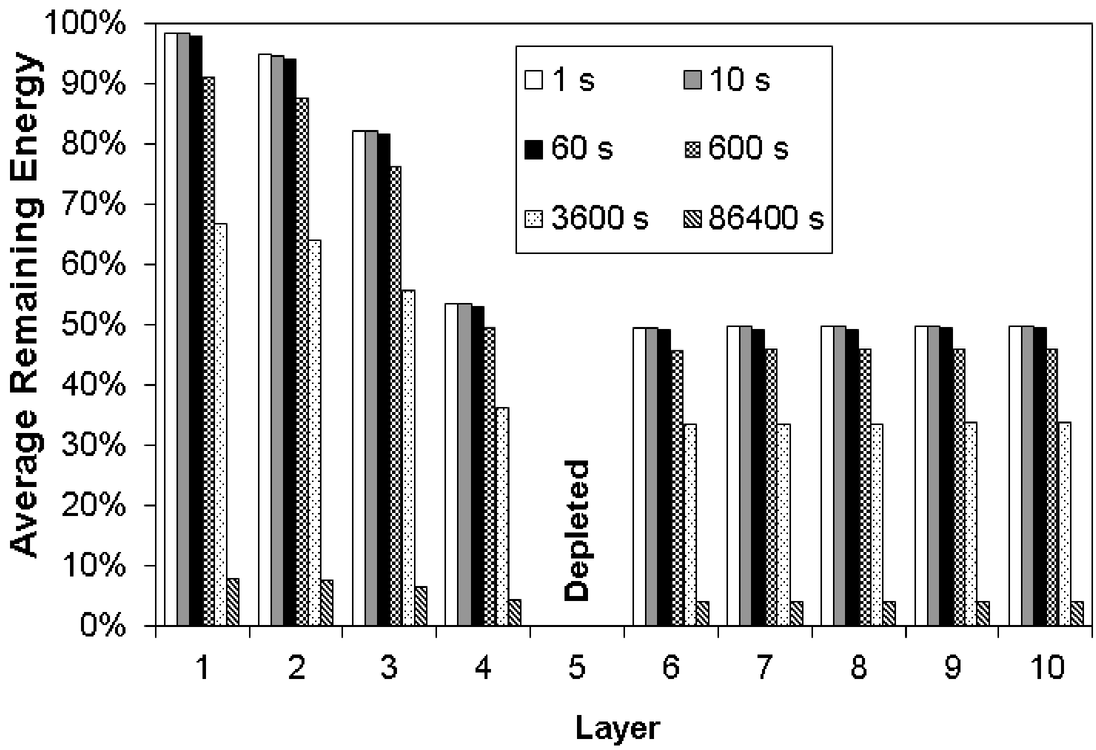

Fig. 35 – Average remaining energy of each layer in this scenario (5*d*).

Table XX – Average remaining energy of each layer in this scenario (5*d*).

Traffic Load (msg/s)	Layer 1	Layer 2	Layer 3	Layer 4	Layer 5	Layer 6	Layer 7	Layer 8	Layer 9	Layer 10
1.16E-05	7.91%	7.61%	6.61%	4.29%	Depleted	3.98%	3.99%	3.99%	4.00%	4.00%
2.78E-04	66.65%	64.13%	55.69%	36.20%	Depleted	33.54%	33.64%	33.64%	33.74%	33.74%
0.00166	91.19%	87.74%	76.20%	49.53%	Depleted	45.89%	46.03%	46.03%	46.17%	46.17%
0.166	97.67%	93.97%	81.62%	53.05%	Depleted	49.15%	49.30%	49.30%	49.45%	49.45%
0.1	98.31%	94.60%	82.15%	53.39%	Depleted	49.47%	49.62%	49.62%	49.77%	49.77%
1	98.43%	94.71%	82.25%	53.46%	Depleted	49.53%	49.68%	49.68%	49.83%	49.83%

3.5.1.4.6 Average Remaining Energy per Layer – Maximum P_{tx} (directly to base station)

Fig. 36 and Table XXI show the average remaining energy per layer of the networks using Maximum P_{tx} (directly to base station). In these simulations, layer 10 was the first to have its energy depleted.

The average remaining energy per layer of the simulations was:

- Layer 1
  - 1 message per second: **99.79%**; 1 message at each 10 seconds: **99.77%**; 1 message at each 60 seconds: **99.65%**; 1 message at each 600 seconds: **98.39%**; 1 message at each 3600 seconds: **91.95%**; 1 message at each 86400 seconds: **32.76%**.
- Layer 2
  - 1 message per second: **99.46%**; 1 message at each 10 seconds: **99.44%**; 1 message at each 60 seconds: **99.32%**; 1 message at each 600 seconds: **98.07%**; 1 message at each 3600 seconds: **91.65%**; 1 message at each 86400 seconds: **32.65%**.

- Layer 3
  - 1 message per second: **98.35%**; 1 message at each 10 seconds: **98.33%**; 1 message at each 60 seconds: **98.22%**; 1 message at each 600 seconds: **96.98%**; 1 message at each 3600 seconds: **90.63%**; 1 message at each 86400 seconds: **32.29%**.
- Layer 4
  - 1 message per second: **95.78%**; 1 message at each 10 seconds: **95.77%**; 1 message at each 60 seconds: **95.65%**; 1 message at each 600 seconds: **94.45%**; 1 message at each 3600 seconds: **88.26%**; 1 message at each 86400 seconds: **31.45%**.
- Layer 5
  - 1 message per second: **91.01%**; 1 message at each 10 seconds: **91.00%**; 1 message at each 60 seconds: **90.88%**; 1 message at each 600 seconds: **89.74%**; 1 message at each 3600 seconds: **83.86%**; 1 message at each 86400 seconds: **29.88%**.

- Layer 6
  - 1 message per second: **83.11%**; 1 message at each 10 seconds: **83.12%**; 1 message at each 60 seconds: **83.00%**; 1 message at each 600 seconds: **81.96%**; 1 message at each 3600 seconds: **76.59%**; 1 message at each 86400 seconds: **27.29%**.
- Layer 7
  - 1 message per second: **71.16%**; 1 message at each 10 seconds: **71.18%**; 1 message at each 60 seconds: **71.06%**; 1 message at each 600 seconds: **70.18%**; 1 message at each 3600 seconds: **65.57%**; 1 message at each 86400 seconds: **23.37%**.
- Layer 8
  - 1 message per second: **54.06%**; 1 message at each 10 seconds: **54.11%**;

1 message at each 60 seconds: **53.99%**; 1 message at each 600 seconds: **53.34%**; 1 message at each 3600 seconds: **49.82%**; 1 message at each 86400 seconds: **17.77%**.

- Layer 9
  - 1 message per second: **30.70%**; 1 message at each 10 seconds: **30.79%**; 1 message at each 60 seconds: **30.67%**; 1 message at each 600 seconds: **30.32%**; 1 message at each 3600 seconds: **28.30%**; 1 message at each 86400 seconds: **10.11%**.
- Layer 10
  - 1 message per second: **depleted**; 1 message at each 10 seconds: **depleted**; 1 message at each 60 seconds: **depleted**; 1 message at each 600 seconds: **depleted**; 1 message at each 3600 seconds: **depleted**; 1 message at each 86400 seconds: **depleted**.

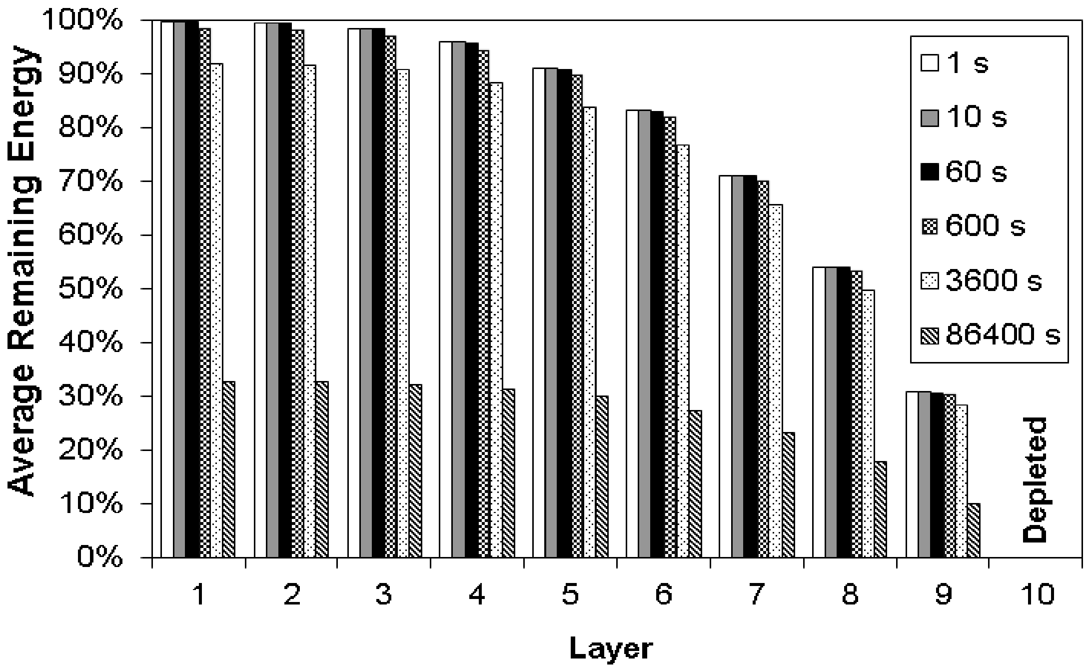

Fig. 36 – Average remaining energy of each layer in this scenario (directly to base station).

Table XXI – Average remaining energy of each layer in this scenario (directly to base station).

Traffic Load (msg/s)	Layer 1	Layer 2	Layer 3	Layer 4	Layer 5	Layer 6	Layer 7	Layer 8	Layer 9	Layer 10
1.16E-05	32.76%	32.65%	32.29%	31.45%	29.88%	27.29%	23.37%	17.77%	10.11%	Depleted
2.78E-04	91.95%	91.65%	90.63%	88.26%	83.86%	76.59%	65.57%	49.82%	28.30%	Depleted
0.00166	98.39%	98.07%	96.98%	94.45%	89.74%	81.96%	70.18%	53.34%	30.32%	Depleted

Traffic Load (msg/s)	Layer 1	Layer 2	Layer 3	Layer 4	Layer 5	Layer 6	Layer 7	Layer 8	Layer 9	Layer 10
0.166	99.65%	99.32%	98.22%	95.65%	90.88%	83.00%	71.06%	53.99%	30.67%	Depleted
0.1	99.77%	99.44%	98.33%	95.77%	91.00%	83.12%	71.18%	54.11%	30.79%	Depleted
1	99.79%	99.46%	98.35%	95.78%	91.01%	83.11%	71.16%	54.06%	30.70%	Depleted

3.5.1.5 Energy Consumption Profile

The transmission power increase also had an impact on the energy consumption profile [33], [137] of the simulated networks. As can be observed in Fig. 37, Fig. 38, Fig. 39, Fig. 40, Fig. 41, Fig. 42 and in

Table XXII, due to the transmission power increase, the energy spent on transmissions (labeled as Radio-TX) increased, following the transmission power increase. The energy consumption profile of secondary states is shown in Fig. 43 and Table XXIII.

The energy consumption profile of the simulations in this scenario was:

- $P_{tx} - 1d$
  - Radio transmission:**32.03%**; Radio reception: **24.70%**; Microcontroller: **41.18%**; Sensor: **2.08%**.
- $11.31P_{tx} - 2d$
  - Radio transmission:**77.47%**; Radio reception: **11.18%**; Microcontroller: **10.38%**; Sensor: **0.96%**.
- $46.76P_{tx} - 3d$
  - Radio transmission: **91.11%**; Radio reception: **4.96%**; Microcontroller: **3.48%**; Sensor: **0.44%**.
- $128P_{tx} - 4d$
  - Radio transmission: **95.57%**; Radio reception: **2.61%**; Microcontroller: **1.56%**; Sensor: **0.24%**.
- $279.50P_{tx} - 5d$
  - Radio transmission: **97.52%**; Radio reception: **1.52%**; Microcontroller: **0.80%**; Sensor: **0.15%**.
- Maximum P_{tx} – directly to base station

- Radio transmission: **99.47%**; Radio reception: **0.34%**; Microcontroller: **0.14%**; Sensor: **0.04%**.

- Secondary States
  - Radio: **47.61%**; Radio reception: **23.81%**; Microcontroller: **28.58%**.

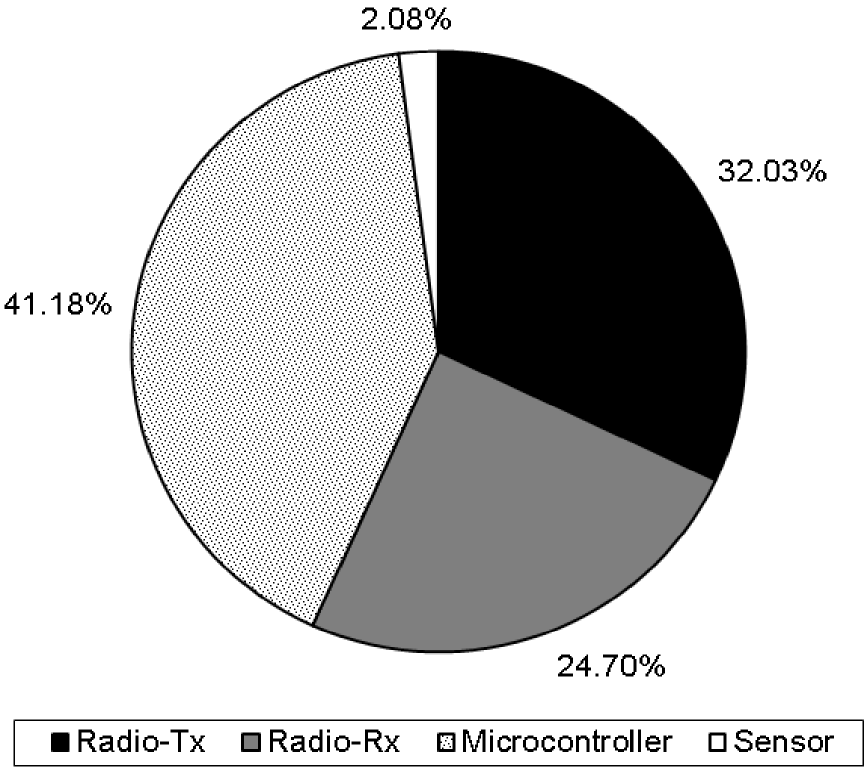

Fig. 37 – Energy consumption profile when using P_{tx} (1 Hop).

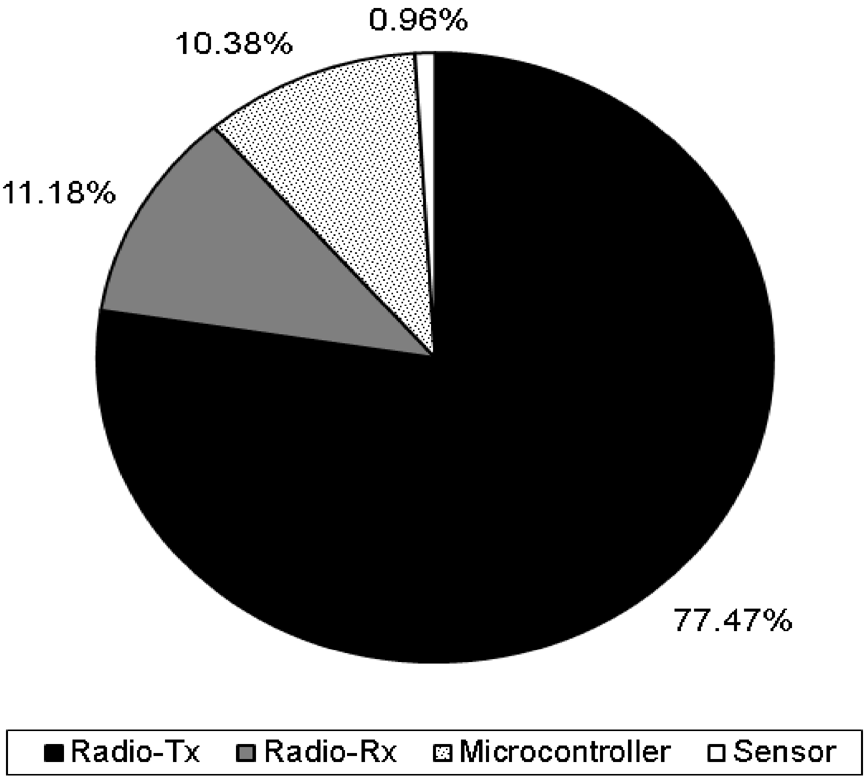

Fig. 38 – Energy consumption profile when using $11.31P_{tx}$ ($2d$).

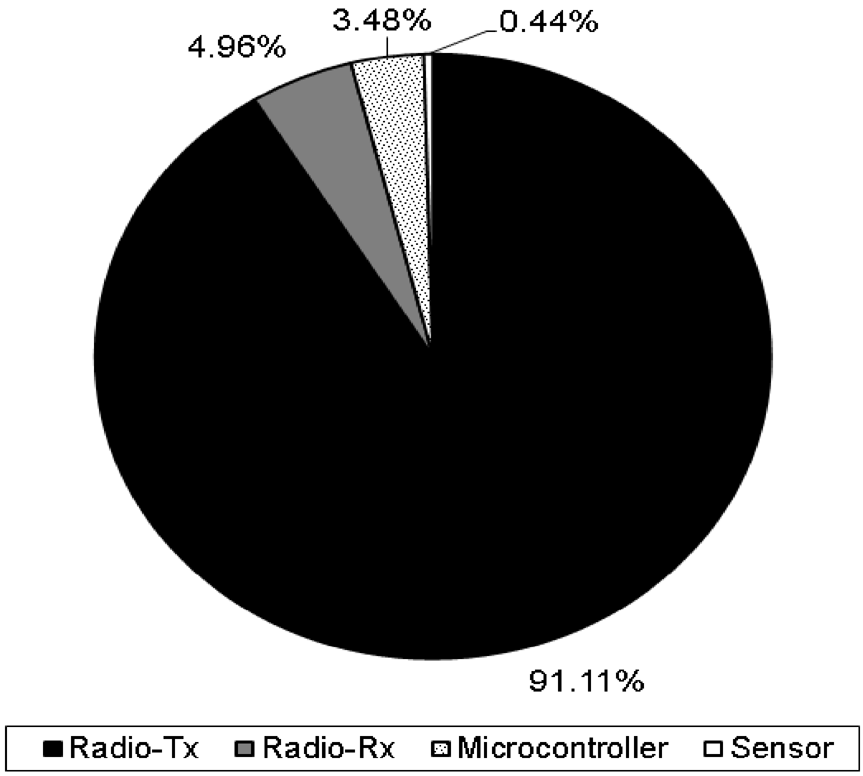

Fig. 39 – Energy consumption profile when using $46.76P_{tx}$ ($3d$).

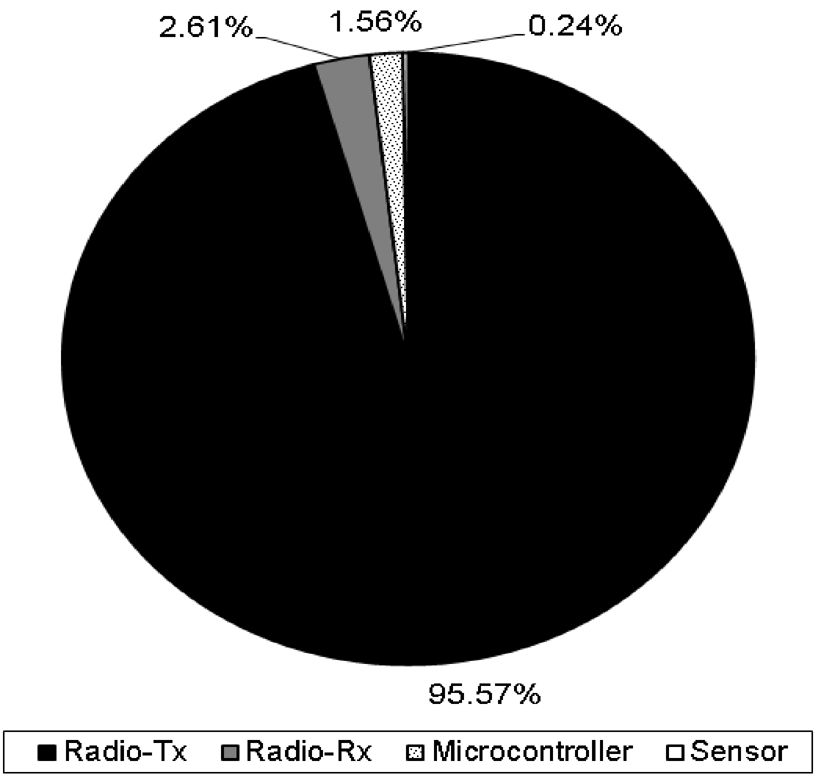

Fig. 40 – Energy consumption profile when using128P_{tx} (4d).

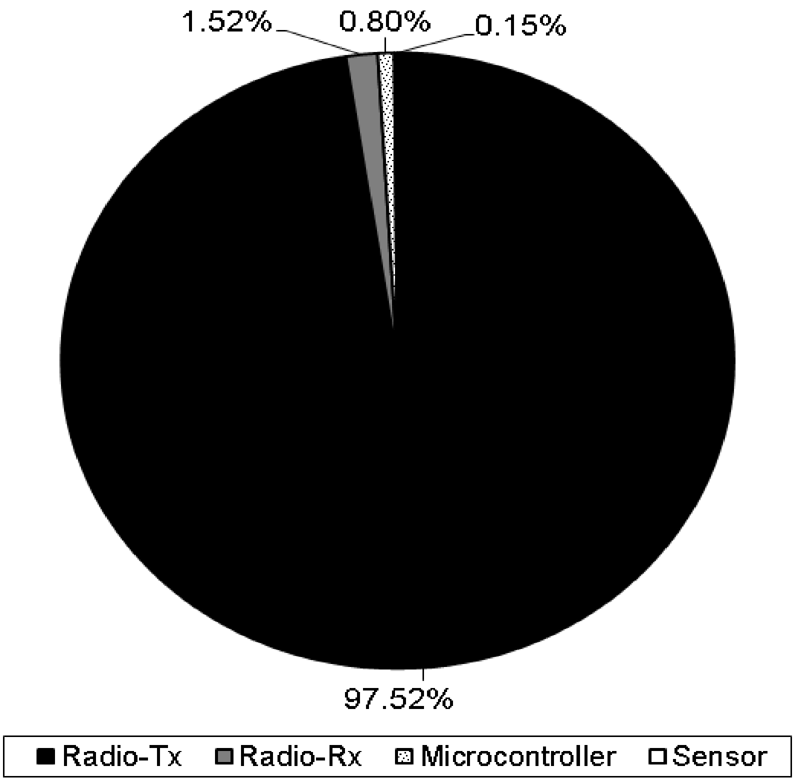

Fig. 41 – Energy consumption profile when using 279.5P_{tx} (5d).

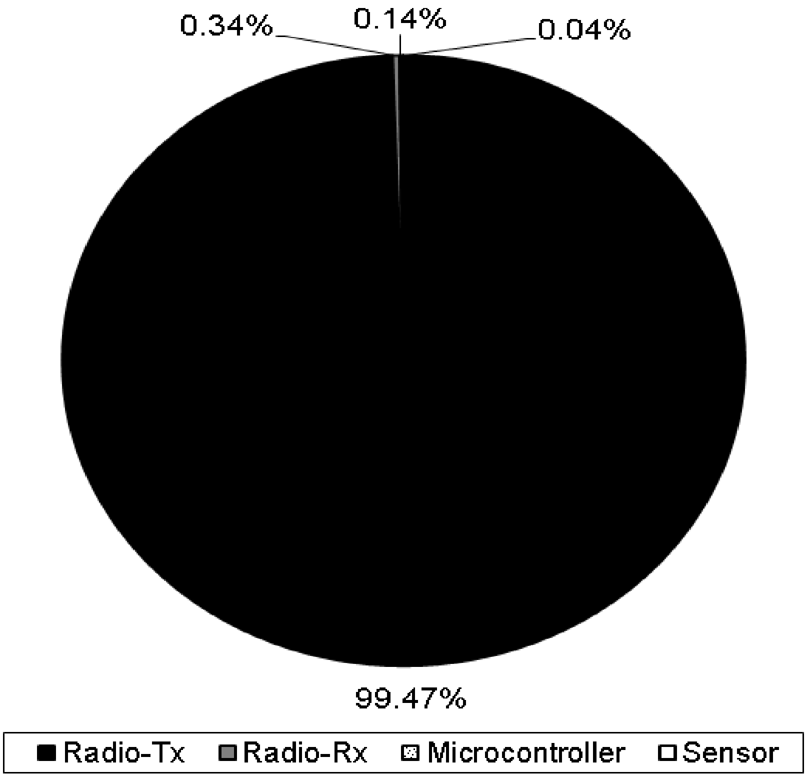

Fig. 42 – Energy consumption profile when using maximum P_{tx} (directly to base station).

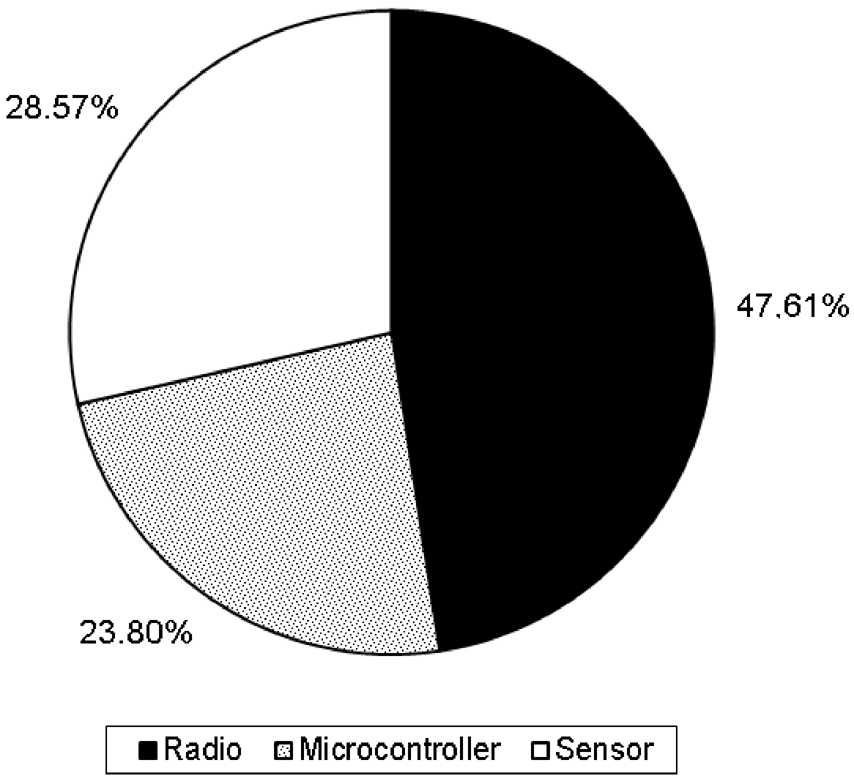

Fig. 43 – Energy consumption profile of the secondary consumption (in all scenarios).

Table XXII – Energy consumption of each part/functionality.

Transmission Power	**Reach**	**Radio-Tx**	**Radio-Rx**	**Microcontroller**	**Sensor**
P_{tx}	1d	32.03%	24.70%	41.18%	2.08%

$11.31P_{tx}$	$2d$	77.47%	11.18%	10.38%	0.96%
$46.76P_{tx}$	$3d$	91.11%	4.96%	3.48%	0.44%
$128P_{tx}$	$4d$	95.57%	2.61%	1.56%	0.24%
$279.50P_{tx}$	$5d$	97.52%	1.52%	0.80%	0.15%
Max P_{tx}	Base Station	99.47%	0.34%	0.14%	0.04%

Table XXIII – Energy consumption profile of Secondary States in all scenarios.

Radio	Microcontroller	Sensor
47.61%	23.81%	28.58%

3.5.2 Message Log

Fig. 44 and Table XXIV shows that the total of listened messages in relation to generated messages decreased with higher transmission power, from 990% to 770%.

Fig. 45 and Table XXIV shows that the total of rerouted messages in relation to generated messages decreased with higher transmission power, from 450% to 0%.

Fig. 46 and Table XXIV shows that the total of overheard messages in relation to generated messages increased with higher transmission power, from 540% to 700%, with peaks of 820%.

The message log of the simulations was:

- $P_{tx} - 1d$
    - Listened Messages: **990%**; Rerouted Messages: **450%**; Overheard Messages: **540%**.
- $11.31P_{tx} - 2d$
    - Listened Messages: **970%**; Rerouted Messages: **200%**; Overheard Messages: **770%**.
- $46.76P_{tx} - 3d$
    - Listened Messages: **940%**; Rerouted Messages: **120%**; Overheard Messages: **820%**.
- $128P_{tx} - 4d$
    - Listened Messages: **900%**; Rerouted Messages: **80%**; Overheard Messages: **820%**.
- $279.50P_{tx} - 5d$
    - Listened Messages: **850%**; Rerouted Messages: **50%**; Overheard Messages: **800%**.

- Maximum P_{tx} – directly to base station
    - Listened Messages: **700%**; Rerouted Messages: **0%**; Overheard Messages: **700%**.

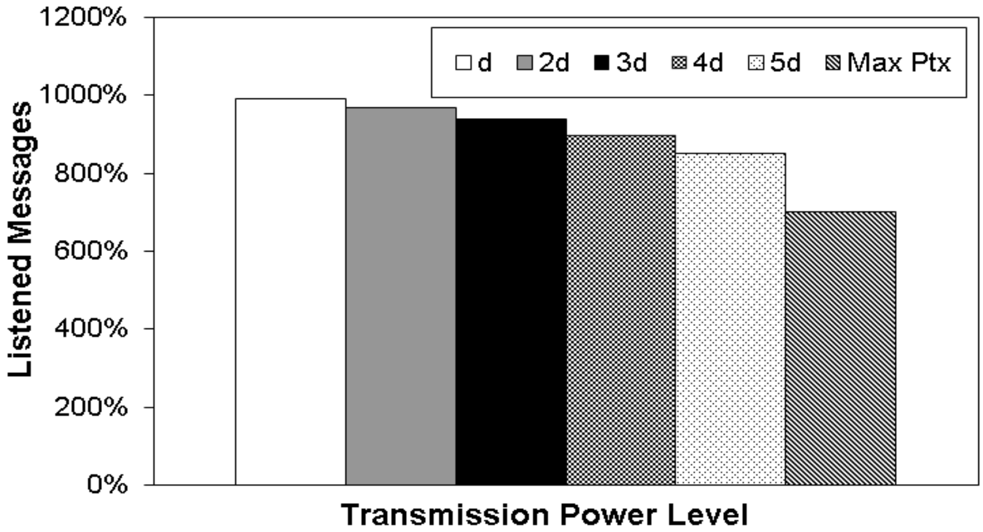

Fig. 44 – Log of listened messages.

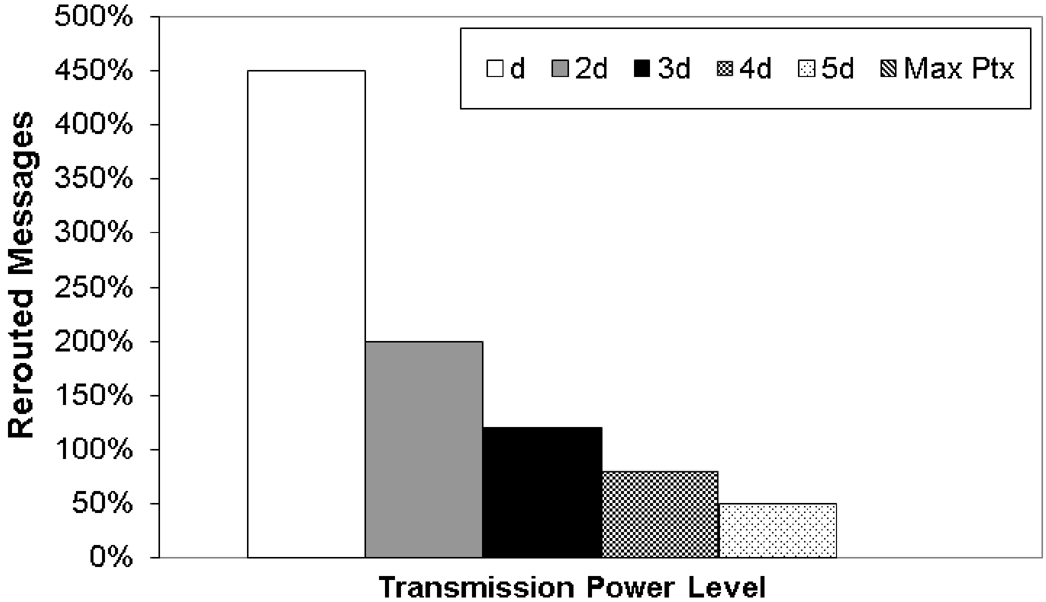

Fig. 45 – Log of rerouted messages.

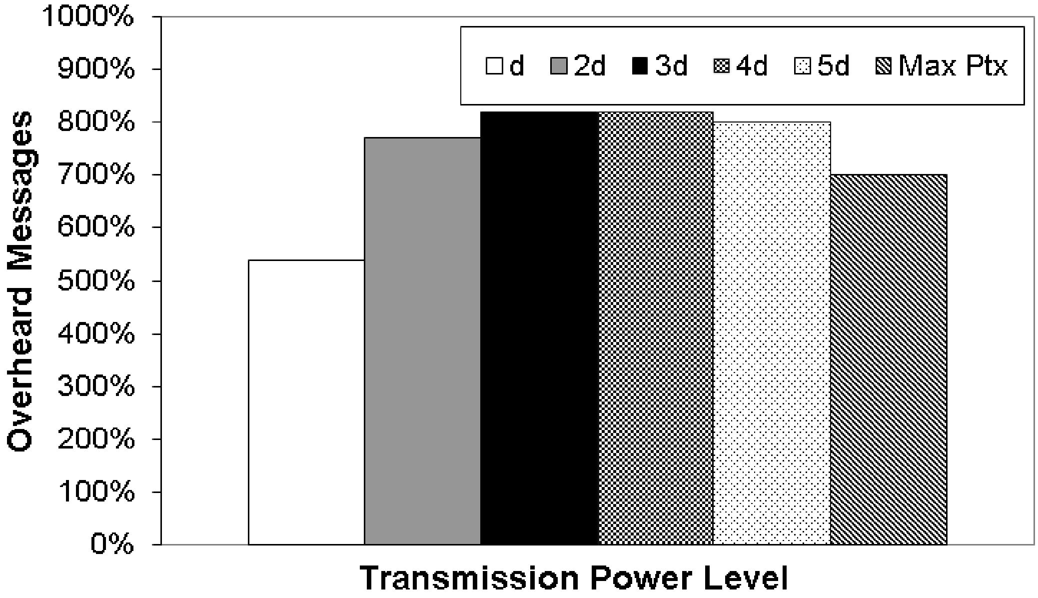

Fig. 46 – Log of overheard messages.

Table XXIV – Message logs of this scenario.

Transmission Power	Reach	Listened Messages	Rerouted Messages	Overheard Messages
P_{tx}	$1d$	990%	450%	540%
$11.31P_{tx}$	$2d$	970%	200%	770%
$46.76P_{tx}$	$3d$	940%	120%	820%
$128P_{tx}$	$4d$	900%	80%	820%
$279.50P_{tx}$	$5d$	850%	50%	800%
Max P_{tx}	Base Station	700%	0%	700%

3.5.2.1 Messages per Hour

As can be observed in Fig. 47 and Table XXV, the quantity of messages per hour generated by the simulated networks were entirely different. As the generation period of the simulated networks varied from one message per second to one message per day, the quantity of messages per hour generated also kept the huge difference of the generation periods used in the simulations.

The quantity of messages per hour generated by the simulated networks was:

- $P_{tx} - 1d$
  - 1 message per second: **216083.65 messages per hour**; 1 message at each 10 seconds: **21600.72 messages per hour**; 1 message at each 60 seconds: **3600.07 messages per hour**; 1 message at each 600 seconds: **360.01 messages per hour**; 1 message at each 3600 seconds: **60.00 messages per hour**; 1 message at each 86400 seconds: **2.51 messages per hour**.
- $11.31P_{tx} - 2d$

  - 1 message per second: **216123.71 messages per hour**; 1 message at each 10 seconds: **21600.47 messages per hour**; 1 message at each 60 seconds: **3600.16 messages per hour**; 1 message at each 600 seconds: **360.00 messages per hour**; 1 message at each 3600 seconds: **60.01 messages per hour**; 1 message at each 86400 seconds: **2.50 messages per hour**.
- $46.76P_{tx} - 3d$
  - 1 message per second: **216487.39 messages per hour**; 1 message at each 10 seconds: **21601.35 messages per hour**; 1 message at each 60 seconds: **3600.40 messages per hour**; 1 message at each 600 seconds: **360.01 messages per hour**; 1 message at each 3600 seconds: **60.01 messages per hour**; 1 message at each 86400 seconds: **2.50 messages per hour**.
- $128P_{tx} - 4d$
  - 1 message per second: **208971.43 messages per hour**; 1 message at each 10 seconds: **21604.15 messages per hour**; 1 message at each 60 seconds: **3600.70 messages per hour**; 1 message at each 600 seconds: **360.06**; 1 message at each 3600 seconds: **60.02 messages per hour**; 1 message at each 86400 seconds: **2.50 messages per hour**.
- $279.50P_{tx} - 5d$
  - 1 message per second: **217595.74 messages per hour**; 1 message at each 10 seconds: **21619.05 messages per hour**; 1 message at each 60 seconds: **3601.06 messages per hour**; 1 message at each 600 seconds: **360.12 messages per hour**; 1 message at each 3600 seconds: **60.03 messages per hour**; 1 message at each 86400 seconds: **2.50 messages per hour**.
- Maximum P_{tx} – directly to base station
  - 1 message per second: **215294.12 messages per hour**; 1 message at each 10 seconds: **21621.30 messages per hour**; 1 message at each 60 seconds: **3607.11 messages per hour**; 1 message at each 600 seconds: **360.60 messages per hour**; 1 message at each 3600 seconds: **60.11 messages per hour**; 1 message at each 86400 seconds: **2.50 messages per hour**.

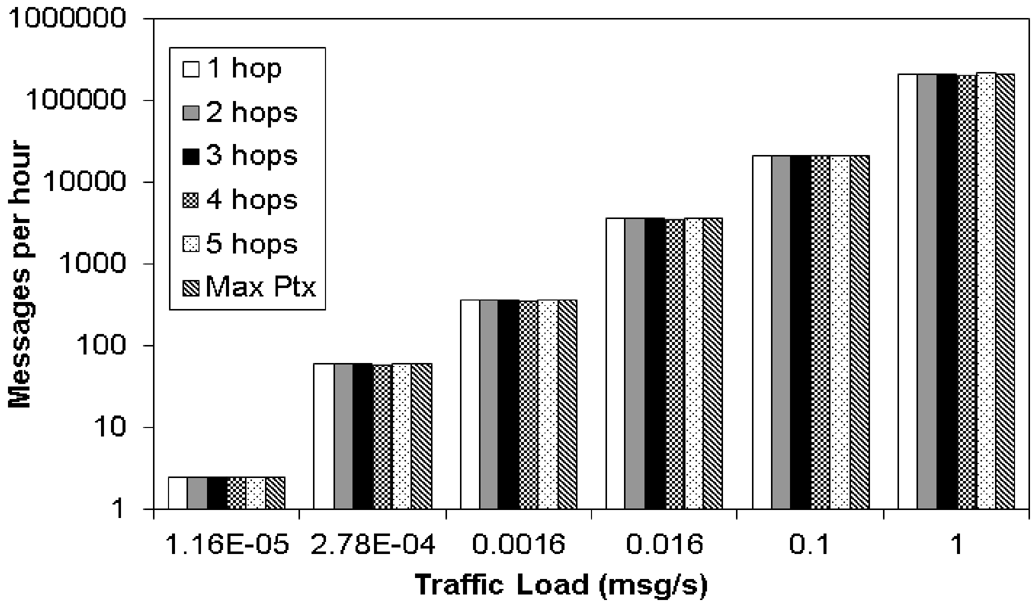

Fig. 47 – Messages per hour of the simulated networks.

Table XXV – Messages per hour of the simulated networks.

Traffic Load (msg/s)	Messages per Hour – 1*d*	Messages per Hour – 2*d*	Messages per Hour – 3*d*	Messages per Hour – 4*d*	Messages per Hour – 5*d*	Messages per Hour – Max Power
1.16E-05	2.51	2.50	2.50	2.50	2.50	2.50
2.78E-04	60.00	60.01	60.01	60.02	60.03	60.11
0.00166	360.01	360.00	360.01	360.06	360.12	360.60
0.166	3600.07	3600.16	3600.40	3600.70	3601.06	3607.11
0.1	21600.72	21600.47	21601.35	21604.15	21619.05	21621.30
1	216083.65	216123.71	216487.39	208971.43	217595.74	215294.12

3.5.2.2 Analysis of the Message Traffic - P_{tx} (1d)

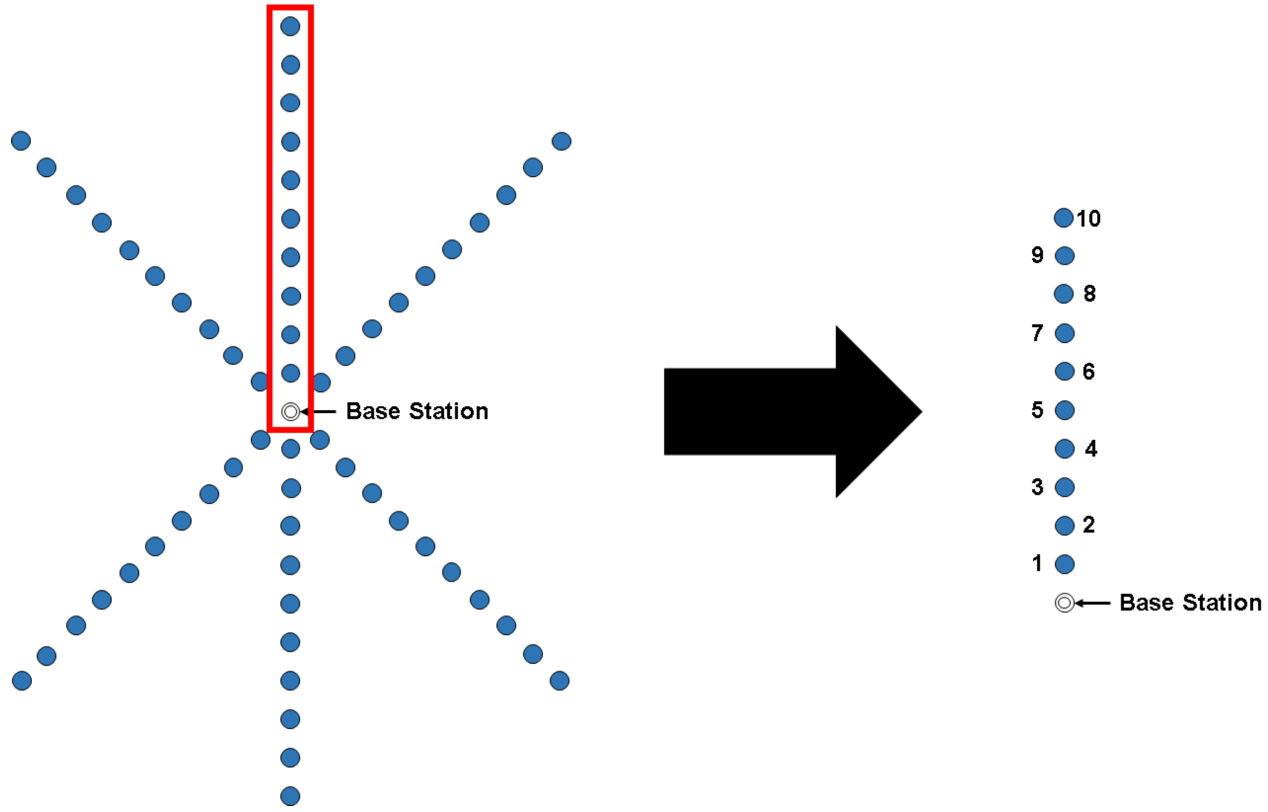

Fig. 48 – The simulated network and one of its branches.

As the simulations adopted a time-driven [104]–[108] and well-defined network cycles for each mote generates and sends its messages, we could analyze the exact traffic that each message had to handle. The simulated network used in this chapter, which is shown in Fig. 48, is formed by six identical and concentric branches with ten motes each, consequently, the analysis of one branch and its motes is perfectly generalizable for the other six that forms the network.

Fig. 49, Fig. 50 and Table XXVI show that the number of messages listened by some motes was very high. Each mote sent just **one** message and the average number of listened messages by each mote was **9.9**.

Being the mote number its linear position in relation to the base station, the message log per mote of a single Network Cycle of the simulations in this scenario using P_{tx} was:

- Mote 1
    - Listened Messages: **9**; Rerouted Messages: **9**;

      Overheard Messages: **0**; Hops to Base Station: **1**.
- Mote 2
    - Listened Messages: **18**; Rerouted Messages: **8**;

      Overheard Messages: **10**; Hops to Base Station: **2**.

- Mote 3
    - Listened Messages: **16**; Rerouted Messages: **7**;
    Overheard Messages: **9**; Hops to Base Station: **3**.
- Mote 4
    - Listened Messages: **14**; Rerouted Messages: **6**;
    Overheard Messages: **8**; Hops to Base Station: **4**.
- Mote 5
    - Listened Messages: **12**; Rerouted Messages: **5**;
    Overheard Messages: **7**; Hops to Base Station: **5**.
- Mote 6
    - Listened Messages: **10**; Rerouted Messages: **4**;
    Overheard Messages: **6**; Hops to Base Station: **6**.
- Mote 7
    - Listened Messages: **8**; Rerouted Messages: **3**;
    Overheard Messages: **5**; Hops to Base Station: **7**.

- Mote 8
    - Listened Messages: **6**; Rerouted Messages: **2**;
    Overheard Messages: **4**; Hops to Base Station: **8**.
- Mote 9
    - Listened Messages: **4**; Rerouted Messages: **1**;
    Overheard Messages: **3**; Hops to Base Station: **9**.
- Mote 10
    - Listened Messages: **2**; Rerouted Messages: **0**;
    Overheard Messages: **2**; Hops to Base Station: **10**.
- Total
    - Listened Messages: **99**; Rerouted Messages:**45**;
    Overheard Messages: **54**; Hops to Base Station: **55**; Generated Messages: **10** (one per mote).
- Averages
    - Listened Messages: **9.9**; Rerouted Messages: **4.5**;
    Overheard Messages: **5.4**; Hops to Base Station: **5.5**.

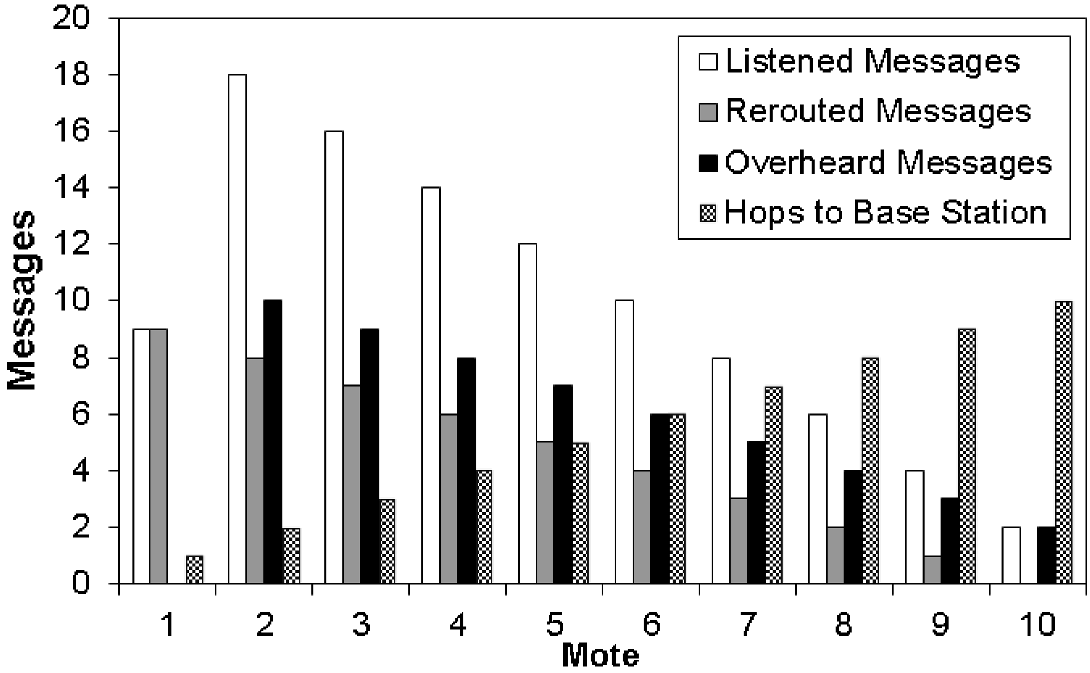

Fig. 49 – Message log per mote (1*d*).

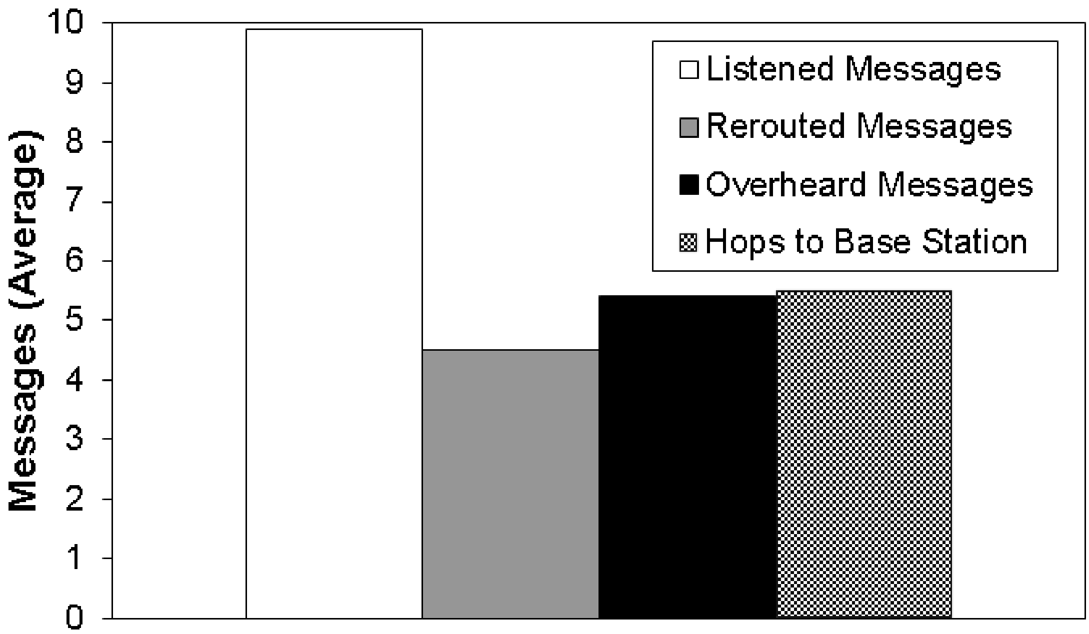

Fig. 50 – Message log per mote – Averages (1 hop).

Table XXVI – Message log per mote (1 hop).

Mote	Listened Messages	Rerouted Messages	Overheard Messages	Hops to Base Station
1	9	9	0	1
2	18	8	10	2
3	16	7	9	3
4	14	6	8	4
5	12	5	7	5
6	10	4	6	6
7	8	3	5	7

8	6	2	4	8
9	4	1	3	9
10	2	0	2	10
Total	**99**	**45**	**54**	**55**
Average	**9.9**	**4.5**	**5.4**	**5.5**
Generated Messages	**10 (one per mote)**			

3.5.2.3 Analysis of the Message Traffic – $11.31P_{tx}$ ($2d$)

Fig. 51, Fig. 52 and Table XXVII show that the average number of listened messages decreased from 9.9 to 9.7, the average number of rerouted messages decreased from 4.5 to 2, the average number of overheard messages increased from 5.4 to 7.7, the average number of hops between the motes and the base station decreased from 5.5 to 3.

Being the mote number its distance in hops to the base station, the message log per mote of a single Network Cycle of the simulations in this scenario using $11.31P_{tx}$ was:

- Mote 1
  - Listened Messages: **9**; Rerouted Messages: **4**;
    Overheard Messages: **5**; Hops to Base Station: **1**.
- Mote 2
  - Listened Messages: **13**; Rerouted Messages: **4**;
    Overheard Messages: **9**; Hops to Base Station: **1**.
- Mote 3
  - Listened Messages: **12**; Rerouted Messages: **3**;
    Overheard Messages: **9**; Hops to Base Station: **2**.
- Mote 4
  - Listened Messages: **15**; Rerouted Messages: **3**;
    Overheard Messages: **12**; Hops to Base Station: **2**.
- Mote 5
  - Listened Messages: **13**; Rerouted Messages: **2**;
    Overheard Messages: **11**; Hops to Base Station: **3**.
- Mote 6
  - Listened Messages: **11**; Rerouted Messages: **2**;
    Overheard Messages: **9**; Hops to Base Station: **3**.
- Mote 7
  - Listened Messages: **9**; Rerouted Messages: **1**;

Overheard Messages: **8**; Hops to Base Station: **4**.

- Mote 8
  - Listened Messages: **7**; Rerouted Messages: **1**;

    Overheard Messages: **6**; Hops to Base Station:**4**.
- Mote 9
  - Listened Messages: **5**; Rerouted Messages: **0**;

    Overheard Messages: **5**; Hops to Base Station: **5**.
- Mote 10
  - Listened Messages: **3**; Rerouted Messages: **0**;

    Overheard Messages: **3**; Hops to Base Station: **5**.
- Total
  - Listened Messages: **97**; Rerouted Messages: **20**;

    Overheard Messages: **77**; Hops to Base Station: **30**; Generated Messages: **10** (one per mote).
- Averages
  - Listened Messages: **9.7**; Rerouted Messages: **2.0**;

    Overheard Messages: **7.7**; Hops to Base Station: **3.0**.

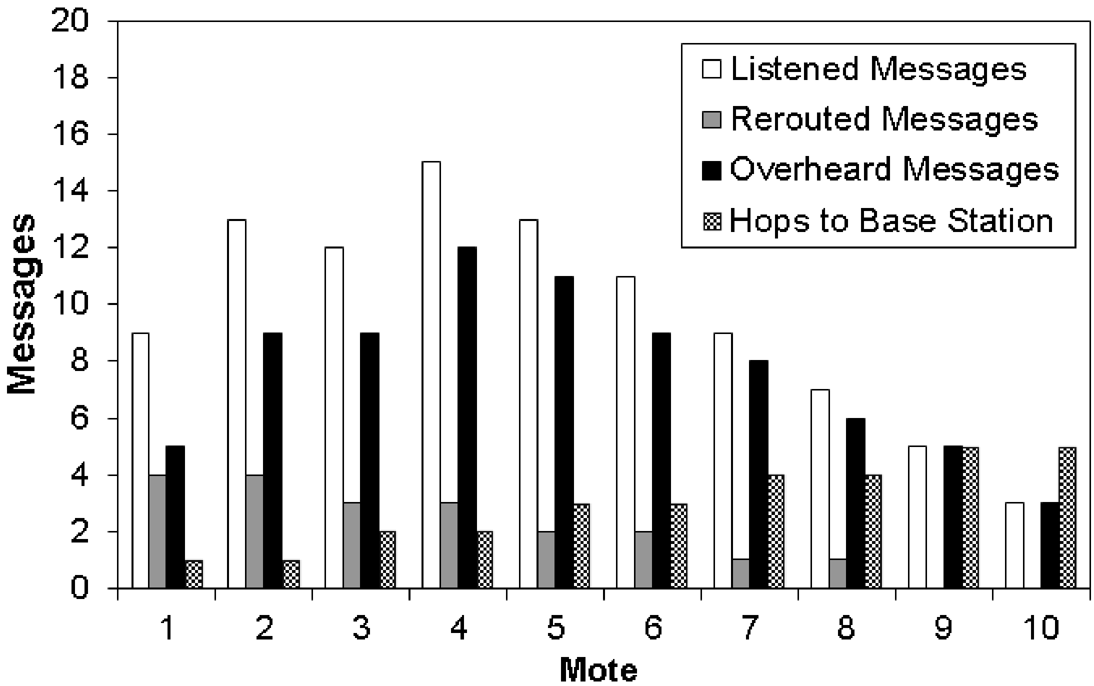

Fig. 51 – Message log per mote (2*d*).

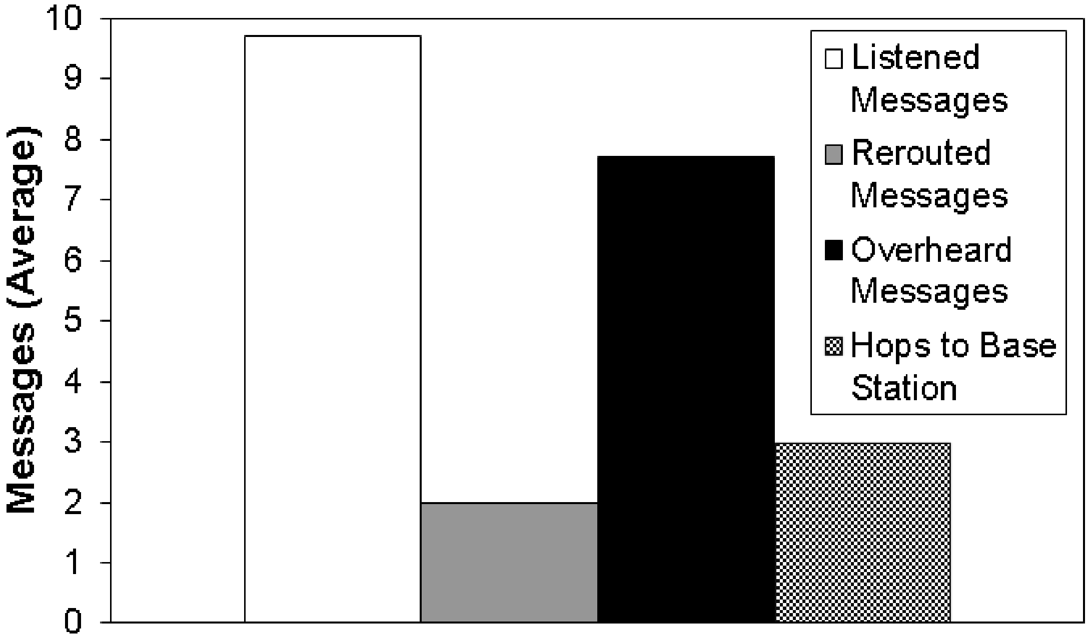

Fig. 52 – Message log per mote – Averages (2*d*).

Table XXVII – Message log per mote (2*d*).

Mote	Listened Messages	Rerouted Messages	Overheard Messages	Hops to Base Station
1	9	4	5	1
2	13	4	9	1
3	12	3	9	2
4	15	3	12	2
5	13	2	11	3
6	11	2	9	3
7	9	1	8	4
8	7	1	6	4
9	5	0	5	5
10	3	0	3	5
Total	**97**	**20**	**77**	**30**
Average	**9.7**	**2**	**7.7**	**3**
Generated Messages	**10 (one per mote)**			

3.5.2.4 Analysis of the Message Traffic – $46.76P_{tx}$ (3*d*)

Fig. 53, Fig. 54 and Table XXVIII show that the average number of listened messages decreased from 9.9 to 9.4, the average number of rerouted messages decreased from 4.5 to 1.2, the average number of overheard messages increased from 5.4 to 8.2, the average number of hops between the motes and the base station decreased from 5.5 to 2.2.

Being the mote number its distance in hops to the base station, the message log per mote of a single Network Cycle of the simulations in this scenario using $46.76P_{tx}$ was:

- Mote 1
    - Listened Messages: **9**; Rerouted Messages: **3**;
      Overheard Messages: **6**; Hops to Base Station: **1**.
- Mote 2
    - Listened Messages: **12**; Rerouted Messages: **2**;
      Overheard Messages: **10**; Hops to Base Station: **1**.
- Mote 3
    - Listened Messages: **10**; Rerouted Messages: **2**;
      Overheard Messages: **8**; Hops to Base Station: **1**.
- Mote 4
    - Listened Messages: **12**; Rerouted Messages:**2**;
      Overheard Messages: **10**; Hops to Base Station: **2**.
- Mote 5
    - Listened Messages: **11**; Rerouted Messages: **1**;
      Overheard Messages: **10**; Hops to Base Station: **2**.
- Mote 6
    - Listened Messages: **12**; Rerouted Messages: **1**;
      Overheard Messages: **11**; Hops to Base Station: **2**.
- Mote 7
    - Listened Messages: **10**; Rerouted Messages: **1**;
      Overheard Messages: **9**; Hops to Base Station: **3**.
- Mote 8
    - Listened Messages: **8**; Rerouted Messages: **0**;
      Overheard Messages: **8**; Hops to Base Station: **3**.
- Mote 9

  - Listened Messages: **6**; Rerouted Messages: **0**;

    Overheard Messages: **6**; Hops to Base Station: **3**.

- Mote 10
  - Listened Messages: **4**; Rerouted Messages: **0**;

    Overheard Messages: **4**; Hops to Base Station: **4**.

- Total
  - Listened Messages: **94**; Rerouted Messages: **12**;

    Overheard Messages: **82**; Hops to Base Station: **22**; Generated Messages: **10** (one per mote).

- Averages
    - Listened Messages: **9.4**; Rerouted Messages: **1.2**;

      Overheard Messages: **8.2**; Hops to Base Station: **2.2**.

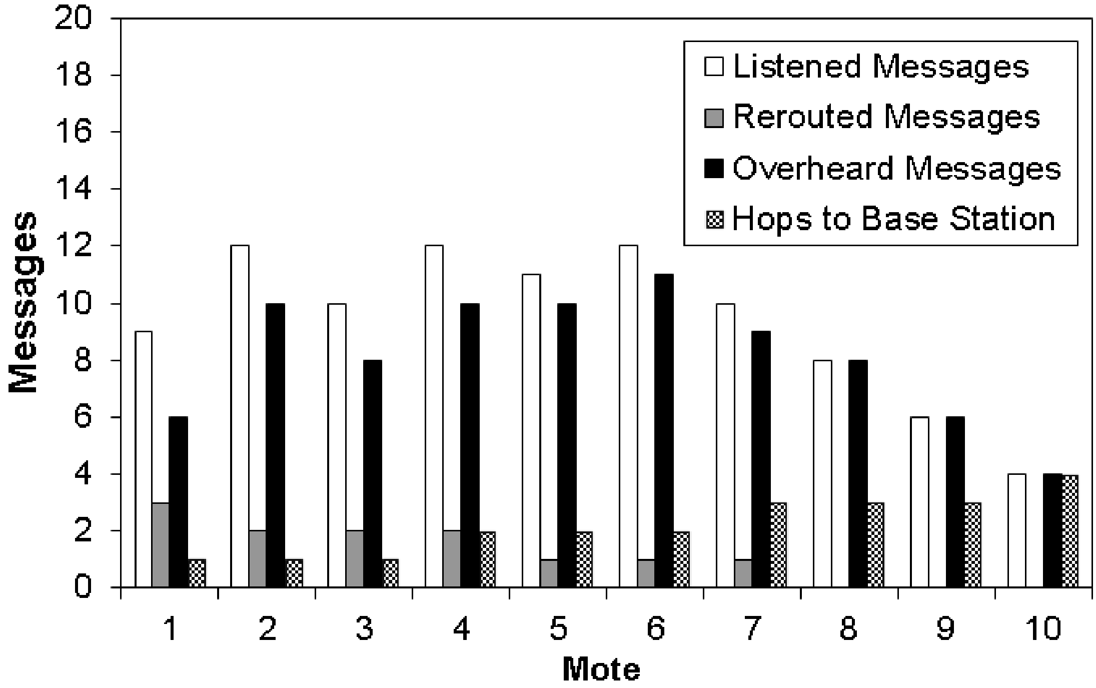

Fig. 53 – Message log per mote (3*d*).

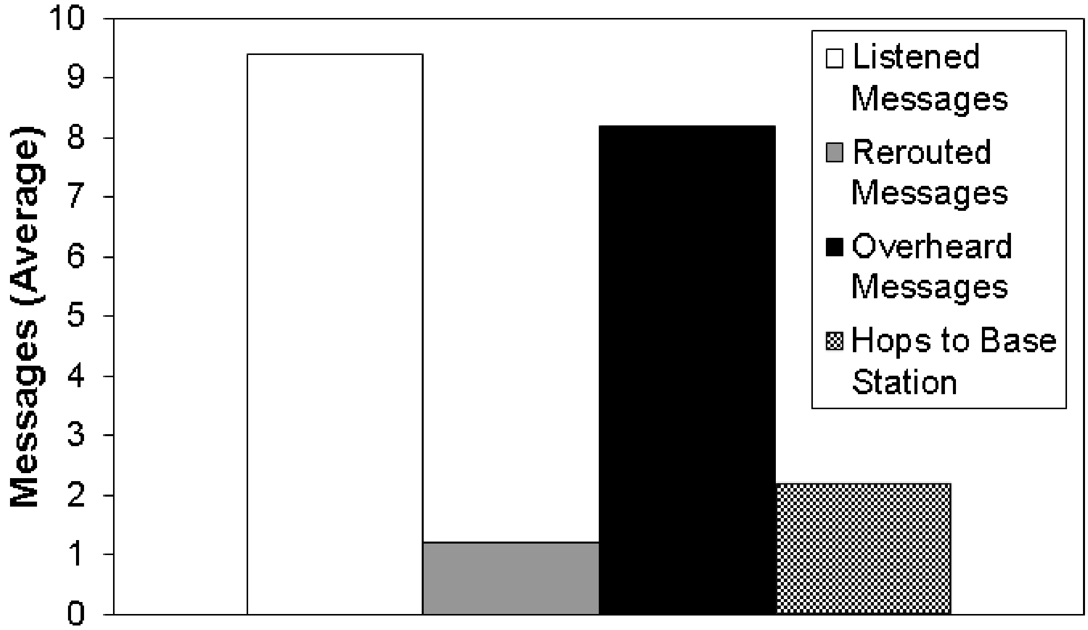

Fig. 54 – Message log per mote – Averages (3*d*).

Table XXVIII – Message log per mote (3d).

Mote	Listened Messages	Rerouted Messages	Overheard Messages	Hops to Base Station
1	9	3	6	1
2	12	2	10	1
3	10	2	8	1
4	12	2	10	2
5	11	1	10	2
6	12	1	11	2
7	10	1	9	3
8	8	0	8	3
9	6	0	6	3
10	4	0	4	4
Total	**94**	**12**	**82**	**22**
Average	**9.4**	**1.2**	**8.2**	**2.2**
Generated Messages	**10 (one per mote)**			

3.5.2.5 Analysis of the Message Traffic – 128P_{tx} (4d)

Fig. 55, Fig. 56 and Table XXIX show that the average number of listened messages decreased from 9.9 to 9, the average number of rerouted messages decreased from 4.5 to 0.8, the average number of overheard messages increased from 5.4 to 8.2, the average number of hops between the motes and the base station decreased from 5.5 to 1.8.

Being the mote number its distance in hops to the base station, the message log per mote of a single Network Cycle of the simulations in this scenario using 128P_{tx} was:

- Mote 1
    - Listened Messages: **9**; Rerouted Messages: **2**;
      Overheard Messages: **7**; Hops to Base Station: **1**.
- Mote 2
    - Listened Messages: **11**; Rerouted Messages: **2**;
      Overheard Messages: **9**; Hops to Base Station: **1**.
- Mote 3
    - Listened Messages: **10**; Rerouted Messages: **1**;
      Overheard Messages: **9**; Hops to Base Station: **1**.

- Mote 4
    - Listened Messages: **11**; Rerouted Messages: **1**;
    Overheard Messages: **10**; Hops to Base Station: **1**.
- Mote 5
    - Listened Messages: **9**; Rerouted Messages: **1**;
    Overheard Messages: **8**; Hops to Base Station: **2**.
- Mote 6
    - Listened Messages: **10**; Rerouted Messages: **1**;
    Overheard Messages: **9**; Hops to Base Station: **2**.
- Mote 7
    - Listened Messages: **10**; Rerouted Messages: **0**;
    Overheard Messages: **9**; Hops to Base Station: **2**.
- Mote 8
    - Listened Messages: **9**; Rerouted Messages: **0**;
    Overheard Messages: **9**; Hops to Base Station: **2**.
- Mote 9
    - Listened Messages: **7**; Rerouted Messages: **0**;
    Overheard Messages: **7**; Hops to Base Station: **3**.
- Mote 10
    - Listened Messages: **5**; Rerouted Messages: **0**;
    Overheard Messages: **5**; Hops to Base Station: **3**.
- Total
    - Listened Messages: **90**; Rerouted Messages: **8**;
    Overheard Messages: **82**; Hops to Base Station: **18**; Generated Messages: **10** (one per mote).

- Averages
  - Listened Messages: **9**; Rerouted Messages: **0.8**;

    Overheard Messages: **8.2**; Hops to Base Station: **1.8**.

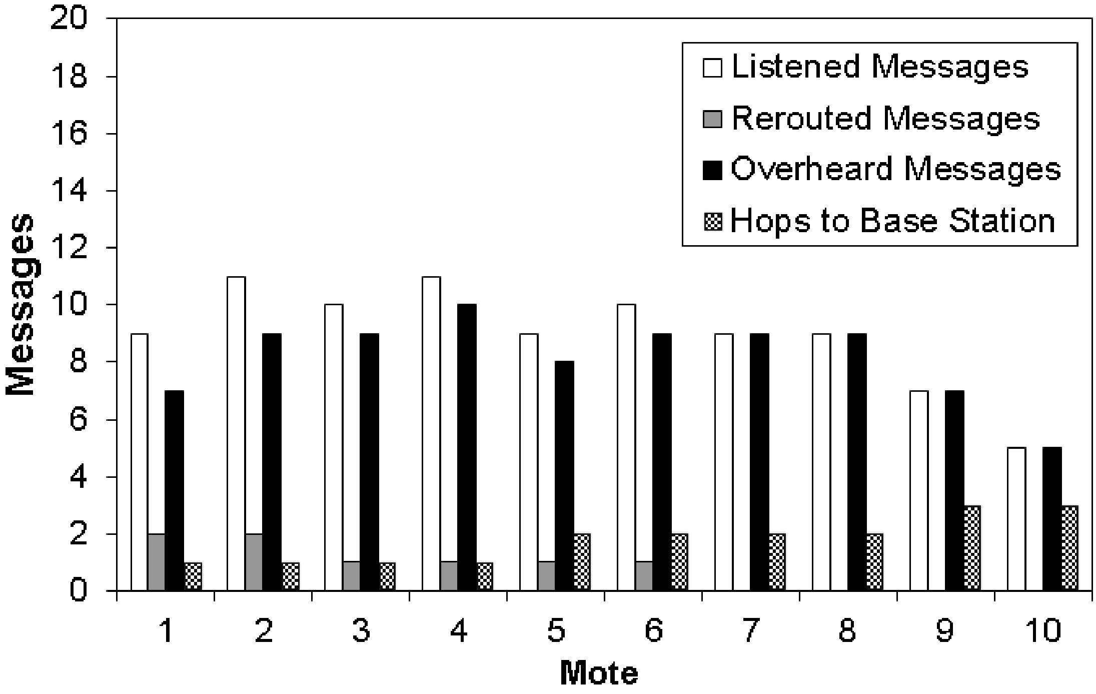

Fig. 55 – Message log per mote (4*d*).

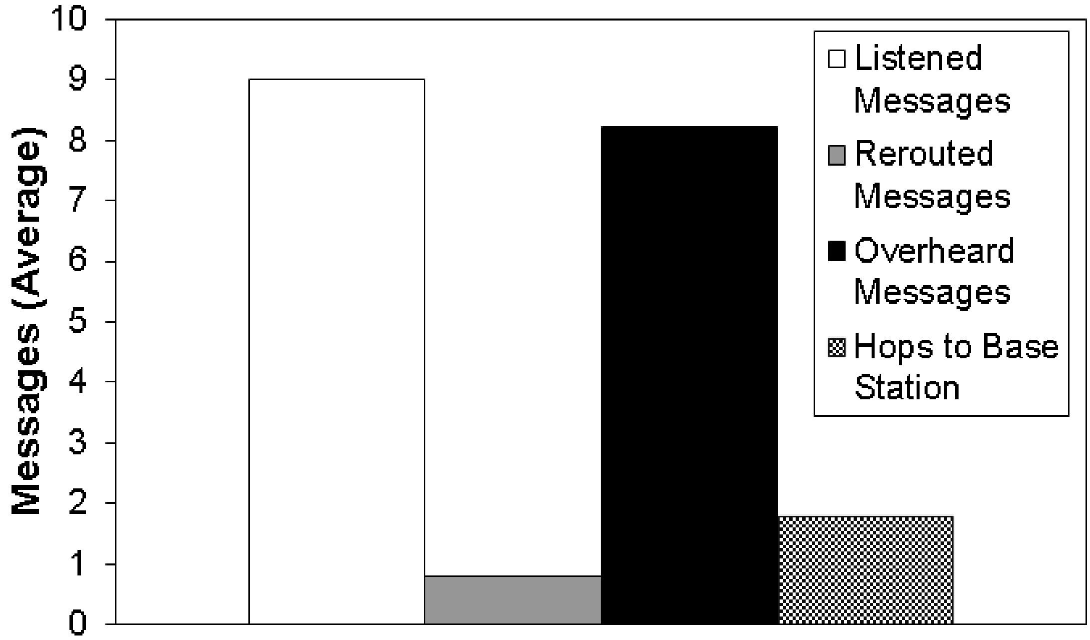

Fig. 56 – Message log per mote – Averages (4*d*).

Table XXIX – Message log per mote (4*d*).

Mote	Listened Messages	Rerouted Messages	Overheard Messages	Hops to Base Station

1	9	2	7	1
2	11	2	9	1
3	10	1	9	1
4	11	1	10	1
5	9	1	8	2
6	10	1	9	2
7	9	0	9	2
8	9	0	9	2
9	7	0	7	3
10	5	0	5	3
Total	**90**	**8**	**82**	**18**
Average	**9**	**0.8**	**8.2**	**1.8**
Generated Messages	**10 (one per mote)**			

3.5.2.6 Analysis of the Message Traffic – 279.50P_{tx} (5d)

Fig. 57, Fig. 58 and Table XXX show that the average number of listened messages decreased from 9.9 to 8.5, the average number of rerouted messages decreased from 4.5 to 0.5, the average number of overheard messages increased from 5.4 to 8, the average number of hops between the motes and the base station decreased from 5.5 to 1.5.

Being the mote number its distance in hops to the base station, the message log per mote of a single Network Cycle of the simulations in this scenario using 279.50P_{tx} were:

- Mote 1
  - Listened Messages: **9**; Rerouted Messages: **1**;

    Overheard Messages: **8**; Hops to Base Station: **1**.
- Mote 2
  - Listened Messages: **10**; Rerouted Messages: **1**;

    Overheard Messages: **9**; Hops to Base Station: **1**.
- Mote 3
  - Listened Messages: **9**; Rerouted Messages: **1**;

    Overheard Messages: **8**; Hops to Base Station: **1**.

- Mote 4
    - Listened Messages: **10**; Rerouted Messages: **1**;

      Overheard Messages: **9**; Hops to Base Station: **1**.
- Mote 5
    - Listened Messages: **9**; Rerouted Messages: **1**;

      Overheard Messages: **8**; Hops to Base Station: **1**.
- Mote 6
    - Listened Messages: **10**; Rerouted Messages: **0**;

      Overheard Messages: **10**; Hops to Base Station: **2**.
- Mote 7
    - Listened Messages: **8**; Rerouted Messages: **0**;

      Overheard Messages: **8**; Hops to Base Station: **2**.
- Mote 8
    - Listened Messages: **8**; Rerouted Messages: **0**;

      Overheard Messages: **8**; Hops to Base Station: **2**.
- Mote 9
    - Listened Messages: **6**; Rerouted Messages: **0**;

      Overheard Messages: **6**; Hops to Base Station: **2**.
- Mote 10
    - Listened Messages: **6**; Rerouted Messages: **0**;

      Overheard Messages: **6**; Hops to Base Station: **2**.
- Total
    - Listened Messages: **85**; Rerouted Messages: **5**;

      Overheard Messages: **80**; Hops to Base Station: **15**; Generated Messages: **10** (one per mote).

- Averages
  - Listened Messages: **8.5**; Rerouted Messages: **0.5**; Overheard Messages: **8**; Hops to Base Station: **1.5**.

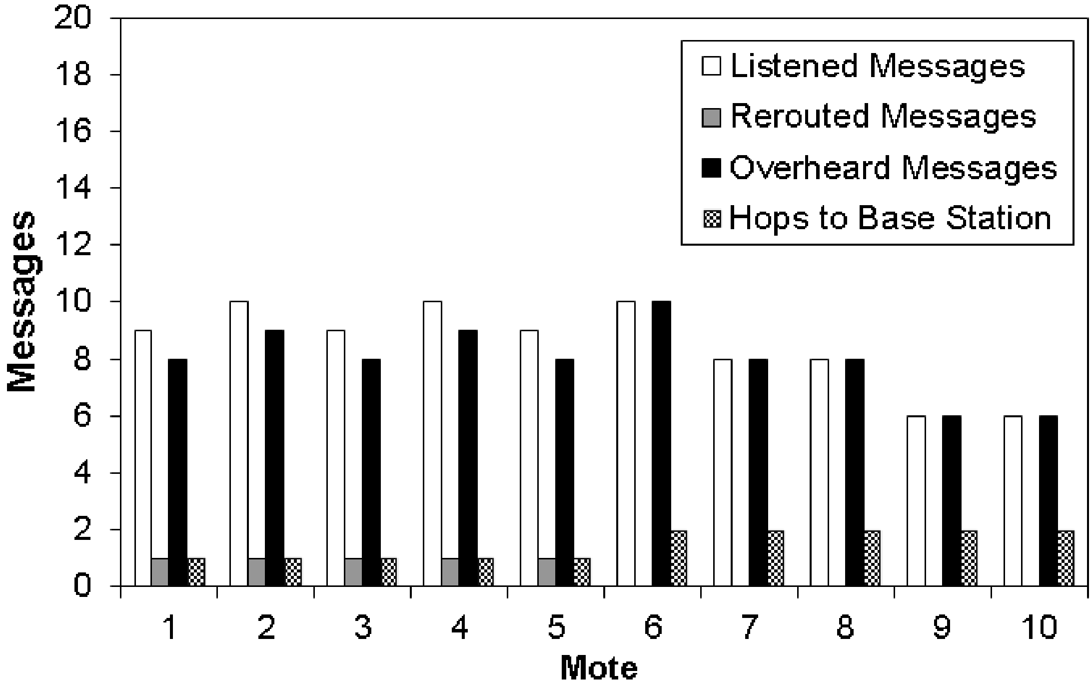

Fig. 57 – Message log per mote (5*d*).

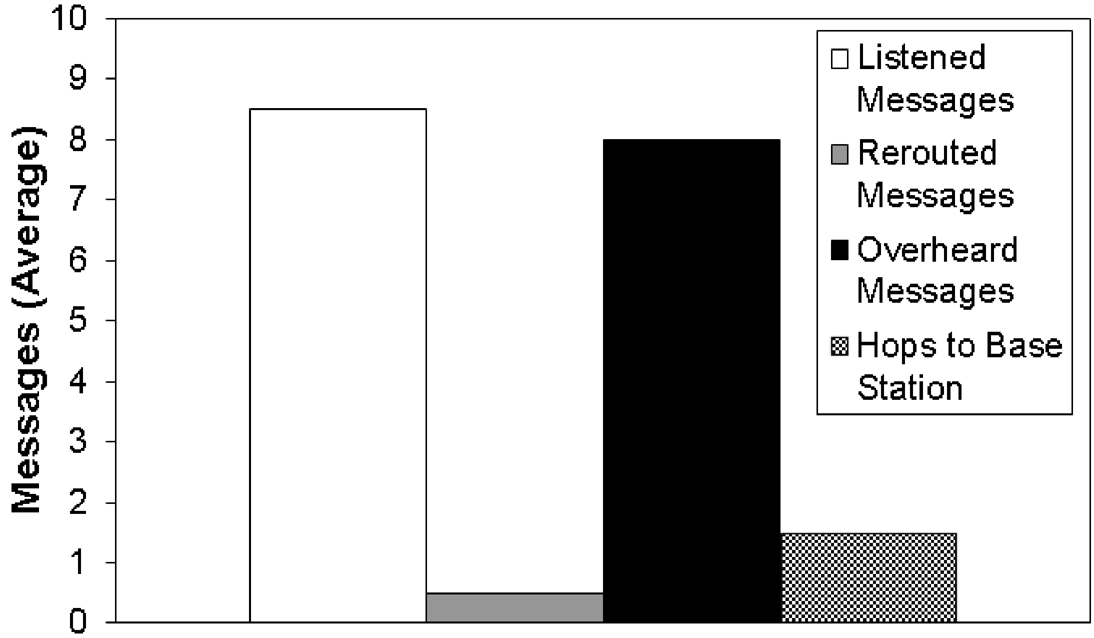

Fig. 58 – Message log per mote – Averages (5*d*).

Table XXX – Message log per mote (5*d*).

Mote	Listened Messages	Rerouted Messages	Overheard Messages	Hops to Base Station

1	9	1	8	1
2	10	1	9	1
3	9	1	8	1
4	10	1	9	1
5	9	1	8	1
6	10	0	10	2
7	8	0	8	2
8	8	0	8	2
9	6	0	6	2
10	6	0	6	2
Total	**85**	**5**	**80**	**15**
Average	**8.5**	**0.5**	**8**	**1.5**
Generated Messages	**10 (one per mote)**			

3.5.2.7 Analysis of the Message Traffic – Maximum P_{tx} (Directly to Base Station)

Fig. 59, Fig. 60 and Table XXXI show that the average number of listened messages decreased from 9.9 to 7, the average number of rerouted messages decreased from 4.5 to 0, the average number of overheard messages increased from 5.4 to 7, the average number of hops between the motes and the base station decreased from 5.5 to 1.

Being the mote number its distance in hops to the base station, the message log per mote of a single Network Cycle of the simulations in this scenario using the maximum P_{tx} were:

- Mote 1
  - Listened Messages: **9**; Rerouted Messages: **0**;
    Overheard Messages: **9**; Hops to Base Station: **1**.
- Mote 2
  - Listened Messages: **9**; Rerouted Messages: **0**;
    Overheard Messages: **9**; Hops to Base Station: **1**.
- Mote 3
  - Listened Messages: **8**; Rerouted Messages: **0**;
    Overheard Messages: **8**; Hops to Base Station: **1**.

- Mote 4
    - Listened Messages: **8**; Rerouted Messages: **0**;

      Overheard Messages: **8**; Hops to Base Station: **1**.
- Mote 5
    - Listened Messages: **7**; Rerouted Messages: **0**;

      Overheard Messages: **7**; Hops to Base Station: **1**.
- Mote 6
    - Listened Messages: **7**; Rerouted Messages: **0**;

      Overheard Messages: **7**; Hops to Base Station: **1**.
- Mote 7
    - Listened Messages: **6**; Rerouted Messages: **0**;

      Overheard Messages: **6**; Hops to Base Station: **1**.
- Mote 8
    - Listened Messages: **6**; Rerouted Messages: **0**;

      Overheard Messages: **6**; Hops to Base Station: **1**.
- Mote 9
    - Listened Messages: **5**; Rerouted Messages: **0**;

      Overheard Messages: **5**; Hops to Base Station: **1**.
- Mote 10
    - Listened Messages: **5**; Rerouted Messages: **0**;

      Overheard Messages: **5**; Hops to Base Station: **1**.
- Total
    - Listened Messages: **70**; Rerouted Messages: **0**;

      Overheard Messages: **70**; Hops to Base Station: **10**; Generated Messages: **10** (one per mote).

- Averages
  - Listened Messages: **7**; Rerouted Messages: **0**;

    Overheard Messages: **7**; Hops to Base Station: **1**.

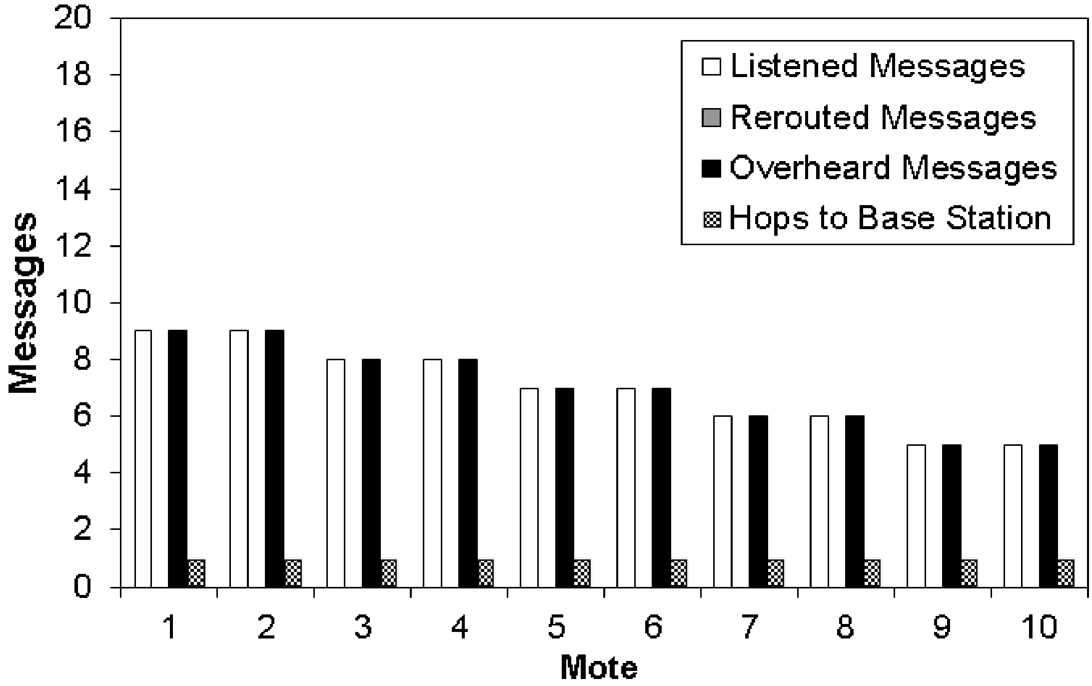

Fig. 59 – Message log per mote (directly to base station).

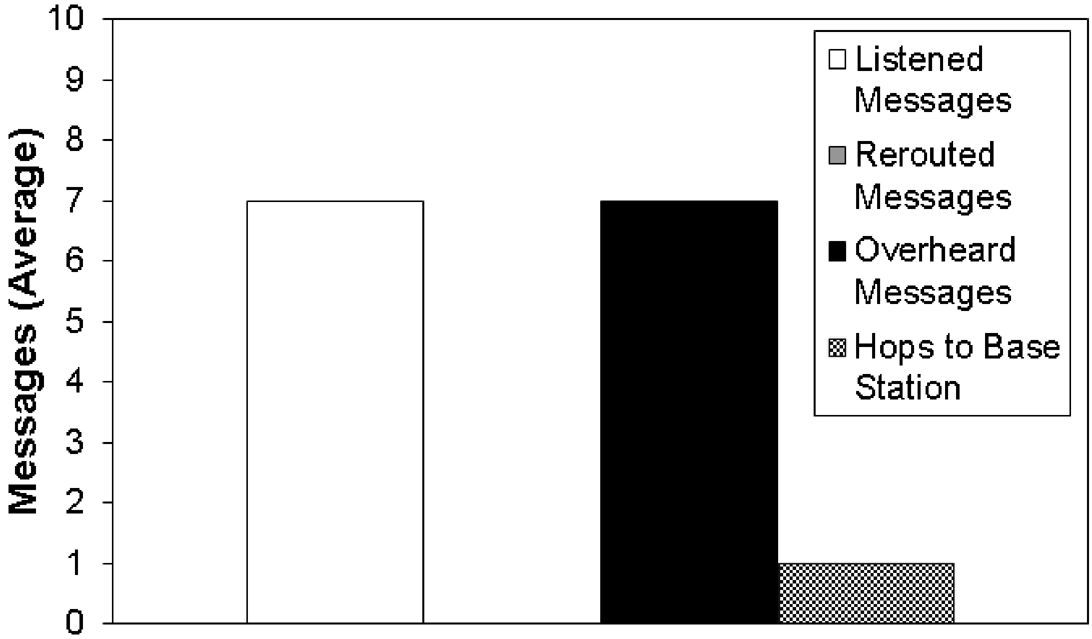

Fig. 60 – Message log per mote – Averages (directly to base station).

Table XXXI – Message log per mote (directly to base station).

Mote	Listened Messages	Rerouted Messages	Overheard Messages	Hops to Base Station

1	9	0	9	1
2	9	0	9	1
3	8	0	8	1
4	8	0	8	1
5	7	0	7	1
6	7	0	7	1
7	6	0	6	1
8	6	0	6	1
9	5	0	5	1
10	5	0	5	1
Total	**70**	**0**	**70**	**10**
Average	**7**	**0**	**7**	**1**
Generated Messages	**10 (one per mote)**			

3.6 Chapter Summary and Concluding Remarks

In order to have a better view of the results presented in this chapter, we divided this section into three parts: Lifetime, Traffic of Messages and General Comments.

3.6.1 Lifetime

The lifetime of the networks using P_{tx} was longer in all simulated scenarios but, when the generation period was low, the difference between the lifetime of the networks using P_{tx} and higher transmission power levels lowered considerably. At the lowest generation period, which was one message per day, the difference between the lifetime of the network using P_{tx} and the networks using up to $128P_{tx}$ was less than 3.5%

These similar lifetimes of low traffic networks can be understood by analyzing the ratio between their primary and secondary energy consumption. As the primary energy consumption is caused by tasks related to active tasks, like reading sensors and sending/receiving messages, its share is larger when the generation period is short and smaller when the generation period is long.

Observing the trend of the primary energy consumption of all simulated networks it is reasonable to infer that the extra energy spent to send messages further impacts less when fewer messages had to be sent, being a plausible strategy for networks with a low message traffic.

3.6.2 Traffic of Messages

As the transmission power increased in order to have a longer range and the radio module used on the model had an omnidirectional antenna [138]–[141], longer transmissions reached not only motes nearer the base station (or the base station itself) and all motes between the sender and the receiver, but also reached motes further the base station, located at the other side of the transmission radius.

Using higher transmission power levels decreased the quantity of messages listened by the motes, however, the number of overheard messages, which are the messages unnecessarily received, increased. As the messages were sent further when using higher transmissions power levels, the quantity of rerouted messages also decreased.

One result that can be inferred, but is not analyzed in this work, is that the less hops a message has to perform, the lower is the chance of it be corrupted or lost.

3.6.3 General Comments

The use of multiple transmission power levels shown both positive and negative results. The results about the traffic of messages were very positive, but, it cannot be analyzed alone, without energy issues, due to the focus of this work on Wireless Sensor Networks.

The lifetime and network cost had very negative results when using short generation periods but, on networks with longer generation periods, the difference between the lifetimes of the simulated networks got lower as the generation period was getting longer. The huge difference between the quantity of messages per hour generated throughout the lifetime of the networks also implies what kind of networks the use of multiple transmission power levels would suit better, as invasion alarms or other networks with low message traffic.

In Computer Sciences, a similar effect is observed in some studies [142]–[145], showing that the greedy routing (the term used when a message is forward to the neighbors closer to the destination) is not always the optimal solution.

Chapter IV

LIFETIME MAXIMIZATION WITH MULTIPLE BATTERY LEVELS IN IRREGULAR TOPOLOGY WIRELESS SENSOR NETWORKS

In this chapter, a novel heuristic method to increment the lifetime of wireless sensor networks is proposed. The main difference between the proposed strategy and the others is that it can be used in networks with no topology restrictions. A model for energy consumption estimation of each mote in a time-driven network is also presented. The heuristic validation was carried out by means of simulations using motes with realistic parameter values. Three different network topologies were evaluated and the results show that the proposed heuristic can be a feasible mean to increase the lifetime of wireless sensor networks, extending the lifetime of some simulated networks more than 200%.

4.1 Introduction

Wireless Sensor Networks (WSNs) [1]–[9] are gaining a significant importance in many economic and social activities, with a pervasive presence in a variety of scenarios in industrial, home, entertainment and medical environments. This scenario is partially explained by the continuing advances in the microelectronics area, making it possible to have commercially available tiny transceivers and microprocessors at low cost. The prediction made by Moore in 1965 [10] is still valid for devices that use integrated electronic circuits, turning computational limitations, for both hardware and software, into just a transient issue. However, all electronic devices require electrical energy to function and, with the worldwide effort to conserve electrical energy, managing and reducing energy consumption in wireless networks have become a key research topic nowadays.

The typical application scenarios of wireless sensor networks impose an additional challenge related to energy consumption. Wireless sensor networks usually rely only on batteries, and replacing or recharging batteries of terminals in many applications may be a difficult task [2], [6]. This situation has motivated investigation into strategies for reducing energy consumption and increasing the network lifetime.

In a wireless sensor network, motes may have different workloads and, therefore, different energy expenditures. For instance, when a mote forwards messages generated by its neighbor motes towards a sink node or base station, that mote will spend additional energy, due to the tasks related to the message forwarding process, such as packet processing, transmission, and reception. Therefore, if all motes in a network are equipped with batteries with the same initial charge, motes with higher energy expenditure will run out of energy sooner, what may cause the whole network to stop functioning properly. Additionally, as pointed out in [1], [11], in some cases a large portion of the energy allocated to the network may end up unused when the network becomes inoperative. Therefore, it is essential to quantify the amount of energy consumed by each task performed by motes in a network, in order to estimate the energy expenditure of each mote and hence make the appropriate distribution of the available energy among motes.

The purpose of this chapter is twofold. Firstly, we propose a mathematical model to estimate the energy consumed by motes in a wireless sensor network, considering the tasks performed by motes, such as sensor reading, data processing, and transmission and reception of messages. We will assume a network with arbitrary topology regarding mote connection and the location of the base station (i.e., sink mote). The evaluation of the consumed energy will also consider tasks related to message forwarding when multi-hop connections between message sources and the base station are required. The model includes both primary states, such as transmission and reception, as well as secondary states, such as sleep mode, of a mote. As we will see, message routing is responsible for a relevant portion of the total energy consumed by a mote, leading to considerable differences in the amounts of energy spent by different motes.

The second purpose of this chapter is to ascertain the effectiveness of the proposed model by presenting an analysis of the effects of different strategies for energy distribution among motes on the lifetime of a wireless sensor network. More specifically, we investigate two strategies, namely, the uniform distribution and the proportional distribution. The uniform distribution strategy assigns the same amount of energy to all motes in the network, while the proportional distribution assigns a larger amount of energy to those motes with higher energy consumption, but keeping fixed the total energy assigned to the whole network. The energy consumed by each mote of the network is estimated using the proposed energy model. Several scenarios regarding traffic intensity and location of the base station are investigated. Results show that the proportional energy distribution always increases the network lifetime, with the highest improvement achieved when there is a significant disparity among the amounts of energy consumed by motes of the network. As will be discussed, this disparity may be exacerbated by the location of the base station with respect to the whole network. If the base station is directly reached (i.e., one hop connection) by a small number of motes, then these motes will have higher workload, which is translated into higher energy consumption in these motes, when compared to other motes.

The remainder of the chapter is organized as follows. In section 4.2, we discuss energy consumption in wireless sensor networks and how this issue is addressed in the literature in the context of lifetime extension. In section 4.3, we present the proposed model for estimating the individual energy consumption of each mote of a given network. In section 4.4, the proportional energy distribution strategy is discussed. Section 4.5 presents the results of a numerical analysis carried out to investigate the effects of energy distribution strategies on the network lifetime. Two energy distribution strategies are studied, namely, the proportional distribution and the uniform distribution. Finally, in section 4.6, we present our concluding remarks and discuss the future works.

4.2 Energy Consumption in Wireless Sensor Networks and Lifetime Maximization Techniques

Energy consumption in wireless sensor networks is a complex subject and has been the focus of a large number of research works, as a literature survey shows. Among several different parameters related to energy consumption, the network lifetime [93]–[96] is a fundamental metric in the analysis of energy consumption of a wireless sensor network. It is widely accepted that, in typical wireless sensor network applications, the network lifetime is limited by the battery charge [1], [6], [9]. Furthermore, depending on the network deployment location and network application, battery replacement can be either prohibitively expensive or hazardous [2], [6]. This situation has motivated a considerable research effort to investigate and design techniques for network lifetime maximization.

These techniques include:

- Resource allocation using cross-layer design;
- Opportunistic transmission schemes/sleep-wake scheduling;
- Routing/clustering;
- Mobile relays and sinks;
- Coverage connectivity/optimal deployment;
- Data gathering/network Coding;
- Data correlation;
- Energy harvesting;
- Beamforming.

Interested readers are referred to the survey presented in [6] for details on these techniques.

According to the analysis presented in [17–21], the levels of energy consumed by different motes of a network are not the same and vary depending on the relative location of motes, particularly when multi-hop routing is employed [15,22–26]. This unbalanced consumption can cause battery depletion in certain regions of the network, which can lead to a fatal disruption in the connections between motes and the base station. This effect was initially studied in circular networks, but it can occur in any network topology, and is commonly called Energy Hole or Doughnut Effect [7,8,18–21,27–31]. Several techniques have been proposed to mitigate the effects of this unbalanced energy consumption, including:

- Clustering-based techniques;
- Non-uniform node distribution techniques;
- Mobility-based techniques;
- Region-based techniques;
- Transmission-based techniques;
- Optimization-based techniques;
- Genetic algorithm-based techniques;
- Node deployment techniques.

Interested readers are referred to the survey presented [8] for details on these techniques.

One strategy for extending network lifetime that has received a great deal of attention is the one based on assigning the amount of energy to motes according to their energy expenditure, or even deploying more motes in a specific highly demanded sector of the network, such that the lifetimes of all motes are about the same [7], [8], [98], [99], [113], [114], [146], [147]. The usage of different sets of batteries, which is a way of assigning distinct amounts of energy to the motes, is addressed with a financial perspective in [98], [99].

As discussed in the following sections, the amount of energy expended by a mote depends on a variety of factors related to the network application (e.g., the size of the messages, the intensity of the traffic generated by the associated sensor), the physical layer (e.g., transmit power and signal processing techniques), and the upper layers protocols (e.g., medium control access and routing algorithms).

Particularly, the location of a mote with respect to the base station, to which all messages are sent, plays a key role in determining the energy expenditure of that mote. In a scenario in which motes use neighbor motes to forward their messages to the base station, motes located close to the base station will have higher energy expenditure, due to the transmissions of messages of neighbor motes. On the other hand, in the opposite scenario, in which all motes transmit directly to the base station, motes located far from the base station tend to have higher energy expenditure, due to the required higher transmit power.

In this chapter, we investigate on the problem of prolonging lifetime of wireless sensor network. More specifically, we propose a mathematical model to evaluate the energy spent by each mote of an arbitrary network, based on the characteristics of the network, such as its topology, traffic pattern, and mote behavior.

4.2.1 Related Literature and Contributions

Energy consumption is a relevant issue in wireless sensor networks and has recently motivated a great deal of research effort. In this section, we present a literature survey on this issue, beginning with works addressing general aspects of energy consumption, and concluding with those closely related to this present work.

One prominent part of the works devoted to energy modeling is based on simulation. In [148]–[151], the authors investigate the energy consumed by motes of wireless sensor networks in different levels of complexities and using different approaches. In [152], a framework to design wireless sensor networks in power consumption constrained environments is proposed. In [153], the authors propose a framework to integrate elements of different simulation tools, which one focusing on a different aspect of the network, in order to obtain a wide view of the network operation and performance. In [151], the authors present a survey of simulation tools for wireless sensor networks.

Motivated by the increasing interest in the use of energy harvesting techniques [29], [154], [155] in wireless sensor networks, the authors in [156] employ an analytical approach to model the energy consumption and to manage the use of solar-based harvesting resources specifically for wireless sensor networks. In [157], a strategy is proposed for enhancing the energy efficiency of the wireless sensor network based on adjusting the number of base stations. In [109], [110], [158], [159], the authors propose strategies for adjusting the network topology based on the energy consumed by motes, in order to control the workload of motes. In [160], the authors investigate the use of renewable energy sources to supply extra energy to the motes with higher energy demands. References [161], [162] present an extensive survey on some existing energy consumption and energy management models for wireless sensor networks.

Several other works provide detailed analysis of energy consumption in wireless sensor network focused on the network operation or mote tasks. In [163]–[165], the authors propose an energy consumption model for both the physical and the medium access control (MAC) layers, considering the internal structure of each exchanged packet. In [166], the authors present a stochastic model to estimate the energy consumed in a network in which the usual tasks performed by motes, such as sensing, message processing, transmission, and reception, are triggered by external events. The authors in [18], [167] also analyze the energy consumption of the components of a mote in event triggered situations, but from a probabilistic perspective. In [27], [88], the authors analyze real motes (either commercially available motes or motes built with off-the-shelf components) to propose a realistic energy consumption model, denoted CSESM (Communication Subsystem Energy Consumption Model), based on the hardware architecture and on the operation states of the components of a mote. In the work presented in [168], the authors propose a model for the energy consumption by a mote considering, among other factors, the cost of sensing and processing tasks. All the works mentioned in this paragraph investigate on the energy consumption problem in a wireless sensor network considering that motes may assume different states regarding energy consumption. Our work employs a similar approach, however, we consider the interrelation not only between transmitters and their respective receivers, but also among neighbor motes of a transmitter or a receiver, analyzing and modeling the effects of this interrelation among motes on the energy consumption. Additionally, our proposed model can be used in any network, regardless its physical network topology.

The focus of the present work is on the estimation of the individual energy consumed by each mote in a network, based on information related to the network topology, message routing, tasks performed by motes and traffic. Based on this estimation, we investigate the problem of lifetime extension and the energy waste reduction. A literature survey shows that several models for energy estimation in wireless sensor network have been proposed in the last years. Some existing works, such as the aforementioned papers [27], [88], [163]–[165], [168], analyze the energy consumption related to the connection between two motes, modeling, in some cases, the energy consumed by each exchanged bit and the effects of propagation environment. However, these works do not consider the inherent cooperative behavior of wireless sensor networks and the interaction among motes.

To the best of our knowledge, our work is the first one to consider different states of energy consumption of motes in an energy estimation strategy that considers the cooperative behavior inherent to multi-hop routing, employed by most wireless sensor networks, and with no physical topology constraints. Differently from the models presented in the aforementioned works, our model focuses on energy demanding tasks, the cooperative behavior of multi-hop networks and how messages transmitted by a mote affects other neighbor motes, providing a more realist description of the interaction among motes, leading to a more precise estimation of the energy consumed by a mote. Our model employs some concepts of network graph and vicinity [169]–[174] to model the interaction among motes. As will be made clear along this work, our proposed model can be used in any network as long as its topology, routing information and energy profile of motes are known, offering a contribution to the field devoted to the analysis of energy in wireless sensor network.

4.3 Energy Consumption Modeling

In this section, we present the proposed model to estimate the energy consumed by each mote in the network that considers, among other features, the individual workload of each mote, i.e., the model assesses the individual energy consumption according to the tasks performed by each mote. For ease of presentation, we introduce the proposed model along with a numerical example.

Before describing the details of the network model, we present in Table XXXII the main variables and their respective descriptions.

4.3.1 Notation and Definitions

Table XXXII shows the main variables used in the model and their respective descriptions. Capital letters in bold style are used for matrices while lowercase in bold style are used for vectors.

For the low vision readers, the authors also prepared a version of this work using a more easily distinguishable notation. For this version, please contact the authors.

Table XXXII – Notations used in this work.

Term	**Description**
α_m	Energy consumed by a mote m to read its sensors and assemble a new message.
$\boldsymbol{\alpha}$	Vector with all α_m of the network.
β_m	Energy consumed by a mote m to transmit a message.
$\boldsymbol{\beta}$	Vector with all β_m of the network.
γ_m	Energy consumed by a mote m to receive and process a message.
$\boldsymbol{\gamma}$	Vector with all γ_m of the network.
P_ω	Power consumed by secondary states.
ω_m	Energy consumed by a mote m when it is in the secondary state.
$\boldsymbol{\omega}$	Vector with all ω_m of the network.
e_m	Total energy consumption of a mote m per network cycle.
$\boldsymbol{e}$	Vector with all e_m of each mote in the network.
b_m	Absolute burden of a mote m.
$\boldsymbol{b}$	Vector with all b_m of the network.
$w_{m,n}$	Number of messages transmitted by mote m and received by mote n.
ρ_m	Generation rate of new messages of a mote m.
$\boldsymbol{\rho}$	Vector with all ρ_m of the network.
μ_m	Quantity of all messages received/listened by a mote m.
$\boldsymbol{\mu}$	Vector with all μ_m in the network.
$f_{m,n}$	Fraction of messages that will be routed through a link connecting mote m to n.
$\boldsymbol{F}$	Adjacency matrix with all $f_{m,n}$ of each link in the network.
$q_{m,n}$	Quantity of all messages transmitted through a link connecting mote m to n.
$\boldsymbol{Q}$	Matrix with all $q_{m,n}$.
T	Network cycle.
T_α	Time spent by a mote to read all its sensors and assemble a new message.
T_p	Time spent by a mote in primary states.
T_{tx}	Time spent by a mote to transmit a message.
T_{rx}	Time spent by a mote to receive and process a message.
$\boldsymbol{N}$	Adjacency matrix representing the network.
Ξ_m	Set of all neighbors of a mote m.
Π_m	Set of all predecessor neighbors of a mote m.
Γ_m	Set of all successor of a mote m.
l, m, n	Mote identifiers.

4.3.2 Network Model and Assumptions

The energy consumption model proposed in this work is based on some widely accepted assumptions. Firstly, we assume a time-driven network [104]–[108], meaning that all tasks performed by motes are repetitive with period, or network cycle, T. Accordingly, mote m periodically generates and transmits ρ_m information messages per network cycle. The time-driven assumption allows for simple mathematical models which can be used to predict the behavior of the network and investigate some energy consumption issues.

The destination of all information messages generated by motes in our network model is a single sink terminal, denoted here as base station. We also assume that motes are only able to communicate with their closest neighbors, such that a multi-hop connection may be required to send a message from the source mote to the base station. In this sense, we assume that an appropriate routing protocol is employed, such that each mote is connected to the base station through the multi-hop route with the smallest number of hops between that mote and the base station [175], [176]. The determination of these multi-hop routes are based on the notion of vicinity [169], [170], using the following classification of neighbor motes of a given mote, according to their relative positions (see Fig. 61) [169]–[173]:

- **Successor neighbor**: A neighbor mote located nearer the base station than the considered mote. A mote uses its successors as the next hop to reach the base station.
- **Equivalent neighbor**: A neighbor located as far to the base station as the considered mote.
- **Predecessor neighbor**: A neighbor located farther to the base station than the considered mote. Predecessor neighbors may use the considered mote as the next hop in their transmissions.
- **Ancestor motes**: Motes connected, directly or indirectly, to a given mote m that are further from the base station and use mote m as a router, *i.e.,* all motes that may depend on mote m to reroute their messages [177].

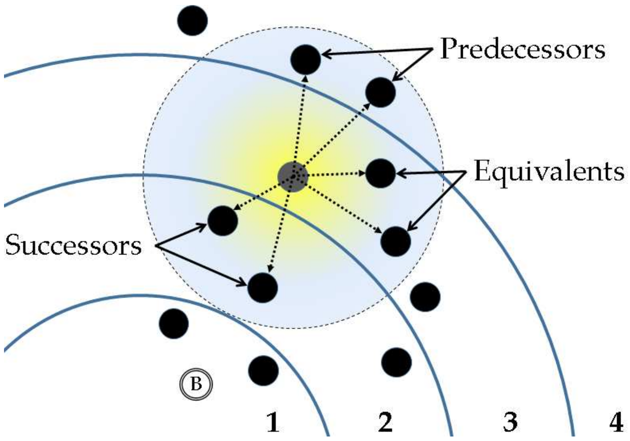

Fig. 61 – Example showing the different types of neighbor motes considered in this work.

We assume that motes are equipped with algorithms to discover and classify all of their neighbors. Many applications and routing protocols require a mote to know its successor neighbors only [175], [178], [179].

Similar to [114], [175], [180]–[182], we assume that the network physical topology, mote placement and links between motes are known. We also consider that the operational characteristics of the components of the mote is known, either by direct measurement [18], [33], [38], [43] or by means of their respective datasheets.

We assume a perfect medium access control (MAC) protocol that guarantees contention-free transmissions. Therefore, there are no collisions or retransmissions when messages are transmitted between motes. This assumption is also adopted in other works, and can be justified by the low message rates expected in many wireless sensor network applications [101], [183]–[186]. For a detailed analysis about these assumptions, readers are referred to references [187]–[189].

4.3.3 Modeling the Individual Energy Consumption of Each Mote

Modeling the energy consumed in wireless sensor networks is usually a difficult task, due to several intrinsic characteristics of this type of network, such as a large number of motes in the network, the cooperative behavior due to possible multi-hop routing [27], [95], [176], [190]–[192] and the intrinsic mutual interference among motes. Therefore, the estimation of the energy consumed by each mote must consider the whole network as a single system.

Clearly, the energy consumed by a mote depends on the number of messages processed by that mote, which include transmitted messages, received messages addressed to that mote, and received message but not addressed to that mote (the so-called *promiscuous reception*, as discussed later). It should be noted that by transmitted messages we mean not only messages generated by the mote, but also those messages routed by that mote. As discussed in the following paragraphs, the number of messages processed by a mote depends on the location of the mote in the network.

For the numerical example, we consider a simple network, represented in the graph shown in Fig. 62.

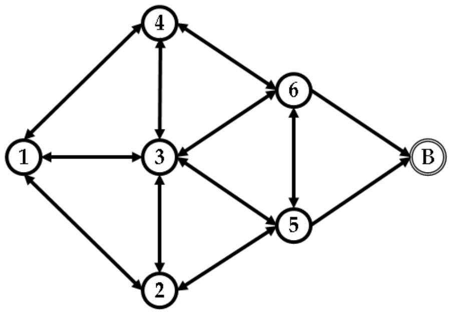

Fig. 62 – Network with 6 motes and a base station (B).

In this graph, numbered circles represent motes and the circle labeled with **B** represents the base station. In this example, all messages generated by motes are sent to the base station. A directed edge connecting, say, mote m to mote n indicates messages transmitted by mote m can be correctly decoded by mote n, i.e., motes m and n are neighbors. On the other hand, the absence of an edge connecting two motes means that messages transmitted by one of these motes cannot be detected and decoded by the other mote, and therefore do not cause any effect on the other mote.

The topology of the network can be described by the so-called adjacency matrix $\boldsymbol{N}$ [172], in which $N_{m,n} = 1$ indicates the existence of a link connecting mote m to mote n. The adjacency matrix for the network shown in Fig. 62 is, therefore,

$$\boldsymbol{N} = [N_{m,n}] = \begin{bmatrix} \mathbf{0} & 1 & 1 & 1 & 0 & 0 & 0 \\ 1 & \mathbf{0} & 1 & 0 & 1 & 0 & 0 \\ 1 & 1 & \mathbf{0} & 1 & 1 & 1 & 0 \\ 1 & 0 & 1 & \mathbf{0} & 0 & 1 & 0 \\ 0 & 1 & 1 & 0 & \mathbf{0} & 1 & 0 \\ 0 & 0 & 1 & 1 & 1 & \mathbf{0} & 0 \\ 0 & 0 & 0 & 0 & 1 & 1 & \mathbf{0} \end{bmatrix}.$$

Note that the base station is included in matrix $\boldsymbol{N}$.

Recalling that we are assuming time-driven networks [104]–[108], the network cycle T is assumed to be long enough such a mote can, within the interval T,

1. assembly its own messages generated within that interval T;
2. transmit messages (their own messages and rerouted messages);
3. receive and process messages transmitted by neighbors.

Overall, T must be adjusted considering the repetitive behavior of time-driven networks, in order to allow the cyclic observation of the tasks performed by all motes.

Returning to our example, we assume that each mote generates one message per network cycle, that is, $\rho_m = 1$. Therefore, the vector $\boldsymbol{\rho}$ is written a

$$\boldsymbol{\rho} = [\rho_m] = [111111]^{\mathrm{T}}$$

where $()^{\mathrm{T}}$ indicates the matrix transpose operation.

As discussed before, motes that are not directly connected to the base station must use a route formed with neighbor motes to send their messages to the base station. Therefore, each mote transmits not only their own messages, but also messages generated by neighbors due to the use of multi-hop routing. Note, in addition, that a mote may have several neighbors to which it can forward its messages (its own messages and messages it is routing for other ancestor motes) towards the base station, as we can see in the network shown in Fig. 62. For instance, mote **1** can forward its messages to either motes **2**, **3** or **4**. The mote selected to forward messages of a given mote depends on the routing protocol employed in the network. Several protocols with different strategies have been proposed in the literature for wireless sensor networks (see, for instance, references [18], [109], [110], [170], [175], [179]–[182]). The effects of the routing technique employed are modeled here by the factor $f_{m,n}$, which denotes the fraction of all messages transmitted by mote m that are routed through link (m,n) connecting mote m and mote n. Therefore, any protocol can be assumed in the proposed energy model, and the only information required are the resulting factors $f_{m,n}$, for all pairs m,n.

Factors $f_{m,n}$ can be represented in a matrix form by means of matrix $\boldsymbol{F}$. For ease of presentation, we assume in this example a simple probabilistic routing protocol, according to which a mote distributes randomly its messages among all its successor neighbors, with equal probability. This means that, for instance, mote **1** randomly selects one of its successor neighbors (motes **2**, **3** and **4**) to forward its messages. Therefore, the matrix $\boldsymbol{F}$ of the network in Fig. 63 is

$$\boldsymbol{F} = [f_{m,n}] = \begin{bmatrix} \mathbf{0} & 0.333 & 0.333 & 0.333 & 0 & 0 & 0 \\ 0 & \mathbf{0} & 0 & 0 & 1 & 0 & 0 \\ 0 & 0 & \mathbf{0} & 0 & 0.5 & 0.5 & 0 \\ 0 & 0 & 0 & \mathbf{0} & 0 & 1 & 0 \\ 0 & 0 & 0 & 0 & \mathbf{0} & 0 & 1 \\ 0 & 0 & 0 & 0 & 0 & \mathbf{0} & 1 \\ 0 & 0 & 0 & 0 & 0 & 0 & \mathbf{0} \end{bmatrix}$$

Fig. 63 shows all non-zero factors $f_{m,n}$ for the network in the example. Note that $f_{m,n}$ is non-zero only for links connecting a mote and one of its successor neighbors.

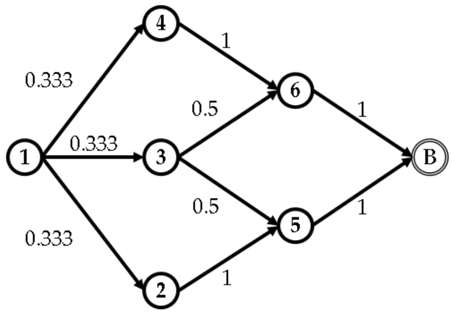

Fig. 63 – Factors $f_{m,n}$ of links in the network.

Now, recalling that each mote generates its own messages at rate ρ_m (messages per network cycle *T*), then the number of messages (generated and rerouted) transmitted by mote *m* through link (*m*,*n*), per network cycle, denoted here as $q_{m,n}$, is given by

$$q_{m,n} = f_{m,n}\left(\rho_m + \sum_{l \in \Pi_m} q_{l,m}\right), \qquad (1)$$

where Π_m is the set of all predecessor motes of mote *m*. Note that the quantity inside the parenthesis in (1) is the number of messages effectively transmitted by mote *m*, either generated or rerouted.

As expected, in order to determine the quantity $q_{m,n}$ of messages generated and rerouted by a given mote *m*, the values of $q_{l,m}$ of predecessor motes *l* are required. Therefore, we must begin the determination of quantities $q_{m,n}$ with motes that do not reroute messages from other motes. For instance, for mote **1** in the example, we have

$$q_{1,n} = f_{1,n}\left(\rho_1 + \sum_{l \in \Pi_1} q_{l,1}\right),$$

where Π_1 is the set of preceding neighbors of mote **1**, *i.e.*, motes whose messages are rerouted by mote **1**. In general, the set Π_m consists of the indexes of non-zero rows of the *m*-th column of matrix ***F***. For *m* = 1, we have

$$\Pi_1 = \{m \mid f_{m,1} \neq 0\} = \{\varnothing\}.$$

Now, using the values of $f_{1,n}$, for *n* = 1, 2, … 7, given in matrix ***F***, we finally have

$$q_{1,n} = \begin{cases} 1/3 & n = \mathbf{2}, \mathbf{3} \text{ and } \mathbf{4} \\ 0 & \text{otherwise} \end{cases}$$

Repeating this procedure for all $q_{m,n}$, the resulting quantities are shown in matrix ***Q*** as

$$\boldsymbol{Q} = [q_{m,n}] = \begin{bmatrix} \mathbf{0} & 0.333 & 0.333 & 0.333 & 0 & 0 & 0 \\ 0 & \mathbf{0} & 0 & 0 & 1.333 & 0 & 0 \\ 0 & 0 & \mathbf{0} & 0 & 0.667 & 0.667 & 0 \\ 0 & 0 & 0 & \mathbf{0} & 0 & 1.333 & 0 \\ 0 & 0 & 0 & 0 & \mathbf{0} & 0 & 3 \\ 0 & 0 & 0 & 0 & 0 & \mathbf{0} & 3 \\ 0 & 0 & 0 & 0 & 0 & 0 & \mathbf{0} \end{bmatrix}.$$

Fig. 64 shows the quantities $q_{m,n}$ of messages transmitted through links of the network in the example.

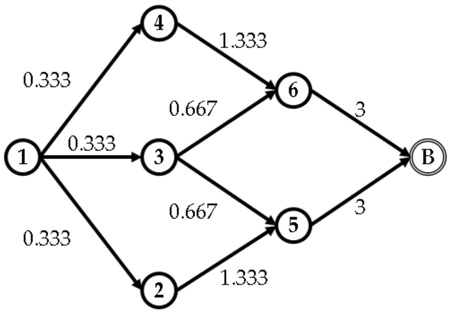

Fig. 64 – Quantities $q_{m,n}$ of all links transmitted through links of the network per cycle.

Returning to the description of the proposed energy model, it should be noted that a mote may receive messages that are not addressed to it but addressed to its neighbors, due to the broadcast nature of wireless transmission [126], [143]. This situation, called *promiscuous reception* [127], leads to an extra energy expenditure in each mote, since the addressee (i.e., the destination mote) of a message is only known by the receiver mote after the message is processed. With promiscuous reception, each mote imposes a burden to all its neighbors. This burden, as far as energy consumption is concerned, can be modeled as the number of all messages transmitted by a mote per network cycle, denoted here as absolute burden b_m, and calculated as

$$b_m = \sum_{l \in \Gamma_m} q_{m,l}, \tag{2}$$

where Γ_m is the set of all successor motes of mote m. Note that b_m can be calculated using matrix $\boldsymbol{Q}$ as

$$\boldsymbol{b} = [b_m] = \boldsymbol{Q}\mathbf{1}$$

where $\boldsymbol{b}$ is the vector with all absolute burden values b_m and $\mathbf{1}$ is the unit column vector. For the network in the example, $\boldsymbol{b}$ is

$$\boldsymbol{b} = \begin{bmatrix} 1 \\ 1.33 \\ 1.33 \\ 1.33 \\ 3 \\ 3 \\ 0 \end{bmatrix}.$$

Fig. 65 shows the absolute burden of all motes of the network in the example. Note that motes closer to the base station has larger burden.

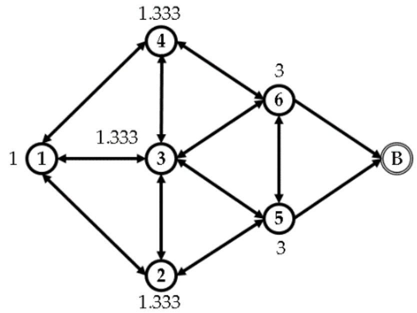

Fig. 65 – Absolute burden b_m of each mote.

Now, the quantity of messages μ_m that mote m receives per network cycle T is the sum of the absolute burdens of all its neighbors, that is

$$\mu_m = \sum_{n \in \Xi_m} b_n, \tag{3}$$

where Ξ_m is the set of all neighbors of mote m (i.e., predecessor, equivalent and successor neighbors, see section 4.3.1) and b_n is the absolute burden of mote n.

The summation in (3) can be performed using vector $\boldsymbol{b}$ and matrix $\boldsymbol{N}$ already presented, as follows. Recall that vector $\boldsymbol{b}$ contains the number of messages transmitted by each mote, while the adjacency matrix $\boldsymbol{N}$ indicates the connection between any two motes. Therefore, by combining $\boldsymbol{b}$ and $\boldsymbol{N}$, we can construct a matrix $\boldsymbol{W}$ whose elements $w_{\mathrm{m,n}}$ represent the number of messages transmitted by mote m and received by mote n (messages addressed and not addressed to n). More specifically, if $N_{\mathrm{m,n}} = 1$, then mote n listens to all b_{m} messages transmitted by mote m. Therefore, the elements of matrix $\boldsymbol{W}$ can be determined as follows:

$$w_{m,n} = \begin{cases} b_m & \text{if } N_{m,n} = 1 \\ 0 & \text{otherwise.} \end{cases}$$

For the network in the example, matrix $\boldsymbol{W}$ is

$$\boldsymbol{W} = [w_{m,n}] = \begin{bmatrix} \mathbf{0} & 1 & 1 & 1 & 0 & 0 & 0 \\ 1.333 & \mathbf{0} & 1.333 & 0 & 1.333 & 0 & 0 \\ 1.333 & 1.333 & \mathbf{0} & 1.333 & 1.333 & 1.333 & 0 \\ 1.333 & 0 & 1.333 & \mathbf{0} & 0 & 1.333 & 0 \\ 0 & 3 & 3 & 0 & \mathbf{0} & 3 & 3 \\ 0 & 0 & 3 & 3 & 3 & \mathbf{0} & 3 \\ 0 & 0 & 0 & 0 & 0 & 0 & \mathbf{0} \end{bmatrix}.$$

Now, the number of all messages received, regarding their addressees, by mote n can be determined by summing the elements of the n-th column of matrix $\boldsymbol{W}$, being represented in vector $\boldsymbol{\mu}$. Alternatively, we can write

$$\boldsymbol{\mu} = [\mu_m] = \boldsymbol{W}^T \mathbf{1}.$$

For the network in the example, $\boldsymbol{\mu}$ is

$$\boldsymbol{\mu} = [\mu_n] = \begin{bmatrix} 4 \\ 5.33 \\ 9.67 \\ 5.33 \\ 5.67 \\ 5.67 \\ 6 \end{bmatrix}.$$

Motes consume energy not only when transmitting or receiving messages, the so-called *primary states* of a mote, by also when they are in the *idle* and *sleep* states, also known as *secondary states* [18]. In our model, we denote the energy consumed in the secondary state per network cycle by ω_m. The energy ω_m is usually very low when compared to the energy spent in the primary states. However, in cases with long network cycles and consequently long secondary states, the energy consumed in secondary states may have a relevant impact in the overall energy consumption, as will be shown in our analysis in section 4.5.

According to the model presented so far, the number of messages transmitted and received by mote m per network cycle are b_m and μ_m, respectively. Let us assume the following notation: (*i*) T_α denotes the time needed to read a sensor and assemble a new message, (*ii*) T_{tx} denotes the time to transmit a message, and (*iii*) T_{rx} denotes the time needed to receive and process a message. Therefore, the total time spent by a mote in the primary state, denoted by $T_{p,m}$, is $T_{p,m} = T_\alpha + b_m T_{tx} + \mu_m T_{rx}$. Consequently, the energy ω_m consumed by mote m in the secondary state is

$$\omega_m = (T - T_{p,m}) \times P_\omega, \tag{4}$$

where T is the network cycle duration and P_ω is the power consumed by a mote in the secondary states. It is important to note that the duration of a transmission or a reception is usually very short, but transmissions and receptions demand considerably higher amounts of energy when compared to secondary states, as shown in [18].

4.3.4 Individual Energy Consumption

Finally, the estimated energy consumption e_m, per network cycle, of mote m is given by

$$e_m = \rho_m \times \alpha_m + b_m \times \beta_m + \mu_m \times \gamma_m + \omega_m, \tag{5}$$

where α_m is the energy consumed to read the associated sensors and assemble a new message, β_m is the energy consumed to transmit a message, γ_m is the energy consumed to receive and process a message, and ω_m is the energy consumed in the secondary state during a network cycle.

Using (5), we can determine the energy e_m consumed by each mote of the network considered in the example. Table XXXIII presents the parameter setting for the example. The values of some of the parameters of the model and the resulting energy e_m are shown in Table XXXIV.

- **Values of the parameters used in the numerical analysis** (also shown in Table XXXIII**)**:
  - ρ_m: 1 message per second; α_m: 0.5 millijoules; β_m: 2.5 millijoules; γ_m: 0.6 millijoules; ω_m: 0.1 millijoules; T: 1 second; T_α: 100 milliseconds; T_{tx}: 10 milliseconds; T_{rx}: 10 milliseconds.

- **Total energy consumption e_m per network cycle** (also shown in Table XXXIV**)**:
  - Mote **1**: b_1: 1, μ_1: 4, ω_1**:** 85 microjoules, e_1**: 4.98 millijoules**.
  - Mote **2**: b_2: 1.33, μ_2: 5.33, ω_2**:** 83 microjoules, e_2**: 6.45 millijoules**.
  - Mote **3**: b_3: 1.33, μ_m: 9.66, ω_3**:** 79 microjoules, e_3**: 9.04 millijoules**.
  - Mote **4**: b_4: 1.33, μ_4: 5.33, ω_4**:** 83 microjoules, e_4**: 6.45 millijoules**.
  - Mote **5**: b_5: 3, μ_5: 5.66, ω_5**:** 81 microjoules, e_5**: 9.98 millijoules**.
  - Mote **6**: b_6: 3, μ_6: 5.66, ω_6**:** 81 microjoules, e_6**: 9.98 millijoules**.

Table XXXIII – Values of the parameters used in the numerical analysis.

Parameters	**Value**
ρ_m	1 msg/cycle
α_m	0.5 mJ
β_m	2 mJ
γ_m	0.6 mJ
ω_m	0.1 mW
T	1 s
T_α	100 ms
T_{tx}	10 ms
T_{rx}	10 ms

Table XXXIV – Total energy consumption e_m per network cycle.

Mote m	b_m	μ_m	ω_m	e_m
1	1	4	85 μJ	**4.98 mJ**
2	1.33	5.33	83 μJ	**6.45 mJ**
3	1.33	9.66	79 μJ	**9.04 mJ**
4	1.33	5.33	83 μJ	**6.45 mJ**
5	3	5.66	81 μJ	**9.98 mJ**
6	3	5.66	81 μJ	**9.98 mJ**

Note that mote **3** has considerably higher energy consumption (9.04 mJ) when compared to the consumption of its equivalent neighbors, i.e., motes **2** and **4** (motes **2**, **3** and **4** are two hops away from the base station and, therefore, they can be considered equivalent to each other). This higher energy consumption of mote **3** can be explained by the fact that this mote listens to a large number of messages from its neighbors, due to its location in the network, as can be inferred from the value of μ_3.

It should be noted that the proposed energy estimation model is general in the sense that it can be applied to any network topology. In particular, this model does not require motes to be organized in tiers, according to the number of hops to reach the base station. Basically, the required information about the network is: its adjacency matrix (matrix $\boldsymbol{N}$), how messages are routed towards the base station (matrix $\boldsymbol{F}$) and how many messages each mote generates during a network cycle (vector $\boldsymbol{\rho}$).

Note that the model proposed here does not explicitly consider accessory messages or *handshake messages*, like r*equest to send/clear to send* (RTS/CTS) messages and acknowledgment (ACK) messages [124], [125], [128]. However, these messages can be easily incorporated in the model.

4.4 Energy Distribution

In this section, we discuss a strategy for extending the lifetime of wireless sensor networks, based on assigning motes energy proportionally to their energy expenditure.

In a typical network configuration, the performance of the network depends on every mote of the network, such that if one of the motes stops working properly, the performance of the network can be severely degraded [13]–[16],[44]. For instance, when motes reroute messages of neighbor motes, a malfunctioned mote will affect all routes passing through that mote. Therefore, a widely accepted measure of the network lifetime is the elapsed time between the beginning of the network operation and the moment when one or more motes stop working properly. In our context, we are interested in the situation in which motes stop working due to battery depletion. Therefore, we formally define the lifetime of a network as the elapsed time from the beginning of the network operation until the battery of one or more motes depletes.

It is important to mention that several other definitions of lifetime of wireless sensor networks can be found in the literature [93]–[96]. In addition to the one related to the battery life, other common definitions are the time until the network communication backbone ceases to exist and the time until the message delivery rate reduces below a pre-defined threshold. The motivation for defining the network lifetime based on the battery life is that the replacement of batteries in a wireless sensor network can be demanding or even impractical, and battery depletion is a common cause of network failure.

As we have seen in section 4.3.4, motes may have different energy expenditure, depending on its traffic and its location in the network. Therefore, if the same amount of energy is provided to all motes in the network, the mote with the highest energy expenditure will determine the network lifetime. For instance, if all motes in the example shown in section 4.3 (see section 4.3.4) receive the same energy, mote **5** and **6** would determine the lifetime of the network. The strategy studied in this work for extending the lifetime of a wireless sensor network is based on assigning each mote a battery with the amount of energy proportional to the energy consumption of the mote during a network cycle. By doing so, all motes will cease working approximately at the same time. An additional and important consequence of this strategy is that the remaining energy at batteries after the network ceases working is minimized, reducing the amount of wasted energy. This distribution strategy based on energy consumption was first studied in [113], and has been investigated in several other works found in the literature [7], [8], [98], [99], [113], [114], [146], [147].

In order to apply the proportional energy assignment strategy, we first need to estimate the energy consumed by each mote, per network cycle. Then, we estimate the total energy consumed by the whole network and the fractions of this total energy consumed by the motes. Finally, the energy available to the whole network is distributed to the motes, proportionally to their respective energy consumption. The steps to implement this strategy are summarized in Algorithm 2.

Algorithm 2 **Battery distribution algorithm.**

INPUT:
Energy consumption e_m of each mote in the network
Energy budget of the network

1. Calculate the total energy consumption of the network (sum of all e_m)
2. Calculate the relative consumption of each mote, with respect to the total energy consumption of the network
3. Distribute the energy available according to the relative consumption of each mote

Batteries are the most common source of energy in wireless sensor networks, and energy in batteries is usually indicated in terms of their electric charges (assuming a fixed battery voltage), measured in *milliampere hour* (mAh). Therefore, we adopt the unit milliampere hour to indicate the energy assigned to motes.

To illustrate the application of this strategy of energy distribution, we consider again the network shown in section 4.3, assuming that the energy available for the whole network corresponds to 840 mAh (energy budget). After applying Algorithm 2 in the example (see Fig. 62), the results are presented in Table XXXV.

- **Total energy consumption e_m per network cycle** (also shown in Table XXXV):
  - Mote **1**: e_1 = 4.98 millijoules, relative consumption = 10.62%, **assigned battery: 89.23 mAh**.
  - Mote **2**: e_2= 6.45 millijoules, relative consumption = 13.75%, **assigned battery: 115.57 mAh**.
  - Mote **3**: e_3= 9.04 millijoules, relative consumption = 19.28%, **assigned battery: 161.98 mAh**.
  - Mote **4**: e_4= 6.45 millijoules, relative consumption = 13.75%, **assigned battery: 115.57 mAh**.
  - Mote **5**: e_5= 9.98 millijoules, relative consumption = 21.28%, **assigned battery: 178.82 mAh**.
  - Mote **6**: e_6= 9.98 millijoules, relative consumption = 21.28%, **assigned battery: 178.82 mAh**.

Table XXXV – Battery distribution of the network used in the example.

Mote m	e_m	Relative Consumption	Assigned Battery
1	4.98 mJ	10.62%	**89.23 mAh**
2	6.45 mJ	13.75%	**115.57 mAh**
3	9.04 mJ	19.28%	**161.98 mAh**
4	6.45 mJ	13.75%	**115.57 mAh**
5	9.98 mJ	21.28%	**178.82 mAh**
6	9.98 mJ	21.28%	**178.82 mAh**
Total	**46.88 mJ**	**100%**	**840 mAh**

The total energy required by all six motes is 46.88 mJ, per network cycle. Table XXXV shows the result of distributing 840 mAh among all six motes proportionally to their energy consumption.

Note that the values of energy assigned to each mote did not consider the restriction that batteries are commercially available in certain values of energy only. The problem of assigning energy to mote considering this additional restriction and the assortment of battery sets available in the market is well addressed in [98], [99], which is out of the scope of the present work.

4.5 Numerical Analysis

In this section, we explore in further details the problem of network lifetime and energy distribution strategies. More specifically, using the energy model proposed in section 4.3, we evaluate the effects of the energy assignment on the lifetime of a wireless sensor network, considering different scenarios in terms of network topology, network cycle duration and different strategies for energy distribution. Two energy distribution strategies are investigated: the *uniform distribution strategy*, according to which motes are assigned the same amount of energy, and the *proportional distribution strategy*, which was discussed in section 4.4.

4.5.1 Network Topology and Parameter Setting

This numerical analysis is carried out by means of simulation, considering a network with 34 motes, shown in Fig. 66 by means of a graph. As before, an edge in this graph connecting two motes means that these motes can communicate with each other without errors. On the other hand, the absence of an edge between two motes means that their transmissions do not disturb each other.

All motes send their messages to a base station, using multi-hop connections. Three different base station locations are tested, as shown in Fig. 67: at the middle of the network (**a**), near the edge of the network (**b**), and outside the network area (**c**). These three base station locations lead to representative scenarios regarding the traffic distribution among motes, which, as we will see, affects the energy consumption and network lifetime, as pointed in [136].

We consider a simple architecture for the motes [85], composed by battery, radio transceiver, microcontroller, and a temperature sensor, as shown in Fig. 68.

We assume that motes are built with off-the-shelf components: Xbee PRO [60] for the radio transceiver, Atmega8L [87] as the microcontroller, and LM75 [86] for the temperature sensor.

The energy consumption and characteristics of each state were both retrieved from datasheets and by direct measurements [18], and are shown in Table XXXVI.

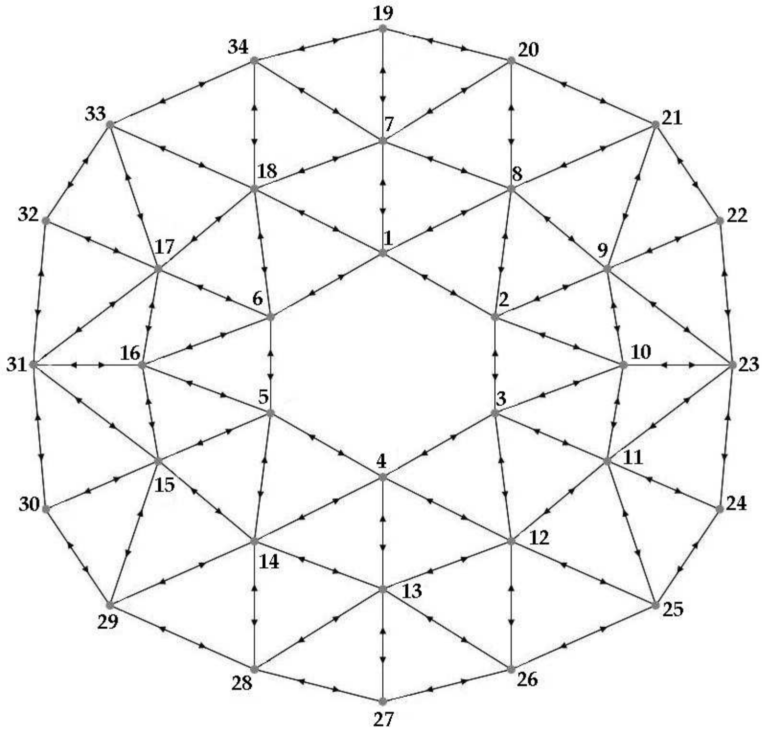

Fig. 66 – Network topology used in the numerical analysis.

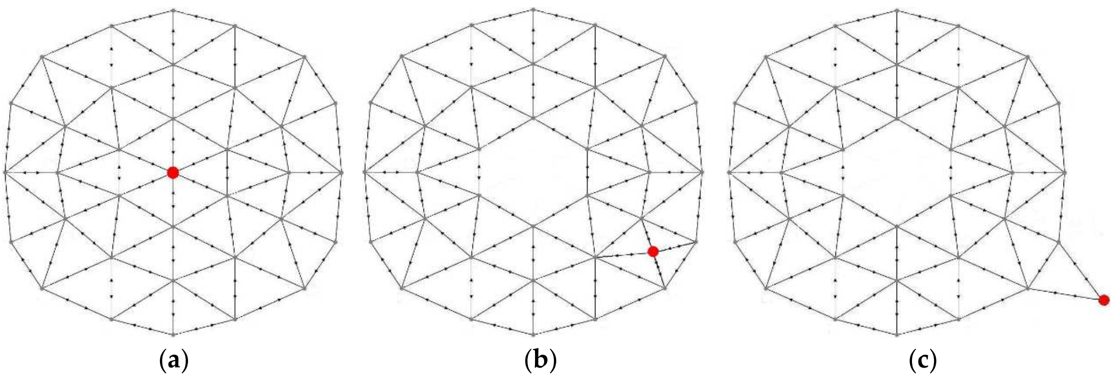

Fig. 67 – Three base station locations were tested: (**a**) at the center of the network; (**b**) near the edge of the network; (**c**) outside the network.

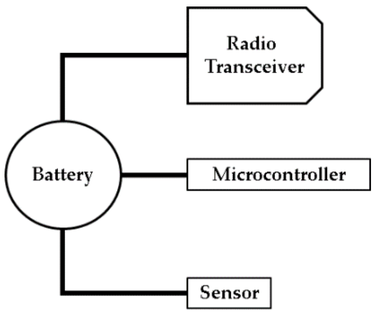

Fig. 68 – Mote architecture.

- **Characteristics of the simulated motes** (also shown in Table XXXVI**)**:
  - Energy for reading sensors – α_m: 0.3 millijoules.

- Transmitting a message – β_m: 1.92 millijoules.
- Receiving a message – γ_m: 0.36 millijoules.
- Secondary states – ω_m: 0.06 milliwatts.
- Time spent by a mote to read all its sensors and assemble a new message – T_α: 100 milliseconds.
- Time spent by a mote to transmit a message – T_{tx}: 3 milliseconds.
- Time spent by a mote to receive and process a message – T_{rx}: 0.6 milliseconds.

Table XXXVI – Characteristics of the simulated motes.

Characteristics	Energy and Power Consumption
Energy for reading sensors – α_m	0.3 mJ
Transmitting a message – β_m	1.92 mJ
Receiving a message – γ_m	0.36 mJ
Secondary states – ω_m	0.06 mW
Time spent by a mote to read all its sensors and assemble a new message – T_α	100 ms
Time spent by a mote to transmit a message – T_{tx}	3 ms
Time spent by a mote to receive and process a message – T_{rx}	0.6 ms

In order to evaluate the effect of traffic load on the performance of both energy distribution strategies, we considered three network cycles T: (*i*) one second; (*ii*) 600 seconds (10 minutes); (*iii*) 86,400 seconds (24 hours). These values are representative for a wide variety of sensor network applications. In all three traffic scenarios, we assume that all motes transmit one message per network cycle, i.e., $\rho_m = 1$, for all m.

The routing protocol adopted in the analysis implements a simple probabilistic routing, according to which a mote forwards its messages (its own messages and routed messages) to one of its closest successor neighbors (in terms of number of hops), randomly chosen, as illustrated in Fig. 69. The final destination of all messages is the base station.

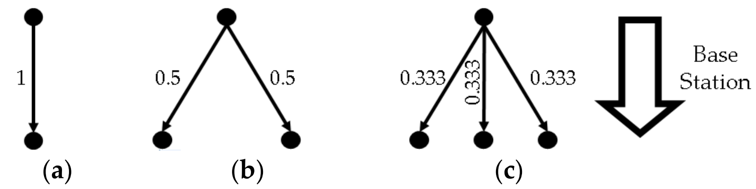

Fig. 69 – Example of a mote with one successor (**a**); two successors (**b**); three successors (**c**).

4.5.2 Simulation Model

The estimation of the network lifetime is performed by means of simulation. The structure of this simulation is organized as follows:

1. The available amount of energy for the whole network is distributed among all motes, according to the considered distribution strategy, i.e., uniform distribution or proportional distribution. In the case of proportional distribution, the amount of energy spent by each mote is determined using the energy model proposed in section 4.3, based on parameters and topology of the network.
2. The simulation then begins, and time advances in fixed steps equal to the chosen network cycle T.
3. At each network cycle, motes perform their respective tasks, i.e., sensor reading (packet generation), packet transmission, and packet reception. After each task is performed the respective amount of energy (indicated in Table XXXVI) is removed from the battery charge. The simulation run stops when any given mote is not able to perform its tasks due to insufficient energy in its battery. The lifetime of the network is then estimated as the duration of the simulation run (i.e., the number of network cycles until the simulation stops).

It should be noted that, in the simulation runs, the energy spent by motes due to each task (i.e., sensor reading, transmission, and reception) are individually removed from the battery as these tasks are performed. The estimated total energy spent by motes per network cycle provided by the proposed model are used only to assign the initial changes of the batteries (in the case of proportional distribution).

In all experiments, the available amount of energy for the whole network is 4760 mAh. Therefore, when the uniform energy distribution strategy is used, each mote is assigned a battery of capacity equals to 140 mAh. When the proportional distribution strategy is employed, two schemes are used in the simulation:

- **Scheme 1**: Each mote is assigned the exact amount of energy calculated using the proportional distribution strategy;
- **Scheme 2**: Each mote is assigned a set of batteries of commercially available values, whose total energy is as close as possible to the exact amount of energy calculated using the proportional distribution strategy. For this scheme, the values of batteries manufactured by Panasonic were adopted [193].

The tasks performed by each mote in the simulation (sensor reading, message assembly, message transmission and message reception) are described in Algorithm 3 and Algorithm 4.

Algorithm 3 **Regular operation of a mote in the simulation.**

1. **REPEAT**
1. Activate microcontroller and read sensor,
2. Assemble and send a message,
3. Switch sensor, radio and microcontroller to sleep mode.
4. **UNTIL** battery energy is not depleted.

Algorithm 4 **Processing a received message.**

PROCEDURE Reception
1. Activate microcontroller and process message
2. **IF** message received is addressed to the receiving mote **THEN**
3. Reroute message to the next hop
4. **END IF**
5. Switch radio and microcontroller to sleep mode

Recall that, as discussed in section 4.3, we assume the network employs a perfect medium access control (MAC) protocol that guarantees contention-free transmissions and error-free reception.

4.5.3 Results

In this section, we analyze the performance of the network presented in Fig. 66 regarding energy consumption. Firstly, we analyze the accuracy of the proposed energy model, by comparing the energy consumptions calculated using the proposed model with the simulated results. Next, we investigate the effects of the network cycle and the location of the base station on the energy expenditures of motes. Then, the network lifetimes under different scenarios are analyzed for both strategies of energy distribution. Finally, we study the remaining energy in the whole network after the network stops working.

4.5.3.1 Accuracy of the proposed energy model

Table XXXVII shows the energy consumed per network cycle by some motes of the network investigated, using the proposed model and simulation.

- **Energy e_m consumed by some motes, per network cycle: calculated (using the proposed model) and simulated values** (also shown in Table XXXVII**)**:
  - Mote **5**: calculated e_5 = 21.787 millijoules, simulated e_5 = 21.786 millijoules.
  - Mote **12**: calculated e_{12} = 40.963 millijoules, simulated e_{12} = 21.962 millijoules.
  - Mote **25**: calculated e_{25} = 51.323 millijoules, simulated e_{25} = 51.324 millijoules.
  - Mote **31**: calculated e_{31} = 6.389 millijoules, simulated e_{31} = 6.389 millijoules.

Table XXXVII – Energy e_m consumed by some motes, per network cycle: calculated (using the proposed model) and simulated values.

Mote *m*	**Calculated e_m**	**Simulated e_m**
5	21.787 mJ	21.786 mJ
12	40.963 mJ	40.962 mJ
25	51.323 mJ	51.324 mJ
31	6.389 mJ	6.389 mJ

The results presented in Table XXXVII show a good agreement between simulated and calculated results, with differences below 1%.

Table XXXVII shows only the results for motes **5**, **12**, **25** and **31** since these motes have different workloads, due to their locations in the network, leading to different energy consumptions. As expected, mote 25 has the largest energy expenditure, since it is the closest one to the base station, while mote 31 has the lowest energy expenditure, as this mote forwards very few packets. Therefore, as discussed in previous sections, some motes are indeed overburdened by other motes depending on their locations in the network, thus, requiring more energy.

4.5.3.2 Distribution of the Energy Expenditure

In this section, we discuss the effect of the base station location and the network cycle on the distribution of energy expenditure throughout the network. Fig. 70 (**a**)-(**c**) present the energy expenditure of each mote, for all three base station locations, with network cycle $T = 1$ second.

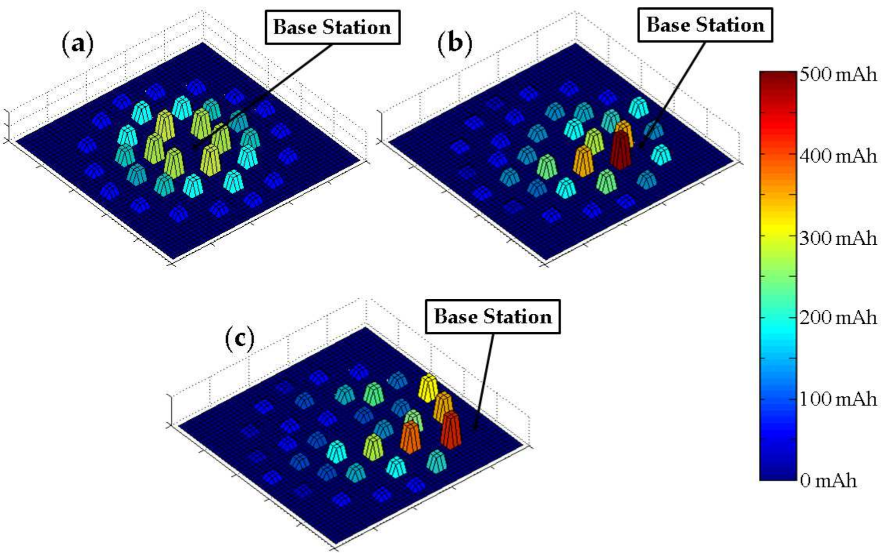

Fig. 70 – Energy distribution for all three base station locations, for network cycle $T = 1$s.

As already pointed out, motes close to the base station have higher energy expenditures due to their extra workloads, caused by message routing and promiscuous reception. Note, however, that when the base station is located near the center of the network, it can be directly reached by a larger number of motes, spreading this extra workload over a larger number of motes. It is important to notice that the energy distribution pattern shown in Fig. 70 (**a**)-(**c**) may lead to the so-called Energy Hole/Doughnut Effect [7], [8], [109]–[114], [194]–[196] when motes are assigned the same amount of energy.

Fig. 71 (a)-(c) show similar results to those presented in Fig. 70, but now for network cycles of 600 seconds and 86400 seconds. We can see that the difference among the energy consumed by motes reduces as the network cycle increases. This result can be explained by recalling that the highest energy consuming tasks are transmission and reception [18]. If the network cycle is large, then the fraction of energy spent with transmission and reception reduces, as the number of transmissions and receptions per time unit reduces. Therefore, the energy spent with secondary states, which does not depend on the physical location of the mote, becomes more relevant, and the levels of energy expenditure throughout the network area tend to be invariant with respect to the mote location.

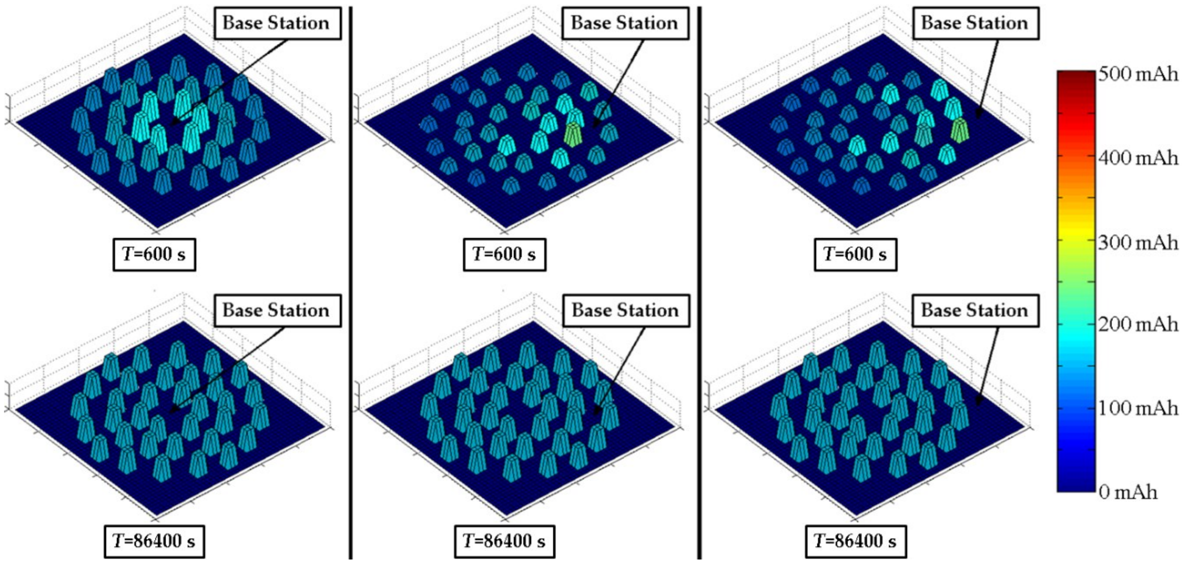

(**a**) (**b**) (**c**)

Fig. 71 – Energy distribution for all three base station locations, for $T = 600$ s and $T = 86400$ s.

4.5.3.3 Lifetime

In this section, we analyze the lifetime extension when the proportional energy distribution strategy is employed. As discussed in section 4.4, we define the lifetime of a network as the length of the interval between the moment the network operation begins until the moment the first mote runs out of battery. Table XXXVIII shows the lifetimes of the network for all three network cycles, under the uniform energy distribution and the two versions of proportional energy distribution strategy (i.e., exact energy is assigned and a combination of commercial battery set is assigned). These results correspond to scenario in which the base station is located at the center of the network area (see Fig. 67 (**a**)).

- **Network lifetimes with base station located at the center of the network** (also shown in Table XXXVIII**)**:
    - o **Network cycle of 1 second**: using uniform battery distribution: 22.9 hours; using battery set: 46.2 hours; using the exact calculated battery values: 46.9 hours.
    - o **Network cycle of 600 seconds:** using uniform battery distribution: 4492.1 hours; using battery set: 5297 hours; using the exact calculated battery values: 5397.6 hours.
    - o **Network cycle of 86400 seconds**: using uniform battery distribution: 6644.3 hours; using battery set: 6655.7 hours; using the exact calculated battery values: 6655.7 hours.

Table XXXVIII – Network lifetimes with base station located at the center of the network.

Network Cycle *T*	**Uniform Dist.**	**Proportional Dist. (Batt. Set)**		**Proportional Dist. (Exact)**	
	Lifetime	**Lifetime**	**Lifetime Enhancement**	**Lifetime**	**Lifetime Enhancement**
1 s	22.9 h	46.2 h	102 %	46.9 h	105 %
600 s	4492.1 h	5297 h	17.9 %	5397.6 h	20 %
86400 s	6644.3 h	6655.7 h	0.2 %	6655.7 h	0.2 %

We can see that the proportional distribution strategy always results in a longer lifetime. We can also see that the lifetime enhancement is more pronounced in networks with lower network cycle times. In fact, the lifetime enhancement achieved with the proportional distribution strategy depends on the degree of the discrepancy among the levels of energy consumed by the motes, which, in turn, is related to the frequency with which messages are generated. If messages are generated more frequently (i.e., low network cycle time), then the energy spent with transmission and reception operations is proportionally higher (with respect to the total energy expenditure of a mote), and the amounts of energy spent by motes will be more heterogeneously distributed throughout the network, as we can see in Fig. 70 and Fig. 71. Therefore, when energy is assigned uniformly, motes with high energy expenditure (i.e., those close to the base station) will collapse sooner and the network lifetime is shortened. On the other hand, when energy is assigned proportionally to the energy expenditure of the mote, all motes tend to stop working at the same time, and the lifetime is increased.

Table XXXIX and Table XL show results similar to those presented in Table XXXVIII, but now for the other two base station locations, i.e., near the edge of the network, and outside the network, respectively.

- **Network lifetimes with base station located near the edge of the network** (also shown in Table XXXIX):
    - **Network cycle of 1 second**: using uniform battery distribution: 7.9 hours; using battery set: 27.3 hours; using the exact calculated battery values: 27.3 29.3 hours.
    - **Network cycle of 600 seconds:** using uniform battery distribution: 2777.8 hours; using battery set: 4775.3 hours; using the exact calculated battery values: 4837.9 hours.
    - **Network cycle of 86400 seconds**: using uniform battery distribution: 6602.3 hours; using battery set: 6643.7 hours; using the exact calculated battery values: 6649.1 hours.
- **Lifetimes of the network with base station located outside the network** (also shown in Table XL):
    - **Network cycle of 1 second**: using uniform battery distribution: 8.2 hours; using battery set: 25.7 hours; using the exact calculated battery values: 27.4 hours.
    - **Network cycle of 600 seconds:** using uniform battery distribution: 2829.5 hours; using battery set: 4661.5 hours; using the exact calculated battery values: 4747.1 hours.
    - **Network cycle of 86400 seconds**: using uniform battery distribution: 6604.3 hours; using battery set: 6647.9 hours; using the exact calculated battery values: 6648 hours.

Table XXXIX – Network lifetimes with base station located near the edge of the network.

Network Cycle *T*	**Uniform Dist.**	**Proportional Dist. (Batt. Set)**		**Proportional Dist. (Exact)**	
	Lifetime	**Lifetime**	**Lifetime Enhancement**	**Lifetime**	**Lifetime Enhancement**
1 s	7.9 h	27.3 h	245 %	29.3 h	270 %
600 s	2777.8 h	4775.3 h	71.9 %	4837.9 h	74 %
86400 s	6602.3 h	6643.7 h	0.62 %	6649.1 h	0.7 %

Table XL – Lifetimes of the network with base station located outside the network.

Network Cycle *T*	Uniform Dist.	Proportional Dist. (Batt. Set)		Proportional Dist. (Exact)	
	Lifetime	Lifetime	Lifetime Enhancement	Lifetime	Lifetime Enhancement
1 s	8.2 h	25.7 h	213.9 %	27.4 h	234 %
600 s	2829.5 h	4661.5 h	64.8 %	4747.1 h	68 %
86400 s	6604.3 h	6647.9 h	0.66 %	6648 h	0.7 %

When we compare the lifetimes of all three base station locations, for a given network cycle time and distribution strategy, we note that the network lifetime consistently reduces as the base station moves from the center to outside the network. This can be explained by noting that when the base station is located at the center of the network, the workload due to message routing is more evenly distributed among the motes. On the other hand, when the base station is located far from the network center, few motes are responsible for a larger fraction of the operations needed to deliver messages to the base station. Consequently, these motes will collapse sooner, unless they are assigned a larger amount of energy, leaving the rest of the motes with a smaller amount of energy. This also explains the larger lifetime enhancement achieve with proportional energy distribution, when the base station is located far from the center of the network [136].

4.5.3.4 Remaining Energy

Lifetime extension is one of the benefits achieved when the proportional energy distribution is employed. Another effect of this energy distribution strategy is that, at the end of the network life, all motes will have their batteries almost completely depleted. On the other hand, with the uniform distribution strategy, some motes will still have a large amount of energy left stored in their batteries at the end of the network operation. For example, for the three network configurations considered in this section, the remaining energy levels after the network stops working are shown in Table XLI.

- **Remaining energy (in percentage of the initial energy) after the network stops working** (also shown in Table XLI**)**:
    - **Uniform distribution in network cycle of 1 second**: base station at center: 32.2%, base station near the edge of the network: 72.9%, base station outside of the network: 70%.
    - **Uniform distribution in network cycle of 600 seconds**: base station at center: 14.4%, base station near the edge of the network: 42.6%, base station outside of the network: 40.4%.

- **Uniform distribution in network cycle of 86400 seconds**: base station at center: 0.2%, base station near the edge of the network: 0.7%, base station outside of the network: 0.7%.
- **Proportional distribution in network cycle of 1 second, using battery set**: base station at center: 1.58%, base station near the edge of the network: 7.62%, base station outside of the network: 6.1%.
- **Proportional distribution in network cycle of 600 second, using battery set:** base station at center: 1.35%, base station near the edge of the network: 1.3%, base station outside of the network: 1.76%.
- **Proportional distribution in network cycle of 86400 second, using battery set:** base station at center: 0.01%, base station near the edge of the network: 0.08%, base station outside of the network: 0.01%.
- **Proportional distribution, using the exact calculated battery values:** less than 0.01% in almost all scenarios.

Table XLI – Remaining energy (in percentage of the initial energy) after the network stops working.

Network Cycle *T*	**Average Remaining Energy**								
	Uniform Dist.			**Proportional Dist. (Batt. Set)**			**Proportional Dist. (Exact)**		
	BS at center	**BS near edge**	**BS outside**	**BS at center**	**BS near edge**	**BS outside**	**BS at center**	**BS near edge**	**BS outside**
1 s	32.2%	72.9%	70.0%	1.58%	7.62%	6.10%	< 0.01%	< 0.02%	< 0.01%
600 s	14.4%	42.6%	40.4%	1.35%	1.3%	1.76%	< 0.01%	< 0.01%	< 0.01%
86400 s	0.2%	0.7%	0.7%	0.01%	0.08%	0.01%	< 0.01%	< 0.01%	< 0.01%

As expected, significant amounts of energy remain in the batteries after the network collapses when the network cycle time is low, which corresponds to the case of the largest lifetime enhancement. In comparison, practically no energy is left in the batteries in all network configurations when the proportional energy distribution is employed.

It should be noted that in a practical implementation of the strategy of proportional energy distribution, the amount of energy assigned to each mote depends on the available set of batteries, and the exact energy distribution may not be feasible. Therefore, lower lifetime enhancement and higher energy waste should be expected.

4.6 Concluding Remarks

The lifetime of wireless sensor networks is one of the main issues that network designers and operators face when deploying and operating a network. In most applications, motes of wireless sensor networks are powered by batteries, which in many situations are difficult to be recharged or replaced, possibly reducing the network lifetime. Appropriate energy distribution among motes is known to be a good strategy to overcome this problem. The estimation of the energy consumed by each mote in a wireless sensor network is an important step in any energy distribution procedure. In this chapter, we proposed a model to estimate the energy consumed by motes in an arbitrary wireless sensor network, with no physical topology constraints. The proposed model assumes a time-driven network and considers the primary states (e.g., transmission and reception operations) as well as the secondary states (e.g., sleep mode) of a mote. The model also includes in the energy budget calculation the effects of message routing and the reception of unsolicited packets. Based on the proposed model, we investigated the effects of energy distribution on the lifetime, among other metrics, of a network with several motes and one base station, which is the destination of all messages. Two different strategies of energy distribution were investigated: (*i*) assigning the same energy to all motes, and (*ii*) assigning an amount of energy proportional to the energy spent by the mote. In order to assess the effectiveness of the proposed model, a numerical analysis was performed with different network topologies and, in all cases, for the sake of comparison, the networks were simulated considering both energy strategies cited above, without increasing the energy budget of whole the network. Results show that a lifetime extension can be achieved when proportional energy distribution is used, and that the benefits of this energy distributing strategy are more pronounced when the degree of discrepancy among the levels of energy spent by different motes is high and when the network cycle is short. The degree of discrepancy among energy consumption levels is affected by tasks related to message routing (motes closer to the base station have a higher workload and, therefore, higher energy expenditure) and by the base station location (when the base station is located near the center of the network, the extra workload due to message forwarding is shared among a larger number of motes). The simulation results have also shown that the estimations of the energy expenditure of motes provided by the proposed model are sufficiently accurate.

Chapter V

IMPACT OF MULTIPLE BATTERY LEVELS AND MULTIPLE TRANSMISSION POWER LEVELS ON WIRELESS SENSOR NETWORKS

In this chapter, the use of multiple transmission levels, analyzed in Chapter III and in [19], [20], and the strategies for calculating the individual energy consumption and the battery distribution heuristic, presented in Chapter IV, are examined on three different network topologies in 54 distinct scenarios. The simulated networks were designed to have different levels of topology irregularity, from a well-organized network, with its base station exactly in its center to a network with its base station isolated from the network cluster. The results are presented and discussed among the sections and some further and associated analysis are presented in the Chapter Summary and Concluding Remarks section.

For supporting an easier usage of screen reader software, this chapter repeats some discussion and definitions already made in previous chapters.

5.1 Introduction

The prediction made by Moore in 1965 [10] is still valid for equipment that uses integrated electronic circuits, turning computational limitations, for both hardware and software, just transient topics. However, all electronic devices need electrical energy to work, making the energy consumption issue a serious problem.

As pointed in [61], the energy consumption of a Wireless Sensor Network mote is the summation of the individual consumption of all its parts. Each one of these components, generally, has multiple states and different consumptions levels related to them. Manufacturers are increasingly achieving low power consumption [62] but, when performing a long-term analysis, even the few microamperes consumed by idle and sleep states are not negligible for a Wireless Sensor Network mote.

The energy amount consumed by inactive states has a direct proportionality to the time spent in these states. Therefore, a Wireless Sensor Network that generates and sends more messages spends less energy on these unimportant states than a low-activity WSN. Among the main active tasks of a WSN mote, transmitting is one that requires more power for being performed [1].

It would be reasonable to imagine that the best solution to increase network lifetime would just give the largest amount of energy possible to each mote. Nevertheless, as pointed out in [1], [11], in some cases, almost 90% of the energy of a network is not used even when the network is inoperative. Therefore, it is essential to understand and quantify the amount of energy consumed by each task performed by motes in a network and hence make the best use of the energy available.

In this work, we present a strategy to increase the lifetime of Wireless Sensor Networks maintaining the same energy budget, i.e., using the same amount of energy and making a Wireless Sensor Network operational for a longer period of time.

The energy consumption is a complex and sensible subject for Wireless Sensor Networks, consequently, it is the main topic in many published works. Among different parameter related to energy consumption, the network lifetime [93]–[96] is a fundamental metric in a Wireless Sensor Network model, therefore, it is also covered in distinguished studies aiming the prolongation of Wireless Sensor Network lifetimes. Besides the emerging energy harvesting techniques [6], [158], it is accepted that the network lifetime is limited by the battery charge [1], [6], [9]. Furthermore, depending on the Wireless Sensor Network deployment place and its application, like battlefields or disaster areas, battery replacement can be either prohibitively expensive or hazardous [2], [6].

In [6], the network lifetime maximization techniques are divided into:

- Resource allocation using cross-layer design;
- Opportunistic transmission schemes/Sleep-wake scheduling;
- Routing/Clustering;
- Mobile relays and sinks;
- Coverage connectivity/Optimal deployment;
- Data gathering/Network Coding;
- Data correlation;
- Energy Harvesting;

- Beamforming.

The works related to the aforementioned network lifetime maximization techniques are referenced in [6].

According to the analysis presented in [109], [110], [113], [114], [159], the energy consumption of each mote is not uniform and varies depending on its the relative placement. As Wireless Sensor Networks rely on multi-hop routing [27], [95], [176], [190]–[192], this unbalanced consumption can cause battery depletion in certain sections of a network, which can lead to a fatal disruption in the connections between some active motes and the base station. This effect was initially more in-depth studied, but not exclusively, in circular networks and is called Energy Hole or Doughnut Effect [7], [8], [109]–[114], [194]–[196]. In [8], the techniques for avoiding Energy Holes are divided into:

- Clustering Based Techniques;
- Non-Uniform Node Distribution Techniques;
- Mobility Based Techniques;
- Region Based Techniques;
- Transmission Based Techniques;
- Optimization Based Techniques;
- Genetic Algorithm Based Techniques;
- Node Deployment Techniques.

The works related to the aforementioned techniques for avoiding Energy Holes are referenced in [8].

Complementing the aforementioned techniques, there is also an approach that, instead of allocating more motes in a specific highly demanded section of the Wireless Sensor Network, allocates more energy for the motes in this particular section [7], [8], [98], [99], [113], [114]. The usage of different sets, which is a way of assigning distinct amounts of energy to the motes, is addressed in a financial perspective in [98], [99].

Regarding the physical topology of a network, in real-world scenarios, many obstacles can forbid a perfect physical or logical organization of a network, which is required by some strategies [6]. Obstacles like trees, lakes, rocks, buildings, walls or even the shape of the field where the network will be deployed can interfere in the construction of a network with a circular pattern or any other type of perfect-organized physical topology.

5.2 Multiple Transmission Power Levels

The use of multiple/dynamic transmission power levels is employed in both in academic works [63]–[67] and commercial products [60], [68]–[70], having the potential to be employed in Wireless Sensor Networks motes. A common and widespread technology that uses multiple/dynamic transmission power levels is the Bluetooth [71], [72], specifically, the Class 1 devices [73], [74].

This subject is further analyzed in Chapter III and in [19], [20].

5.3 Energy Distribution

The operation of Wireless Sensor Networks is based on the cooperative behavior of many motes spread over a given area, generally relying only on their supplied batteries. Since motes have no other energy source and replacing the batteries of each mote spread over a wide area is such a challenging task [2], [6], strategies for reducing energy consumption have recently received a great deal of attention.

It would be reasonable to imagine that the best solution to increase network lifetime would just give the largest amount of energy possible to each mote. Nevertheless, as pointed out in [1], [11], in some cases, almost 90% of the energy of a network is not used even when the network is inoperative.

As pointed in [109], [110], [113], [114], [159], the energy consumption of each mote is not uniform and varies depending on the mote's location. This effect was more in-depth studied in circular networks and the consequence of the unbalanced consumption, which leads to a fatal interruption of message flow toward the base station, has been called Energy Hole or Doughnut Effect [7], [8], [109]–[114], [194]–[196]. Two known strategies have proven to be effective mechanisms to increase the lifetime of circular networks: one is based on increasing the number of motes (density) near the base station [109], [110] while the other suggests to allocate more batteries on the motes near the base station [113], [114]. Both strategies address the problem of a Wireless Sensor Networks lifetime by allocating more energy to motes located in a specific area of the network.

The strategies of energy reallocation proposed in [7], [8], [98], [99], [113], [114] are very effective, but restricted to circular networks.

In this chapter, we use the energy distribution technique presented and analyzed in Chapter IV, that calculates and assigns a proportional battery set to each mote according to their energy consumption, regarding the network topology.

5.4 The Cost of a Wireless Sensor Network

Besides the Wireless Sensor Networks paradigm states that they are made of inexpensive motes, the price of many parts used in these motes still not insignificant. Some commercial motes have even higher prices, over US$60 [75]–[79], due to their integrated and assembled equipment. As Wireless Sensor Network motes are high technology tools, it is feasible that they are not very cheap when they are produced.

As a Wireless Sensor Network can be constituted by thousands of motes, its total cost has a direct proportionality with both the price of its motes and its dimension. Another issue, which can cause both monetary and environmental damages, is the deployment of potentially harmful parts, especially batteries, in a sensible environment [80]–[84].

5.5 Methodology

This chapter was made using Matlab simulations [12]–[17], data acquired from both direct measurements (detailed in Chapter II and in [18]) and the respective datasheets of each component, and, Mathematical models used in related academic literature (referenced along the text). The results were also confronted with some previous academic works in order to ascertain their validity.

5.5.1 Mote Architecture

The motes considered in the analysis presented in this chapter follow a basic architecture, having one battery, one microcontroller, one radio transceiver and one sensor [85], as shown in Fig. 72. Each mote used Digi XBee PRO [60] as its radio transceiver, Texas Instruments LM75 [86] as its sensor, Atmel Atmega8L [87] as its microcontroller and CR 1632 as its battery (140 mAh; one per mote).

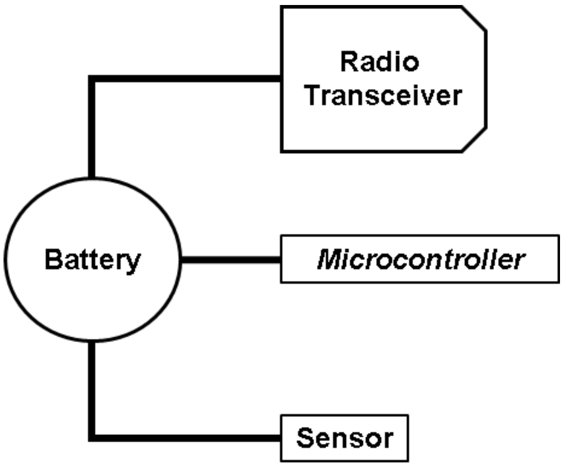

Fig. 72 – Mote architecture.

5.5.2 Energy Consumption

The motes considered in the analysis presented in this chapter follow a simple architecture, having a battery, a microcontroller, a radio transceiver and a sensor [19], [20], [85]. The energy consumption model used in this chapter is shown in Equation (1) and described below:

- The total energy consumption of a mote at a given time is equals to the summation of the energy consumption of its radio module, its sensor, and its microcontroller.

$$c_m(t) = c_r(t)+c_s(t)+c_\mu(t), \tag{1}$$

where c_m is the total consumption of a mote and c_r, c_s and c_μ are, respectively, the consumption of its radio module, sensor and microcontroller. In order to achieve accurate results, we followed the current consumption of each component given by direct measurements [18] (Xbee active states) and their respective datasheets. As shown in their datasheets [60], [86], [87], all parts have different consumption levels according to their current states, consequently, these different levels were computed in our simulations. The sleep state was the standard state of all parts, thus, all parts just changed to active states when a new message had to be generated or only the radio module and the microcontroller when a mote had to receive a message.

5.5.2.1 Primary and Secondary Energy Consumption

We divide the energy consumption into two categories: Primary and Secondary. Primary energy consumption refers to the energy consumed by active states, like reading sensors, processing data, transmitting or receiving messages etc. Secondary energy consumption refers to the energy consumed by inactive states, like idle and power-down/sleep states [60], [86]–[88].

It is important to note that every electronic part used in a mote consumes energy, including when they are in secondary states, like idle and sleep and that the energy consumption of secondary states is usually very low when compared to the primary states [18].

5.5.3 Transmission Power Levels

In order to calculate the power of the received signal, denoted by P_{rx}, by motes at a given distance, we assumed the Plane Earth Propagation Model [89], which is shown in Equation (2) and described below:

- The reception power is equals to the multiplication of the transmission power, the antenna gain of the transmitter, the antenna gain of the receiver, the square of the antenna height of the transmitter and the square of the antenna height of the receiver, all them divided by the distance between the antennas raised to the power of the path loss exponent of the medium which, in this chapter, is set to **3.5** in all scenarios.

$$P_{rx} = \frac{P_{tx} G_{tx} G_{rx} h_{tx}{}^2 h_{rx}{}^2}{d^\gamma}, \tag{2}$$

where P_{tx} is the transmission power which, in this chapter, is the Xbee PRO [60] maximum transmission power; G_{tx} and G_{rx} are the antenna gains of the transmitter and the receiver, respectively; h_{tx} and h_{rx} are, respectively, the heights of the transmitter and receiver antennas; d is the distance between transmitter and receiver antennas, and γ is the path loss exponent, which, in this chapter, is set to **3.5** [90]–[92].

As all motes have the same antenna gains and heights, in order to keep the same P_{rx} at different distances, the transmission power P_{tx} was the only adjustable parameter. Letting d be denoted by the maximum distance that two motes can communicate with the standard transmission power P_{tx}, the transmission power levels used in this chapter are:

- **Path loss exponent set to <u>3.5</u>** (also shown in Table XLII**)**:
    - P_{tx} reaching d; $11.31P_{tx}$ reaching $2d$; $46.76P_{tx}$ reaching $3d$.

Table XLII – Transmission power levels used for a path loss exponent set to **3.5**.

Distance	**Transmission Power**
d	P_{tx}
$2d$	$11.31P_{tx}$
$3d$	$46.76P_{tx}$

In the simulations of this chapter, we analyzed three different situations (also shown in Fig. 73):

- All motes transmitting for reaching one hop.
- Motes transmitting for reaching two hops.
- Motes transmitting for reaching three hops.

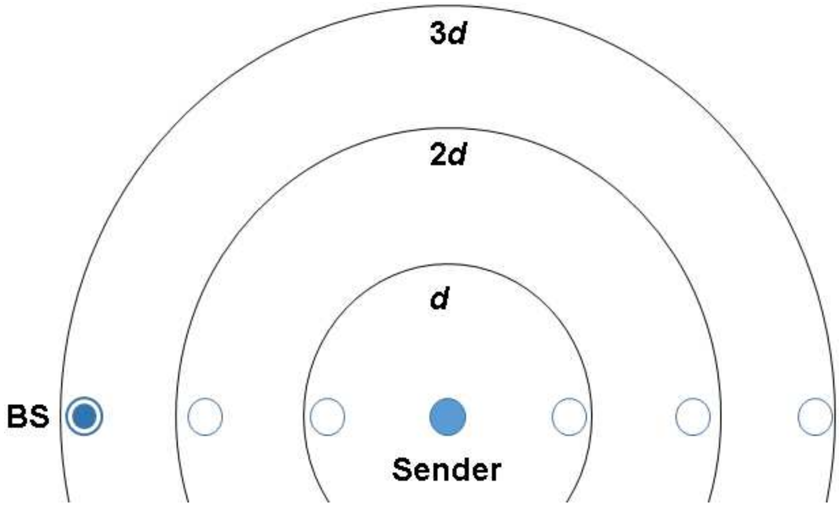

Fig. 73 – Transmission radius with different power levels.

As all motes transmit their messages towards a single base station, their maximum transmission power levels did not exceed the power needed to reach the base station in any situation.

5.5.4 Network Lifetime

The network lifetime [93]–[96] of a WSN can have different definitions: the time until the network communication backbone ceases to exist; the time until the message delivery rate is bellow a threshold or when one or more motes have their battery depleted. Since this work focuses on energy consumption, the adopted definition of network lifetime does not account for other factors but tasks that consumes the battery charge of the WSN motes.

In this chapter, we defined the lifetime of a WSN as the period of time from the moment the network operation begins until the first mote runs out of battery, as considered in [19], [93]–[97]. The energy budget of all networks is 4760 mAh, which is equally divided into the homogeneous distribution scenarios, assigning 140 mAh batteries to each mote. Assuming our simulated mote model, a 140 mAh battery provides the maximum lifetime, i.e., when the mote neither sends nor receives messages, of 6666.67 hours.

5.5.5 Energy Distribution Heuristic

In order to extend the network lifetime, each mote should receive amounts of energy proportional to its energy consumption. After calculating the energy consumption of each mote in the network, the amount of energy assigned to each mote is adjusted to be proportional to its consumption per network cycle.

Due to the repetitive behavior time-driven networks have at each network cycle, the energy consumption of each mote can be used to calculate both the total network consumption per network cycle and the energy required by each mote in order to efficiently perform its tasks. By using our proposed heuristic, presented in Algorithm 5, each mote can receive a percentage of the total energy available to the network according to its individual consumption, therefore, keeping the energy budget unchanged.

Algorithm 5 – Battery redistribution algorithm.

INPUT:
Energy consumption e_m of each mote in the network
Energy budget of the network activate microcontroller and read sensor

1. Calculate the total energy consumption of the network (summation of all e_m)
2. Calculate the relative consumption of each mote in comparison to the total energy consumption of the network
3. Distribute the energy available according to the relative consumption of each mote

Batteries are the primary power source used in Wireless Sensor Network motes [1], [6], [9] and, for this reason, the energy redistribution can be performed by assigning larger capacity batteries or battery sets to each mote [7], [8], [98], [99], [113], [114].

In this chapter, we defined the lifetime of a Wireless Sensor Network as the period of time from the moment the network operation begins until the first mote runs out of battery, as considered in [19], [93]–[97]. The energy budget of all networks is 4760 mAh, which is equally divided into the homogeneous distribution scenarios, assigning 140 mAh batteries to each mote.

5.5.6 Batteries

The batteries models used in the simulations of this chapter followed the charges available in the commercial coin models manufactured by Panasonic Corporation [197]. The choice of using coin batteries relied on the fact that they already have compatible voltage with all parts used in the simulated motes and also have different capacities (charges), allowing the assemblage of different batteries sets [98], [99] according with calculated to each mote using the technique shown in Chapter IV.

The battery models of Lithium – Manganese Dioxide, Lithium – Carbon Monofluoride and Lithium – High Temperature Operation [193] used to assemble the batteries sets used in the simulations are shown, respectively, in Table XLIII, Table XLIV, Table XLV and described below:

- Lithium – Manganese Dioxide Batteries
  - CR 1025: 30 mAh; CR 1216: 25 mAh; CR 1220: 35 mAh; CR 1612: 40 mAh; CR 1616: 55 mAh; CR 1620: 75 mAh; CR 1632: 140 mAh; CR 2012: 55 mAh; CR 2016: 90 mAh; CR 1025: 30 mAh; CR 1216: 25 mAh; CR 1220: 35 mAh; CR 1612: 40 mAh; CR 1616: 55 mAh; CR 1620: 75 mAh; CR 1632: 140 mAh; CR 2012: 55 mAh; CR 2016: 90 mAh; CR 2025: 165 mAh.
- Lithium – Carbon Monofluoride Batteries
  - BR 1220: 35 mAh; BR 1225: 48 mAh; BR 1632: 120 mAh; BR 2032: 200 mAh; BR 2325: 165 mAh; BR 2330: 255 mAh; BR 3032: 500 mAh;
- Lithium – High Temperature Operation Batteries
  - BR 1225A: 48 mAh; BR 1632A: 120 mAh; BR 2330A: 255 mAh; BR 2450A: 550 mAh; BR 3477A: 1000 mAh.

Table XLIII – Lithium – Manganese Dioxide batteries.

Model	Capacity	Voltage
CR 1025	30 mAh	3 V
CR 1216	25 mAh	3 V
CR 1220	35 mAh	3 V
CR 1612	40 mAh	3 V
CR 1616	55 mAh	3 V
CR 1620	75 mAh	3 V
CR 1632	140 mAh	3 V
CR 2012	55 mAh	3 V
CR 2016	90 mAh	3 V
CR 2025	165 mAh	3 V

Table XLIV – Lithium – Carbon Monofluoride batteries.

Model	Capacity	Voltage
BR 1220	35 mAh	3 V
BR 1225	48 mAh	3 V
BR 1632	120 mAh	3 V
BR 2032	200 mAh	3 V
BR 2325	165 mAh	3 V
BR 2330	255 mAh	3 V
BR 3032	500 mAh	3 V

Table XLV – Lithium – High Temperature Operation Batteries.

Model	Capacity	Voltage
BR 1225A	48 mAh	3 V
BR 1632A	120 mAh	3 V
BR 2330A	255 mAh	3 V
BR 2450A	550 mAh	3 V
BR 3477A	1000 mAh	3 V

5.5.7 Network Cost

We defined the network cost as the summation of the price of all parts used in the simulated networks. The quotation of all components was made on Mouser and Farnell [77], [78] during 2017, and their average prices are shown in Table XLVI.

- **Average prices of all components** (also shown in Table XLVI**)**:
  - **Battery** – model: CR 1632, price: US$4.99.
  - **Radio Module** – model: Xbee PRO 2.4 GHz, price: US$34.00.
  - **Microcontroller** – model: Atmega8L, price: US$3.66.
  - **Sensor** – model: LM75, price: US$1.86.

Table XLVI – Average prices of all components.

Part	Model	Price
Battery	CR 1632	US$4.99
Radio Module	Xbee PRO 2.4 GHz	US$34.00
Microcontroller	Atmega8L	US$3.66
Sensor	LM75	US$1.86

The total network cost of the simulated network, with 34 motes, was US$1,513.34.

Facing the waste of its remaining parts, it is feasible to relate the cost a Wireless Sensor Networks with its lifetime. In this chapter, we also use the metric cost per hour relating the total cost of a network with its lifetime, as shown in Equation (3) and described below:

- Network Cost per hour is equals to the total cost of the network divided by its lifetime in hours.

$$h = \frac{c}{l}, \tag{3}$$

where h is the cost per hour of the network, c is the total cost of the network and l is its lifetime (in hours).

5.5.7.1 The Nonlinearity of the Energy Price

Due to the different charges and nonlinear prices, the assortment of battery sets under cost constraints is quite a complex problem. This problem is well addressed in [98], [99].

5.5.8 Messages per Hour

As the simulations have different generation periods, when each mote generates a new message, there is also a need to analyze how many messages a network generates throughout its lifetime. We decided to associate the number of generated messages with the network lifetime, as shown in Equation. (4) and described below:

- Messages generated per hour is equals to the total number of messages generated by a network divided by its lifetime.

$$M = \frac{m}{l}, \tag{4}$$

where M is the quantity of messages per hour of the network, m is the summation of all messages generated by the network and l is its lifetime (in hours).

5.5.9 Message Log

After the end of each simulation, all messages were accounted and divided into four categories:

- **Listened Messages**: All messages **received** by a mote, regardless the addressee of them.
- **Rerouted Messages**: All messages that a mote had to **reroute** in order to reach the base station, in other words, all messages addressed to others motes that had to perform multiple hops towards the base station.
- **Overheard Messages**: Only the messages that a mote received but were **not** addressed to it, in other words, the messages that were **unnecessarily** received/listened by a mote.
- **Generated Messages**: All messages **created** and **sent** by a mote. These messages have the data that a mote wants to transmit to the base station and are created at each network cycle.

The occurrence of overheard messages is a problem that has multiple strategies to be avoided, like using different channels, synchronized sleep cycles or letting the radio module discarding messages not addressed to them [60], [100]–[103]. Xbee PRO, the radio module used as basis of the simulations, can discard messages not addressed to them without using the microcontroller but, as not all radio modules have this feature of discarding messages, the simulations were made with all messages being processed by the microcontroller of each mote, and just after that they were discarded or rerouted.

5.5.10 Implemented Protocols

There are two different protocols considered to make the simulations presented in this chapter: the first is the media access control protocol, which is a built-in software of the Xbee radio module [60] and second is the protocol for sensing the environment, transmitting, receiving and processing messages. The aforementioned protocols are described in the next subsections.

5.5.10.1 Protocol for Sensing, Transmitting, Receiving and Processing Messages

This protocol was implemented on all network motes and it is responsible for all basic tasks performed by them. All motes have same functions, parts and settings and the equal roles, and tasks on the network.

5.5.10.1.1 Network Cycle

Similar to [19], [20], this work employed simulations using energy consumption data acquired from both direct measurements [18], [19] and the datasheets of the electronic componentes. The simulations followed the rules of a time-driven network [104]–[108], therefore, all motes performed their tasks following a network cycle, similarly to [108]–[116]. All motes kept their microcontrollers, sensors and radio transceivers on the power-down/sleep states [60], [86]–[88] until the moment when they had to sense the environment and send their messages or to reroute messages of other motes. The algorithm presented in Algorithm 6 and its resulting flowchart presented in Fig. 74 shows the routine abide by a mote at each network cycle.

Algorithm 6 – Algorithm abide by a mote at each network cycle.

1. Activate microcontroller
2. Read sensor
3. Assembly message
4. Send message
5. Put transceiver, sensor and microcontroller in sleep state
6. Wait a network cycle

Each network cycle T starts over after a settled period of time, it is when all motes generate a new message and send it, directly or with the help of other motes, to the base station. In this chapter, we used six different periods of time (also shown in Table XLVII): 1 second; 10 seconds; 60 seconds (one minute); 600 seconds (10 minutes); 3600 seconds (one hour) and 86400 seconds (one day).

Table XLVII – Network cycles used in this chapter.

Network Cycle *T* / Generation Period (in seconds)	**Traffic Load (msg/s)**
86400	1.16E-05
3600	2.78E-04
600	0.00166
60	0.166
10	0.1
1	1

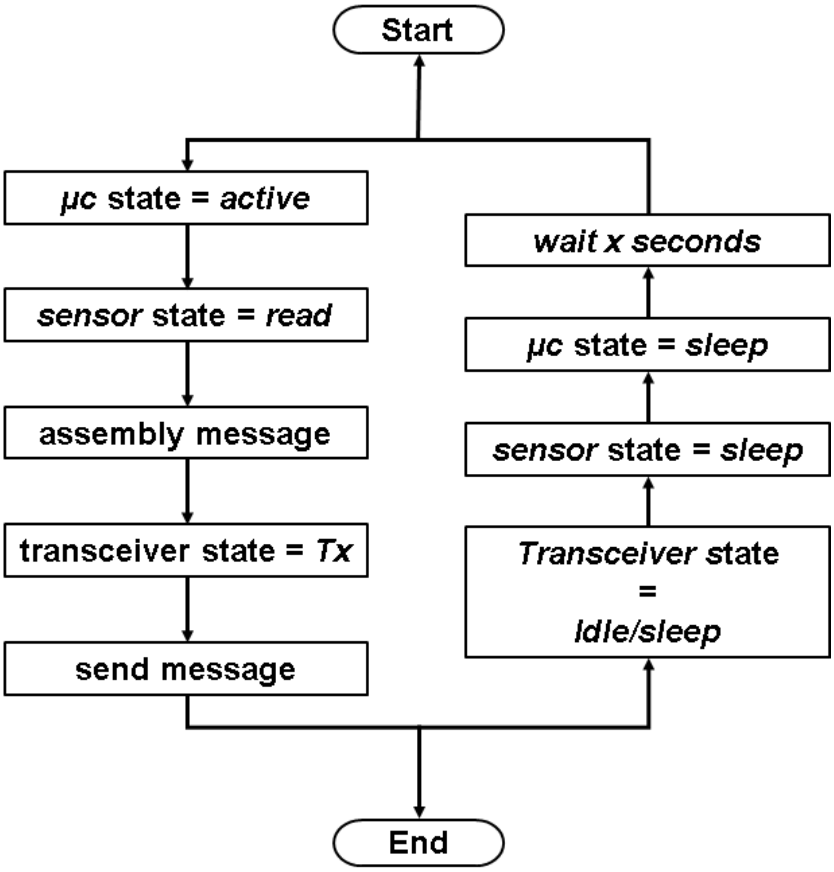

Fig. 74 – Algorithm abide by a mote at each network cycle.

5.5.10.1.2 Receiving and Processing Messages

The situation of receiving messages was modeled after interruptions [117], [118], when the radio transceiver calls an interruption at the microcontroller, waking it, and passing the message to the microcontroller every time a new one is received. This routine is also referred as Wake-up Radio [119]–[123]. In our simulations, to keep the simulations closer to real situations, every message had to be processed, obligatorily, by the microcontroller of the receiver mote.

Xbee transceiver offers the option of filtering received packages which were not addressed to the receiver, but, on our simulations, the identification of the addressee was not made in the same layer [124], [125] of the receiver, thus, always having to be processed by the microcontroller of the receiver [126]. This promiscuous reception [127], which is common when using simpler radio modules [57], [59], was kept to perform more embracing simulations.

After receiving and processing a message, two actions can be performed by a mote (also shown in Fig. 75):

- **Rerouting** the message to a successor mote, **IF** the received message was addressed to the receiver.
- **Discarding** the message, **IF** the received message was **NOT** addressed to the receiver.

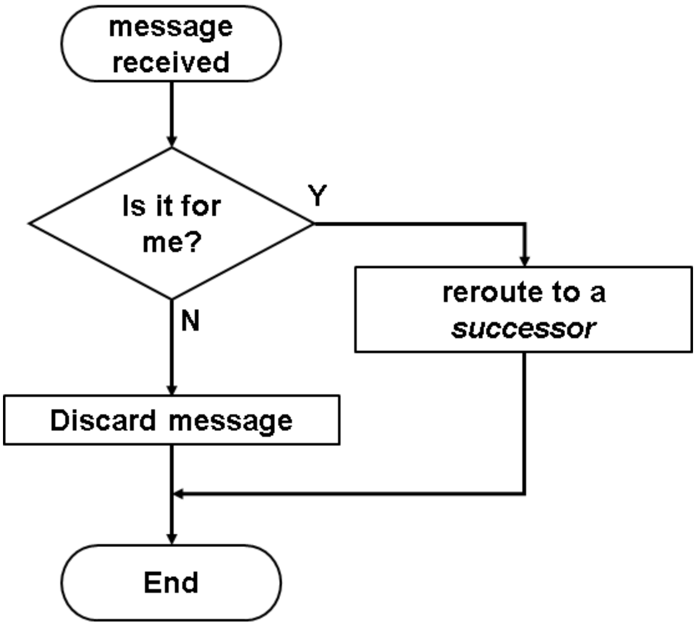

Fig. 75 – Algorithm abide by a mote after receiving a message.

5.5.10.2 Medium/Media Access Control

Xbee PRO radio module has built-in functions and protocols for Medium/Media Access Control (MAC) [124], [125], [128] in order to allow multiple modules to use the shared medium. The Carrier Sense Multiple Access with Collision Avoidance (CSMA/CA) [124], [125], [128]–[131], used in Xbee PRO modules, provides a reliable way to send and receive messages without major problems caused by collisions [132]–[135].

The additional reliability of RTS/CTS handshake (**R**equest **T**o **S**end and **C**lear **T**o **S**end) [89], [124], [125], [128] and the possible retransmissions of corrupted packages are also already implemented on Xbee modules, but, in order to keep the analysis focused just on energy consumption issues, neither RTS/CTS handshake nor collisions/retransmissions were considered on our simulations.

5.6 Simulations and Results

In this chapter we investigated three different scenarios, all using path loss exponent set to 3.5. All simulations used the same identical parts/motes and three circular networks, all with 34 motes each:

- **Scenario I** – base station allocated in the center of the network, as shown in Fig. 76 (**a**).
- **Scenario II** – base station little dislocated to the southeast of the network, but still inside the network cluster, as shown in Fig. 76 (**b**).
- **Scenario III** – base station dislocated to the southeast of the network, outside the network cluster, as shown in Fig. 76 (**c**).

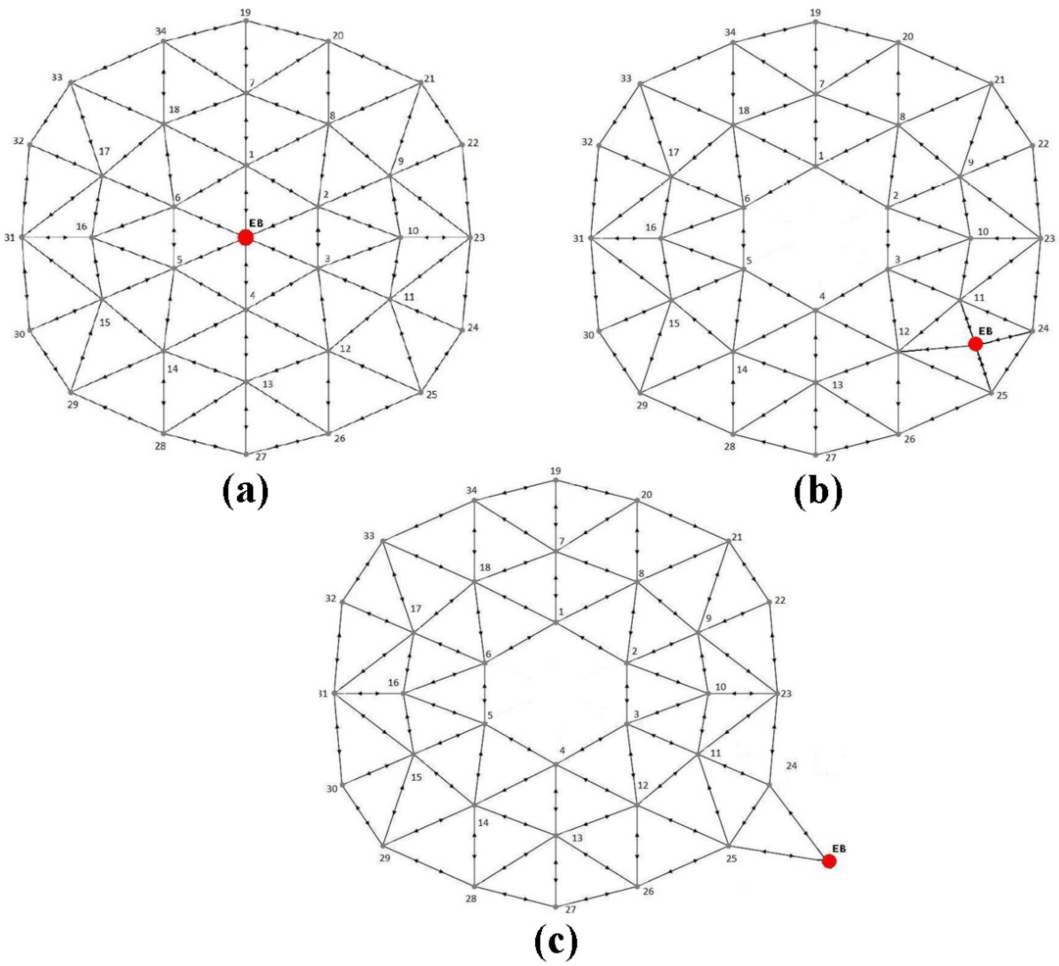

Fig. 76 – Network with base station in the center **(a)**; Network with base station displaced from the center **(b)**; Network with base station out of the mote cluster **(c)**.

5.6.1 Scenario I

In Scenario I, the 34-mote network shown in Fig. 77 was simulated using the path loss exponent set to 3.5. Its base station was located in the exact center of its circular topology, similarly to performed in[109], [110], [113], [114], which is pointed as the best topology in [136].

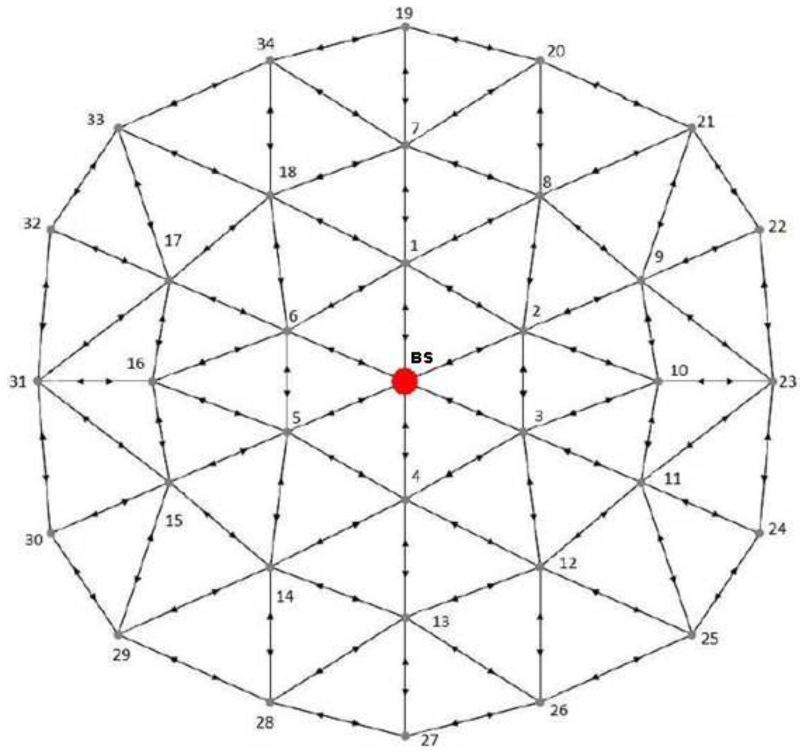

Fig. 77 – Network simulated in Scenario I.

In Scenario I, when using $46.76P_{tx}$, all messages were sent directly to the base station.

5.6.1.1 Battery Redistribution

Using the techniques presented in Chapter IV, each mote on all cases had its individual energy consumption calculated and received a battery set according to its energy needs. As shown in Table XLIII, Table XLIV and Table XLV, the batteries used to assemble the batteries sets had fixed capacities, making some energy values impossible to be arranged exactly. Even with this impossibility, the energy budget, which is the total energy received by a network, of the networks with redistributed energy did not exceed the energy budget of the network with homogeneous energy distribution in any case, being in fact lower in almost all cases.

The energy distribution for the networks with different base station placement, shown in Fig. 78 (**a**)-(**c**), reveals the higher energy consumption of the motes nearer base station, caused by the extra workload of both receiving and rerouting messages of farther motes which, therefore, demands more energy. It is important to notice that the energy distribution pattern shown in Fig. 78

(**a**)-(**c**) indicates the occurrence of Energy Hole/Doughnut Effect, which can be explicated by the higher demanding workloads, of both listening and rerouting messages, that the motes nearer to the base station have to handle.

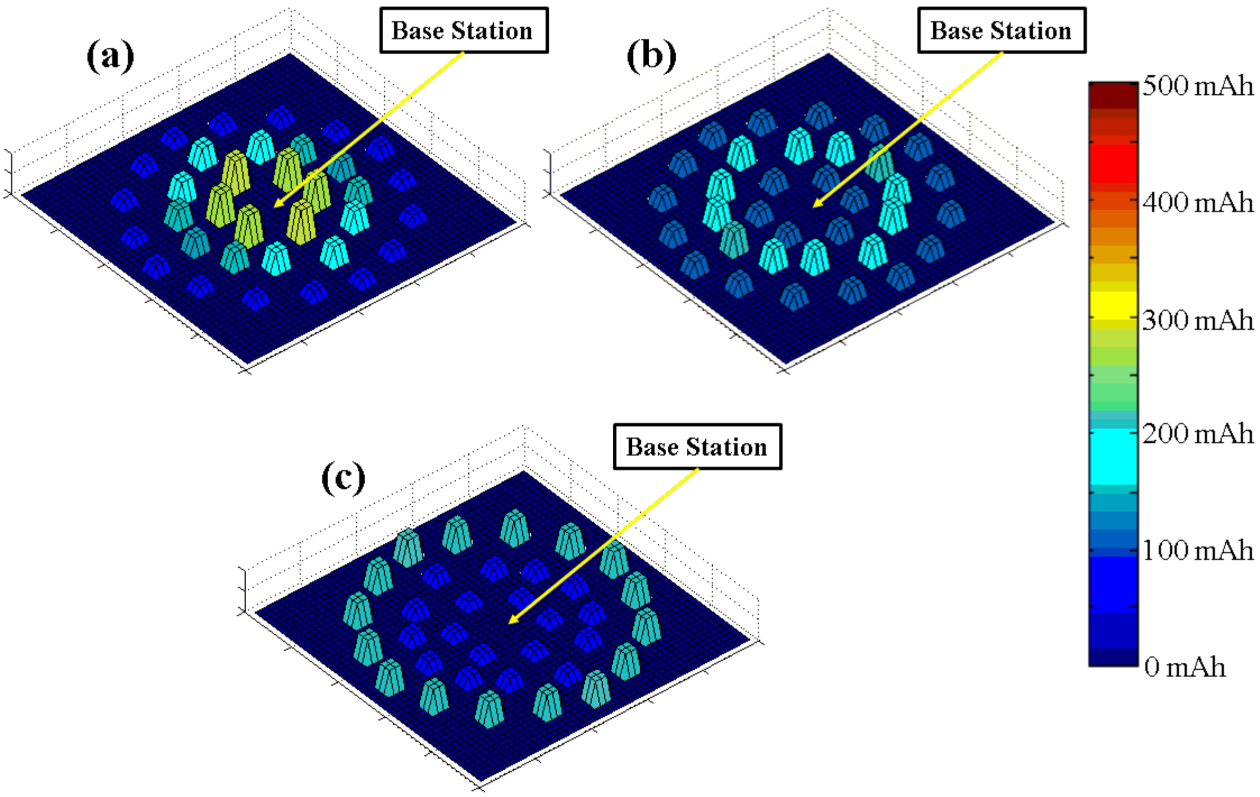

Fig. 78 – Energy distribution among motes of the networks simulated in Scenario I with T = 1s using P_{tx} (**a**); using 11.31P_{tx} (**b**); using 46.76P_{tx} (**c**).

The complete energy assignment of Scenario I is presented in Appendix A, B and C.

5.6.1.2 Transmission Power Levels

As all motes transmit their messages towards a single base station, their maximum transmission power levels did not exceed the power needed to reach the base station in any situation. Fig. 79 (**a**)-(**c**) shows the transmission power level of each mote in the networks simulated in Scenario I: Fig. 79 (**a**) all motes using P_{tx}, reaching a maximum distance d; Fig. 79 (**b**) some motes using up to 11.31P_{tx}, reaching a maximum distance 2d; Fig. 79 (**c**) some motes using up to 46.76P_{tx}, reaching a maximum distance 3d.

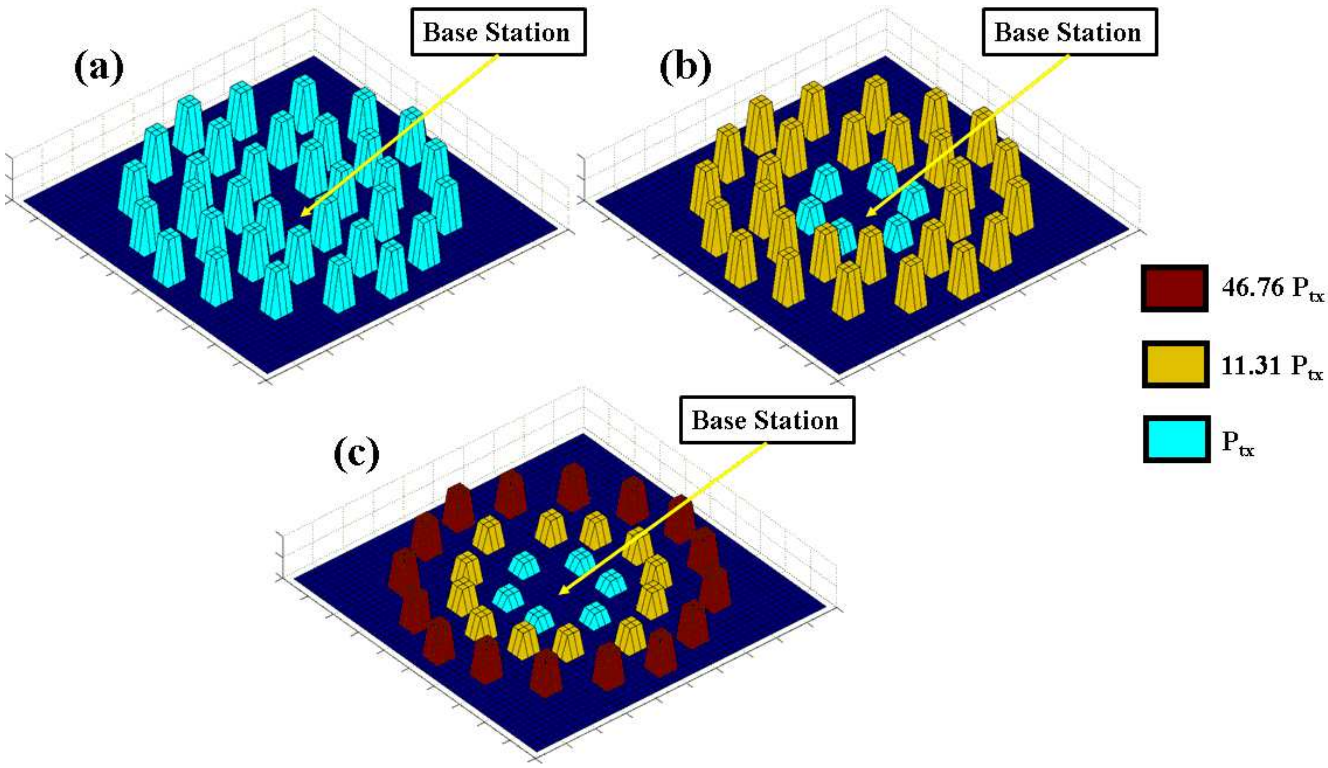

Fig. 79 – Transmission power levels of the networks simulated in Scenario I using P_{tx} (**a**); using $11.31P_{tx}$ (**b**); using $46.76P_{tx}$ (**c**).

The individual transmission power level of each mote of Scenario I is show in Appendix J.

5.6.1.3 Primary and Secondary Consumption

As can be observed in Fig. 80 and Table XLVIII, the average primary energy consumption, which is the consumption for reading sensors, transmitting/receiving and processing messages, got a descendant share on the total consumption of the network when the message generation got lower. This trend was maintained on all cases.

The average primary energy consumptions in Scenario I were:

- $P_{tx} - 1d$
  - 1 message per second: **99.33%**; 1 message at each 10 seconds: **93.41%**; 1 message at each 60 seconds: **70.18%**; 1 message at each 600 seconds: **19.04%**; 1 message at each 3600 seconds: **3.77%**; 1 message at each 86400 seconds: **0.16%**.
- $11.31P_{tx} - 2d$
  - 1 message per second: **99.71%**; 1 message at each 10 seconds: **97.04%**; 1 message at each 60 seconds: **84.48%**; 1 message at each 600 seconds: **35.22%**; 1 message at each 3600 seconds: **8.31%**; 1 message at each 86400 seconds: **0.37%**.
- $46.76P_{tx} - 3d$
  - 1 message per second: **99.81%**; 1 message at each 10 seconds: **98.10%**; 1 message at each 60 seconds: **89.56%**; 1 message at each 600 seconds: **46.16%**; 1

message at each 3600 seconds: **12.50%**; 1 message at each 86400 seconds: **0.50%**.

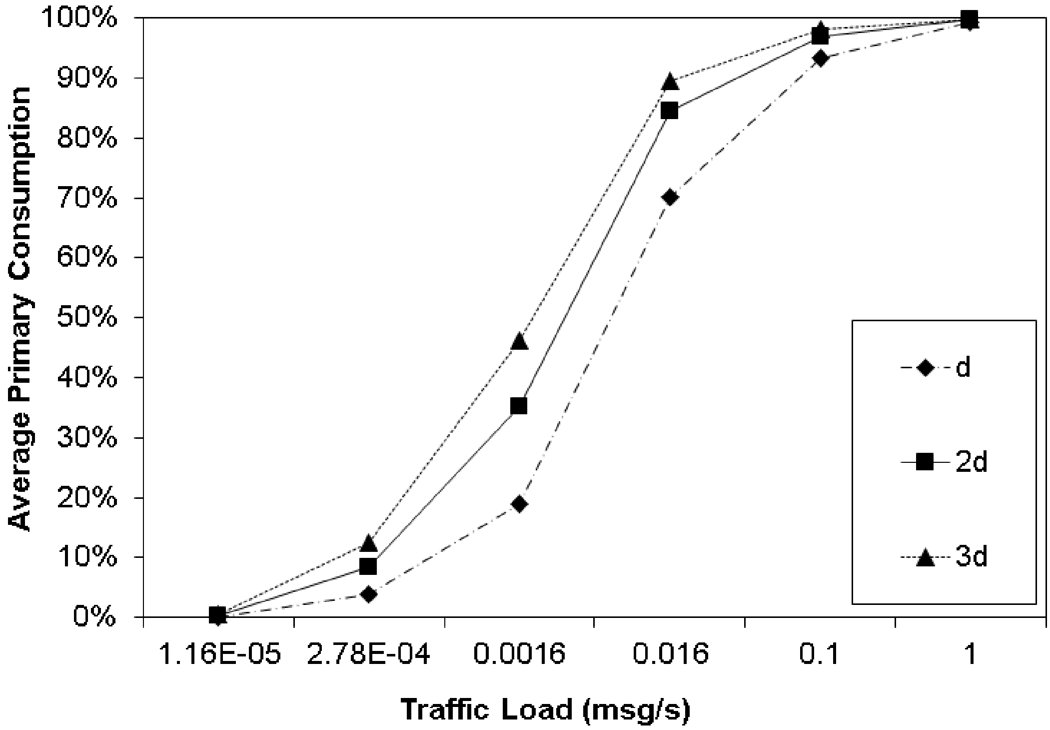

Fig. 80 – Average primary/secondary energy consumption of the networks in Scenario I.

Table XLVIII – Average primary energy consumption in Scenario I.

Traffic Load (msg/s)	**Average Primary Consumption – 1*d***	**Average Primary Consumption – 2*d***	**Average Primary Consumption – 3*d***
1.16E-05	0.16%	0.37%	0.59%
2.78E-04	3.77%	8.31%	12.50%
0.00166	19.04%	35.22%	46.16%
0.166	70.18%	84.48%	89.56%
0.1	93.41%	97.04%	98.10%
1	99.33%	99.71%	99.81%

5.6.1.4 Lifetime

Fig. 81 and Table XLIX show that the lifetime of the simulated networks using standard power with energy redistribution were longer when compared to standard power with homogenous energy distribution. Fig. 81 and Table XLIX also show that the difference between the lifetime of the simulated networks decreased when the traffic load got lower. As the traffic load was being reduced, networks using higher transmission power almost attained the same lifetime of the standard transmission power network.

Fig. 81 and Table XLIX also show that the network using the standard transmission power with the energy redistribution had longer lifetime on all cases.

The lifetimes of the simulations in Scenario I were:

- $P_{tx} - 1d$
    - 1 message per second: **22.87 hours**; 1 message at each 10 seconds: **221.90 hours**; 1 message at each 60 seconds: **1141.46 hours**; 1 message at each 600 seconds: **4492.21 hours**; 1 message at each 3600 seconds: **6168.98 hours**; 1 message at each 86400 seconds: **6644.31 hours**.
- $P_{tx} - 1d$ with energy redistribution
    - 1 message per second: **46.20 hours**; 1 message at each 10 seconds: **425.15 hours**; 1 message at each 60 seconds: **1959.83 hours**; 1 message at each 600 seconds: **5297.01 hours**; 1 message at each 3600 seconds: **6355.68 hours**; 1 message at each 86400 seconds: **6655.70 hours**.
- $11.31P_{tx} - 2d$ with energy redistribution
    - 1 message per second: **20.04 hours**; 1 message at each 10 seconds: **194.02 hours**; 1 message at each 60 seconds: **1022.86 hours**; 1 message at each 600 seconds: **4258.31 hours**; 1 message at each 3600 seconds: **6074.16 hours**; 1 message at each 86400 seconds: **6641.40 hours**.
- $46.76P_{tx} - 3d$ with energy redistribution
    - 1 message per second: **12.71 hours**; 1 message at each 10 seconds: **84.73 hours**; 1 message at each 60 seconds: **691.26 hours**; 1 message at each 600 seconds: **3544.66 hours**; 1 message at each 3600 seconds: **5797.58 hours**; 1 message at each 86400 seconds: **6626.96 hours**.

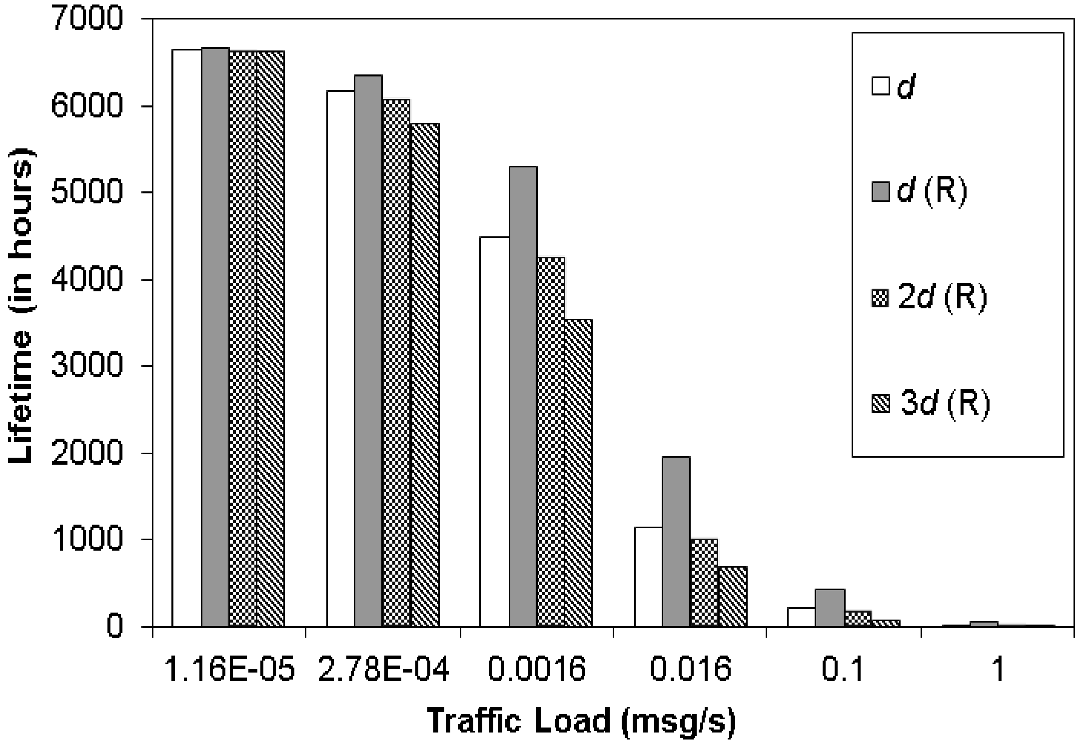

Fig. 81 – Lifetime of the networks with different transmission powers in Scenario I.

Table XLIX – Lifetime of the networks with different transmission powers in Scenario I.

Traffic Load (msg/s)	**Lifetime (in hours) – 1*d***	**Lifetime (in hours) – 1*d* Redistributed**	**Lifetime (in hours) – 2*d* Redistributed**	**Lifetime (in hours) – 3*d* Redistributed**
1.16E-05	6644.31	6655.70	6641.40	6626.96
2.78E-04	6168.98	6355.68	6074.16	5797.58
0.00166	4492.21	5297.01	4258.31	3544.66
0.166	1141.46	1959.83	1022.86	691.26
0.1	221.90	425.15	194.02	84.73
1	22.87	46.20	20.04	12.71

5.6.1.5 Network Cost per Working Hour

Fig. 82 and Table L show the cost of each network per hour of their lifetime. As the network cost is the same on all simulated networks (US$1,513.34), the lifetime was the key issue in Scenario I, making the cost of each network cheaper according the traffic generation got lower.

In Scenario I, all network costs got lower when the traffic generation was reduced and the network using the standard transmission power with the energy redistribution had the lowest network cost on all cases.

The network cost of the simulations in Scenario I were:

- $P_{tx} - 1d$
  - 1 message per second: **US$66.17**; 1 message at each 10 seconds: **US$6.82**;

    1 message at each 60 seconds: **US$1.32**; 1 message at each 600 seconds: **US$0.34**; 1 message at each 3600 seconds: **US$0.25**; 1 message at each 86400 seconds: **US$0.23**.
- $P_{tx} - 1d$ with energy redistribution
  - 1 message per second: **US$32.76**; 1 message at each 10 seconds: **US$3.56**;

    1 message at each 60 seconds: **US$0.77**; 1 message at each 600 seconds: **US$0.29**; 1 message at each 3600 seconds: **US$0.24**; 1 message at each 86400 seconds: **US$0.23**.
- $11.31P_{tx} - 2d$ with energy redistribution
  - 1 message per second: **US$75.52**; 1 message at each 10 seconds: **US$7.80**;

    1 message at each 60 seconds: **US$1.48**; 1 message at each 600 seconds: **US$0.36**; 1 message at each 3600 seconds: **US$0.25**; 1 message at each 86400 seconds: **US$0.23**.
- $46.76P_{tx} - 3d$ with energy redistribution
  - 1 message per second: **US$119.07**; 1 message at each 10 seconds: **US$17.86**;

    1 message at each 60 seconds: **US$2.19**; 1 message at each 600 seconds: **US$0.43**; 1 message at each 3600 seconds: **US$0.26**; 1 message at each 86400 seconds: **US$0.23**.

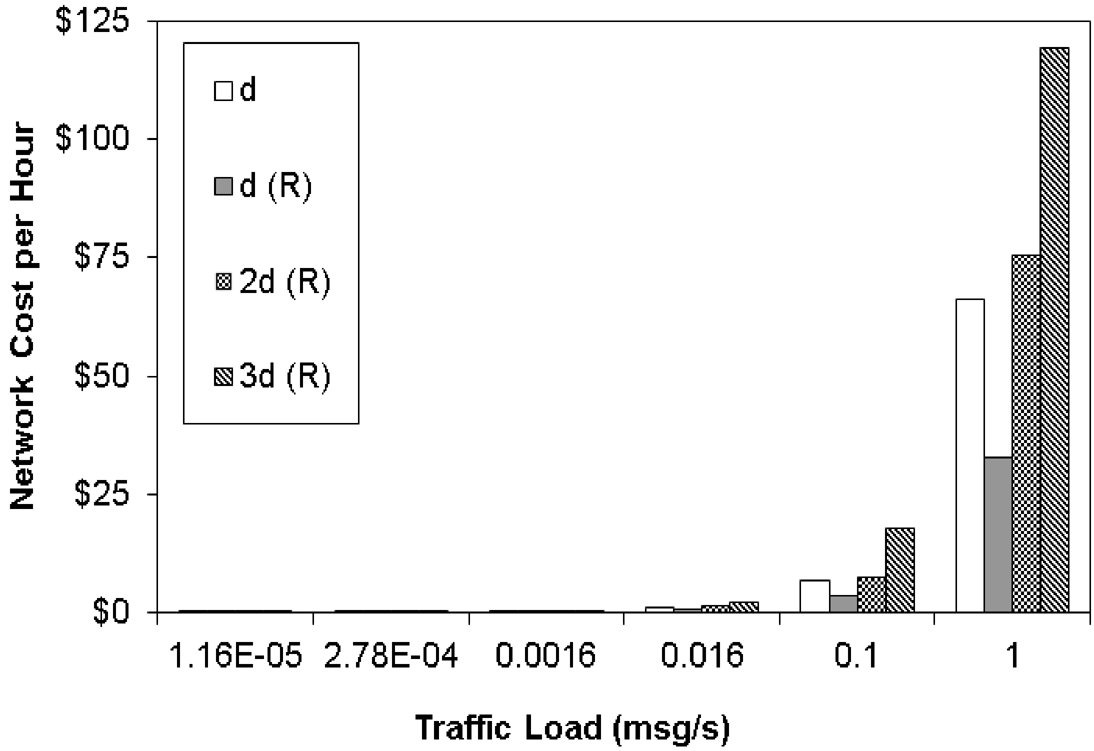

Fig. 82 – Network cost of the networks simulated in Scenario I.

Table L – Network cost of the networks simulated in Scenario I.

Traffic Load (msg/s)	Network Cost per Hour – 1*d*	Network Cost per Hour – 1*d* Redistributed	Network Cost per Hour – 2*d* Redistributed	Network Cost per Hour – 3*d* Redistributed
1.16E-05	US$0.,23	US$0.23	US$0.23	US$0.23
2.78E-04	US$0.25	US$0.24	US$0.25	US$0.26
0.00166	US$0.34	US$0.29	US$0.36	US$0.43
0.166	US$1.32	US$0.77	US$1.48	US$2.19
0.1	US$6.82	US$3.56	US$7.80	US$17.86
1	US$66.17	US$32.76	US$75.52	US$119.07

5.6.1.6 Remaining Energy

Fig. 83 and Table LI show the average remaining energy of the networks simulated in Scenario I. The average remaining energy was way higher when the network used the homogeneous energy distribution.

The average remaining energy of the simulations in Scenario I were:

- $P_{tx} - 1d$
    - 1 message per second: **51.25%**; 1 message at each 10 seconds: **49.71%**; 1 message at each 60 seconds: **42.62%**; 1 message at each 600 seconds: **16.77%**; 1 message at each 3600 seconds: **3.84%**; 1 message at each 86400 seconds: **0.17%**.
- $P_{tx} - 1d$ with energy redistribution
    - 1 message per second: **1.46%**; 1 message at each 10 seconds: **3.53%**; 1 message at each 60 seconds: **1.40%**; 1 message at each 600 seconds: **1.75%**; 1 message at each 3600 seconds: **0.92%**; 1 message at each 86400 seconds: **0.01%**.
- $11.31P_{tx} - 2d$ with energy redistribution
    - 1 message per second: **1.58%**; 1 message at each 10 seconds: **2.10%**; 1 message at each 60 seconds: **1.06%**; 1 message at each 600 seconds: **1.35%**; 1 message at each 3600 seconds: **0.54%**; 1 message at each 86400 seconds: **0.01%**.
- $46.76P_{tx} - 3d$ with energy redistribution
    - 1 message per second: **1.60%**; 1 message at each 10 seconds: **3.77%**; 1 message at each 60 seconds: **0.69%**; 1 message at each 600 seconds: **1.24%**; 1 message at each 3600 seconds: **0.56%**; 1 message at each 86400 seconds: **0.01%**.

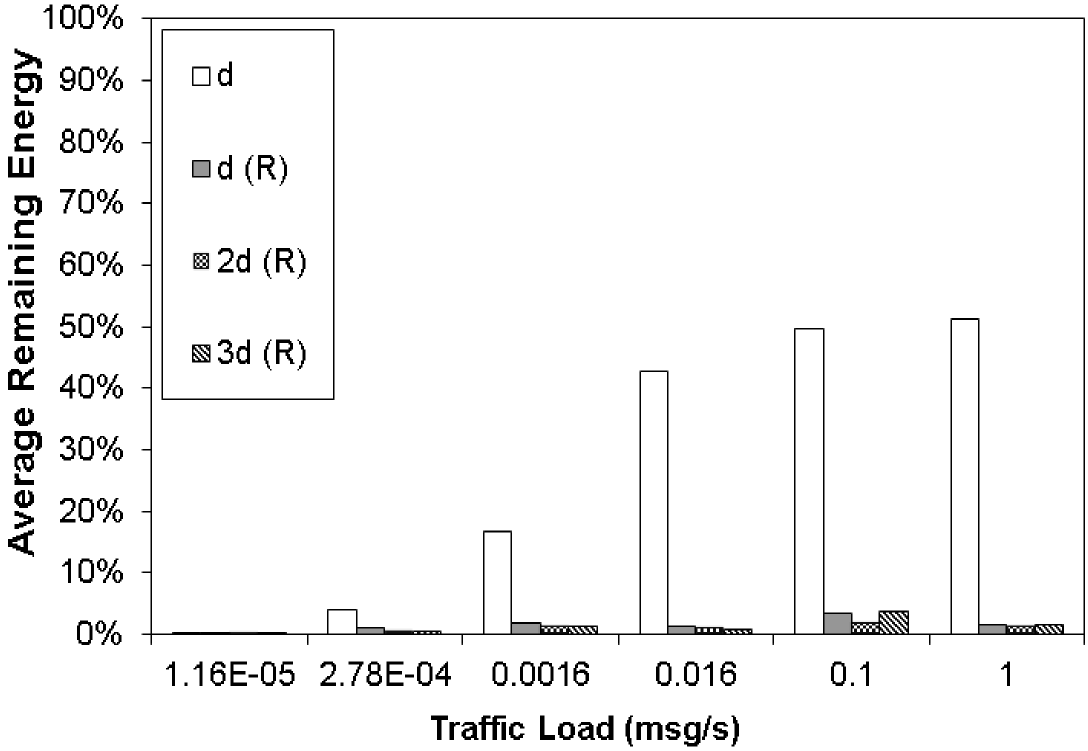

Fig. 83 – Average remaining energy of each network in Scenario I.

Table LI – Average remaining energy of each network in Scenario I.

Traffic Load (msg/s)	**Average Remaining Energy – 1*d***	**Average Remaining Energy – 1*d* Redistributed**	**Average Remaining Energy – 2*d* Redistributed**	**Average Remaining Energy – 3*d* Redistributed**
1.16E-05	0.17%	0.01%	0.01%	0.01%
2.78E-04	3.84%	0.92%	0.54%	0.56%
0.00166	16.77%	1.75%	1.35%	1.24%
0.166	42.62%	1.40%	1.06%	0.69%
0.1	49.71%	3.53%	2.10%	3.77%
1	51.25%	1.46%	1.58%	1.60%

5.6.1.7 Energy Consumption Profile

As can be observed in Fig. 84, Fig. 85, Fig. 86 and in Table LII, due to the transmission power increase, the energy spent on transmissions (labeled as Radio-TX) increased, following the transmission power increase. The energy consumption profile of Secondary states is the same on all cases and is shown in Fig. 87 and Table LIII.

The energy consumption profile of the simulations in Scenario I were:

- $P_{tx} - 1d$
  - Radio transmission:**21.67%**; Radio reception:**47.08%**; Microcontroller:**27.86%**; Sensor: **3.37%**.
- $11.31P_{tx} - 2d$
  - Radio transmission:**53.86%**; Radio reception:**36.94%**; Microcontroller:**7.72%**; Sensor: **1.46%**.
- $46.76P_{tx} - 3d$
  - Radio transmission:**67.84%**; Radio reception:**27.90%**; Microcontroller:**3.33%**; Sensor: **0.92%**.
- Secondary Consumption
  - Radio: **47.62%**; Microcontroller :**23.80%**; Sensor: **28.58%**.

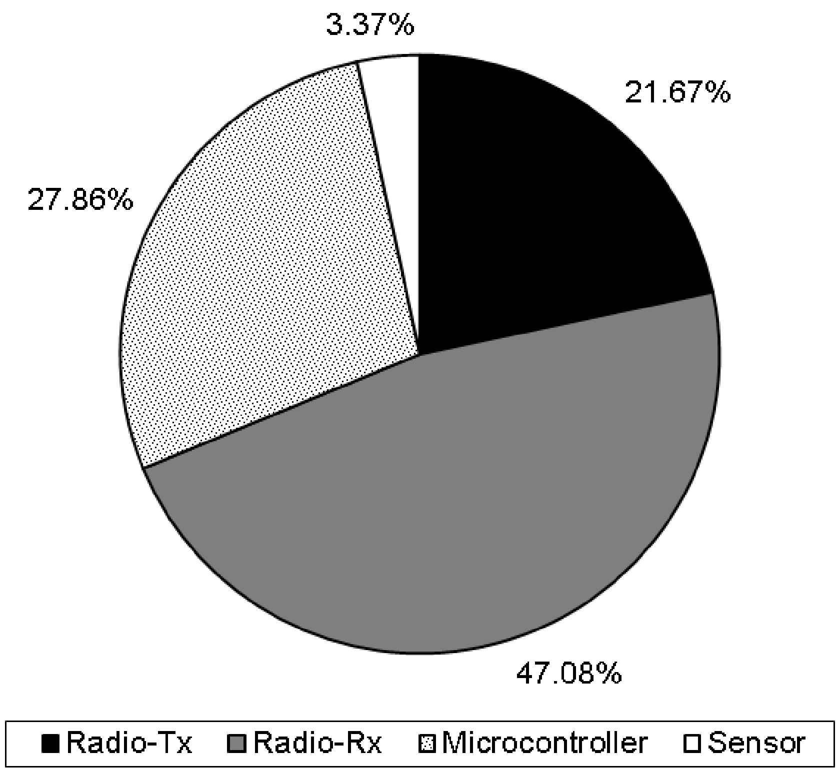

Fig. 84 – Energy consumption profile in Scenario I – P_{tx} (1d).

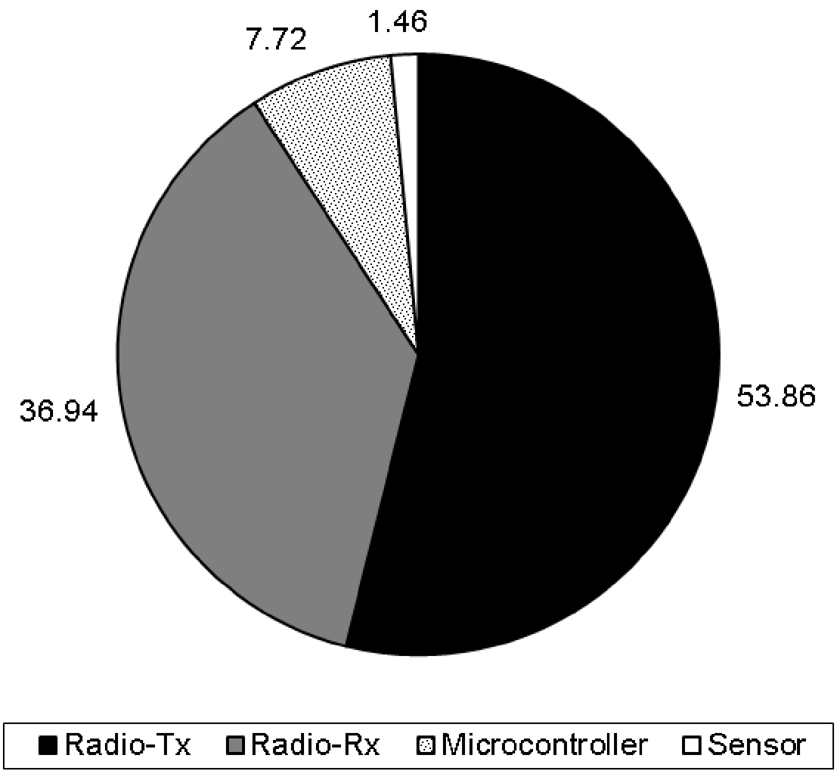

Fig. 85 – Energy consumption profile in Scenario I – 11.31P_{tx} (2d).

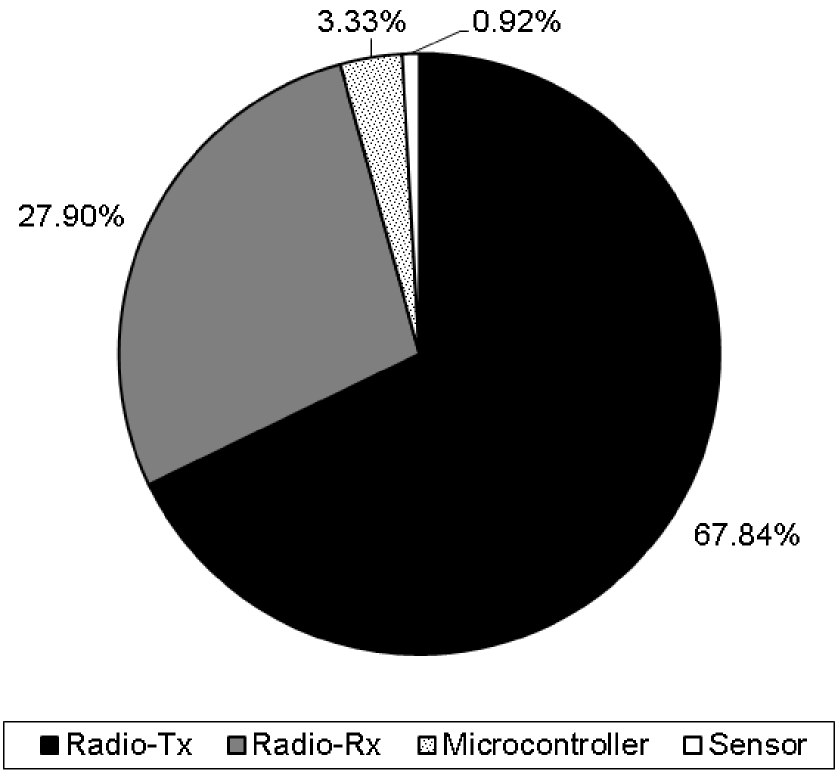

Fig. 86 – Energy consumption profile in Scenario I – 46.76P_{tx} (3d).

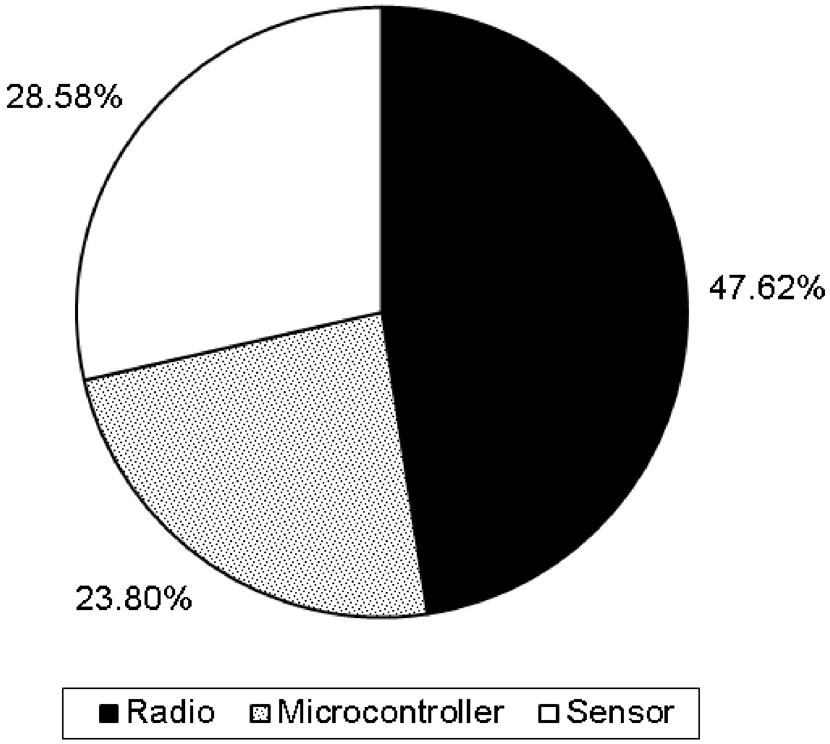

Fig. 87 – Energy consumption profile in Scenario I – Secondary Consumption.

Table LII – Energy consumption of each part of the networks in Scenario I.

Transmission Power	Reach	Radio-Tx	Radio-Rx	Microcontroller	Sensor
P_{tx}	$1d$	21.67%	47.08%	27.86%	3.37%
$11.31P_{tx}$	$2d$	53.86%	36.94%	7.72%	1.46%
$46.76P_{tx}$	$3d$	67.84%	27.90%	3.33%	0.92%

Table LIII – Energy consumption profile of Secondary States in Scenario I.

Radio	Microcontroller	Sensor
47.62%	23.80%	28.58%

5.6.1.8 Message Log

Fig. 88 and Table LIV show that the total of listened messages in relation to generated messages increased with higher transmission power, from 1163% to 2512%.

Fig. 89 and Table LIV show that the total of rerouted messages in relation to generated messages decreased with higher transmission power, from 129% to 0%.

Fig. 90 and Table LIV show that the total of overheard messages in relation to generated messages increased with higher transmission power, from 1033% to 2512%.

The message log of the simulations in Scenario I were:

- $P_{tx} - 1d$

  - Listened Messages: **1163%**; Rerouted Messages: **129%**; Overheard Messages: **1033%**.

- $11.31P_{tx} - 2d$
  - Listened Messages: **2110%**; Rerouted Messages: **47%**; Overheard Messages: **2063%**.

- $46.76P_{tx} - 3d$
  - Listened Messages: **2512%**; Rerouted Messages: **0%**; Overheard Messages: **2512%**.

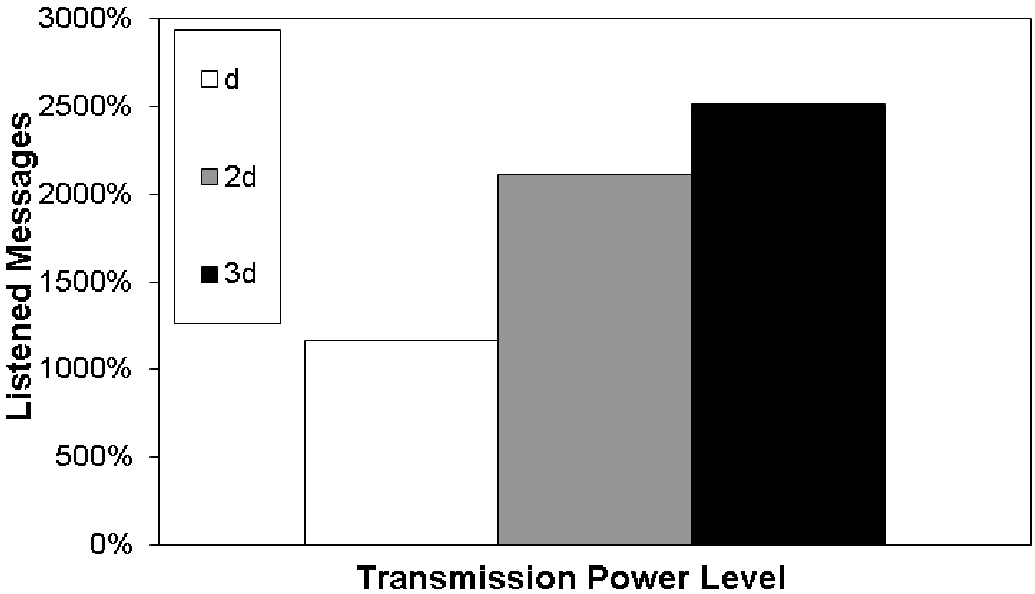

Fig. 88 – Log of listened messages of the simulations in Scenario I.

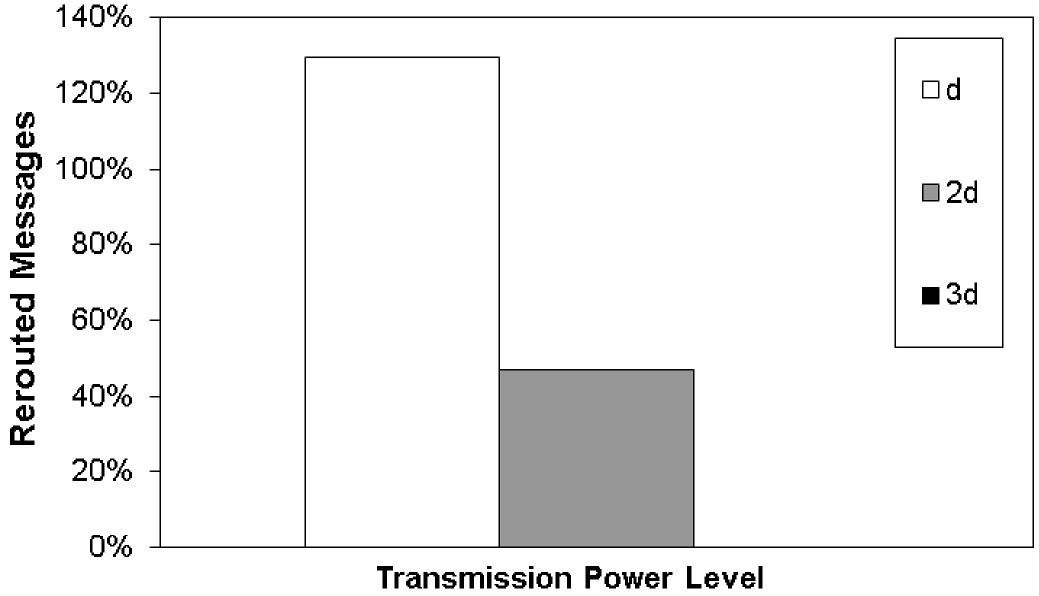

Fig. 89 – Log of rerouted messages of the simulations in Scenario I.

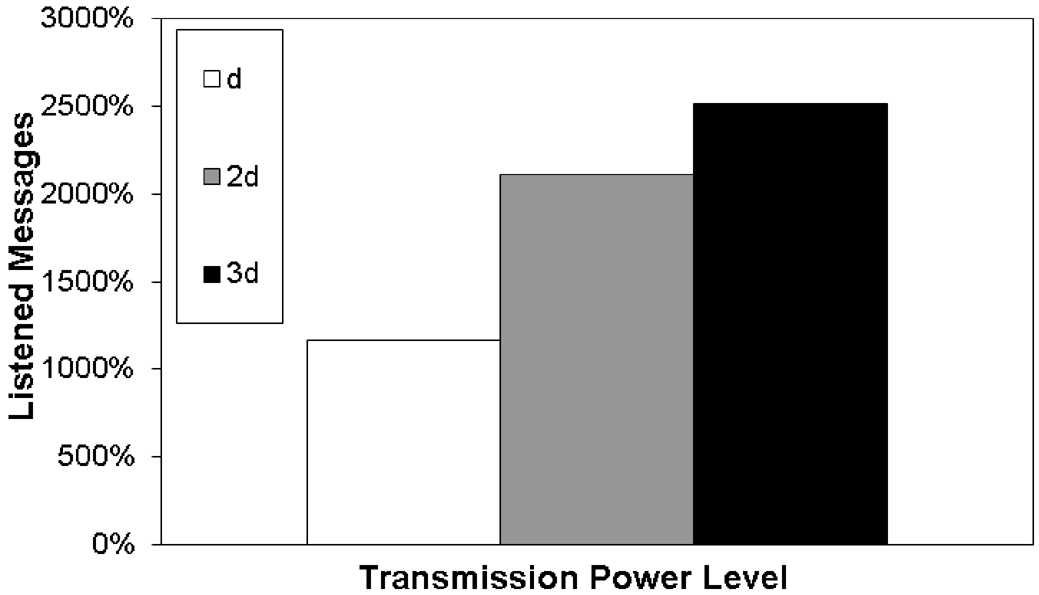

Fig. 90 – Log of overheard messages of the simulations in Scenario I.

Table LIV – Message logs of Scenario I.

Transmission Power	Reach	Listened Messages	Rerouted Messages	Overheard Messages
P_{tx}	$1d$	1163%	129%	1033%
$11.31P_{tx}$	$2d$	2110%	47%	2063%
$46.76P_{tx}$	$3d$	2512%	0%	2512%

5.6.1.9 Energy Consumption Calculation Error

Using the mathematical models presented in Chapter IV and [147], we could estimate both the individual energy consumption of each mote and the network energy consumption per network cycle. Fig. 91 and Table LV show the average error of the calculated individual energy consumption in relation to the simulated values and Fig. 92 and Table LVI show the error of the calculated network energy consumption in relation to the simulated values.

It is important to state that the calculated individual energy consumption errors were due both overestimation and underestimation, resulting in different errors of the calculated network energy consumption.

The average error of the calculated individual energy consumption of the simulations in Scenario I were:

- $P_{tx} - 1d$
  - 1 message per second: **0.01%**; 1 message at each 10 seconds: **0.01%**; 1 message at each 60 seconds: **0.01%**; 1 message at each 600 seconds: **less than 0.01%**; 1 message at each 3600 seconds: **less than 0.01%**; 1 message at each 86400 seconds: **less than 0.01%**.
- $11.31P_{tx} - 2d$
  - 1 message per second: **0.49%**; 1 message at each 10 seconds: **0.48%**; 1 message at each 60 seconds: **0.42%**; 1 message at each 600 seconds: **0.18%**; 1 message at each 3600 seconds: **0.04%**; 1 message at each 86400 seconds: **0.50%**.
- $46.76P_{tx} - 3d$
  - 1 message per second: **0.51%**; 1 message at each 10 seconds: **0.49%** 1 message at each 60 seconds: **0.43%**; 1 message at each 600 seconds: **0.18%**; 1 message at each 3600 seconds: **0.04%**; 1 message at each 86400 seconds: **0.47%**.

The average error of the calculated network energy consumption of the simulations in Scenario I were:

- $P_{tx} - 1d$
  - 1 message per second: **less than 0.01%**; 1 message at each 10 seconds: **less than 0.01%**; 1 message at each 60 seconds: **less than 0.01%**; 1 message at each 600 seconds: **less than 0.01%**; 1 message at each 3600 seconds: **less than 0.01%**; 1 message at each 86400 seconds: **less than 0.01%**.
- $11.31P_{tx} - 2d$
  - 1 message per second: **0.45%**; 1 message at each 10 seconds: **0.44%**; 1 message at each 60 seconds: **0.38%**; 1 message at each 600 seconds: **0.16%**; 1 message at each 3600 seconds: **0.04%**; 1 message at each 86400 seconds: **0.49%**.

- $46.76P_{tx} - 3d$
  - 1 message per second: **0.11%**; 1 message at each 10 seconds: **0.11%**; 1 message at each 60 seconds: **0.10%**; 1 message at each 600 seconds: **0.05%**; 1 message at each 3600 seconds: **0.01%**; 1 message at each 86400 seconds: **0.27%**.

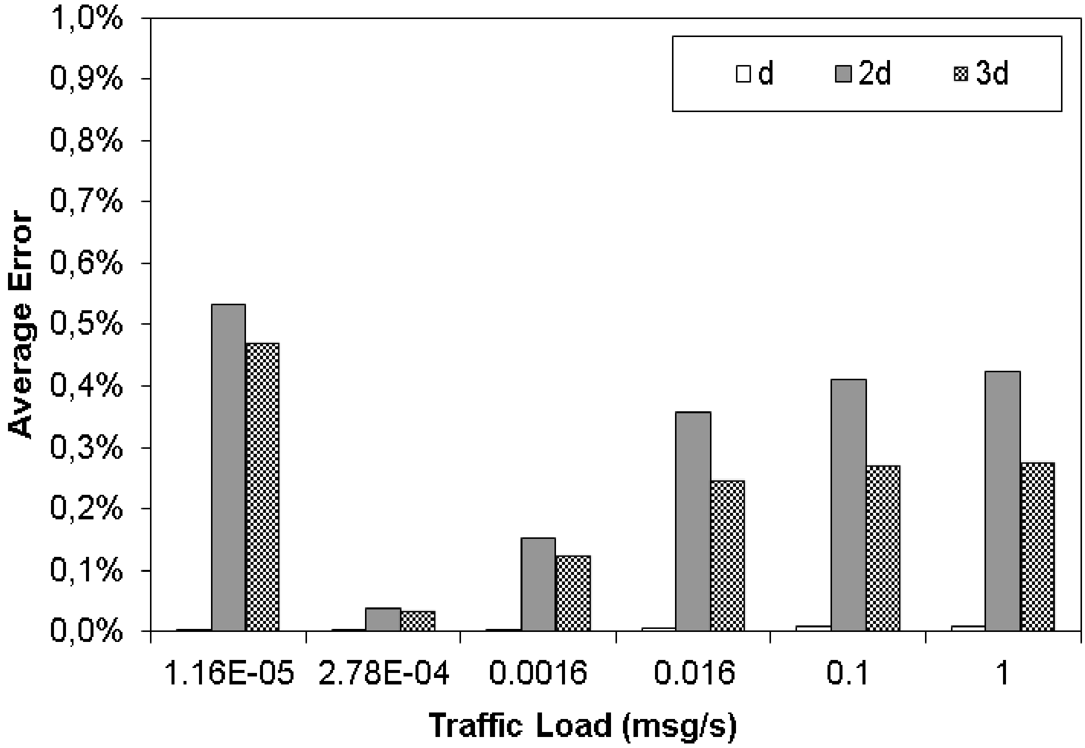

Fig. 91 – Average consumption error (calculated x simulated) of Scenario I.

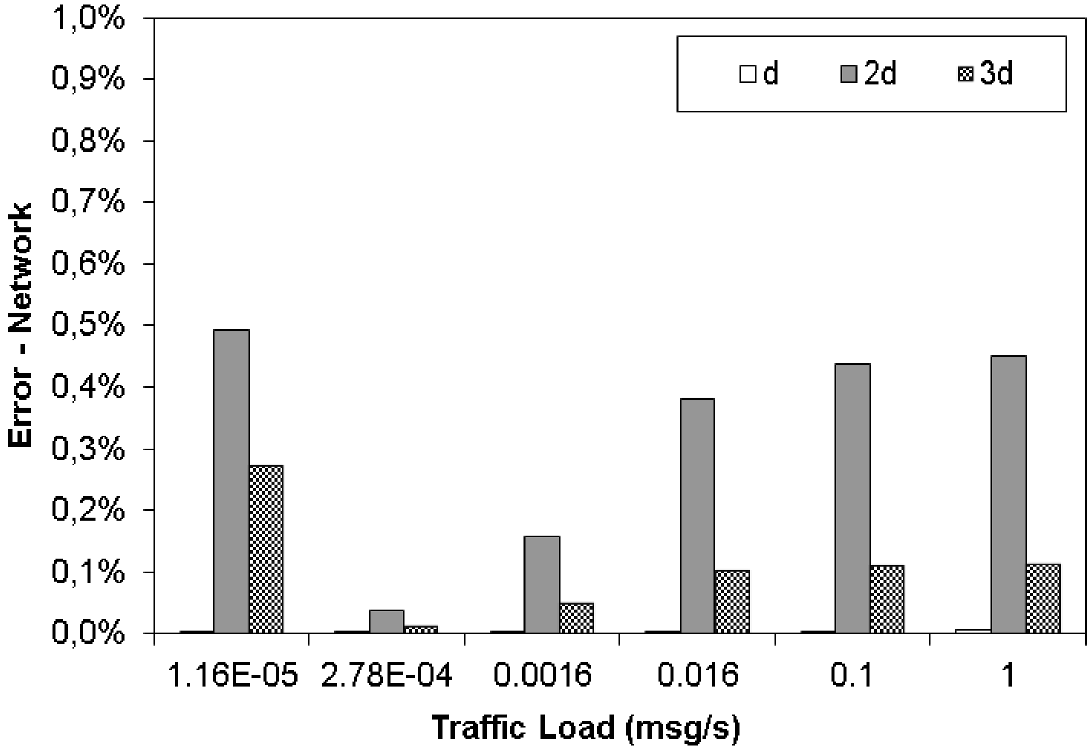

Fig. 92 – Network consumption error (calculated x simulated) of Scenario I.

Table LV – Average consumption error (calculated x simulated) of Scenario I.

Traffic Load (msg/s)	**Average Error – 1*d***	**Average Error – 2*d***	**Average Error – 3*d***
1.16E-05	<0.01%	0.50%	0.47%
2.78E-04	<0.01%	0.04%	0.04%
0.00166	<0.01%	0.18%	0.18%
0.166	0.01%	0.42%	0.43%
0.1	0.01%	0.48%	0.49%
1	0.01%	0.49%	0.51%

Table LVI – Network consumption error (calculated x simulated) of Scenario I.

Traffic Load (msg/s)	**Network Error – 1*d***	**Network Error – 2*d***	**Network Error – 3*d***
1.16E-05	<0.01%	0.49%	0.27%
2.78E-04	<0.01%	0.04%	0.01%
0.00166	<0.01%	0.16%	0.05%
0.166	<0.01%	0.38%	0.10%
0.1	<0.01%	0.44%	0.11%
1	<0.01%	0.45%	0.11%

5.6.2 Scenario II

In Scenario II, the 34-mote network shown in Fig. 93 was simulated using the path loss exponent set to **3.5**. Its base station was little dislocated to the southeast of the network, but still inside the network cluster.

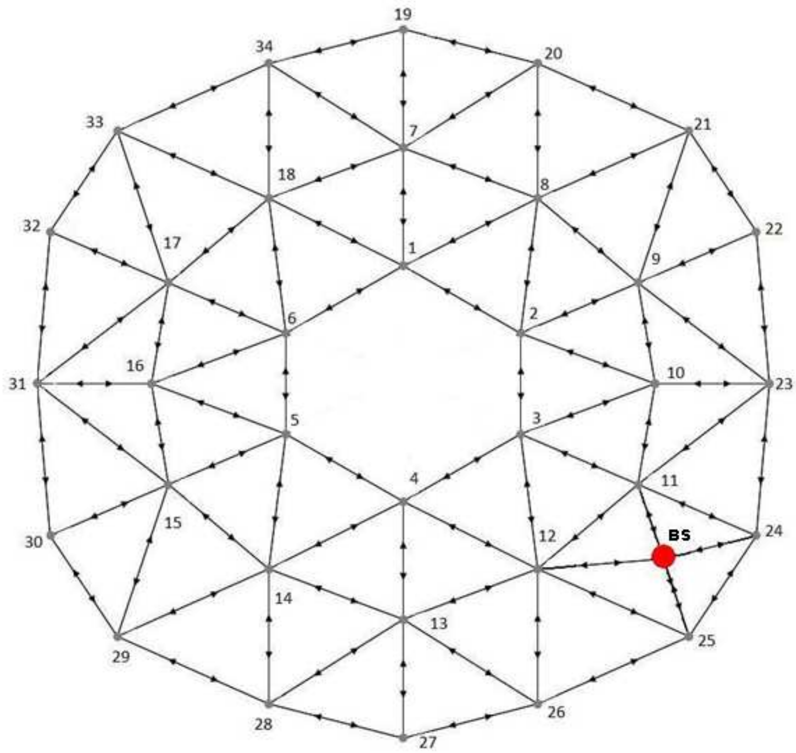

Fig. 93 – Network simulated in Scenario II.

5.6.2.1 Battery Redistribution

Using the techniques presented in Chapter IV, each mote on all cases had its individual energy consumption calculated and received a battery set according to its energy needs. As shown in Table XLIII, Table XLIV and Table XLV, the batteries used to assemble the batteries sets had fixed capacities, making some energy values impossible to be arranged exactly. Even with this impossibility, the energy budget, which is the total energy received by a network, of the networks with redistributed energy did not exceed the energy budget of the network with homogeneous energy distribution in any case, being in fact lower in almost all cases.

The energy distribution for the networks with different base station placement, shown in Fig. 94 (a)-(c), reveals the higher energy consumption of the motes nearer base station, caused by the extra workload of both receiving and rerouting messages of farther motes which, therefore, demands more energy. It is important to notice that the energy distribution pattern shown in Fig. 94 (a)-(c) indicates the occurrence of Energy Hole/Doughnut Effect, which can be explicated by the higher demanding workloads, of both listening and rerouting messages, that the motes nearer to the base station have to handle.

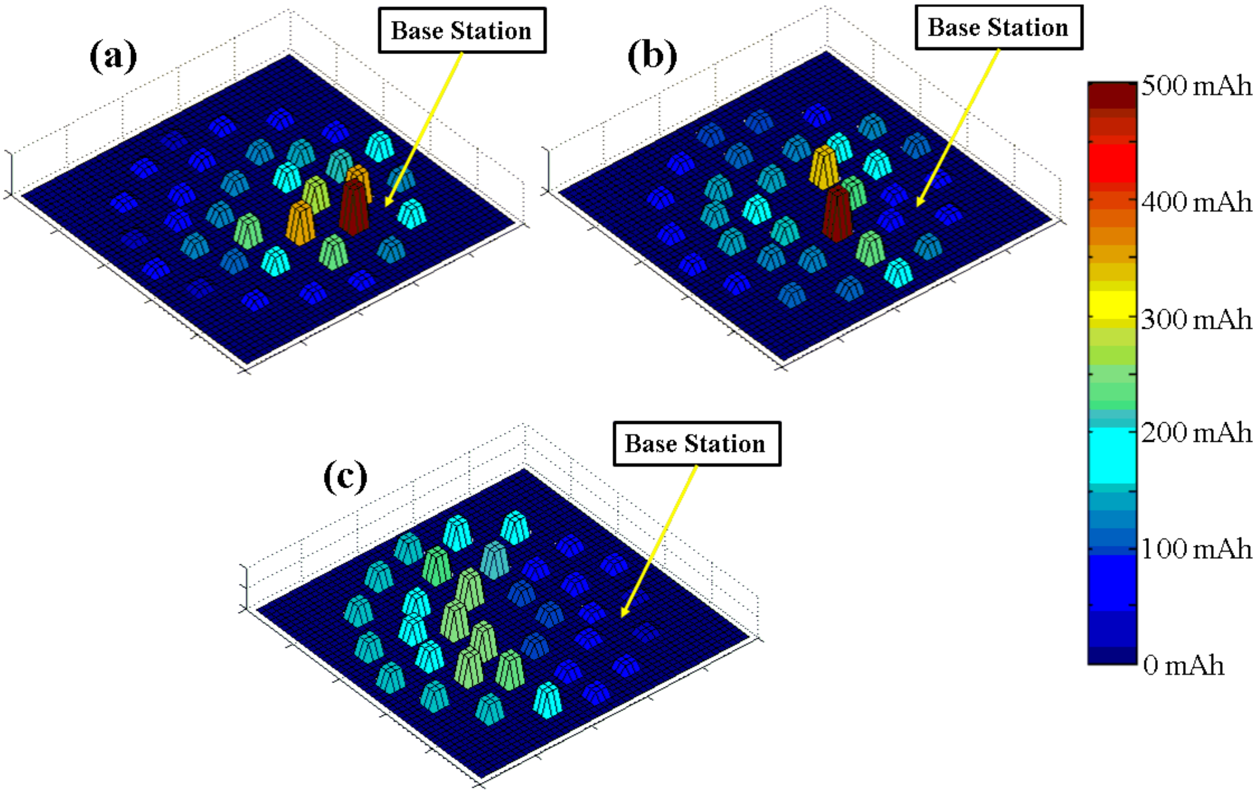

Fig. 94 – Energy distribution among motes of the networks simulated in Scenario II with T = 1s using P_{tx} (**a**); using 11.31P_{tx} (**b**); using 46.76P_{tx} (**c**).

The complete energy assignment of Scenario I is presented in Appendix D, E and F.

5.6.2.2 Transmission Power Levels

As all motes transmit their messages towards a single base station, their maximum transmission power levels did not exceed the power needed to reach the base station in any situation. Fig. 95 (**a**)-(**c**) shows the transmission power level of each mote in the networks simulated in Scenario II: Fig. 95 (**a**) all motes using P_{tx}, reaching a maximum distance d; Fig. 95 (**b**) some motes using up to 11.31P_{tx}, reaching a maximum distance 2d; Fig. 95 (**c**) some motes using up to 46.76P_{tx}, reaching a maximum distance 3d.

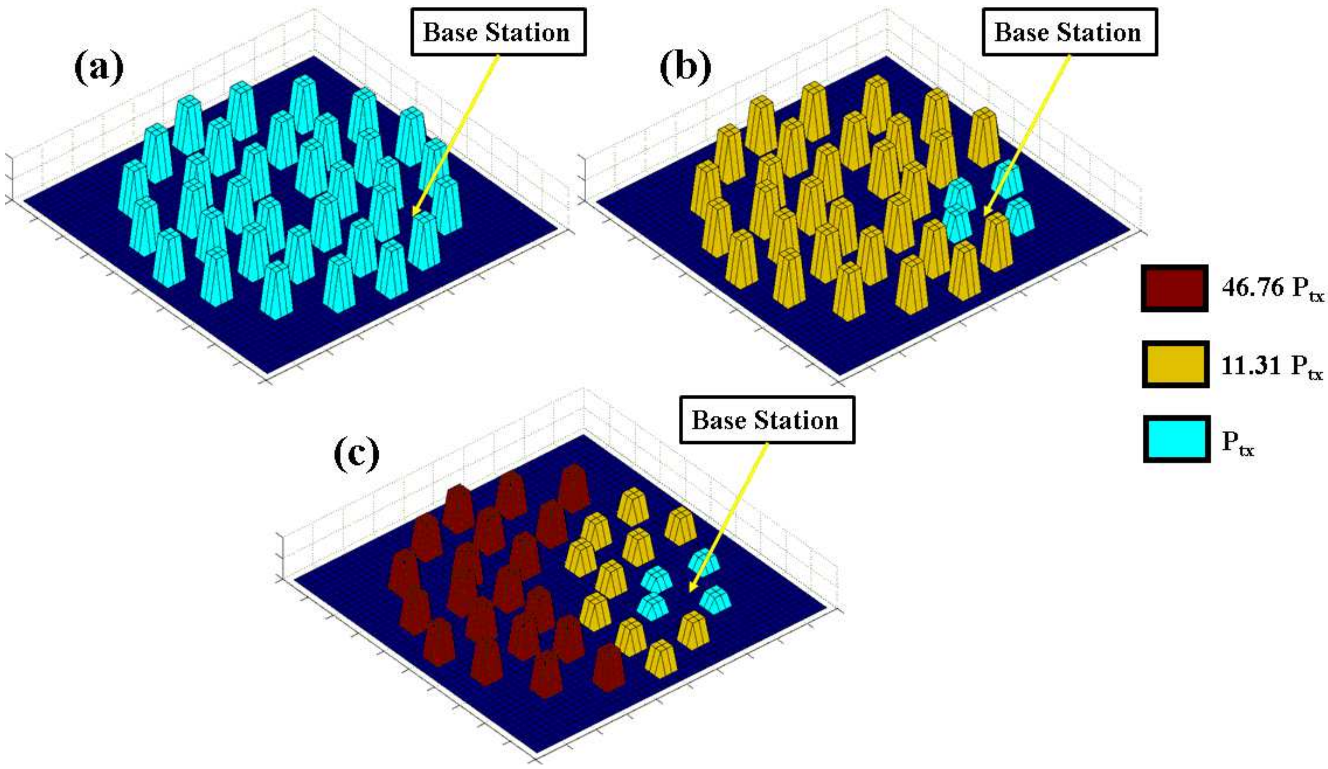

Fig. 95 – Transmission power levels of the networks simulated in Scenario II using P_{tx} (**a**); using $11.31P_{tx}$ (**b**); using $46.76P_{tx}$ (**c**).

The individual transmission power level of each mote of Scenario II is show in Appendix J.

5.6.2.3 Primary and Secondary Consumption

As can be observed in Fig. 96 and Table LVII, the average primary energy consumption, which is the consumption for reading sensors, transmitting/receiving and processing messages, got a descendant share on the total consumption of the network when the message generation got lower. This trend was maintained on all cases.

The average primary energy consumptions in Scenario II were:

- P_{tx} – 1 hop
  - 1 message per second: **99.58%**; 1 message at each 10 seconds: **95.80%**; 1 message at each 60 seconds: **79.09%**; 1 message at each 600 seconds: **27.43%**; 1 message at each 3600 seconds: **5.92%**; 1 message at each 86400 seconds: **0.26%**.

- $11.31P_{tx} – 2d$

- 1 message per second: **99.77%**; 1 message at each 10 seconds: **97.72%**; 1 message at each 60 seconds: **87.68%**; 1 message at each 600 seconds: **41.55%**; 1 message at each 3600 seconds: **10.59%**; 1 message at each 86400 seconds: **0.49%**.

- $46.76P_{tx} - 3d$
  - 1 message per second: **99.87%**; 1 message at each 10 seconds: **98.69%**; 1 message at each 60 seconds: **92.61%**; 1 message at each 600 seconds: **55.61%**; 1 message at each 3600 seconds: **17.27%**; 1 message at each 86400 seconds: **0.86%**.

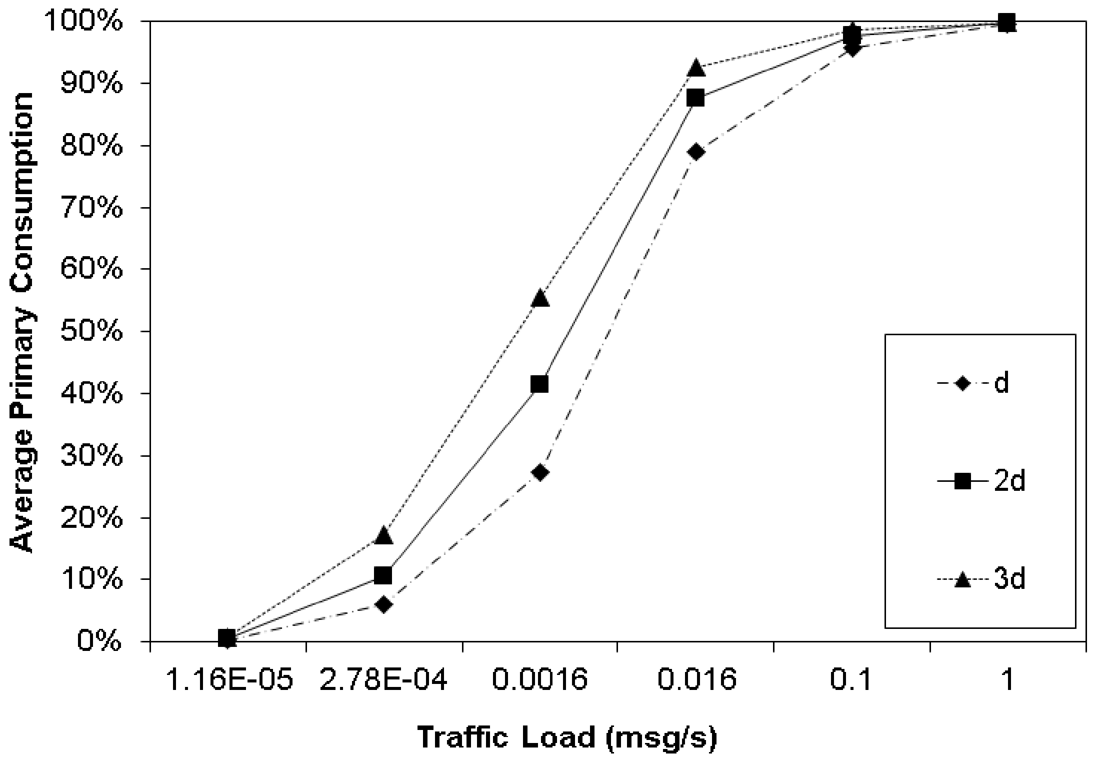

Fig. 96 – Average primary/secondary energy consumption of the networks in Scenario II.

Table LVII – Average primary energy consumption in Scenario II.

Traffic Load (msg/s)	**Average Primary Consumption – 1*d***	**Average Primary Consumption – 2*d***	**Average Primary Consumption – 3*d***
1.16E-05	0.26%	0.49%	0.86%
2.78E-04	5.92%	10.59%	17.27%
0.00166	27.43%	41.55%	55.61%
0.166	79.09%	87.68%	92.61%
0.1	95.80%	97.72%	98.69%
1	99.58%	99.77%	99.87%

5.6.2.4 Lifetime

Fig. 97 and Table LVIII show that, again, the lifetime of the simulated networks using standard power with energy redistribution and the networks using $11.31P_{tx}$ $(2d)$ with energy redistribution were longer when compared to standard power with homogenous energy distribution. Fig. 97 and Table LVIII also show that the difference between the lifetime of the simulated networks decreased when the traffic load got lower. As the traffic load was being reduced, networks using higher transmission power almost attained the same lifetime of the standard transmission power network.

Fig. 97 and Table LVIII also show that the networks using the standard power with energy redistribution and the networks using $11.31P_{tx}$ $(2d)$ with energy redistribution had longer lifetime on all cases.

The lifetimes of the simulations in Scenario II were:

- $P_{tx} - 1d$
  - 1 message per second: **7.92 hours**; 1 message at each 10 seconds: **78.43 hours**;

    1 message at each 60 seconds: **476.2 hours**; 1 message at each 600 seconds: **2777.81 hours**; 1 message at each 3600 seconds: **5405.3 hours**; 1 message at each 86400 seconds: **6602.26 hours**.
- $P_{tx} - 1d$ with energy redistribution
  - 1 message per second: **27.74 hours**; 1 message at each 10 seconds: **267.79 hours**;

    1 message at each 60 seconds: **1320.66 hours**; 1 message at each 600 seconds: **4623 hours**; 1 message at each 3600 seconds: **6153.29 hours**; 1 message at each 86400 seconds: **6643.69 hours**.
- $11.31P_{tx} - 2d$ with energy redistribution
  - 1 message per second: **15.36 hours**; 1 message at each 10 seconds: **148.99 hours**;

    1 message at each 60 seconds: **805.56 hours**; 1 message at each 600 seconds: **3825.5 hours**; 1 message at each 3600 seconds: **5862.29 hours**; 1 message at each 86400 seconds: **6630.8 hours**.
- $46.76P_{tx} - 3d$ with energy redistribution
  - 1 message per second: **8.41 hours**; 1 message at each 10 seconds: **82.84 hours**;

1 message at each 60 seconds: **478.81 hours**; 1 message at each 600 seconds: **2891.21 hours**; 1 message at each 3600 seconds: **5417.8 hours**; 1 message at each 86400 seconds: **6608.32 hours**.

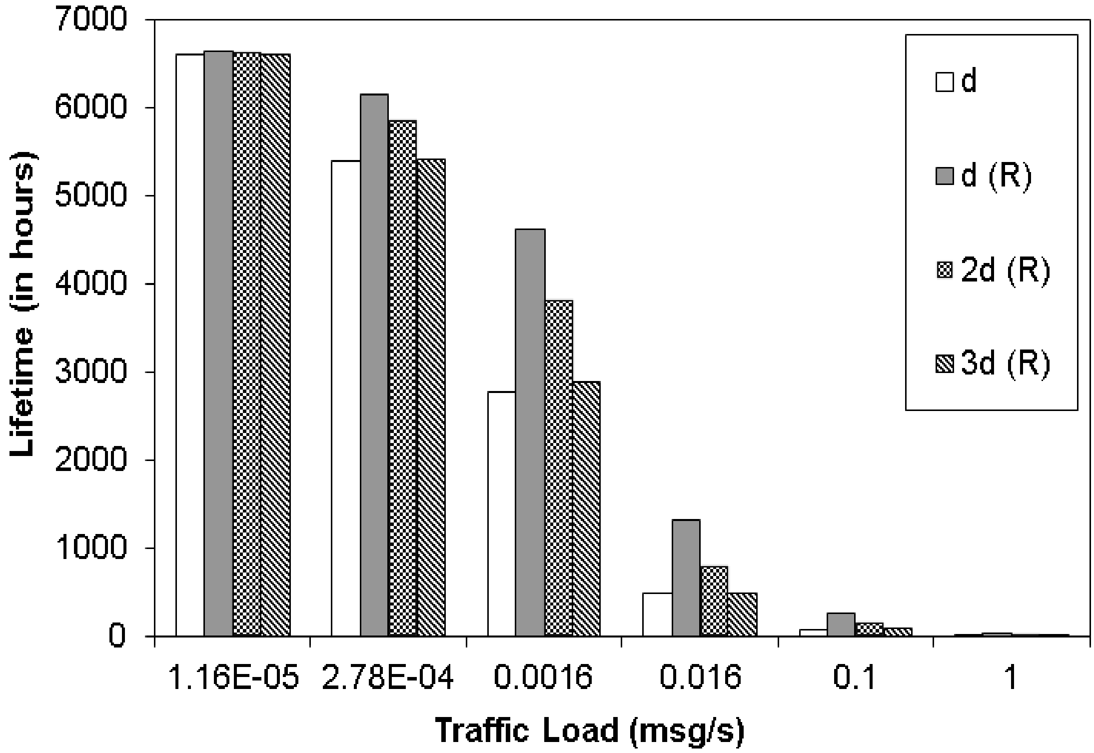

Fig. 97 – Lifetime of the networks with different transmission powers in Scenario II.

Table LVIII – Lifetime of the networks with different transmission powers in Scenario II.

Traffic Load (msg/s)	Lifetime (in hours) – 1*d*	Lifetime (in hours) – 1*d* Redistributed	Lifetime (in hours) – 2*d* Redistributed	Lifetime (in hours) – 3*d* Redistributed
1.16E-05	6602.26	6643.69	6630.8	6608.32
2.78E-04	5405.3	6153.29	5862.29	5417.8
0.00166	2777.81	4623	3825.5	2891.21
0.166	476.2	1320.66	805.56	478.81
0.1	78.43	267.79	148.99	82.84
1	7.92	27.74	15.36	8.41

5.6.2.5 Network Cost

Fig. 98 and Table LIX show the cost of each network per hour of their lifetime. As the network cost is the same on all simulated networks (US$1,513.34), the lifetime was the key issue in Scenario II, making the cost of each network cheaper according the traffic generation got lower.

In Scenario II, all network costs got lower when the traffic generation was reduced and the networks using the standard transmission power and $11.31P_{tx}$, both using the energy redistribution, had the lowest network cost on all cases.

The network cost of the simulations in Scenario II were:

- $P_{tx} - 1d$
  - 1 message per second: **US$191.08**; 1 message at each 10 seconds: **US$19.30**;

    1 message at each 60 seconds: **US$3.18**; 1 message at each 600 seconds: **US$0.54**; 1 message at each 3600 seconds: **US$0.28**; 1 message at each 86400 seconds: **US$0.23**.
- $P_{tx} - 1d$ with energy redistribution
  - 1 message per second: **US$54.55**; 1 message at each 10 seconds: **US$5.65**;

    1 message at each 60 seconds: **US$1.15**; 1 message at each 600 seconds: **US$0.33**; 1 message at each 3600 seconds: **US$0.25**; 1 message at each 86400 seconds: **US$0.23**.
- $11.31P_{tx} - 2d$ with energy redistribution
  - 1 message per second: **US$98.52**; 1 message at each 10 seconds: **US$10.16**;

    1 message at each 60 seconds: **US$1.88**; 1 message at each 600 seconds: **US$0.40**; 1 message at each 3600 seconds: **US$0.26**; 1 message at each 86400 seconds: **US$0.23**.

- $46.76P_{tx}$ – $3d$ with energy redistribution
  - 1 message per second: **US$179.95**; 1 message at each 10 seconds: **US$18.27**; 1 message at each 60 seconds: **US$3.16**; 1 message at each 600 seconds: **US$0.52**; 1 message at each 3600 seconds: **US$0.28**; 1 message at each 86400 seconds: **US$0.23**.

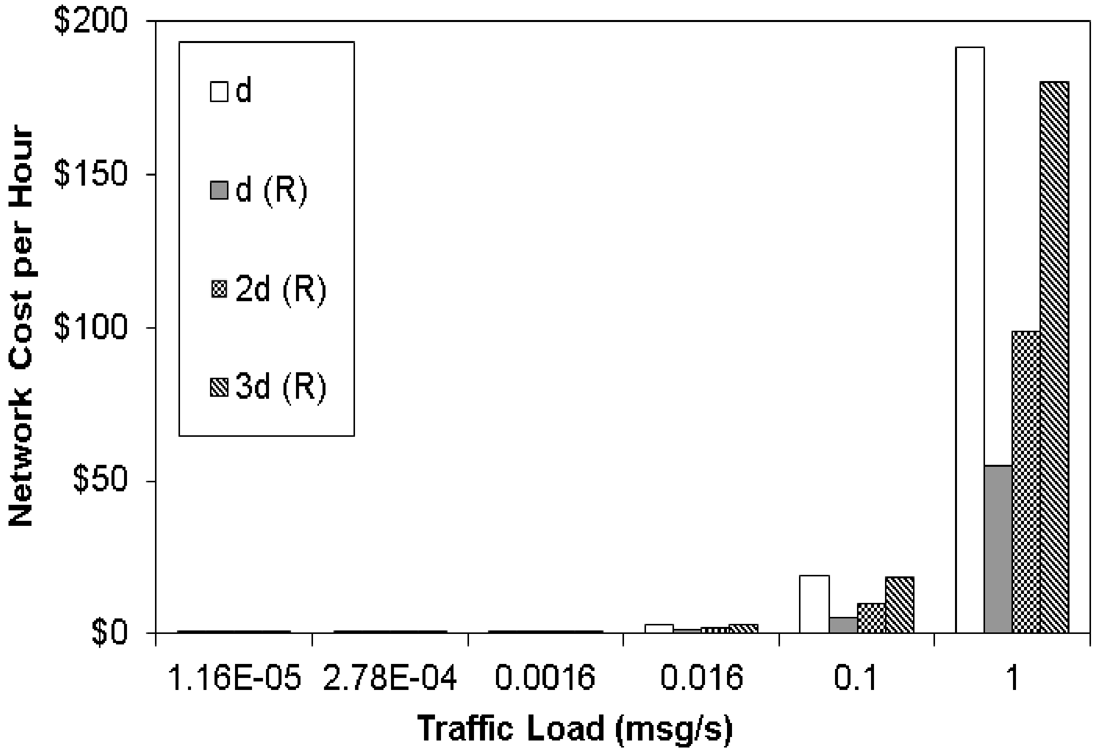

Fig. 98 – Network cost of the networks simulated in Scenario II.

Table LIX – Network cost of the networks simulated in Scenario II.

Traffic Load (msg/s)	**Network Cost – 1*d***	**Network Cost – 1*d* Redistributed**	**Network Cost – 2*d* Redistributed**	**Network Cost – 3*d* Redistributed**
1.16E-05	US$0.23	US$0.23	US$0.23	US$0.23
2.78E-04	US$0.28	US$0.25	US$0.26	US$0.28
0.00166	US$0.54	US$0.33	US$0.40	US$0.52
0.166	US$3.18	US$1.15	US$1.88	US$3.16
0.1	US$19.30	US$5.65	US$10.16	US$18.27
1	US$191.08	US$54.55	US$98.52	US$179.95

5.6.2.6 Remaining Energy

Fig. 99 and Table LX show the average remaining energy of the networks simulated in Scenario II. The average remaining energy was way higher when the network used the homogeneous energy distribution.

The average remaining energy of the simulations in Scenario II were:

- $P_{tx} - 1d$
  - 1 message per second: **72.91%**; 1 message at each 10 seconds: **72.14%**; 1 message at each 60 seconds: **68.13%**; 1 message at each 600 seconds: **42.58%**; 1 message at each 3600 seconds: **13.81%**; 1 message at each 86400 seconds: **0.70%**.
- $P_{tx} - 1d$ with energy redistribution
  - 1 message per second: **5.16%**; 1 message at each 10 seconds: **4.86%**; 1 message at each 60 seconds: **5.16%**; 1 message at each 600 seconds: **4.40%**; 1 message at each 3600 seconds: **1.86%**; 1 message at each 86400 seconds: **0.08%**.
- $11.31P_{tx} - 2d$ with energy redistribution
  - 1 message per second: **1.30%**; 1 message at each 10 seconds: **2.35%**; 1 message at each 60 seconds: **1.97%**; 1 message at each 600 seconds: **1.78%**; 1 message at each 3600 seconds: **1.54%**; 1 message at each 86400 seconds: **0.04%**.
- $46.76P_{tx} - 3d$ with energy redistribution
  - 1 message per second: **4.96%**; 1 message at each 10 seconds: **5.33%**; 1 message at each 60 seconds: **2.82%**; 1 message at each 600 seconds: **2.23%**; 1 message at each 3600 seconds: **1.68%**; 1 message at each 86400 seconds: **0.01%**.

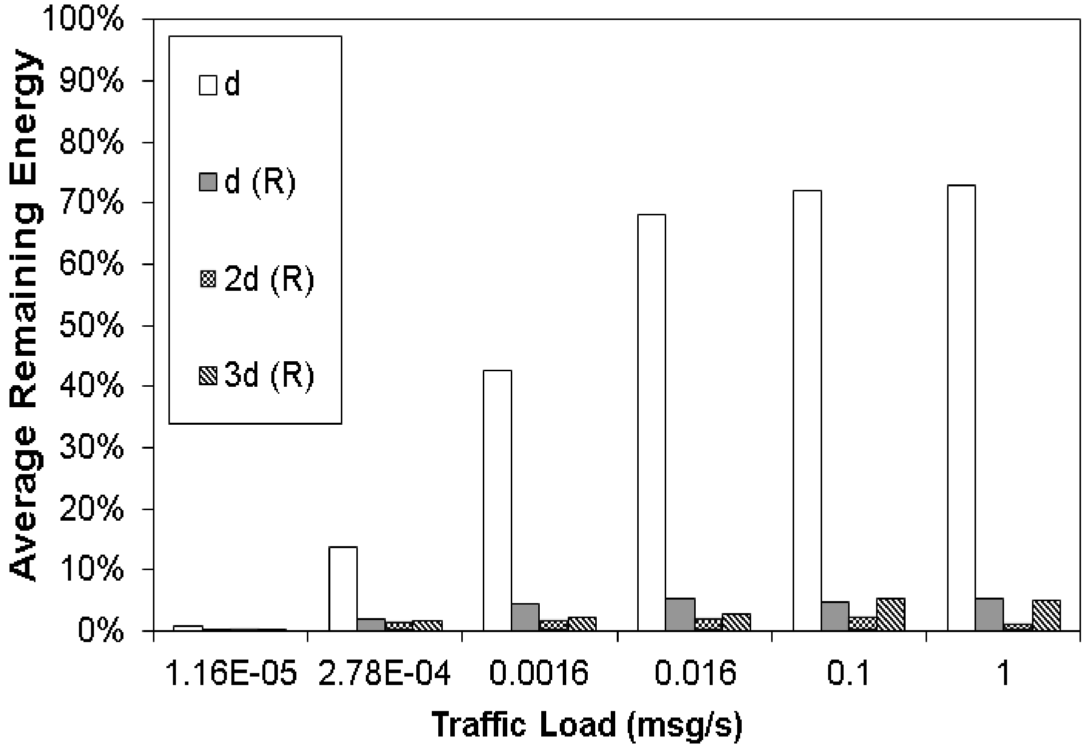

Fig. 99 – Average remaining energy of each network in Scenario II.

Table LX – Average remaining energy of each network in Scenario II.

Traffic Load (msg/s)	Average Remaining Energy – 1*d*	Average Remaining Energy – 1*d* Redistributed	Average Remaining Energy – 2*d* Redistributed	Average Remaining Energy – 3*d* Redistributed
1.16E-05	0.70%	0.08%	0.04%	0.01%
2.78E-04	13.81%	1.86%	1.54%	1.68%
0.00166	42.58%	4.40%	1.78%	2.23%
0.166	68.13%	5.16%	1.97%	2.82%
0.1	72.14%	4.86%	2.35%	5.33%
1	72.91%	5.16%	1.30%	4.96%

5.6.2.7 Energy Consumption Profile

As can be observed in Fig. 100, Fig. 101, Fig. 102 and in Table LXI, due to the transmission power increase, the energy spent on transmissions (labeled as Radio-TX) increased, following the transmission power increase. The energy consumption profile of Secondary states is the same on all cases and is shown in Fig. 103 and Table LXII.

The energy consumption profile of the simulations in Scenario II were:

- $P_{tx} - 1d$
  - Radio transmission:**20.57%**; Radio reception:**45.62%**; Microcontroller:**26.45%**; Sensor: **7.34%**.
- $11.31P_{tx} - 2d$
  - Radio transmission:**56.44%**; Radio reception:**34.64%**; Microcontroller:**6.97%**; Sensor: **1.93%**.
- $46.76P_{tx} - 3d$
  - Radio transmission:**70.89%**; Radio reception:**25.52%**; Microcontroller:**2.95%**; Sensor: **0.63%**.
- Secondary Consumption
  - Radio: **47.61%**; Microcontroller :**23.81%**; Sensor: **28.58%**.

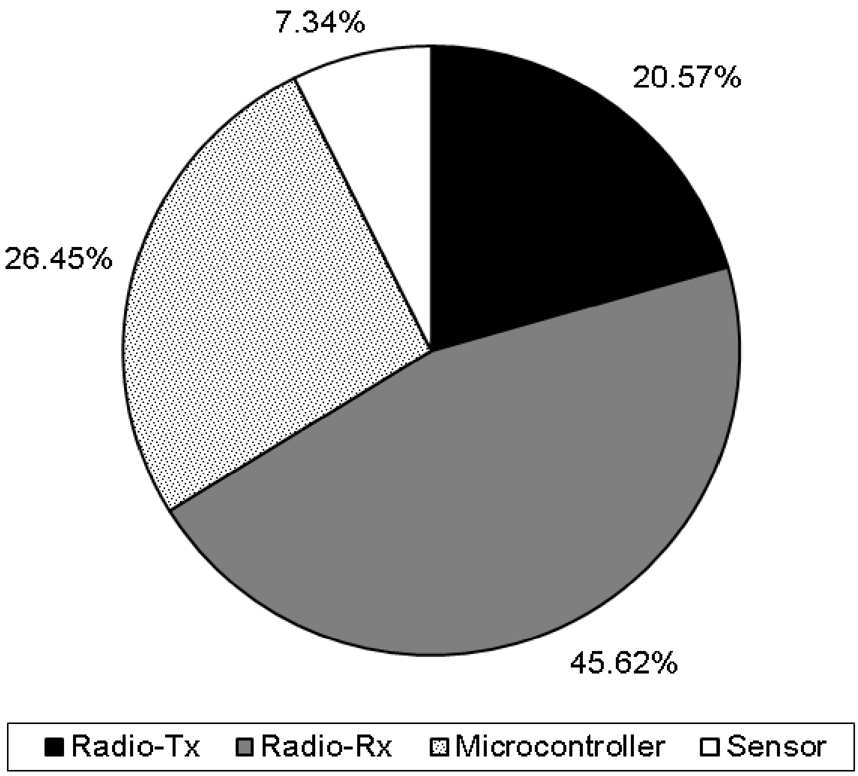

Fig. 100 – Energy consumption profile in Scenario II – P_{tx} ($1d$).

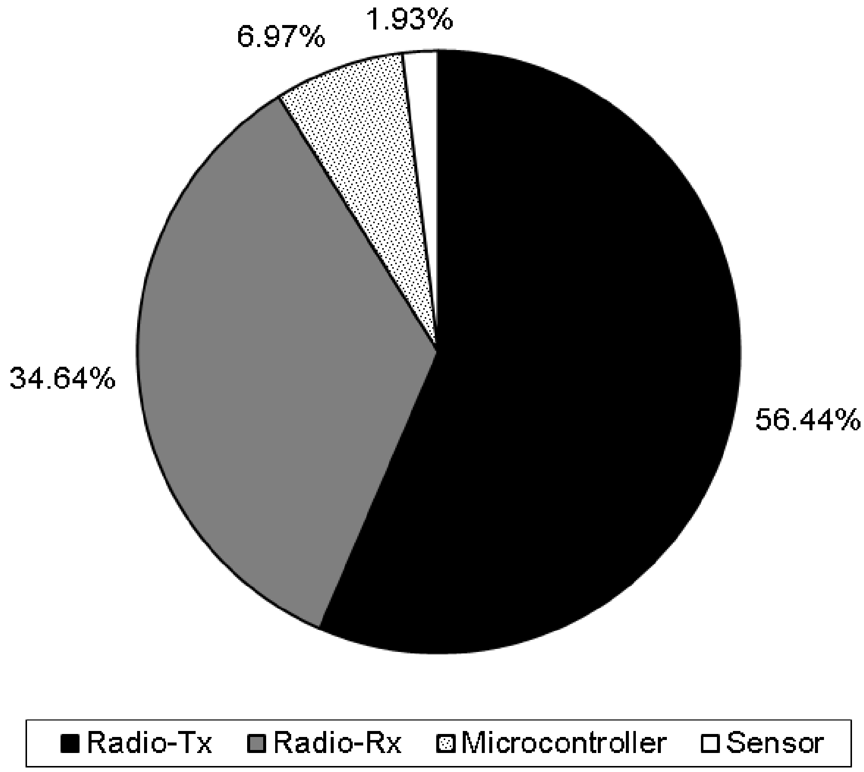

Fig. 101 – Energy consumption profile in Scenario II – $11.31P_{tx}$ ($2d$).

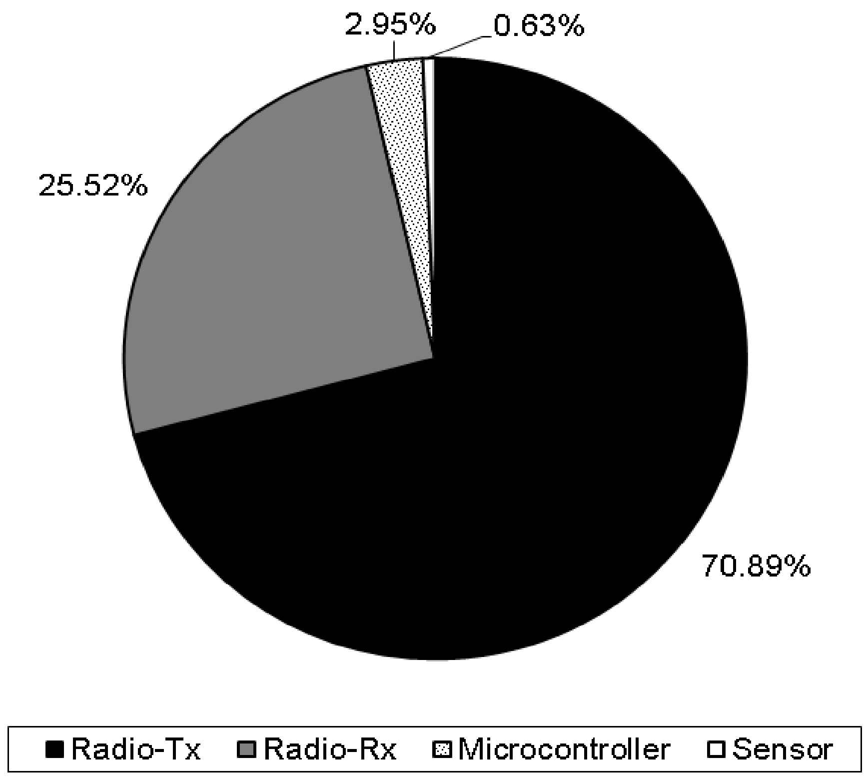

Fig. 102 – Energy consumption profile in Scenario II – $46.76P_{tx}$ ($3d$).

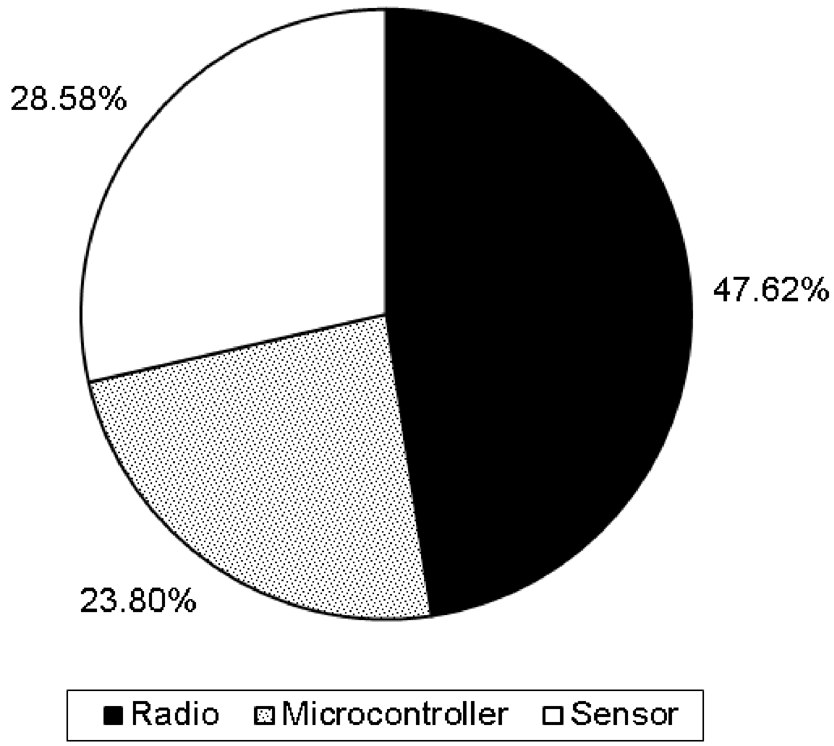

Fig. 103 – Energy consumption profile in Scenario II – Secondary Consumption.

Table LXI – Energy consumption of each part of the networks in Scenario II.

Transmission Power	Reach	Radio-Tx	Radio-Rx	Microcontroller	Sensor
P_{tx}	$1d$	20.57%	45.62%	26.45%	7.34%
$11.31P_{tx}$	$2d$	56.44%	34.64%	6.97%	1.93%
$46.76P_{tx}$	$3d$	70.89%	25.52%	2.95%	0.63%

Table LXII – Energy consumption profile of Secondary States in Scenario II.

Radio	Microcontroller	Sensor
47.61%	23.81%	28.58%

5.6.2.8 Message Log

Fig. 104 and Table LXIII show that the total of listened messages in relation to generated messages increased with higher transmission power, from 1811% to 3359%.

Fig. 105 and Table LXIII show that the total of rerouted messages in relation to generated messages decreased with higher transmission power, from 250% to 29%.

Fig. 106 and Table LXIII show that the total of overheard messages in relation to generated messages increased with higher transmission power, from 1561% to 3330%.

The message log of the simulations in Scenario II were:

- $P_{tx} - 1d$
    - Listened Messages: **1811%**; Rerouted Messages: **250%**; Overheard Messages: **1561%**.
- $11.31P_{tx} - 2d$
    - Listened Messages: **2587%**; Rerouted Messages: **74%**; Overheard Messages: **2514%**.
- $46.76P_{tx} - 3d$
    - Listened Messages: **3359%**; Rerouted Messages: **29%**; Overheard Messages: **3330%**.

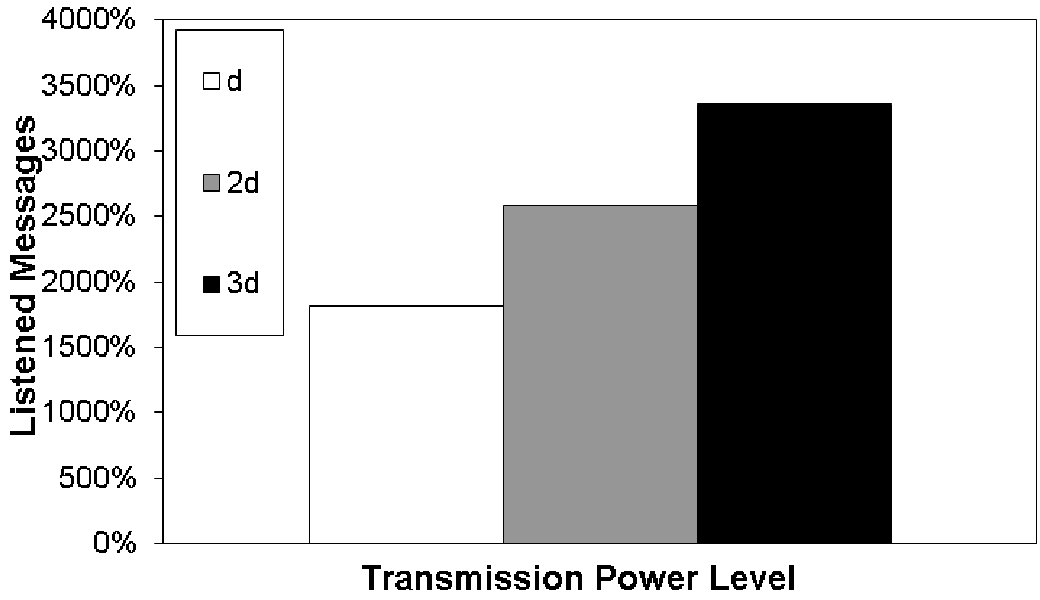

Fig. 104 – Log of listened messages of the simulations in Scenario II.

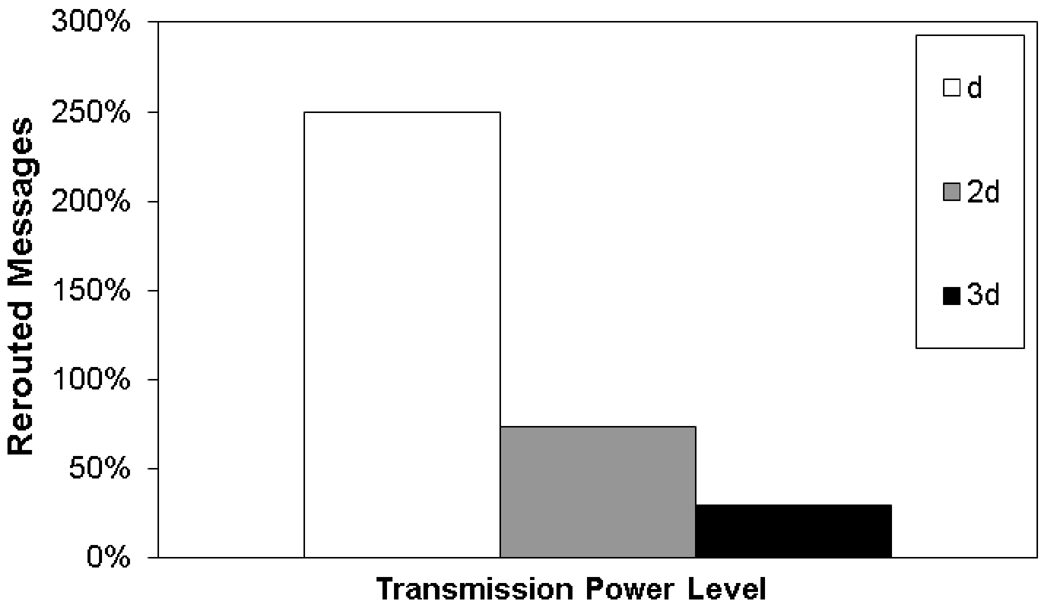

Fig. 105 – Log of rerouted messages of the simulations in Scenario II.

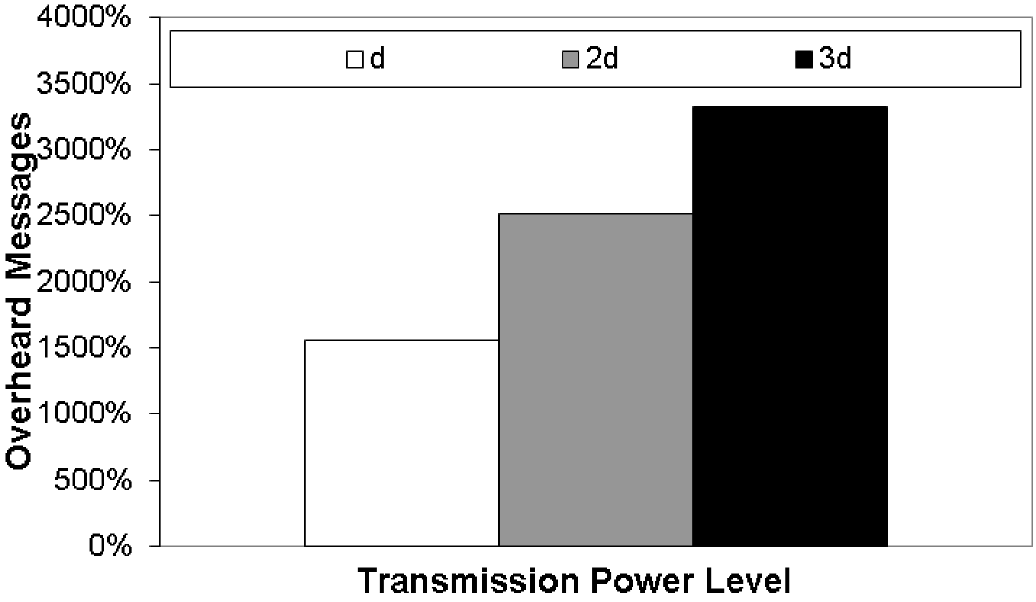

Fig. 106 – Log of overheard messages of the simulations in Scenario II.

Table LXIII – Message logs of Scenario II.

Transmission Power	Reach	Listened Messages	Rerouted Messages	Overheard Messages
P_{tx}	$1d$	1811%	250%	1561%
$11.31P_{tx}$	$2d$	2587%	74%	2514%
$46.76P_{tx}$	$3d$	3359%	29%	3330%

5.6.2.9 Energy Consumption Calculation Error

Using the mathematical models presented in Chapter IV and [147], we could estimate both the individual energy consumption of each mote and the network energy consumption per network cycle. Fig. 107 and Table LXIV show the average error of the calculated individual energy consumption in relation to the simulated values and Fig. 108 and Table LXV show the error of the calculated network energy consumption in relation to the simulated values.

It is important to state that the calculated individual energy consumption errors were due both overestimation and underestimation, resulting in different errors of the calculated network energy consumption.

The average error of the calculated individual energy consumption of the simulations in Scenario II were:

- $P_{tx} - 1d$

  - 1 message per second: **3.86%**; 1 message at each 10 seconds: **3.72%**; 1 message at each 60 seconds: **3.09%**; 1 message at each 600 seconds: **1.22%**; 1 message at each 3600 seconds: **0.30%**; 1 message at each 86400 seconds: **0.01%**.
- $11.31P_{tx} - 2d$
  - 1 message per second: **1.00%**; 1 message at each 10 seconds: **0.98%**; 1 message at each 60 seconds: **0.89%**; 1 message at each 600 seconds: **0.45%**; 1 message at each 3600 seconds: **0.13%**; 1 message at each 86400 seconds: **0.01%**.
- $46.76P_{tx} - 3d$
  - 1 message per second: **0.29%**; 1 message at each 10 seconds: **0.28%**; 1 message at each 60 seconds: **0.26%**; 1 message at each 600 seconds: **0.15%**; 1 message at each 3600 seconds: **0.05%**; 1 message at each 86400 seconds: **less than 0.01%**.

The average error of the calculated network energy consumption of the simulations in Scenario II were:

- $P_{tx} - 1d$
  - 1 message per second: **5.52%**; 1 message at each 10 seconds: **5.30%**; 1 message at each 60 seconds: **4.34%**; 1 message at each 600 seconds: **1.46%**; 1 message at each 3600 seconds: **0.31%**; 1 message at each 86400 seconds: **0.01%**.
- $11.31P_{tx} - 2d$
  - 1 message per second: **1.31%**; 1 message at each 10 seconds: **1.29%**; 1 message at each 60 seconds: **1.16%**; 1 message at each 600 seconds: **0.54%**; 1 message at each 3600 seconds: **0.14%**; 1 message at each 86400 seconds: **0.01%**.
- $46.76P_{tx} - 3d$
  - 1 message per second: **0.16%**; 1 message at each 10 seconds: **0.15%**; 1 message at each 60 seconds: **0.14%**; 1 message at each 600 seconds: **0.08%**; 1 message at each 3600 seconds: **0.02%**; 1 message at each 86400 seconds: **less than 0.01%**.

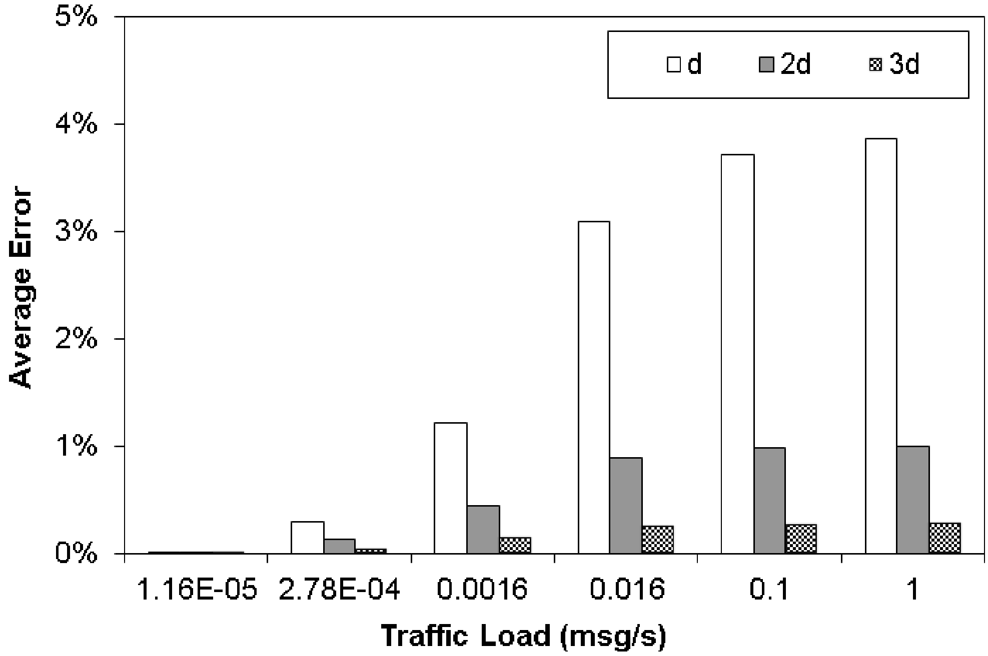

Fig. 107 – Average consumption error (calculated x simulated) of Scenario II.

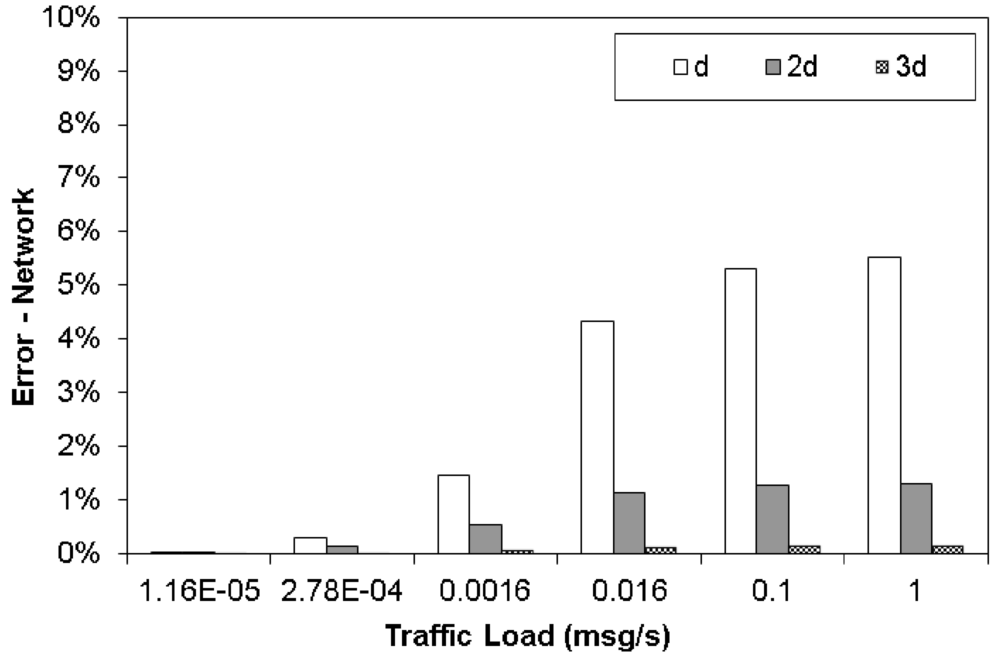

Fig. 108 – Network consumption error (calculated x simulated) of Scenario II.

Table LXIV – Average consumption error (calculated x simulated) of Scenario II.

Traffic Load (msg/s)	Average Error – 1*d*	Average Error – 2*d*	Average Error – 3*d*
1.16E-05	0.01%	0.01%	<0.01%
2.78E-04	0.30%	0.13%	0.05%
0.00166	1.22%	0.45%	0.15%
0.166	3.09%	0.89%	0.26%
0.1	3.72%	0.98%	0.28%
1	3.86%	1.00%	0.29%

Table LXV – Network consumption error (calculated x simulated) of Scenario II.

Traffic Load (msg/s)	Network Error – 1*d*	Network Error – 2*d*	Network Error – 3*d*
1.16E-05	0.01%	0.01%	<0.01%
2.78E-04	0.31%	0.14%	0.02%
0.00166	1.46%	0.54%	0.08%
0.166	4.34%	1.16%	0.14%
0.1	5.30%	1.29%	0.15%
1	5.52%	1.31%	0.16%

5.6.3 Scenario III

In Scenario III, the 34-mote network shown in Fig. 109 was simulated using the path loss exponent set to **3.5**. Its base station was dislocated to the southeast of the network, outside the network cluster.

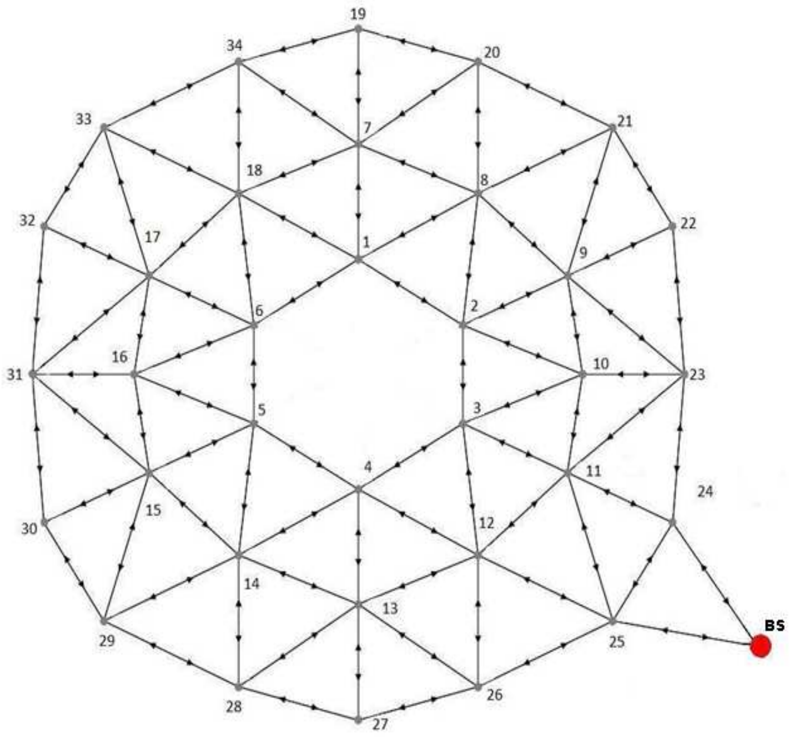

Fig. 109 – Network simulated in Scenario III.

5.6.3.1 Battery Redistribution

Using the techniques presented in Chapter IV, each mote on all cases had its individual energy consumption calculated and received a battery set according to its energy needs. As shown in Table XLIII, Table XLIV and Table XLV, the batteries used to assemble the batteries sets had fixed capacities, making some energy values impossible to be arranged exactly. Even with this impossibility, the energy budget, which is the total energy received by a network, of the networks with redistributed energy did not exceed the energy budget of the network with homogeneous energy distribution in any case, being in fact lower in almost all cases.

The energy distribution for the networks with different base station placement, shown in Fig. 110 (a)-(c), reveals the higher energy consumption of the motes nearer base station, caused by the extra workload of both receiving and rerouting messages of farther motes which, therefore, demands more energy. It is important to notice that the energy distribution pattern shown in Fig. 110 (a)-(c) indicates the occurrence of Energy Hole/Doughnut Effect, which can be explicated by the higher demanding workloads, of both listening and rerouting messages, that the motes nearer to the base station have to handle.

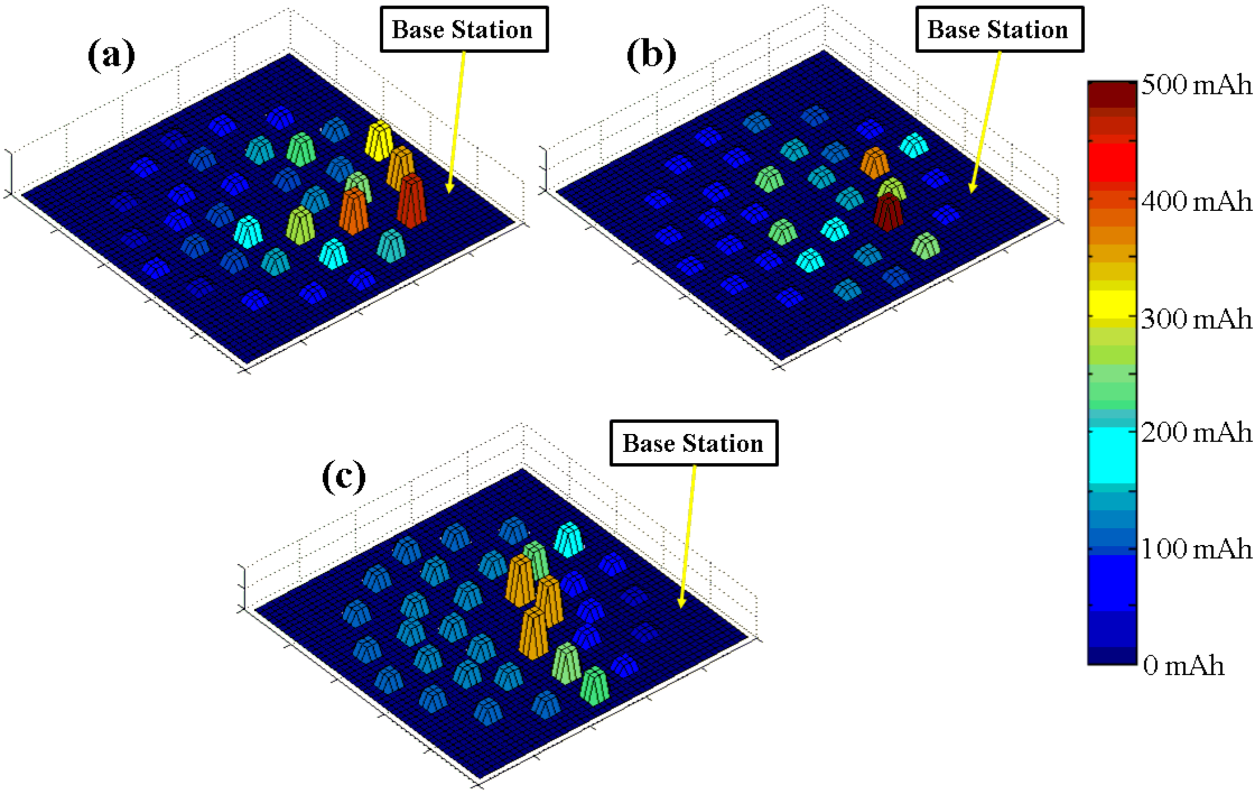

Fig. 110 – Energy distribution among motes of the networks simulated in Scenario III with T = 1s using P_{tx} (**a**); using 11.31P_{tx} (**b**); using 46.76P_{tx} (**c**).

The complete energy assignment of Scenario I is presented in Appendix G, H and I.

5.6.3.2 Transmission Power Levels

As all motes transmit their messages towards a single base station, their maximum transmission power levels did not exceed the power needed to reach the base station in any situation. Fig. 111 (**a**)-(**c**) shows the transmission power level of each mote in the networks simulated in Scenario I: Fig. 111 (**a**) all motes using P_{tx}, reaching a maximum distance d; Fig. 111 (**b**) some motes using up to 11.31P_{tx}, reaching a maximum distance 2d; Fig. 111 (**c**) some motes using up to 46.76P_{tx}, reaching a maximum distance 3d.

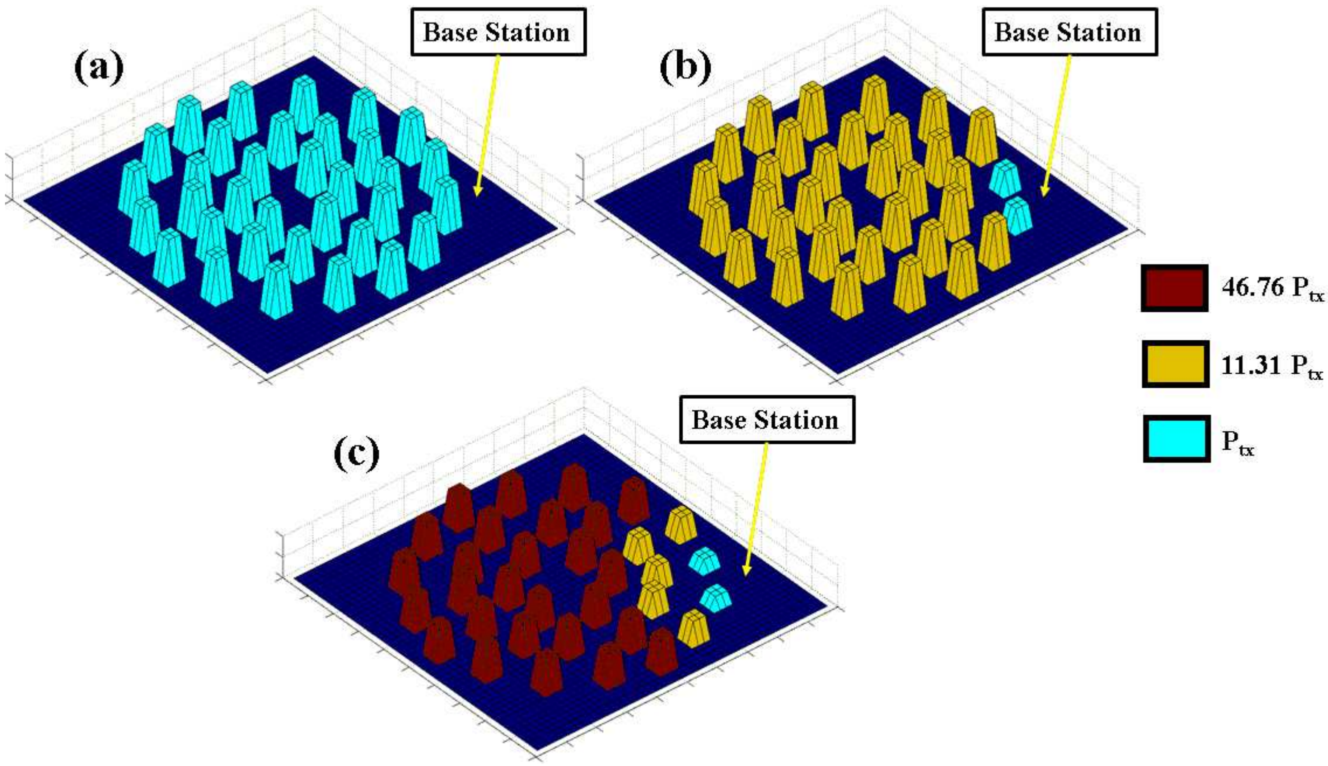

Fig. 111 – Transmission power levels of the networks in Scenario III using P_{tx} (**a**); using $11.31P_{tx}$ (**b**); using $46.76P_{tx}$ (**c**).

The individual transmission power level of each mote of Scenario III is show in Appendix J.

5.6.3.3 Primary and Secondary Consumption

As can be observed in Fig. 112 and Table LXVI, the average primary energy consumption, which is the consumption for reading sensors, transmitting/receiving and processing messages, got a descendant share on the total consumption of the network when the message generation got lower. This trend was maintained on all cases.

The average primary energy consumptions in Scenario III were:

- $P_{tx} - 1d$
  - 1 message per second: **99.61%**; 1 message at each 10 seconds: **96.06%**; 1 message at each 60 seconds: **80.19%**; 1 message at each 600 seconds: **28.80%**; 1 message at each 3600 seconds: **6.31%**; 1 message at each 86400 seconds: **0.28%**.

- $11.31P_{tx} - 2d$

- 1 message per second: **99.82%**; 1 message at each 10 seconds: **98.15%**; 1 message at each 60 seconds: **89.81%**; 1 message at each 600 seconds: **46.84%**; 1 message at each 3600 seconds: **12.80%**; 1 message at each 86400 seconds: **0.61%**.

- $46.76P_{tx} - 3d$
  - 1 message per second: **99.91%**; 1 message at each 10 seconds: **99.06%**; 1 message at each 60 seconds: **94.62%**; 1 message at each 600 seconds: **63.74%**; 1 message at each 3600 seconds: **22.66%**; 1 message at each 86400 seconds: **1.21%**.

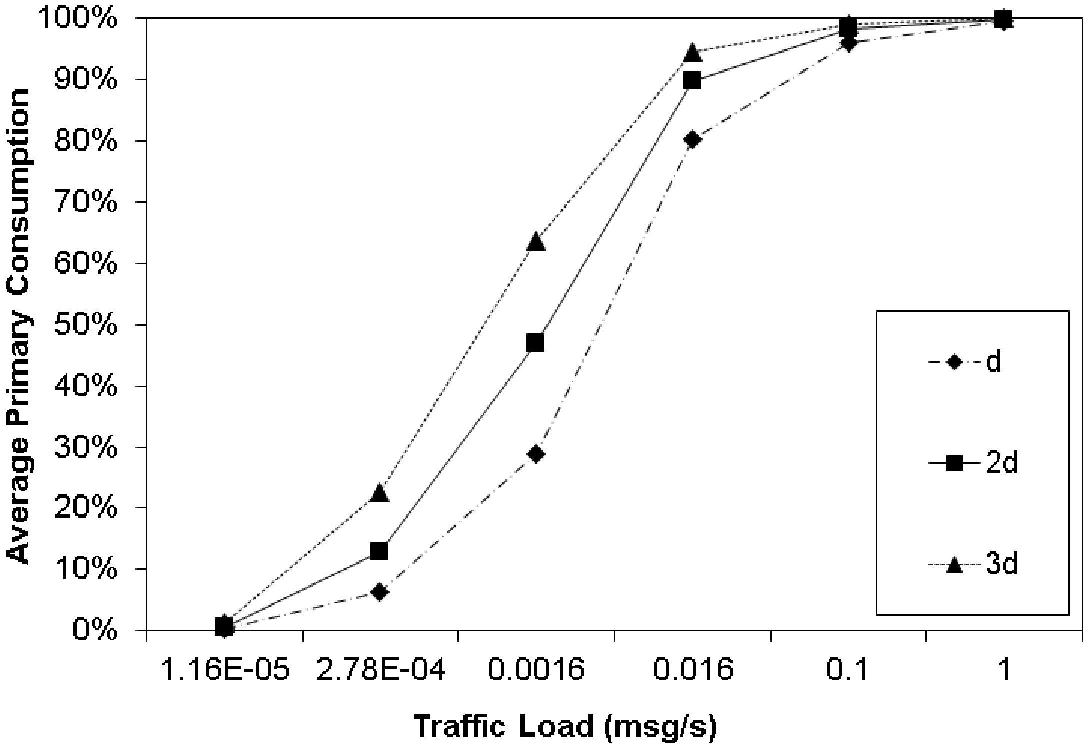

Fig. 112 – Average primary/secondary energy consumption of the networks in Scenario III.

Table LXVI – Average primary energy consumption in Scenario III.

Traffic Load (msg/s)	Average Primary Consumption – 1*d*	Average Primary Consumption – 2*d*	Average Primary Consumption – 3*d*
1.16E-05	0.28%	0.61%	1.21%
2.78E-04	6.31%	12.80%	22.66%
0.00166	28.80%	46.84%	63.74%
0.166	80.19%	89.81%	94.62%
0.1	96.06%	98.15%	99.06%
1	99.61%	99.82%	99.91%

5.6.3.4 Lifetime

Fig. 113 and Table LXVII show that, again, the lifetime of the simulated networks using standard power with energy redistribution and the networks using $11.31P_{tx}$ ($2d$) with energy redistribution were longer when compared to standard power with homogenous energy distribution. Fig. 113 and Table LXVII also show that the difference between the lifetime of the simulated networks decreased when the traffic load got lower. As the traffic load was being reduced, networks using higher transmission power almost attained the same lifetime of the standard transmission power network.

Fig. 113 and Table LXVII also show that the networks using the standard power with energy redistribution and the networks using $11.31P_{tx}$ ($2d$) with energy redistribution had longer lifetime on all cases.

The lifetimes of the simulations in Scenario III were:

- $P_{tx} - 1d$
  - 1 message per second: **8.18 hours**; 1 message at each 10 seconds: **80.94 hours**; 1 message at each 60 seconds: **457.84 hours**; 1 message at each 600 seconds: **2829.5 hours**; 1 message at each 3600 seconds: **5437.59 hours**; 1 message at each 86400 seconds: **6604.29 hours**.
- $P_{tx} - 1d$ with energy redistribution
  - 1 message per second: **25.68 hours**; 1 message at each 10 seconds: **245.57 hours**;

    1 message at each 60 seconds: **1282.66 hours**; 1 message at each 600 seconds: **4661.51 hours**; 1 message at each 3600 seconds: **6184.2 hours**; 1 message at each 86400 seconds: **6647.93 hours**.
- $11.31P_{tx} - 2d$ with energy redistribution
  - 1 message per second: **12.33 hours**; 1 message at each 10 seconds: **120.23 hours**;

    1 message at each 60 seconds: **662.66 hours**; 1 message at each 600 seconds: **3491.33 hours**; 1 message at each 3600 seconds: **5718.05 hours**; 1 message at each 86400 seconds: **6624.62 hours**.
- $46.76P_{tx} - 3d$ with energy redistribution
  - 1 message per second: **6.02 hours**; 1 message at each 10 seconds: **58.37 hours**;

    1 message at each 60 seconds: **340.63 hours**; 1 message at each 600 seconds: **2382.33 hours**; 1 message at each 3600 seconds: **5086.9 hours**; 1 message at each 86400 seconds: **6584.85 hours**.

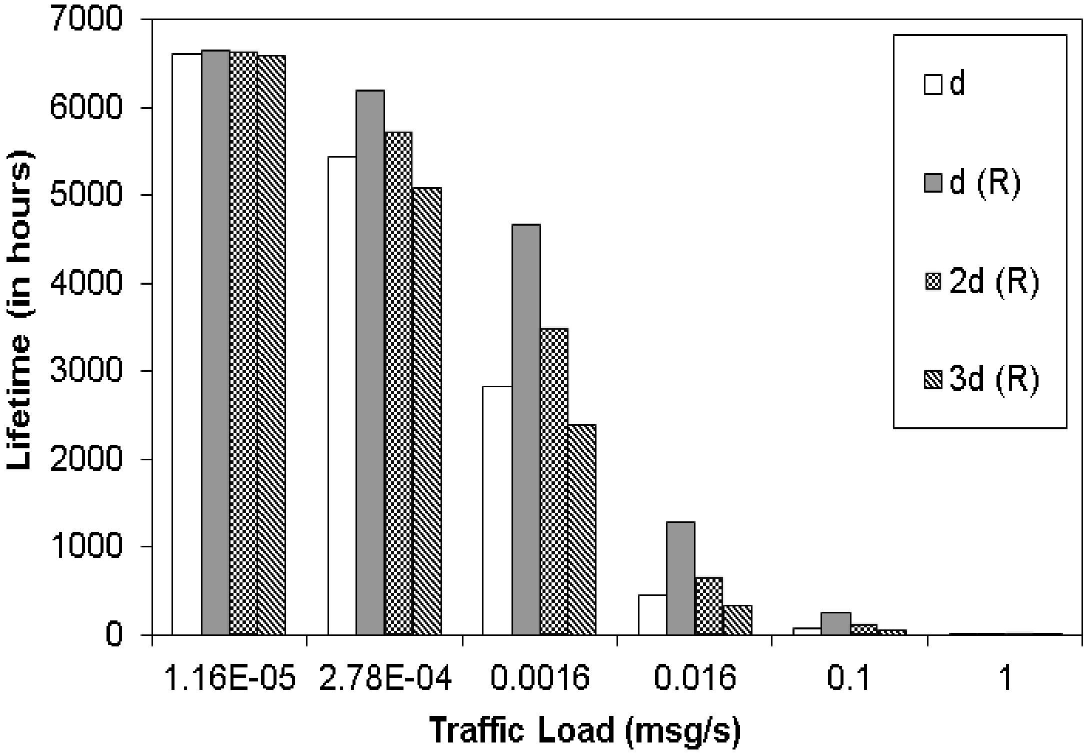

Fig. 113 – Lifetime of the networks with different transmission powers in Scenario III.

Table LXVII – Lifetime of the networks with different transmission powers in Scenario III.

Traffic Load (msg/s)	Lifetime (in hours) – 1d	Lifetime (in hours) – 1d Redistributed	Lifetime (in hours) – 2d Redistributed	Lifetime (in hours) – 3d Redistributed
1.16E-05	6604.29	6647.93	6624.62	6584.85
2.78E-04	5437.59	6184.2	5718.05	5086.9
0.00166	2829.5	4661.51	3491.33	2382.33
0.166	457.84	1282.66	662.66	340.63
0.1	80.94	245.57	120.24	58.37
1	8.18	25.68	12.23	6.02

5.6.3.5 Network Cost

Fig. 114 and Table LXVIII show the cost of each network per hour of their lifetime. As the network cost is the same on all simulated networks (US$1,513.34), the lifetime was the key issue in Scenario III, making the cost of each network cheaper according the traffic generation got lower.

In Scenario III, all network costs got lower when the traffic generation was reduced and the networks using the standard transmission power and 11.31P_{tx}, both using the energy redistribution, had the lowest network cost on all cases.

The network cost of the simulations in Scenario III were:

- $P_{tx} - 1d$

- 1 message per second: **US$185.00**; 1 message at each 10 seconds: **US$18.70**;

  1 message at each 60 seconds: **US$3.31**; 1 message at each 600 seconds: **US$0.53**; 1 message at each 3600 seconds: **US$0.28**; 1 message at each 86400 seconds: **US$0.23**.

- $P_{tx} - 1d$ with energy redistribution
  - 1 message per second: **US$58.93**; 1 message at each 10 seconds: **US$6.16**;

    1 message at each 60 seconds: **US$1.18**; 1 message at each 600 seconds: **US$0.32**; 1 message at each 3600 seconds: **US$0.24**; 1 message at each 86400 seconds: **US$0.23**.

- $11.31P_{tx} - 2d$ with energy redistribution
  - 1 message per second: **US$123.74**; 1 message at each 10 seconds: **US$12.59**;

    1 message at each 60 seconds: **US$2.28**; 1 message at each 600 seconds: **US$0.43**; 1 message at each 3600 seconds: **US$0.26**; 1 message at each 86400 seconds: **US$0.23**.

- $46.76P_{tx} - 3d$ with energy redistribution
  - 1 message per second: **US$251.39**; 1 message at each 10 seconds: **US$25.93**;

    1 message at each 60 seconds: **US$4.44**; 1 message at each 600 seconds: **US$0.64**; 1 message at each 3600 seconds: **US$0.30**; 1 message at each 86400 seconds: **US$0.23**.

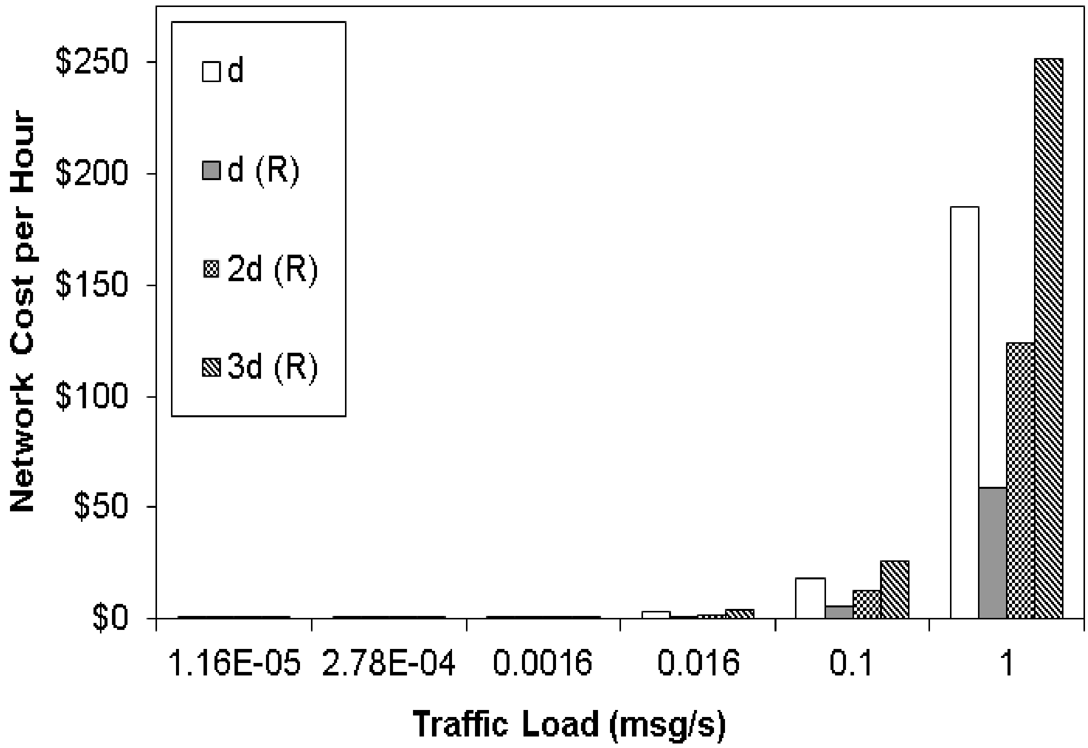

Fig. 114 – Network cost of the networks simulated in Scenario III.

Table LXVIII – Network cost of the networks simulated in Scenario III.

Traffic Load (msg/s)	**Network Cost – 1*d***	**Network Cost – 1*d* Redistributed**	**Network Cost – 2*d* Redistributed**	**Network Cost – 3*d* Redistributed**
1.16E-05	US$0.23	US$0.23	US$0.23	US$0.23
2.78E-04	US$0.28	US$0.24	US$0.26	US$0.30
0.00166	US$0.53	US$0.32	US$0.43	US$0.64
0.166	US$3.31	US$1.18	US$2.28	US$4.44
0.1	US$18.70	US$6.16	US$12.59	US$25.93
1	US$185.00	US$58.93	US$123.74	US$251.39

5.6.3.6 Remaining Energy

Fig. 115 and Table LXIX show the average remaining energy of the networks simulated in Scenario III. The average remaining energy was, again, way higher when the network used the homogeneous energy distribution.

The average remaining energy of the simulations in Scenario III were:

- $P_{tx} - 1d$
    - 1 message per second: **70.09%**; 1 message at each 10 seconds: **69.33%**; 1 message at each 60 seconds: **65.36%**; 1 message at each 600 seconds: **40.39%**; 1 message at each 3600 seconds: **12.93%**; 1 message at each 86400 seconds: **0.65%**.
- $P_{tx} - 1d$ with energy redistribution
    - 1 message per second: **6.10%**; 1 message at each 10 seconds: **6.77%**; 1 message at each 60 seconds: **2.91%**; 1 message at each 600 seconds: **1.76%**; 1 message at each 3600 seconds: **0.90%**; 1 message at each 86400 seconds: **0.01%**.
- $11.31P_{tx} - 2d$ with energy redistribution
    - 1 message per second: **2.67%**; 1 message at each 10 seconds: **2.82%**; 1 message at each 60 seconds: **2.45%**; 1 message at each 600 seconds: **1.36%**; 1 message at each 3600 seconds: **1.52%**; 1 message at each 86400 seconds: **0.02%**.
- $46.76P_{tx} - 3d$ with energy redistribution
    - 1 message per second: **4.48%**; 1 message at each 10 seconds: **6.74%**; 1 message at each 60 seconds: **4.58%**; 1 message at each 600 seconds: **1.31%**; 1 message at each 3600 seconds: **1.27%**; 1 message at each 86400 seconds: **0.09%**.

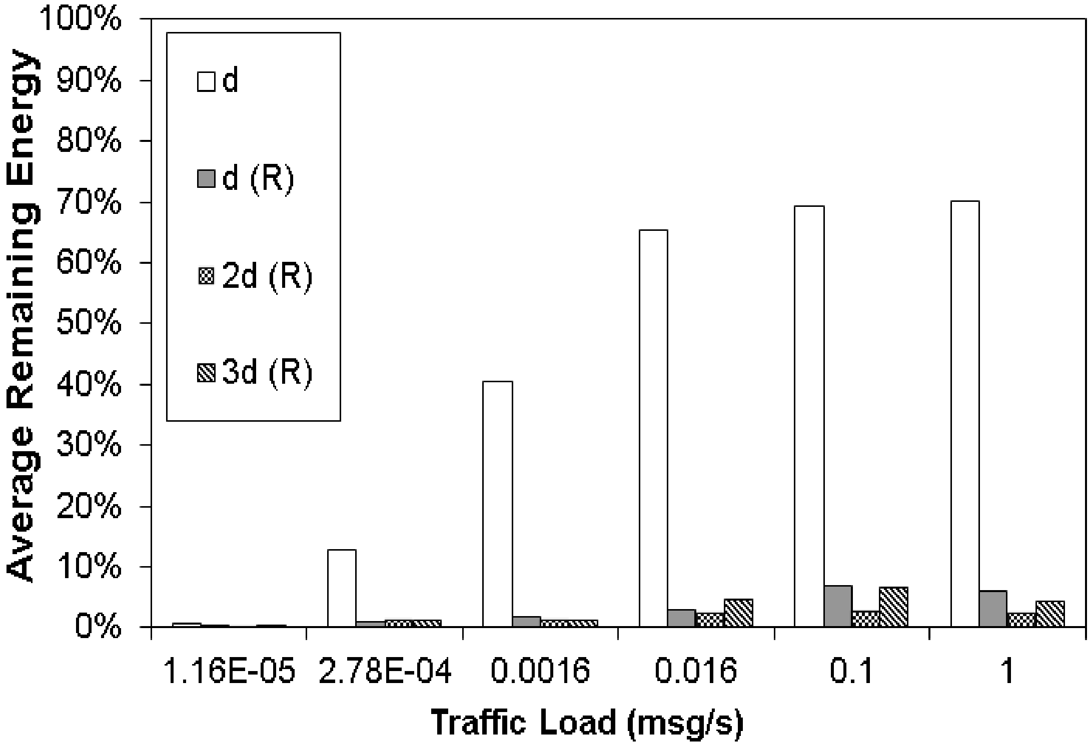

Fig. 115 – Average remaining energy of each network in Scenario III.

Table LXIX – Average remaining energy of each network in Scenario III.

Traffic Load (msg/s)	**Average Remaining Energy – 1*d***	**Average Remaining Energy – 1*d* Redistributed**	**Average Remaining Energy – 2*d* Redistributed**	**Average Remaining Energy – 3*d* Redistributed**
1.16E-05	0.65%	0.01%	0.02%	0.09%
2.78E-04	12.93%	0.90%	1.52%	1.27%
0.00166	40.39%	1.76%	1.36%	1.31%
0.166	65.36%	2.91%	2.45%	4.58%
0.1	69.33%	6.77%	2.82%	6.74%
1	70.09%	6.10%	2.67%	4.48%

5.6.3.7 Energy Consumption Profile

As can be observed in Fig. 116, Fig. 117, Fig. 118 and Table LXX, due to the transmission power increase, the energy spent on transmissions (labeled as Radio-TX) increased, following the transmission power increase. The energy consumption profile of Secondary states is the same on all cases and is shown in Fig. 119 and Table LXXI.

The energy consumption profile of the simulations in Scenario III were:

- $P_{tx} - 1d$

- Radio transmission:**22.62%**; Radio reception:**46.32%**; Microcontroller:**29.08%**; Sensor: **1.96%**.

- $11.31P_{tx} - 2d$
  - Radio transmission:**58.76%**; Radio reception:**33.27%**; Microcontroller:**7.05%**; Sensor: **0.90%**.

- $46.76P_{tx} - 3d$
  - Radio transmission:**74.40%**; Radio reception:**22.57%**; Microcontroller:**2.58%**; Sensor: **0.45%**.

- Secondary Consumption
  - Radio: **47.61%**; Microcontroller :**23.81%**; Sensor: **28.58%**.

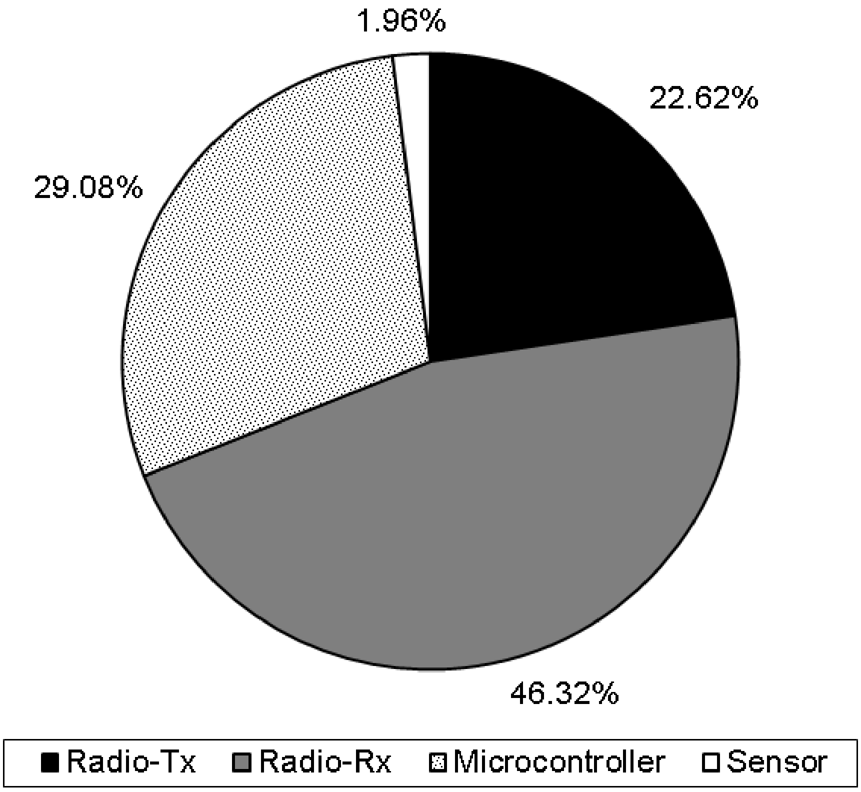

Fig. 116 – Energy consumption profile in Scenario III – P_{tx} (1d).

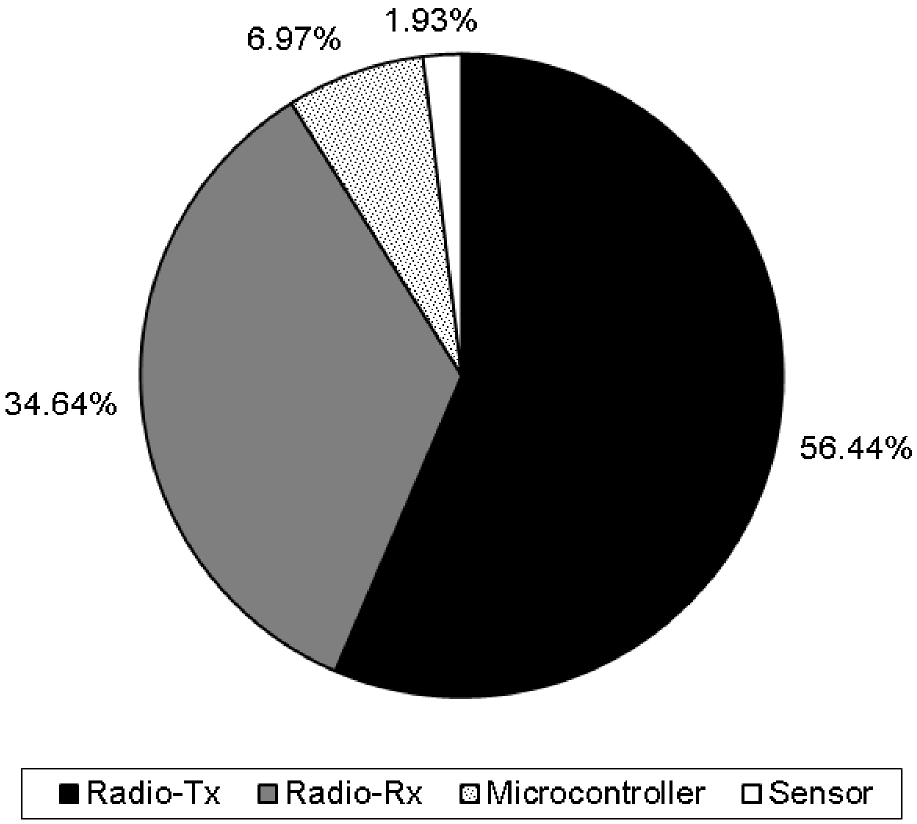

Fig. 117 – Energy consumption profile in Scenario III – $11.31P_{tx}$ ($2d$).

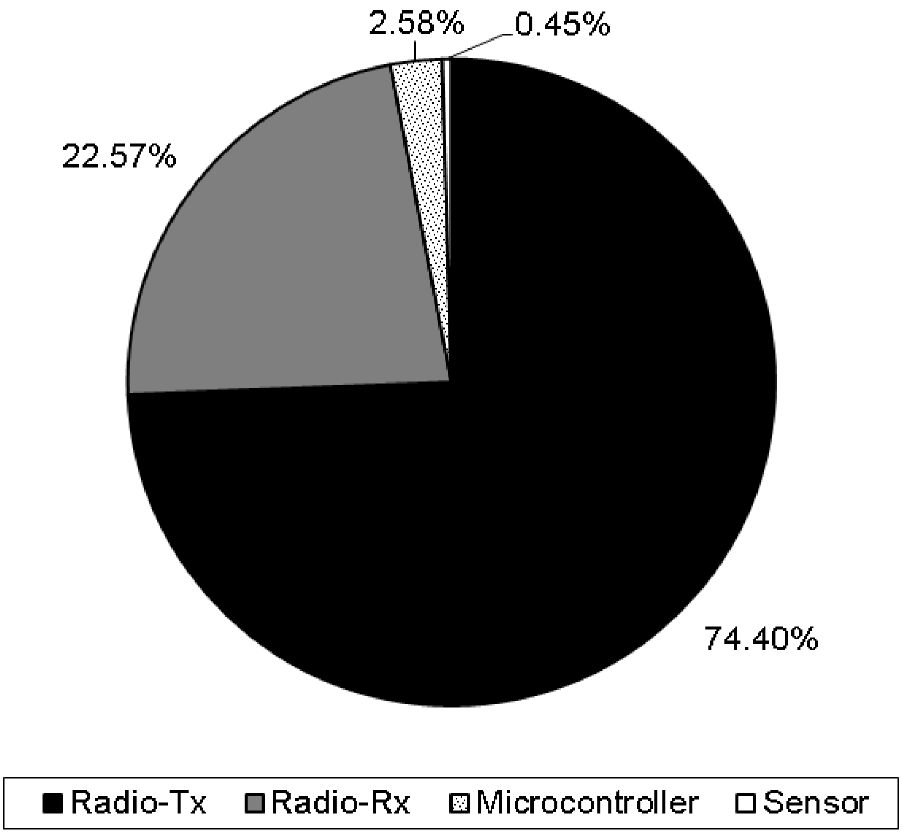

Fig. 118 – Energy consumption profile in Scenario III – $46.76P_{tx}$ ($3d$).

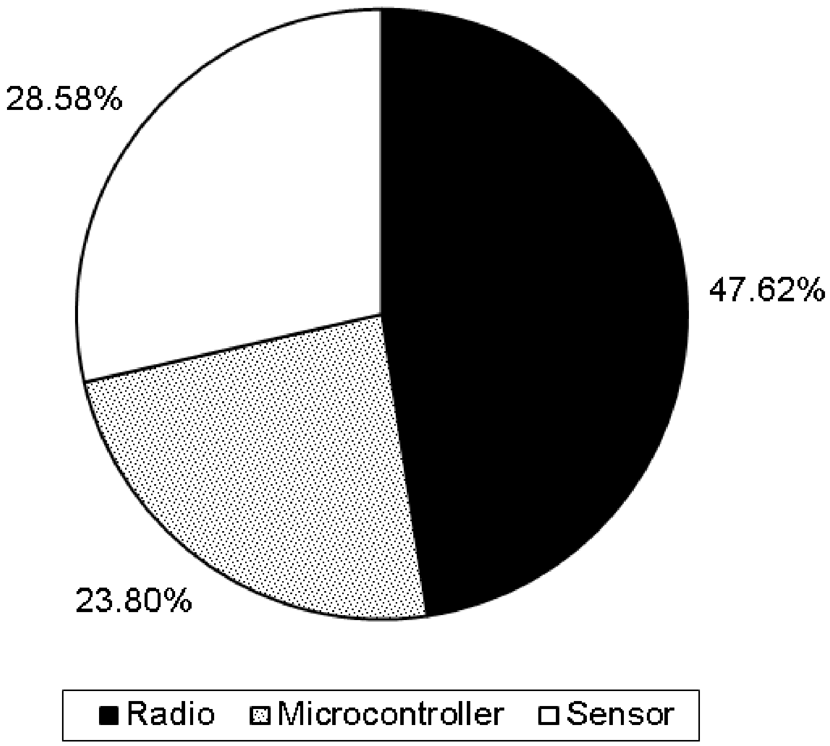

Fig. 119 – Energy consumption profile in Scenario III – Secondary Consumption.

Table LXX – Energy consumption of each part of the networks in Scenario III.

Transmission Power	Reach	Radio-Tx	Radio-Rx	Microcontroller	Sensor
P_{tx}	$1d$	22.62%	46.32%	29.08%	1.96%
$11.31P_{tx}$	$2d$	58.76%	33.27%	7.05%	0.90%
$46.76P_{tx}$	$3d$	74.40%	22.57%	2.58%	0.45%

Table LXXI – Energy consumption profile of Secondary States in Scenario III.

Radio	Microcontroller	Sensor
47.61%	23.81%	28.58%

5.6.3.8 Message Log

Fig. 120 and Table LXIII show that the total of listened messages in relation to generated messages increased with higher transmission power, from 1967% to 4166%.

Fig. 121 and Table LXIII show that the total of rerouted messages in relation to generated messages decreased with higher transmission power, from 312% to 59%.

Fig. 106Fig. 122 and Table LXIII show that the total of overheard messages in relation to generated messages increased with higher transmission power, from 1656% to 4107%.

The message log of the simulations in Scenario III were:

- $P_{tx} - 1d$

  - Listened Messages: **1967%**; Rerouted Messages: **312%**; Overheard Messages: **1656%**.
- $11.31P_{tx} - 2d$
  - Listened Messages: **3079%**; Rerouted Messages: **118%**; Overheard Messages: **2961%**.
- $46.76P_{tx} - 3d$
  - Listened Messages: **4166%**; Rerouted Messages: **59%**; Overheard Messages: **4107%**.

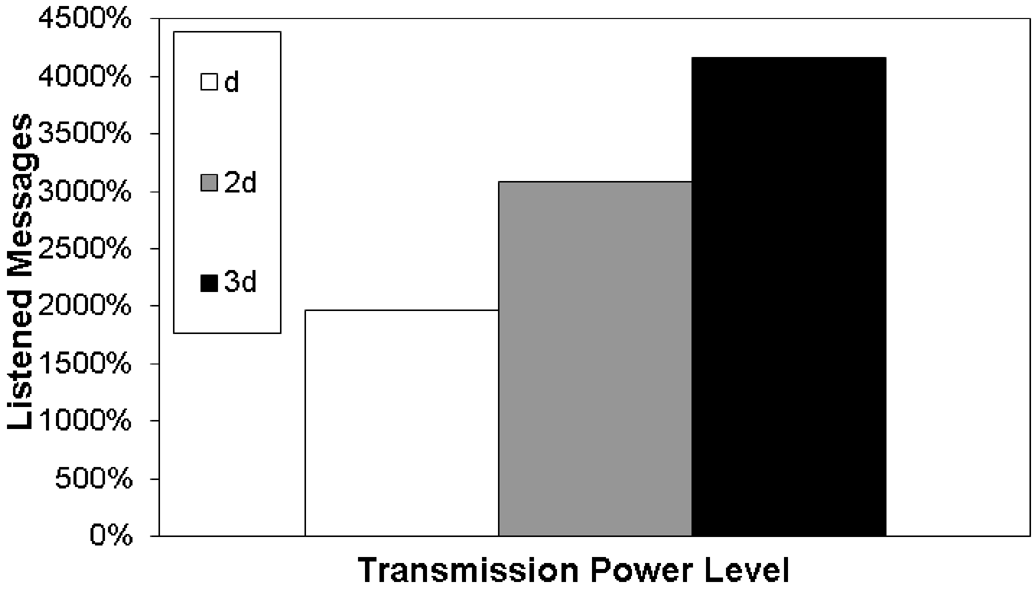

Fig. 120 – Log of listened messages of the simulations in Scenario III.

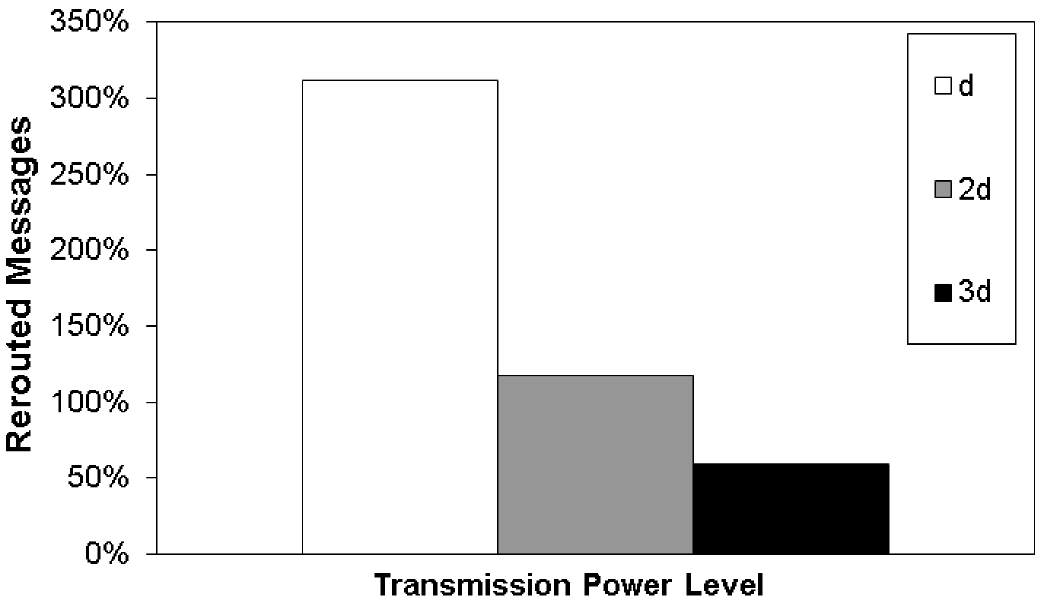

Fig. 121 – Log of rerouted messages of the simulations in Scenario III.

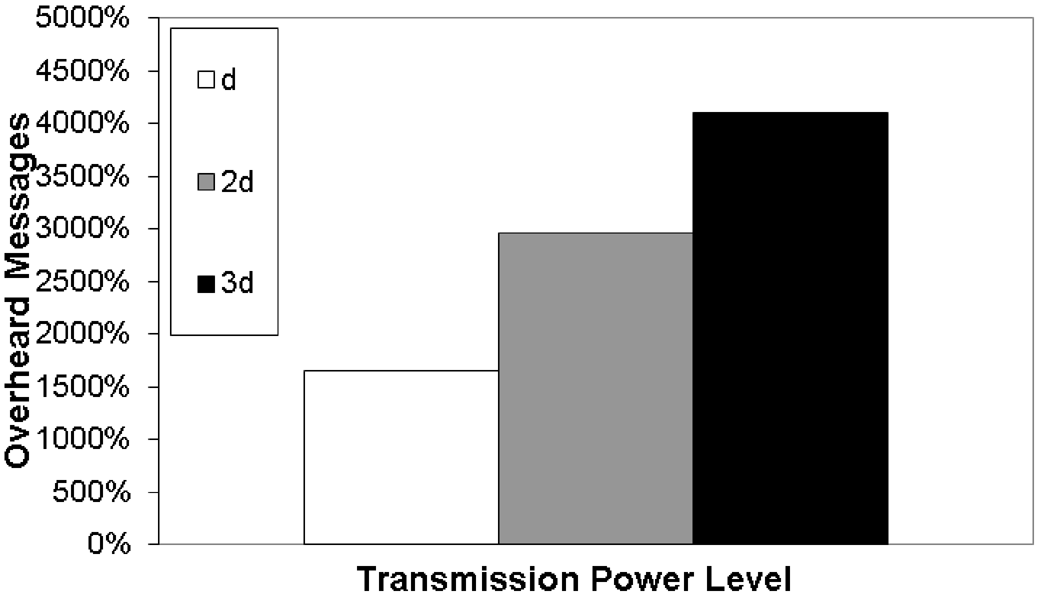

Fig. 122 – Log of overheard messages of the simulations in Scenario III.

Table LXXII – Message logs of Scenario III.

Transmission Power	Reach	Listened Messages	Rerouted Messages	Overheard Messages
P_{tx}	$1d$	1967%	312%	1656%
$11.31P_{tx}$	$2d$	3079%	118%	2961%
$46.76P_{tx}$	$3d$	4166%	59%	4107%

5.6.3.9 Energy Consumption Calculation Error

Using the mathematical models presented in Chapter IV and [147], we could estimate both the individual energy consumption of each mote and the network energy consumption per network cycle. Fig. 123 and Table LXXIII show the average error of the calculated individual energy consumption in relation to the simulated values and Fig. 124 and Table LXXIV show the error of the calculated network energy consumption in relation to the simulated values.

It is important to state that the calculated individual energy consumption errors were due both overestimation and underestimation, resulting in different errors of the calculated network energy consumption.

The average error of the calculated individual energy consumption of the simulations in Scenario III were:

- $P_{tx} - 1d$
  - 1 message per second: **0.01%**; 1 message at each 10 seconds: **0.01%**; 1 message at each 60 seconds: **less than 0.01%**; 1 message at each 600 seconds: **less than 0.01%**; 1 message at each 3600 seconds: **less than 0.01%**; 1 message at each 86400 seconds: **less than 0.01%**.
- $11.31P_{tx} - 2d$

- 1 message per second: **0.45%**; 1 message at each 10 seconds: **0.44%**; 1 message at each 60 seconds: **0.40%**; 1 message at each 600 seconds: **0.20%**; 1 message at each 3600 seconds: **0.06%**; 1 message at each 86400 seconds: **less than 0.01%**.

- $46.76P_{tx} - 3d$
  - 1 message per second: **0.47%**; 1 message at each 10 seconds: **0.27%**; 1 message at each 60 seconds: **0.25%**; 1 message at each 600 seconds: **0.16%**; 1 message at each 3600 seconds: **0.06%**; 1 message at each 86400 seconds: **0.55%**.

The average error of the calculated network energy consumption of the simulations in Scenario III were:

- $P_{tx} - 1d$
  - 1 message per second: **less than 0.01%**; 1 message at each 10 seconds: **less than 0.01%**; 1 message at each 60 seconds: **less than 0.01%**; 1 message at each 600 seconds: **less than 0.01%**; 1 message at each 3600 seconds: **less than 0.01%**; 1 message at each 86400 seconds: **less than 0.01%**.
- $11.31P_{tx} - 2d$
  - 1 message per second: **0.50%**; 1 message at each 10 seconds: **0.50%**; 1 message at each 60 seconds: **0.45%**; 1 message at each 600 seconds: **0.24%**; 1 message at each 3600 seconds: **0.07%**; 1 message at each 86400 seconds: **less than 0.01%**.
- $46.76P_{tx} - 3d$
  - 1 message per second: **0.11%**; 1 message at each 10 seconds: **0.20%**; 1 message at each 60 seconds: **0.19%**; 1 message at each 600 seconds: **0.12%**; 1 message at each 3600 seconds: **0.04%**; 1 message at each 86400 seconds: **0.35%**.

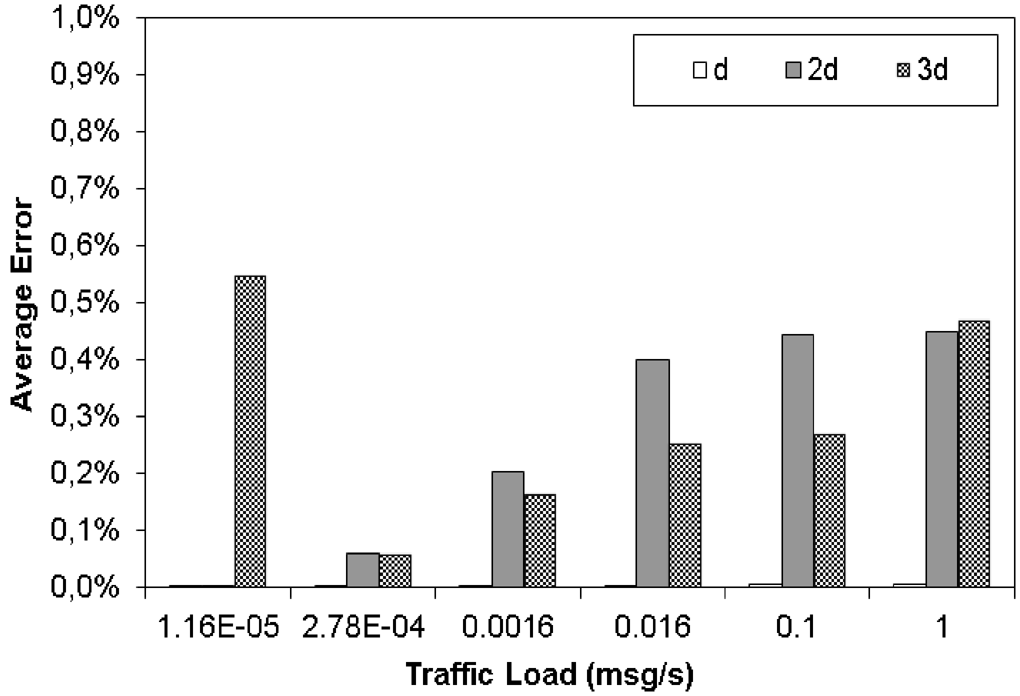

Fig. 123 – Average consumption error (calculated x simulated) of Scenario III.

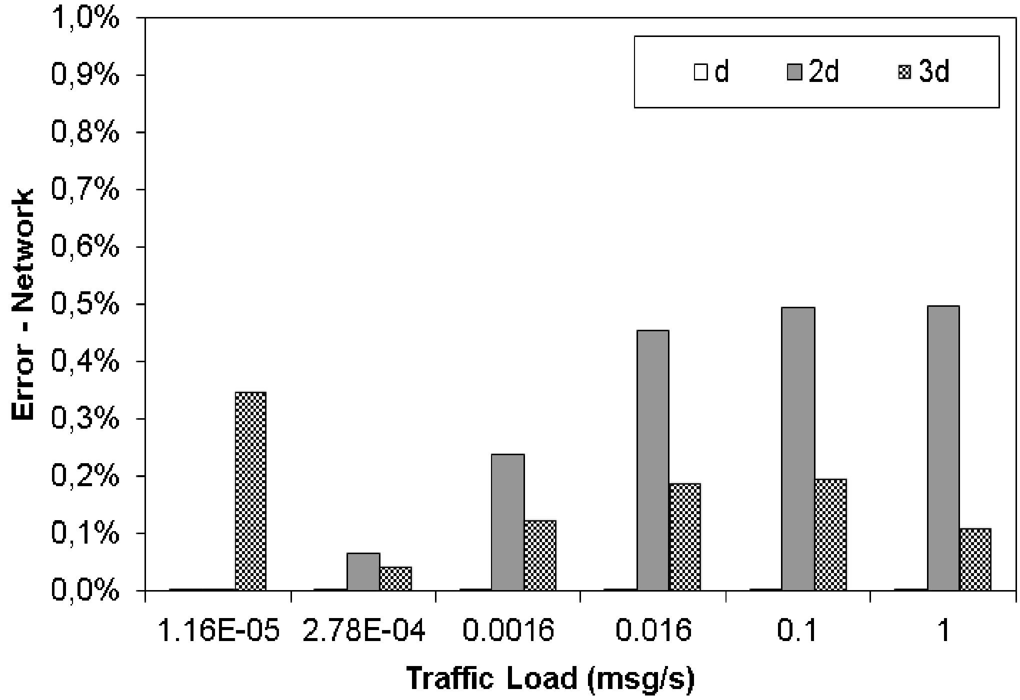

Fig. 124 – Network consumption error (calculated x simulated) of Scenario III.

Table LXXIII – Average consumption error (calculated x simulated) of Scenario III.

Traffic Load (msg/s)	**Average Error – 1*d***	**Average Error – 2*d***	**Average Error – 3*d***
1.16E-05	<0.01%	<0.01%	0.55%
2.78E-04	<0.01%	0.06%	0.06%
0.00166	<0.01%	0.20%	0.16%
0.166	<0.01%	0.40%	0.25%

Traffic Load (msg/s)	Average Error – $1d$	Average Error – $2d$	Average Error – $3d$
0.1	0.01%	0.44%	0.27%
1	0.01%	0.45%	0.47%

Table LXXIV – Network consumption error (calculated x simulated) of Scenario III.

Traffic Load (msg/s)	Network Error – $1d$	Network Error – $2d$	Network Error – $3d$
1.16E-05	<0.01%	<0.01%	0.35%
2.78E-04	<0.01%	0.07%	0.04%
0.00166	<0.01%	0.24%	0.12%
0.166	<0.01%	0.45%	0.19%
0.1	<0.01%	0.50%	0.20%
1	<0.01%	0.50%	0.11%

5.7 Chapter Summary and Concluding Remarks

In order to have a better view of the results presented in this chapter, we divided this section in four parts: (*i*) lifetime; (*ii*) traffic of messages; (*iii*) energy consumption calculation and (*iv*)general comments.

5.7.1 Lifetime

As observed in Chapter III and [19], [20], the use of multiple transmission power levels had negative to neutral results on the lifetime of the networks, depending on the generation period of the network. As an example, in Scenario III, in the generation period of 1 message per second case, the lifetime of the network using just the energy redistribution strategy had a lifetime 213.94% longer than the standard network while the network using the energy redistribution strategy and the transmission power level of $11.31P_{tx}$ had a lifetime increase of 49.51%. The lifetime of the networks using energy redistribution and higher transmission power levels were always shorter than the lifetimes of the networks using just the energy redistribution strategy, but, in the cases with longer generation periods, the gap between the lifetimes of all networks was getting minimized.

These similar lifetimes of low traffic networks can be understood by analyzing the ratio between their primary and secondary energy consumption. As the primary energy consumption is caused by tasks related to active tasks, like reading sensors and sending/receiving messages, its share is larger when the generation period is short and smaller when the generation period is long.

The lifetime of the networks using the standard transmission power P_{tx} and the energy redistribution strategy was the longer in all simulated scenarios. This result can be explained by the fact that when the energy was redistributed among the motes, the ones that demanded more energy received more energy. When those motes received the same amount of energy of the others, they were the first to have its batteries depleted.

As shown in Appendix A, B and C, the energy consumption estimations indicate that the generation periods had a sensible impact on difference between the individual energy consumption of the motes. While the difference between the energy consumption of the most overburdened motes was very noticeable when using short generation periods, this difference was very attenuated by major share of the energy consumed by secondary states (idle, sleep etc.) when using longer generation periods.

5.7.2 Traffic of Messages

As the transmission power increased in order to have a longer range and the radio module used on the model had an omnidirectional antenna [138]–[141], longer transmissions reached not only motes nearer the base station (or the base station itself) and all motes between the sender and the receiver, but also reached motes further the base station, located at the other side of the transmission radius.

Using higher transmission power levels decreased the quantity of messages listened by the motes but, in other hand, the number of overheard messages, which are the messages unnecessarily received, increased. As the messages were sent further when using higher transmissions power levels, the quantity of rerouted messages also decreased.

One result that can be inferred, but is not analyzed in this work, is that the less hops a message has to perform, the lower is the chance of it be corrupted or lost.

5.7.3 Energy Consumption Calculation

The strategy using the mathematical models presented in Chapter IV and [147] for calculating the energy consumption of each mote and giving them a battery amount proportional to its energy needs had positive results on the lifetime of all simulated networks. It shows, similarly to another works with circular networks [7], [8], [109]–[114], [195] that some motes are indeed overburdened by other motes depending on their locations in the network, thus, needing more energy.

The simulations show a low error rate between the calculated values in comparison to the simulated ones, most cases with less than 1% of error, indicating that the models can be used with both regularly and irregularly topologies.

It is important to state that those error levels were very low because all motes consumed the same energy for performing the same tasks, there were no deviations between them. In real-life parts, it is common to have little differences between their characteristics and some effects [198]–[202] can also affect the estimations adding, consequently, more error to the calculations.

5.7.4 Concluding Remarks

The use of the mathematical models and the energy redistribution strategy, presented in Chapter IV and [147], had positive results on all simulations and analysis, even on the networks with irregular topologies. The use of the mathematical models can also be positive when designing a network and not redistributing its batteries, by finding which motes would be overburdened by the other motes.

The use of multiple transmission power levels, presented in Chapter III and in [19], [20], reveals both positive and negative results. The results about the traffic of messages were very positive, but, they cannot be analyzed alone, without energy issues, due to the focus of this work on Wireless Sensor Networks. The lifetime and network cost had very negative results when using short generation periods but, on networks with longer generation periods, the difference between the lifetimes of the simulated networks got lower as the generation period was getting longer. The huge difference between the quantity of messages per hour generated throughout the lifetime of the networks also implies what kind of networks the use of multiple transmission power levels would suit better, as invasion alarms or other networks with low low message traffic.

Chapter VI

WORK SUMMARY AND CONCLUDING REMARKS

This chapter presents the comments and concluding remarks about this work and a brief discussion about the planned future researches.

6.1 Comments and Concluding Remarks per Chapter

In this section, we summarize our comments and concluding remarks about the specific analysis made in each chapter.

6.1.1 Chapter II: Current Consumption in Radio Modules for Wireless Sensor Networks

The measurements presented in this chapter shows how the current consumptions of radio modules typically employed in Wireless Sensor Networks can be more complex and intricate than the constant values presented in their respective datasheets. The complexity of the observed waveforms is closely related to the complexity of the radio module.

All measurements show, as expected, that the datasheets present reliable information about an electronic device. However, when precise information about current consumption is required, the information available in datasheet may not be enough, and a more detailed analysis of the current consumption profile of the involved devices may be necessary. The use of detailed energy consumption profiles is very needed when designing energy-aware techniques for Wireless Sensor Networks, or when motes in a Wireless Sensor Networks are powered by alternative power supplies, such as energy harvesting power supplies.

The measurement setup employed in this work provided both sufficient resolution and clear waveforms, being suitable for the future steps of this work, namely, analysis of other radio modules and evaluation of external factors that affect current consumption in Wireless Sensor Networks.

6.1.2 Chapter III: The Impact of Multiple Transmission Power Levels on Wireless Sensor Networks

In order to have a better view of the results presented in this chapter, we divided this section into two parts: Lifetime and Traffic of Messages.

6.1.2.1 Lifetime

The lifetime of the networks using the standard transmission power P_{tx} was longer in all simulated scenarios but, when the generation period was low, the difference between the lifetime of the networks using P_{tx} and higher transmission power levels lowered considerably. At the lowest generation period, which was one message per day, the difference between the lifetime of the network using P_{tx} and the networks using up to $128P_{tx}$ was less than 3.5%

These similar lifetimes of low traffic networks can be understood by analyzing the ratio between their primary and secondary energy consumption. As the primary energy consumption is caused by tasks related to active tasks, like reading sensors and sending/receiving messages, its share is larger when the generation period is short and smaller when the generation period is long.

Observing the trend of the primary energy consumption of all simulated networks it is reasonable to infer that the extra energy spent to send messages further impacts less when fewer messages had to be sent, being a plausible strategy for networks with a low message traffic.

6.1.2.2 Traffic of Messages

As the transmission power increased in order to have a longer range and the radio module used on the model had an omnidirectional antenna [138]–[141], longer transmissions reached not only motes nearer the base station (or the base station itself) and all motes between the sender and the receiver, but also reached motes further the base station, located at the other side of the transmission radius.

Using higher transmission power levels decreased the quantity of messages listened by the motes, however, the number of overheard messages, which are the messages unnecessarily received, increased. As the messages were sent further when using higher transmissions power levels, the quantity of rerouted messages also decreased.

One result that can be inferred, but is not analyzed in this work, is that the less hops a message has to perform, the lower is the chance of it be corrupted or lost.

6.1.3 Chapter IV: Lifetime Maximization with Multiple Battery Levels in Irregular Topology Wireless Sensor Networks

The simulations results show that it is possible to increase the lifetime of irregular topology Wireless Sensor Networks, without energy budget increases, by using mathematical analysis. The results indicate that the use of the proposed analysis and the battery distribution heuristic had significant effects on lifetime increase and consequent energy wasting reduction. The simulations also show that the best results were in the "worst" scenarios (base station in the periphery), which is more likely to happen on real networks, with more than 200% of lifetime increase in networks with higher message traffic. For expanding the boundary conditions of our models and make them more embracing, the next steps of our work will analyze and add the stochastic behavior of event-driven networks and the impact of retransmissions due to message losses.

6.1.4 Chapter V: Impact of Multiple Battery Levels and Multiple Transmission Power Levels on Wireless Sensor Networks

The use of the mathematical models and the energy redistribution strategy, presented in Chapter IV and [147], had positive results on all simulations and analysis, even on the networks with irregular topologies. The use of the mathematical models can also be positive when designing a network and not redistributing its batteries, by finding which motes would be overburdened by the other motes.

The use of multiple transmission power levels, presented in Chapter III and in [19], [20], reveals both positive and negative results. The results about the traffic of messages were very positive, but, they cannot be analyzed alone, without energy issues, due to the focus of this work on Wireless Sensor Networks. The lifetime and network cost had very negative results when using short generation periods but, on networks with longer generation periods, the difference between the lifetimes of the simulated networks got lower as the generation period was getting longer. The huge difference between the quantity of messages per hour generated throughout the lifetime of the networks also implies what kind of networks the use of multiple transmission power levels would suit better, as invasion alarms or other networks with low message traffic.

6.2 Concluding Remarks and Contributions

This work focused on analyzing and presenting strategies to make efficient usage of the batteries and to increase the lifetime of Wireless Sensor Networks maintaining the same energy budget.

The first step was investigating, measuring and analyzing the current consumption of the components used in a typical mote architecture. This analysis gave the basis for understanding how the current consumption profile of the components used in a mote are and how much energy is spent in their different operation states.

After the analysis of the current consumption profile of the components of a mote, we noted that a significant amount of energy is spent on secondary states, i.e., when a mote is idle or in power-saving states. We proceeded to investigate the impact of using multiple transmission power level in order to each message having to course fewer hops to reach the base station. The impact on the lifetimes of the networks was negative, in higher traffic scenarios, to negligible, in low traffic scenarios. The impact on the message traffic can be interpreted as very positive according to the purpose of the network and its traffic. As the difference in the lifetimes are negligible when the message traffic is low, each increase in the transmission power has a direct impact on the number of hops that a message has to perform, reducing expressively the chances of any losses.

The next investigation was made using our proposed strategy for maximizing the lifetime of any Wireless Sensor Networks, regardless its physical topologies and keeping the same energy budget. Our proposal is based in a mathematical analysis, to calculate the individual energy consumption of each mote in a network. The second step of our strategy is based in battery assign heuristic, providing batteries according to the individual energy consumption of each mote. Our strategy achieved expressive lifetime increases in all scenarios, exceeding 200% in some cases and reducing the energy waste to less than 7% in most cases.

In addition to the aforementioned results, this work also proposed metrics for analyzing Wireless Sensor Networks, viz.: the network cost, energy consumption profile, primary and secondary consumption, message logs etc.

6.3 Future Works

Based in our investigation about the use of multiple transmission power levels, we plan to propose a protocol based on the use of multiple transmission power levels, with each mote adapting its transmission power levels to a set of metrics set by the network operator.

Due to the difficult task of assembling a specific battery set to each mote in a network, the next step of our research on this subject will address the use of a predetermined number of electric charge levels, in order to study the point where the network can have a lifetime maximization with a reduced number of different battery sets. We also plan to make more measurements using newer radio modules, providing more data to the literature.

REFERENCES

[1] I. F. Akyildiz, W. Su, Y. Sankarasubramaniam, and E. Cayirci, "Wireless sensor networks: a survey," *Comput. Networks*, vol. 38, no. 4, pp. 393–422, Mar. 2002.

[2] V. Potdar, a. Sharif, and E. Chang, "Wireless Sensor Networks: A Survey," *2009 Int. Conf. Adv. Inf. Netw. Appl. Work.*, vol. 38, pp. 393–422, 2009.

[3] G. Anastasi, M. Conti, M. Di Francesco, and A. Passarella, "Energy conservation in wireless sensor networks: A survey," *Ad Hoc Networks*, vol. 7, no. 3, pp. 537–568, 2009.

[4] R. Mulligan and H. M. Ammari, "Coverage in Wireless Sensor Networks: A Survey," *Netw. Protoc. Algorithms*, vol. 2, no. 2, pp. 27–53, 2010.

[5] L. M. Oliveira and J. J. Rodrigues, "Wireless Sensor Networks: a Survey on Environmental Monitoring," *J. Commun.*, vol. 6, no. 2, 2011.

[6] H. Yetgin, K. T. K. Cheung, M. El-Hajjar, and L. Hanzo, "A Survey of Network Lifetime Maximization Techniques in Wireless Sensor Networks," *IEEE Commun. Surv. Tutorials*, vol. 19, no. 2, pp. 828–854, 2017.

[7] N. Jabeur, N. Sahli, and I. M. Khan, "Survey on sensor holes: A cause-effect-solution perspective," *Procedia Comput. Sci.*, vol. 19, pp. 1074–1080, 2013.

[8] R. Sharma, "Energy Holes Avoiding Techniques in Sensor Networks: A survey," *Int. J. Eng. Trends Technol.*, vol. 20, no. 4, pp. 204–208, Feb. 2015.

[9] I. F. Akyildiz and M. C. Vuran, *Wireless Sensor Networks*. Chichester, UK: John Wiley & Sons, Ltd, 2010.

[10] G. E. Moore, "Cramming more components onto integrated circuits (Reprinted from Electronics, pg 114-117, April 19, 1965)," *Proc. Ieee*, vol. 86, no. 1, pp. 82–85, 1965.

[11] J. Lian, K. Naik, and G. B. Agnew, "Data capacity improvement of wireless sensor networks using non-uniform sensor distribution," *Int. J. Distrib. Sens. Networks*, vol. 2, no. 2, pp. 121–145, 2006.

[12] The Mathworks Inc., "MATLAB - MathWorks," *www.mathworks.com/products/matlab*, 2016. [Online]. Available: http://www.mathworks.com/products/matlab/.

[13] M. Documentation, "Matlab documentation," *Matlab*. p. R2012b, 2012.

[14] The Mathworks Inc., "MATLAB (R2015a)," *The MathWorks Inc.* 2015.

[15] E. a Sobie, *An introduction to MATLAB.*, vol. 4, no. 191. 2011.

[16] S. E. Lyshevski, "MATLAB Basics," *Eng. Sci. Comput. Using MATLAB®*, pp. 1–26, 2003.

[17] B. Paris, "Modeling of Wireless Communication Systems using MATLAB Characterization of the wireless channel and its impact on Outline Part III : Learning Objectives Pathloss and Link Budget From Physical Propagation to Multi-Path Fading Statistical Characterization ," *Communications*, 2010.

[18] F. A. M. Miranda and P. Cardieri, "Current Consumption in Radio Modules for Wireless Sensor Networks," in *XXXV Simpósio Brasileiro de Telecomunicações e Processamento de Sinais – SBrT2017*, 2017.

[19] F. A. M. Miranda and P. Cardieri, "The impact of multiple power levels on the lifetime of Wireless Sensor Networks," in *2016 IEEE International Symposium on Consumer Electronics (ISCE)*, 2016, pp. 103–104.

[20] F. Miranda and P. Cardieri, "An Analysis of the Use of Multiple Transmission Power Levels on Wireless Sensor Networks," in *Proceedings of 5th International Electronic Conference on Sensors and Applications*, 2018, p. 5739.

[21] J. J. Lazzaro, "The principles of universal design," *E Media Prof.*, vol. 10, no. 2, pp. 56–57, 1997.

[22] S. Choi, "Universal Design," *Int. J. Divers.*, vol. 5, no. 6, pp. 115–124, 2005.

[23] M. F. Story, "Maximizing Usability: The Principles of Universal Design," *Assist. Technol.*, vol. 10, no. 1, pp. 4–12, 1998.

[24] W. Lidwell, K. Holden, and J. Butler, "Universal Principles of Design," *Univers. Princ. Des. 125 ways to Enhanc. usability, Influ. perception, increase appeal, make beter Des. Decis. teach through Des.*, pp. 1–271, 2010.

[25] M. Story, J. L. Mueller, and R. L. Mace, "The Universal Design File: Designing for People of All Ages and Abilities," *Des. Res. Methods J.*, vol. 1, no. 5, p. 165, 1998.

[26] C. for U. D. A. N. S. Ncus, *The Principles of Universal Design (version 2.0)*. 2011.

[27] Q. W. Q. Wang, M. Hempstead, and W. Yang, "A Realistic Power Consumption Model for Wireless Sensor Network Devices," *2006 3rd Annu. IEEE Commun. Soc. Sens. Ad Hoc Commun. Networks*, vol. 1, pp. 286–295, 2006.

[28] R. Soua and P. Minet, "A survey on energy efficient techniques in wireless sensor networks," in *2011 4th Joint IFIP Wireless and Mobile Networking Conference (WMNC 2011)*, 2011, pp. 1–9.

[29] S. Akbari, "Energy Harvesting for Wireless Sensor Networks Review," in *Proceedings of the 2014 Federated Conference on Computer Science and Information Systems*, 2014, pp. 987–992.

[30] E. Lattanzi and A. Bogliolo, "WSN Design for Unlimited Lifetime," in *Sustainable Energy Harvesting Technologies - Past, Present and Future*, InTech, 2011.

[31] E. Lattanzi and A. Bogliolo, "VirtualSense: A java-based open platform for ultra-low-power wireless sensor nodes," *Int. J. Distrib. Sens. Networks*, vol. 2012, 2012.

[32] P. Spies, M. Pollak, and L. Mateu, *Handbook of Energy Harvesting Power Supplies and Applications*, 1st ed. Singapore: Pan Stanford, 2015.

[33] A. Moschitta and I. Neri, "Power consumption Assessment in Wireless Sensor Networks," in *ICT - Energy - Concepts Towards Zero - Power Information and Communication Technology*, InTech, 2014.

[34] D. Macii and D. Petri, "An Effective Power Consumption Measurement Procedure for Bluetooth Wireless Modules," *IEEE Trans. Instrum. Meas.*, vol. 56, no. 4, pp. 1355–1364, Aug. 2007.

[35] T. Laopoulos, P. Neofotistos, C. Kosmatopoulos, and S. Nikolaidis, "Current variations measurements for the estimation of software-related power consumption," in *IMTC/2002. Proceedings of the 19th IEEE Instrumentation and Measurement Technology Conference (IEEE Cat. No.00CH37276)*, 2014, vol. 2, pp. 1637–1642.

[36] H. G. Lee, K. Lee, Y. Choi, and N. Chang, "Cycle-Accurate Energy Measurement and Characterization of FPGAs," *Analog Integr. Circuits Signal Process.*, vol. 42, no. 3, pp. 239–251, Mar. 2005.

[37] T. Laopoulos, P. Neofotistos, C. A. Kosmatopoulos, and S. Nikolaidis,

"Measurement of current variations for the estimation of software-related power consumption," *IEEE Trans. Instrum. Meas.*, vol. 52, no. 4, pp. 1206–1212, 2003.

[38] T. Savolainen, N. Javed, and B. Silverajan, "Measuring energy consumption for RESTful interactions in 3GPP IoT nodes," in *2014 7th IFIP Wireless and Mobile Networking Conference (WMNC)*, 2014, pp. 1–8.

[39] A. Hergenröder, J. Horneber, and J. Wilke, "SANDbed: A WSAN Testbed for Network Management and Energy Monitoring," *Proc. 8th GIITG KuVS Fachgespräch Drahtlose Sensornetze*, pp. 71–73, 2009.

[40] Zhang Fan and Li Wenfeng, "Energy efficiency testbed for wireless sensor networks," in *2010 IEEE International Conference on Systems, Man and Cybernetics*, 2010, pp. 3807–3812.

[41] G. Werner-Allen, P. Swieskowski, and M. Welsh, "MoteLab: a wireless sensor network testbed," in *IPSN 2005. Fourth International Symposium on Information Processing in Sensor Networks, 2005.*, pp. 483–488.

[42] J. Horneber and A. Hergenroder, "A Survey on Testbeds and Experimentation Environments for Wireless Sensor Networks," *IEEE Commun. Surv. Tutorials*, vol. 16, no. 4, pp. 1820–1838, 2014.

[43] X. Jiang, P. Dutta, D. Culler, and I. Stoica, "Micro power meter for energy monitoring of wireless sensor networks at scale," in *Proceedings of the 6th international conference on Information processing in sensor networks - IPSN '07*, 2007, p. 186.

[44] P. Dutta, Y. Kuo, A. Ledeczi, and T. Schmid, "Putting the software radio on a low-calorie diet," *Proc. Ninth*, 2010.

[45] Agilent Technologies Inc., "Agilent 34405A Multimeter Manual." 2013.

[46] Agilent Technologies Inc., "Agilent 34401A Service Guide." 2013.

[47] Fluke Corporation, "Fluke 45 Dual Display Multimeter Users Manual." 1989.

[48] Agilent Technologies Inc., "Agilent 34410A/11A Digital Multimeter User's Guide." 2012.

[49] Agilent Technologies Inc., "Agilent InfiniiVision 2000 X-Series Oscilloscopes User's Guide." 2011.

[50] Minipa do Brasil Ltda., "Minipa Digital Oscilloscope MO-2025 / MO-2061 / MO-2100 / MO-2200 Instructions Manual." 2009.

[51] Tektronix Inc., "Tektronix TDS 420A, TDS 430A & TDS 460A Digitizing Oscilloscopes Service Manual." 1996.

[52] Teledyne LeCroy Inc., "Teledyne HDO4000 Operator's Manual." 2013.

[53] R. Feynman, R. Leighton, M. Sands, and S. Treiman, *The Feynman lectures on physics - Mainly Electromagnetism and Matter*. 1964.

[54] P. A. Tipler and G. Mosca, *Physics for Scientists and Engineers*, 6th ed. New York, New York, USA: W. H. Freeman, 2007.

[55] Valhalla Scientific Inc., "Model 2575 A – Precision AC/DC Active Current Shunt Datasheet." 2016.

[56] Murata Manufacturing Co., "Murata DR3000 Datasheet." 2015.

[57] Linx Technologies, "Linx LT Series Transceiver Module Data Guide." 2015.

[58] Telecontrolli SRL, "Telecontrolli RT4-XXX Radio Transmitter Datasheet." .

[59] Telecontrolli SRL, "Telecontrolli RR3 Radio Receiver Datasheet." .

[60] Digi International Inc., “Digi XBee/XBee-PRO OEM RF Modules Product Manual.” 2009.
[61] G. Girban and M. Popa, “A glance on WSN lifetime and relevant factors for energy consumption,” in *2010 International Joint Conference on Computational Cybernetics and Technical Informatics*, 2010, pp. 523–528.
[62] R. Min *et al.*, “Low-power wireless sensor networks,” in *VLSI Design 2001. Fourteenth International Conference on VLSI Design*, pp. 205–210.
[63] Z. Chen, F. Gao, X. Zhang, J. C. F. Li, and M. Lei, “Sensing and Power Allocation for Cognitive Radio with Multiple Primary Transmit Powers,” *IEEE Wirel. Commun. Lett.*, vol. 2, no. 3, pp. 319–322, Jun. 2013.
[64] T. O. Olwal, B. J. van Wyk, K. Djouani, Y. Hamam, P. Siarry, and N. Ntlatlapa, “Autonomous Transmission Power Adaptation for Multi-Radio Multi-Channel Wireless Mesh Networks,” 2009, pp. 284–297.
[65] Wei Ren, Qing Zhao, and A. Swami, “Power control in cognitive radio networks: how to cross a multi-lane highway,” *IEEE J. Sel. Areas Commun.*, vol. 27, no. 7, pp. 1283–1296, Sep. 2009.
[66] F. Gao, J. Li, T. Jiang, and W. Chen, “Sensing and Recognition When Primary User Has Multiple Transmit Power Levels,” *IEEE Trans. Signal Process.*, vol. 63, no. 10, pp. 2704–2717, May 2015.
[67] F. Zhao and H. Xiao, “Transmit power allocation algorithm in cognitive radio MISO system based QPSK constellation,” *IEEJ Trans. Electr. Electron. Eng.*, vol. 9, no. 3, pp. 258–261, May 2014.
[68] Microchip Technology Inc., “Microchip MRF24J40MA Data Sheet.” 2008.
[69] Freescale Semiconductor Inc., “Freescale MC13202 Datasheet with Addendum.” 2015.
[70] Atmel Corporation, “Atmel AT86RF232 Datasheet.” 2011.
[71] Bluetooth Special Interest Group, “Bluetooth Technology Website,” 2018. [Online]. Available: https://www.bluetooth.com/.
[72] Bluetooth Special Interest Group, “What is Bluetooth Technology?,” *Bluetooth SIG, Inc.*, 2014. .
[73] LitePoint, “Practical Manufacturing Testing of Bluetooth Wireless Devices,” 2016.
[74] T. L. Ericsson, I. B. M. Corporation, I. Corporation, N. Corporation, and . T. C., “Specification of the Bluetooth System.” 1999.
[75] J. L. Hill and D. E. Culler, “Mica: A wireless platform for deeply embedded networks,” *IEEE Micro*, vol. 22, no. 6, pp. 12–24, 2002.
[76] Libelium Comunicaciones Distribuidas S.L., “Libelium Waspmote Technical Guide.” 2017.
[77] Mouser Electronics, “Mouser Electronics.” [Online]. Available: www.mouser.com.
[78] Premier Farnell, “Premier Farnell.” [Online]. Available: http://www.farnell.com/.
[79] Digi-Key, “Digi-Key.” [Online]. Available: www.digikey.com.
[80] Y. Yu, B. Chen, K. Huang, X. Wang, and D. Wang, “Environmental Impact Assessment and End-of-Life Treatment Policy Analysis for Li-Ion Batteries and Ni-MH Batteries,” *Int. J. Environ. Res. Public Health*, vol. 11, no. 3, pp. 3185–3198, Mar. 2014.

[81] G. Majeau-Bettez, T. R. Hawkins, and A. H. StrØmman, "Life cycle environmental assessment of lithium-ion and nickel metal hydride batteries for plug-in hybrid and battery electric vehicles," *Environ. Sci. Technol.*, vol. 45, no. 10, pp. 4548–4554, 2011.

[82] J. Xu, H. R. Thomas, R. W. Francis, K. R. Lum, J. Wang, and B. Liang, "A review of processes and technologies for the recycling of lithium-ion secondary batteries," *J. Power Sources*, vol. 177, no. 2, pp. 512–527, Mar. 2008.

[83] T. C. Chang, S. J. You, B. S. Yu, and K. F. Yao, "A material flow of lithium batteries in Taiwan," *J. Hazard. Mater.*, vol. 163, no. 2–3, pp. 910–915, Apr. 2009.

[84] N. Gandhi, M. A. J. Huijbregts, D. van de Meent, W. J. G. M. Peijnenburg, J. Guinée, and M. L. Diamond, "Implications of geographic variability on Comparative Toxicity Potentials of Cu, Ni and Zn in freshwaters of Canadian ecoregions," *Chemosphere*, vol. 82, no. 2, pp. 268–277, Jan. 2011.

[85] M. A. M. Vieira, C. N. Coelho, D. C. da Silva, and J. M. da Mata, "Survey on wireless sensor network devices," in *EFTA 2003. 2003 IEEE Conference on Emerging Technologies and Factory Automation. Proceedings (Cat. No.03TH8696)*, vol. 1, pp. 537–544.

[86] Maxim Integrated, "National Semiconductor LM75 Digital Temperature Sensor and Thermal Watchdog with Two - Wire Interface." 2009.

[87] Atmel Corporation, "8-bit Atmel with 8KBytes In- System Programmable Flash ATmega8 ATmega8L." 2013.

[88] Q. Wang and W. Yang, "Energy consumption model for power management in wireless sensor networks," *4th Annu. IEEE Commun. Soc. Conf. Sensor, Mesh Ad Hoc Commun. Networks*, pp. 142–151, 2007.

[89] T. S. Rappaport, *Wireless Communications: Principles and Practice*, 2nd ed. Upper Saddle River, NJ, USA: Prentice Hall, 2002.

[90] S. Y. Seidel and T. S. Rappaport, "914 MHz path loss prediction models for indoor wireless communications in multifloored buildings," *IEEE Trans. Antennas Propag.*, vol. 40, no. 2, pp. 207–217, 1992.

[91] G. Mao, B. D. O. Anderson, and B. Fidan, "Path loss exponent estimation for wireless sensor network localization," *Comput. Networks*, vol. 51, no. 10, pp. 2467–2483, Jul. 2007.

[92] S. S. Ghassemzadeh, R. Jana, C. W. Rice, W. Turin, and V. Tarokh, "A statistical path loss model for in-home UWB channels," in *2002 IEEE Conference on Ultra Wideband Systems and Technologies (IEEE Cat. No.02EX580)*, pp. 59–64.

[93] N. H. Mak and W. K. G. Seah, "How Long is the Lifetime of a Wireless Sensor Network?," in *2009 International Conference on Advanced Information Networking and Applications*, 2009, pp. 763–770.

[94] Y. Chen and Q. Zhao, "On the lifetime of wireless sensor networks," *IEEE Commun. Lett.*, vol. 9, no. 11, pp. 976–978, 2005.

[95] J. W. Jung and M. A. Weitnauer, "On using cooperative routing for lifetime optimization of multi-hop wireless sensor networks: Analysis and guidelines," *IEEE Trans. Commun.*, vol. 61, no. 8, pp. 3413–3423, 2013.

[96] I. Dietrich and F. Dressler, "On the lifetime of wireless sensor networks," *ACM Trans. Sens. Networks*, vol. 5, no. 1, pp. 1–39, 2009.

[97] C. G. Cassandras, W. Tao, and S. Pourazarm, "Optimal routing and energy allocation for lifetime maximization of wireless sensor networks with nonideal batteries," *IEEE Trans. Control Netw. Syst.*, vol. 1, no. 1, pp. 86–98, 2014.

[98] H. Long, Y. Liu, Y. Wang, R. Dick, and H. Yang, "Battery allocation for wireless sensor network lifetime maximization under cost constraints," *Proc. 2009 …*, no. 10, pp. 705–712, 2009.

[99] Y. Liu, Y. Wang, H. Long, and H. Yang, "Lifetime-aware battery allocation for wireless sensor network under cost constraints," *IEICE Trans. Commun.*, vol. E95–B, no. 5, pp. 1651–1660, 2012.

[100] S. Hu and M. Motani, "Early overhearing avoidance in wireless sensor networks," in *Lecture Notes in Computer Science (including subseries Lecture Notes in Artificial Intelligence and Lecture Notes in Bioinformatics)*, 2008, vol. 4982 LNCS, pp. 26–35.

[101] B. Abid, H. Seba, and S. Mbengue, "Collision Free Communication for Energy Saving in Wireless Sensor Networks," in *Wireless Sensor Networks - Technology and Applications*, InTech, 2012.

[102] G. Cardone, A. Corradi, and L. Foschini, "Reliable communication for mobile MANET-WSN scenarios," in *Proceedings - IEEE Symposium on Computers and Communications*, 2011, pp. 1085–1091.

[103] S. C. Misra, I. Woungang, and S. Misra, Eds., *Guide to Wireless Sensor Networks*. London: Springer London, 2009.

[104] F.-Y. Leu and H.-W. Huang, "An Event-Driven Mobile Assistant Control Protocol for Wireless Sensor Networks," in *2010 13th International Conference on Network-Based Information Systems*, 2010, pp. 521–526.

[105] M. Hodon *et al.*, "Maximizing performance of low-power WSN node on the basis of event-driven-programming approach: Minimization of operational energy costs of WSN node control unit," in *2015 IEEE Symposium on Computers and Communication (ISCC)*, 2015, pp. 204–209.

[106] N. Sazak, I. Erturk, E. Koklukaya, and M. Cakiroglu, "An energy efficient MAC protocol for cluster based event driven WSN applications," *Software, Telecommun. Comput. Networks (SoftCOM), 2010 Int. Conf.*, pp. 76–81, 2010.

[107] B. Wang, D. Xie, C. Chen, J. Ma, and S. Cheng, "Deploying Multiple Mobile Sinks in Event-Driven WSNs," in *2008 IEEE International Conference on Communications*, 2008, pp. 2293–2297.

[108] Y. Wenguo and G. Tiande, "The Non-uniform Property of Energy Consumption and its Solution to the Wireless Sensor Network," in *2010 Second International Workshop on Education Technology and Computer Science*, 2010, pp. 186–192.

[109] X. Wu, G. Chen, and S. K. Das, "On the Energy Hole Problem of Nonuniform Node Distribution in Wireless Sensor Networks," in *2006 IEEE International Conference on Mobile Ad Hoc and Sensor Systems*, 2006, pp. 180–187.

[110] Xiaobing Wu, Guihai Chen, and S. K. Das, "Avoiding Energy Holes in Wireless Sensor Networks with Nonuniform Node Distribution," *IEEE Trans. Parallel Distrib. Syst.*, vol. 19, no. 5, pp. 710–720, May 2008.

[111] J. Li and P. Mohapatra, "An analytical model for the energy hole problem in many-to-one sensor networks," *IEEE Veh. Technol. Conf.*, vol. 4, pp. 2721–2725, 2005.

[112] J. Li and P. Mohapatra, "Analytical modeling and mitigation techniques for the energy hole problem in sensor networks," *Pervasive Mob. Comput.*, vol. 3, no. 3, pp. 233–254, 2007.

[113] M. L.Sichitiu and R. Dutta, "Benefits of Multiple Battery Levels for the Lifetime of Large Wireless Sensor Networks," 2005, pp. 1440–1444.

[114] M. L. Sichitiu and R. Dutta, "On the Lifetime of Large Wireless Sensor Networks with Multiple Battery Levels," *Ad Hoc Sens. Wirel. Networks*, vol. 00, pp. 1–27, 2007.

[115] S. Madden, M. J. Franklin, J. M. Hellerstein, and U. C. Berkeley, "The Design of an Acquisitional Query Processor For Sensor Networks," *SIGMOD '03 Proc. 2003 ACM SIGMOD Int. Conf. Manag. data*, pp. 491–502, 2003.

[116] M. L. Sichitiu, "Cross-layer scheduling for power efficiency in wireless sensor networks," *Ieee Infocom 2004*, vol. 3, no. C, pp. 1740–1750, 2004.

[117] L. Null and J. Lobur, "The essentials of computer organization and architecture," *essentials Comput. Organ. Archit.*, vol. 10, pp. 93–144, 2010.

[118] W. Stallings, "Computer Architecture and Organization," *Organization*, p. 25, 1998.

[119] L. Gu and J. A. Stankovic, "Radio-Triggered Wake-Up for Wireless Sensor Networks," *Real-Time Syst.*, vol. 29, no. 2–3, pp. 157–182, Mar. 2005.

[120] A. Report, "CC430 Wake-On-Radio Functionality," no. July, pp. 1–8, 2012.

[121] Lin Gu and J. A. Stankovic, "Radio-triggered wake-up capability for sensor networks," in *Proceedings. RTAS 2004. 10th IEEE Real-Time and Embedded Technology and Applications Symposium, 2004.*, pp. 27–36.

[122] I. Demirkol, C. Ersoy, and E. Onur, "Wake-up receivers for wireless sensor networks: benefits and challenges," *IEEE Wirel. Commun.*, vol. 16, no. 4, pp. 88–96, Aug. 2009.

[123] F. Hutu, A. Khoumeri, G. Villemaud, and J.-M. Gorce, "A new wake-up radio architecture for wireless sensor networks," *EURASIP J. Wirel. Commun. Netw.*, vol. 2014, no. 1, p. 177, Dec. 2014.

[124] A. S. Tanenbaum and D. J. Wetherall, *Computer Networks*. Prentice Hall, 2010.

[125] J. F. Kurose and K. W. Ross, *Computer Networking: A Top-Down Approach*, 6th ed. Pearson, 2012.

[126] C. B. Margi and K. Obraczka, "Instrumenting network simulators for evaluating energy consumption in power-aware ad-hoc network protocols," in *The IEEE Computer Society's 12th Annual International Symposium on Modeling, Analysis, and Simulation of Computer and Telecommunications Systems, 2004. (MASCOTS 2004). Proceedings.*, pp. 337–346.

[127] L. M. Feeney and M. Nilsson, "Investigating the energy consumption of a wireless network interface in an ad hoc networking environment," in *Proceedings IEEE INFOCOM 2001. Conference on Computer Communications. Twentieth Annual Joint Conference of the IEEE Computer and Communications Society (Cat. No.01CH37213)*, vol. 3, pp. 1548–1557.

[128] IEEE Standard for Information technology, *IEEE Standard for Information technology — Telecommunications and information Local and metropolitan area networks — Part 11 : Wireless LAN Medium Access Control (MAC)*, vol. 2007, no. June. 2007.

[129] IEEE 802.11 Working Group, "IEEE Std 802.11. Wireless LAN Medium Access

Control (MAC) and Physical Layer (PHY) Specifications of IEEE 802.11." 1999.

[130] L. Kleinrock and F. Tobagi, "Packet Switching in Radio Channels: Part I--Carrier Sense Multiple-Access Modes and Their Throughput-Delay Characteristics," *IEEE Trans. Commun.*, vol. 23, no. 12, pp. 1400–1416, 1975.

[131] I. Howitt and G. Jore A., "IEEE 802.15.4: Low-Rate Wireless Personal Area Networks (LR-WPANs)," *Wirel. Commun. Netw.*, vol. 2011, no. September, p. 314, 2011.

[132] A. Koubaa, M. Alves, and E. Tovar, "A comprehensive simulation study of slotted CSMA/CA for IEEE 802.15.4 wireless sensor networks," in *2006 IEEE International Workshop on Factory Communication Systems*, 2006, pp. 183–192.

[133] A. Vutukuri, S. Bhattacharya, T. Raj, Sridhar, and V. Geetha, "Enhanced Back-Off Technique for IEEE 802.15.4 WSN Standard," 2014, pp. 21–29.

[134] S. U. Rehman, S. Berber, and A. Swain, "Performance analysis of CSMA/CA algorithm for wireless sensor network," in *TENCON 2010 - 2010 IEEE Region 10 Conference*, 2010, pp. 2012–2017.

[135] Z. Dahham, A. Sali, B. M. Ali, and M. S. Jahan, "An efficient CSMA-CA algorithm for IEEE 802.15.4 Wireless Sensor Networks," in *2012 International Symposium on Telecommunication Technologies*, 2012, pp. 118–123.

[136] O. N. Koyi, H. S. Yang, and Y. Kwon, "Impact of Base Station Location on Wireless Sensor Networks," pp. 151–162, 2015.

[137] A. Di Nisio, T. Di Noia, C. G. C. Carducci, and M. Spadavecchia, "High Dynamic Range Power Consumption Measurement in Microcontroller-Based Applications," *IEEE Trans. Instrum. Meas.*, vol. 65, no. 9, pp. 1968–1976, Sep. 2016.

[138] T. S. Rappaport, *Wireless Communications : Principles and Practice*. 2002.

[139] A. Committee, I. Antennas, and P. Society, *IEEE Standard Definitions of Terms for Antennas*, vol. 2013. 2014.

[140] Y. Huang and K. Boyle, *Antennas: From Theory to Practice*. 2008.

[141] J. D. Kraus and R. J. Marhefka, "Antennas for all applications," *Antennas for all applications, by Kraus, John Daniel; Marhefka, Ronald J. New York: McGraw-Hill, c2002.*, vol. 1, no. 34. pp. 6307–6311, 2002.

[142] A. Kosowski and Ł. Kuszner, "On Greedy Graph Coloring in the Distributed Model," 2006, pp. 592–601.

[143] P. Minet and S. Mahfoudh, "SERENA: SchEduling RoutEr Nodes Activity in wireless ad hoc and sensor networks," in *IWCMC 2008 - International Wireless Communications and Mobile Computing Conference*, 2008, pp. 511–516.

[144] P. Minet, S. Mahfoudh, G. Chalhoub, and A. Guitton, "Node Coloring in a Wireless Sensor Network with Unidirectional Links and Topology Changes," in *2010 IEEE Wireless Communication and Networking Conference*, 2010, pp. 1–6.

[145] A. Boukerche, Ed., *Algorithms and Protocols for Wireless Sensor Networks*. Hoboken, NJ, USA: John Wiley & Sons, Inc., 2008.

[146] Q.-Q. Li, H. Gong, M. Liu, M. Yang, and J. Zheng, "On Prolonging Network Lifetime through Load-Similar Node Deployment in Wireless Sensor Networks," *Sensors*, vol. 11, no. 4, pp. 3527–3544, Mar. 2011.

[147] F. A. M. Miranda and C. Al. dos Reis Filho, "Lifetime Maximization With Multiple Battery Levels in Irregularly Distributed Wireless Sensor Networks," in *10th*

International Symposium on Ambient Intelligence and Embedded Systems, 2011.

[148] O. Landsiedel, K. Wehrle, and S. Gotz, "Accurate prediction of power consumption in sensor networks," *Proc. 2nd IEEE Work. Embed. Networked Sensors*, 2005.

[149] W. Du, F. Mieyeville, and D. Navarro, "Modeling Energy Consumption of Wireless Sensor Networks by SystemC," *2010 Fifth Int. Conf. Syst. Networks Commun.*, pp. 94–98, Aug. 2010.

[150] L. M. Kamarudin, R. B. Ahmad, B. L. Ong, a. Zakaria, and D. Ndzi, "Modeling and simulation of near-earth wireless sensor networks for agriculture based application using OMNeT," *2010 Int. Conf. Comput. Appl. Ind. Electron.*, no. Iccaie, pp. 131–136, Dec. 2010.

[151] A. Dâmaso, D. Freitas, N. Rosa, B. Silva, and P. Maciel, "Evaluating the Power Consumption of Wireless Sensor Network Applications Using Models," *Sensors*, vol. 13, no. 3, pp. 3473–3500, Mar. 2013.

[152] D. Sánchez-Álvarez, M. Linaje, and F.-J. Rodríguez-Pérez, "A Framework to Design the Computational Load Distribution of Wireless Sensor Networks in Power Consumption Constrained Environments," *Sensors*, vol. 18, no. 4, p. 954, Mar. 2018.

[153] L. Riliskis and E. Osipov, "Symphony: A Framework for Accurate and Holistic WSN Simulation," *Sensors*, vol. 15, no. 3, pp. 4677–4699, Feb. 2015.

[154] M. Prauzek, J. Konecny, M. Borova, K. Janosova, J. Hlavica, and P. Musilek, "Energy Harvesting Sources, Storage Devices and System Topologies for Environmental Wireless Sensor Networks: A Review," *Sensors*, vol. 18, no. 8, p. 2446, Jul. 2018.

[155] S. Sudevalayam and P. Kulkarni, "Energy harvesting sensor nodes: Survey and implications," *IEEE Commun. Surv. Tutorials*, 2011.

[156] S. Galmés and S. Escolar, "Analytical Model for the Duty Cycle in Solar-Based EH-WSN for Environmental Monitoring," *Sensors*, vol. 18, no. 8, p. 2499, Aug. 2018.

[157] L. Xiao, F. Wu, D. Yang, T. Zhang, and X. Zhu, "Energy Efficient Wireless Sensor Network Modelling Based on Complex Networks," *J. Sensors*, vol. 2016, pp. 1–8, 2016.

[158] Y. Wu, W. Liu, and Q. Shen, "Joint optimal placement, routing, and energy allocation in wireless sensor networks with a shared energy harvesting module," *Int. J. Distrib. Sens. Networks*, vol. 13, no. 5, p. 155014771770944, May 2017.

[159] C.-S. Ok, S. Lee, P. Mitra, and S. Kumara, "Distributed energy balanced routing for wireless sensor networks," *Comput. Ind. Eng.*, vol. 57, no. 1, pp. 125–135, Aug. 2009.

[160] R. Asorey-Cacheda, A. García-Sánchez, F. García-Sánchez, J. García-Haro, and F. González-Castano, "On Maximizing the Lifetime of Wireless Sensor Networks by Optimally Assigning Energy Supplies," *Sensors*, vol. 13, no. 8, pp. 10219–10244, Aug. 2013.

[161] M. Abo-zahhad, O. Amin, M. Farrag, and A. Ali, "Survey on Energy Consumption Models in Wireless Sensor Networks," *Open Trans. Wirel. Commun.*, vol. 4, no. 2, pp. 1–17, 2015.

[162] J. A. Khan, H. K. Qureshi, and A. Iqbal, "Energy management in Wireless Sensor Networks: A survey," *Comput. Electr. Eng.*, vol. 41, pp. 159–176, Jan. 2015.

[163] M. Abo-Zahhad, M. Farrag, A. Ali, and O. Amin, "An energy consumption model for wireless sensor networks," in *5th International Conference on Energy Aware*

Computing Systems & Applications, 2015, pp. 1–4.

[164] A. Ali, M. Abo-Zahhad, and M. Farrag, "Modeling of Wireless Sensor Networks with Minimum Energy Consumption," *Arab. J. Sci. Eng.*, vol. 42, no. 7, pp. 2631–2639, Jul. 2017.

[165] M. Ram and S. Kumar, "Analytical energy consumption model for MAC protocols in wireless sensor networks," in *2014 International Conference on Signal Processing and Integrated Networks (SPIN)*, 2014, pp. 444–447.

[166] V. Agarwal, R. A. DeCarlo, and L. H. Tsoukalas, "Modeling Energy Consumption and Lifetime of a Wireless Sensor Node Operating on a Contention-Based MAC Protocol," *IEEE Sens. J.*, vol. 17, no. 16, pp. 5153–5168, Aug. 2017.

[167] H.-Y. Zhou, "Modeling of Node Energy Consumption for Wireless Sensor Networks," *Wirel. Sens. Netw.*, 2011.

[168] A. Ahmad, N. Javaid, M. Imran, M. Guizani, and A. A. Alhamed, "An Advanced Energy Consumption Model for terrestrial Wireless Sensor Networks," in *2016 International Wireless Communications and Mobile Computing Conference (IWCMC)*, 2016, pp. 790–793.

[169] J. Broch, D. A. Maltz, D. B. Johnson, Y.-C. Hu, and J. Jetcheva, "A performance comparison of multi-hop wireless ad hoc network routing protocols," in *Proceedings of the 4th annual ACM/IEEE international conference on Mobile computing and networking - MobiCom '98*, 1998, pp. 85–97.

[170] M. Caesar, M. Castro, E. B. Nightingale, G. O'Shea, and A. Rowstron, "Virtual ring routing," *ACM SIGCOMM Comput. Commun. Rev.*, vol. 36, no. 4, p. 351, Aug. 2006.

[171] S. Androutsellis-Theotokis and D. Spinellis, "A survey of peer-to-peer content distribution technologies," *ACM Comput. Surv.*, vol. 36, no. 4, pp. 335–371, Dec. 2004.

[172] D. West, *Introduction to Graph Theory*, 2nd ed. London United Kingdon: Pearson, 2017.

[173] J. Bang-Jensen and G. Z. Gutin, *Digraphs*. London: Springer London, 2009.

[174] N. A. Pantazis, S. A. Nikolidakis, and D. D. Vergados, "Energy-Efficient Routing Protocols in Wireless Sensor Networks: A Survey," *IEEE Commun. Surv. Tutorials*, vol. 15, no. 2, pp. 551–591, 2013.

[175] J. N. Al-Karaki and A. E. Kamal, "Routing techniques in wireless sensor networks: a survey," *IEEE Wirel. Commun.*, vol. 11, no. 6, pp. 6–28, Dec. 2004.

[176] M. Radi, B. Dezfouli, K. A. Bakar, and M. Lee, "Multipath Routing in Wireless Sensor Networks: Survey and Research Challenges," *Sensors*, vol. 12, no. 12, pp. 650–685, Jan. 2012.

[177] K. Mehlhorn and P. Sanders, *Algorithms and Data Structures*. Berlin, Heidelberg: Springer Berlin Heidelberg, 2008.

[178] A. Mohammed and Z. Yang, "A Survey on Routing Protocols for Wireless Sensor Networks," in *Sustainable Wireless Sensor Networks*, InTech, 2010.

[179] K. Akkaya and M. Younis, "A survey on routing protocols for wireless sensor networks," *Ad Hoc Networks*, vol. 3, no. 3, pp. 325–349, May 2005.

[180] R. R. Selmic, V. V. Phoha, and A. Serwadda, *Wireless Sensor Networks*. Cham: Springer International Publishing, 2016.

[181] J.-S. Li, H.-C. Kao, and J.-D. Ke, "Voronoi-based relay placement scheme for wireless

sensor networks," *IET Commun.*, vol. 3, no. 4, p. 530, 2009.
[182] R. Ahlswede, Ning Cai, S.-Y. R. Li, and R. W. Yeung, "Network information flow," *IEEE Trans. Inf. Theory*, vol. 46, no. 4, pp. 1204–1216, Jul. 2000.
[183] Shiann-Tsong Sheu, T. Chen, Jenhui Chen, and Fun Ye, "The impact of RTS threshold on IEEE 802.11 MAC protocol," in *Ninth International Conference on Parallel and Distributed Systems, 2002. Proceedings.*, pp. 267–272.
[184] J. Kabara and M. Calle, "MAC Protocols Used by Wireless Sensor Networks and a General Method of Performance Evaluation," *Int. J. Distrib. Sens. Networks*, vol. 8, no. 1, p. 834784, Jan. 2012.
[185] I. Demirkol, C. Ersoy, and F. Alagoz, "MAC protocols for wireless sensor networks: a survey," *IEEE Commun. Mag.*, vol. 44, no. 4, pp. 115–121, Apr. 2006.
[186] T. Stathopoulos, R. Kapur, D. Estrin, J. Heidemann, and Lixia Zhang, "Application-based collision avoidance in wireless sensor networks," in *29th Annual IEEE International Conference on Local Computer Networks*, pp. 506–514.
[187] K. Langendoen and A. Meier, "Analyzing MAC protocols for low data-rate applications," *ACM Trans. Sens. Networks*, 2010.
[188] C.-K. Chau, M. Chen, and S. C. Liew, "Capacity of Large-Scale CSMA Wireless Networks," *IEEE/ACM Trans. Netw.*, vol. 19, no. 3, pp. 893–906, Jun. 2011.
[189] S. Rajba and T. Rajba, "The probability of collisions in Wireless Sensor Network with random sending," *Przegld Elektrotechniczny*, vol. 88, pp. 243–246, 2012.
[190] S. Rani and S. H. Ahmed, *Multi-hop Routing in Wireless Sensor Networks*. Singapore: Springer Singapore, 2016.
[191] N. Xiong, L. Zhang, W. Zhang, A. Vasilakos, and M. Imran, "Design and Analysis of an Efficient Energy Algorithm in Wireless Social Sensor Networks," *Sensors*, vol. 17, no. 10, p. 2166, Sep. 2017.
[192] J. Song, Y. Miao, E. Song, M. Hossain, and M. Alhamid, "Reliability-Aware Cooperative Node Sleeping and Clustering in Duty-Cycled Sensors Networks," *Sensors*, vol. 18, no. 1, p. 127, Jan. 2018.
[193] Panasonic Corporation of North America, "Panasonic Batteries Energy Catalog." Panasonic Corporation of North America, Rolling Meadows, IL, USA, 2011.
[194] N. Ahmed, S. S. Kanhere, and S. Jha, "The holes problem in wireless sensor networks," *ACM SIGMOBILE Mob. Comput. Commun. Rev.*, vol. 9, no. 2, p. 4, Apr. 2005.
[195] W. Bentz and D. Panagou, "An energy-aware redistribution method for multi-agent dynamic coverage networks," in *2016 IEEE 55th Conference on Decision and Control (CDC)*, 2016, vol. 1, no. 5, pp. 2644–2651.
[196] G. Ma and Z. Tao, "A Nonuniform Sensor Distribution Strategy for Avoiding Energy Holes in Wireless Sensor Networks," *Int. J. Distrib. Sens. Networks*, vol. 9, no. 7, p. 564386, Jul. 2013.
[197] "Panasonic Corporation." [Online]. Available: https://industrial.panasonic.com/ww/products/batteries.
[198] S. Borkar, T. Karnik, S. Narendra, J. Tschanz, A. Keshavarzi, and V. De, "Parameter variations and impact on circuits and microarchitecture," in *Proceedings of the 40th conference on Design automation - DAC '03*, 2003, p. 338.

[199] A. Golda, "Temperature influence on power consumption and time delay," *Digit. Syst. Des. 2003. Proceedings.*, pp. 0–4, 2003.

[200] D. Meekhun, V. Boitier, J. Dilhac, and C. Roche, "Study of the ambient temperature effect on the characteristics and the lifetime of Nickel-Metal Hydride secondary battery," pp. 3–6, 2009.

[201] V. Reddy *et al.*, "Impact of negative bias temperature instability on digital circuit reliability," *Microelectron. Reliab.*, vol. 45, no. 1, pp. 31–38, Jan. 2005.

[202] F. Leng, C. M. Tan, and M. Pecht, "Effect of Temperature on the Aging rate of Li Ion Battery Operating above Room Temperature," *Sci. Rep.*, vol. 5, no. 1, p. 12967, Oct. 2015.

Appendix A

COMPLEMENTARY DATA OF CHAPTER V: SCENARIO I USING P_{TX}

Table LXXV – Complementary data of Scenario I using P_{tx} @ T = 1s.

	Mote m	**Calculated e_m (in mAh)**	**Simulated e_m (in mAh)**	**Calculated battery (in mAh)**	**Assigned battery (in mAh)**	**Battery Set (in mAh)**
	1	0.001699944	0.0017	287	285	200+55+30
	2	0.001599944	0.0016	270	270	200+35+35
	3	0.001599944	0.0016	270	270	200+35+35
	4	0.001699944	0.0017	287	285	200+55+30
	5	0.001599944	0.0016	270	270	200+35+35
	6	0.001599944	0.0016	270	270	200+35+35
	7	0.000999944	0.001	169	168	120+48
	8	0.001033278	0.001033333	175	175	120+55
	9	0.000931426	0.000931389	157	156	48+48+35+25
	10	0.000859204	0.000859167	145	145	120+25
	11	0.000931426	0.000931389	157	156	48+48+35+25
	12	0.001033278	0.001033333	175	175	120+55
	13	0.000999944	0.001	169	168	120+48
	14	0.001033278	0.001033333	175	175	120+55
	15	0.000931426	0.000931389	157	156	48+48+35+25
	16	0.000859204	0.000859167	145	145	120+25
	17	0.000931426	0.000931389	157	156	48+48+35+25
	18	0.001033278	0.001033333	175	175	120+55
	19	0.000377722	0.000377778	64	65	35+30
	20	0.000444389	0.000444444	75	75	75
	21	0.000438833	0.000438889	74	75	75
	22	0.000372167	0.000372222	63	65	35+30
	23	0.000511056	0.000511111	86	85	55+30
	24	0.000372167	0.000372222	63	65	35+30
	25	0.000438833	0.000438889	74	73	48+25
	26	0.000444389	0.000444444	75	75	75
	27	0.000377722	0.000377778	64	65	35+30
	28	0.000444389	0.000444444	75	75	75
	29	0.000438833	0.000438889	74	73	48+25
	30	0.000372167	0.000372222	63	65	35+30
	31	0.000511056	0.000511111	86	85	55+30
	32	0.000372167	0.000372222	63	65	35+30
	33	0.000438833	0.000438889	74	75	75
	34	0.000444389	0.000444444	75	75	75
Total	**-**	**0.028177222**	**0.028177222**	**4758**	**4756**	**4756**

Table LXXVI – Complementary data of Scenario I using P_{tx} @ T = 10s.

	Mote m	Calculated e_m (in mAh)	Simulated e_m (in mAh)	Calculated battery (in mAh)	Assigned battery (in mAh)	Battery Set (in mAh)
	1	0.001752444	0.0017525	278	278	200+48+30
	2	0.001652444	0.0016525	263	263	165+48+25+25
	3	0.001652444	0.0016525	263	263	165+48+25+25
	4	0.001752444	0.0017525	278	278	200+48+30
	5	0.001652444	0.0016525	263	263	165+48+25+25
	6	0.001652444	0.0016525	263	263	165+48+25+25
	7	0.001052444	0.0010525	167	168	120+48
	8	0.001085778	0.001085833	173	173	75+48+25+25
	9	0.000983926	0.000983889	156	156	48+48+30+30
	10	0.000911704	0.000911667	145	145	120+25
	11	0.000983926	0.000983889	156	156	48+48+30+30
	12	0.001085778	0.001085833	173	173	75+48+25+25
	13	0.001052444	0.0010525	167	168	120+48
	14	0.001085778	0.001085833	173	173	75+48+25+25
	15	0.000983926	0.000983889	156	156	48+48+30+30
	16	0.000911704	0.000911667	145	145	120+25
	17	0.000983926	0.000983889	156	156	48+48+30+30
	18	0.001085778	0.001085833	173	173	75+48+25+25
	19	0.000430222	0.000430278	68	70	35+35
	20	0.000496889	0.000496944	79	78	48+30
	21	0.000491333	0.000491389	78	78	48+30
	22	0.000424667	0.000424722	67	65	35+30
	23	0.000563556	0.000563611	90	90	90
	24	0.000424667	0.000424722	67	65	35+30
	25	0.000491333	0.000491389	78	78	48+30
	26	0.000496889	0.000496944	79	78	48+30
	27	0.000430222	0.000430278	68	70	35+35
	28	0.000496889	0.000496944	79	78	48+30
	29	0.000491333	0.000491389	78	78	48+30
	30	0.000424667	0.000424722	67	65	35+30
	31	0.000563556	0.000563611	90	90	90
	32	0.000424667	0.000424722	67	65	35+30
	33	0.000491333	0.000491389	78	78	48+30
	34	0.000496889	0.000496944	79	78	48+30
Total	**-**	**0.029960888**	**0.029962222**	**4760**	**4754**	**4754**

Table LXXVII – Complementary data of Scenario I using P_{tx} @ T = 60s.

	Mote m	**Calculated e_m (in mAh)**	**Simulated e_m (in mAh)**	**Calculated battery (in mAh)**	**Assigned battery (in mAh)**	**Battery Set (in mAh)**
	1	0.002044111	0.002044167	244	245	165+40+40
	2	0.001944111	0.001944167	232	230	165+35+30
	3	0.001944111	0.001944167	232	230	165+35+30
	4	0.002044111	0.002044167	244	245	165+40+40
	5	0.001944111	0.001944167	232	230	165+35+30
	6	0.001944111	0.001944167	232	230	165+35+30
	7	0.001344111	0.001344167	160	160	120+40
	8	0.001377444	0.0013775	164	165	165
	9	0.001275593	0.001275556	152	150	120+30
	10	0.00120337	0.001203333	144	145	120+25
	11	0.001275593	0.001275556	152	150	120+30
	12	0.001377444	0.0013775	164	165	165
	13	0.001344111	0.001344167	160	160	120+40
	14	0.001377444	0.0013775	164	165	165
	15	0.001275593	0.001275556	152	150	120+30
	16	0.00120337	0.001203333	144	145	120+25
	17	0.001275593	0.001275556	152	150	120+30
	18	0.001377444	0.0013775	164	165	165
	19	0.000721889	0.000721944	86	85	55+30
	20	0.000788556	0.000788611	94	95	55+40
	21	0.000783	0.000783056	93	95	55+40
	22	0.000716333	0.000716389	86	85	55+30
	23	0.000855222	0.000855278	102	103	55+48
	24	0.000716333	0.000716389	86	85	55+30
	25	0.000783	0.000783056	93	95	55+40
	26	0.000788556	0.000788611	94	95	55+40
	27	0.000721889	0.000721944	86	85	55+30
	28	0.000788556	0.000788611	94	95	55+40
	29	0.000783	0.000783056	93	95	55+40
	30	0.000716333	0.000716389	86	85	55+30
	31	0.000855222	0.000855278	102	103	55+48
	32	0.000716333	0.000716389	86	85	55+30
	33	0.000783	0.000783056	93	95	55+40
	34	0.000788556	0.000788611	94	95	55+40
Total	**-**	**0.039877555**	**0.039878889**	**4756**	**4756**	**4756**

Table LXXVIII – Complementary data of Scenario I using P_{tx} @ T = 600s.

	Mote m	**Calculated e_m (in mAh)**	**Simulated e_m (in mAh)**	**Calculated battery (in mAh)**	**Assigned battery (in mAh)**	**Battery Set (in mAh)**
	1	0.005194111	0.005194167	168	168	120+48
	2	0.005094111	0.005094167	165	165	140+25
	3	0.005094111	0.005094167	165	165	140+25
	4	0.005194111	0.005194167	168	168	120+48
	5	0.005094111	0.005094167	165	165	140+25
	6	0.005094111	0.005094167	165	165	140+25
	7	0.004494111	0.004494167	146	145	120+25
	8	0.004527444	0.0045275	147	148	75+48+25
	9	0.004425593	0.004425556	143	143	55+48+40
	10	0.00435337	0.004353333	141	140	140
	11	0.004425593	0.004425556	143	143	55+48+40
	12	0.004527444	0.0045275	147	148	75+48+25
	13	0.004494111	0.004494167	146	145	120+25
	14	0.004527444	0.0045275	147	148	75+48+25
	15	0.004425593	0.004425556	143	143	55+48+40
	16	0.00435337	0.004353333	141	140	140
	17	0.004425593	0.004425556	143	143	55+48+40
	18	0.004527444	0.0045275	147	148	75+48+25
	19	0.003871889	0.003871944	125	125	90+35
	20	0.003938556	0.003938611	128	128	48+40+40
	21	0.003933	0.003933056	127	128	48+40+40
	22	0.003866333	0.003866389	125	125	90+35
	23	0.004005222	0.004005278	130	130	90+40
	24	0.003866333	0.003866389	125	125	90+35
	25	0.003933	0.003933056	127	125	90+35
	26	0.003938556	0.003938611	128	128	48+40+40
	27	0.003871889	0.003871944	125	125	90+35
	28	0.003938556	0.003938611	128	128	48+40+40
	29	0.003933	0.003933056	127	125	90+35
	30	0.003866333	0.003866389	125	125	90+35
	31	0.004005222	0.004005278	130	130	90+40
	32	0.003866333	0.003866389	125	125	90+35
	33	0.003933	0.003933056	127	125	90+35
	34	0.003938556	0.003938611	128	128	48+40+40
Total	**-**	**0.146977555**	**0.146978889**	**4760**	**4755**	**4755**

Table LXXIX – Complementary data of Scenario I using P_{tx} @ T = 3600s.

	Mote m	**Calculated e_m (in mAh)**	**Simulated e_m (in mAh)**	**Calculated battery (in mAh)**	**Assigned battery (in mAh)**	**Battery Set (in mAh)**
	1	0.022694111	0.022694167	146	146	48+48+25+25
	2	0.022594111	0.022594167	145	145	120+25
	3	0.022594111	0.022594167	145	145	120+25
	4	0.022694111	0.022694167	146	146	48+48+25+25
	5	0.022594111	0.022594167	145	145	120+25
	6	0.022594111	0.022594167	145	145	120+25
	7	0.021994111	0.021994167	141	140	140
	8	0.022027444	0.0220275	141	140	140
	9	0.021925593	0.021925556	141	140	140
	10	0.02185337	0.021853333	140	140	140
	11	0.021925593	0.021925556	141	140	140
	12	0.022027444	0.0220275	141	140	140
	13	0.021994111	0.021994167	141	140	140
	14	0.022027444	0.0220275	141	140	140
	15	0.021925593	0.021925556	141	140	140
	16	0.02185337	0.021853333	140	140	140
	17	0.021925593	0.021925556	141	140	140
	18	0.022027444	0.0220275	141	140	140
	19	0.021371889	0.021371944	137	138	90+48
	20	0.021438556	0.021438611	138	138	90+48
	21	0.021433	0.021433056	137	138	90+48
	22	0.021366333	0.021366389	137	138	90+48
	23	0.021505222	0.021505278	138	138	90+48
	24	0.021366333	0.021366389	137	138	90+48
	25	0.021433	0.021433056	137	138	90+48
	26	0.021438556	0.021438611	138	138	90+48
	27	0.021371889	0.021371944	137	138	90+48
	28	0.021438556	0.021438611	138	138	90+48
	29	0.021433	0.021433056	137	138	90+48
	30	0.021366333	0.021366389	137	138	90+48
	31	0.021505222	0.021505278	138	138	90+48
	32	0.021366333	0.021366389	137	138	90+48
	33	0.021433	0.021433056	137	138	90+48
	34	0.021438556	0.021438611	138	138	90+48
Total	**-**	**0.741977555**	**0.741978889**	**4760**	**4760**	**4760**

Table LXXX – Complementary data of Scenario I using P_{tx} @ T = 86400s.

	Mote m	Calculated e_m (in mAh)	Simulated e_m (in mAh)	Calculated battery (in mAh)	Assigned battery (in mAh)	Battery Set (in mAh)
	1	0.505694111	0.505695556	140.24	140.24	–
	2	0.505594111	0.505595278	140.21	140.21	–
	3	0.505594111	0.505594722	140.21	140.21	–
	4	0.505694111	0.505695	140.24	140.24	–
	5	0.505594111	0.505595	140.21	140.21	–
	6	0.505594111	0.505594167	140.21	140.21	–
	7	0.504994111	0.504995278	140.05	140.05	–
	8	0.505027444	0.505028333	140.06	140.06	–
	9	0.504925593	0.504926389	140.03	140.03	–
	10	0.50485337	0.504853611	140.01	140.01	–
	11	0.504925593	0.504926111	140.03	140.03	–
	12	0.505027444	0.505028056	140.06	140.06	–
	13	0.504994111	0.504994722	140.05	140.05	–
	14	0.505027444	0.505028056	140.06	140.06	–
	15	0.504925593	0.504926389	140.03	140.03	–
	16	0.50485337	0.504853611	140.01	140.01	–
	17	0.504925593	0.504925833	140.03	140.03	–
	18	0.505027444	0.5050275	140.06	140.06	–
	19	0.504371889	0.504372222	139.87	139.87	–
	20	0.504438556	0.504438889	139.89	139.89	–
	21	0.504433	0.504433333	139.89	139.89	–
	22	0.504366333	0.504366667	139.87	139.87	–
	23	0.504505222	0.504505556	139.91	139.91	–
	24	0.504366333	0.504366667	139.87	139.87	–
	25	0.504433	0.504433333	139.89	139.89	–
	26	0.504438556	0.504438889	139.89	139.89	–
	27	0.504371889	0.504372222	139.87	139.87	–
	28	0.504438556	0.504438889	139.89	139.89	–
	29	0.504433	0.504433333	139.89	139.89	–
	30	0.504366333	0.504366667	139.87	139.87	–
	31	0.504505222	0.504505556	139.91	139.91	–
	32	0.504366333	0.504366667	139.87	139.87	–
	33	0.504433	0.504433056	139.89	139.89	–
	34	0.504438556	0.504438889	139.89	139.89	–
Total	**-**	**17.163977555**	**17.163994444**	**4760**	**4760**	–

Appendix B

COMPLEMENTARY DATA OF CHAPTER V: SCENARIO I USING $11.31P_{TX}$

Table LXXXI – Complementary data of Scenario I using 11.31P_{tx} @ T = 1s.

	Mote m	**Calculated e_m (in mAh)**	**Simulated e_m (in mAh)**	**Calculated battery (in mAh)**	**Assigned battery (in mAh)**	**Battery Set (in mAh)**
	1	0.00153169	0.001531667	113	113	48+35+30
	2	0.001395447	0.001395556	103	103	55+48
	3	0.001395447	0.001395556	103	103	55+48
	4	0.00153169	0.001531667	113	113	48+35+30
	5	0.001395447	0.001395556	103	103	55+48
	6	0.001395447	0.001395556	103	103	55+48
	7	0.002503516	0.002516944	184	185	120+35+30
	8	0.002735261	0.002749722	202	200	200
	9	0.002502722	0.002516111	184	185	120+35+30
	10	0.002800473	0.002816111	206	205	165+40
	11	0.002502722	0.002516111	184	185	120+35+30
	12	0.002735261	0.002749722	202	200	200
	13	0.002503516	0.002516944	184	185	120+35+30
	14	0.002735261	0.002749722	202	200	200
	15	0.002502722	0.002516111	184	185	120+35+30
	16	0.002800473	0.002816111	206	205	165+40
	17	0.002502722	0.002516111	184	185	120+35+30
	18	0.002735261	0.002749444	202	200	200
	19	0.001516611	0.001524167	112	113	48+35+30
	20	0.001511056	0.001518611	111	110	55+55
	21	0.001516611	0.001524167	112	113	48+35+30
	22	0.001522167	0.001529722	112	113	48+35+30
	23	0.001586452	0.001593889	117	115	75+40
	24	0.001522167	0.001529722	112	113	48+35+30
	25	0.001516611	0.001524167	112	113	48+35+30
	26	0.001511056	0.001518611	111	110	55+55
	27	0.001516611	0.001524167	112	113	48+35+30
	28	0.001511056	0.001518611	111	110	55+55
	29	0.001516611	0.001524167	112	113	48+35+30
	30	0.001522167	0.001529722	112	113	48+35+30
	31	0.001586452	0.001593889	117	115	75+40
	32	0.001522167	0.001529722	112	113	48+35+30
	33	0.001516611	0.001524167	112	113	48+35+30
	34	0.001511056	0.001518611	111	110	55+55
Total	**-**	**0.064610541**	**0.064900833**	**4760**	**4758**	**4758**

Table LXXXII – Complementary data of Scenario I using $11.31P_{tx}$ @ T = 10s.

	Mote m	Calculated e_m (in mAh)	Simulated e_m (in mAh)	Calculated battery (in mAh)	Assigned battery (in mAh)	Battery Set (in mAh)
	1	0.00158419	0.001584167	114	113	48+35+30
	2	0.001447947	0.001448056	104	103	55+48
	3	0.001447947	0.001448056	104	103	55+48
	4	0.00158419	0.001584167	114	113	48+35+30
	5	0.001447947	0.001448056	104	103	55+48
	6	0.001447947	0.001448056	104	103	55+48
	7	0.002556016	0.002569444	183	183	75+48+30+30
	8	0.002787761	0.002802222	200	200	200
	9	0.002555222	0.002568611	183	183	75+48+30+30
	10	0.002852973	0.002868611	205	205	165+40
	11	0.002555222	0.002568611	183	183	75+48+30+30
	12	0.002787761	0.002802222	200	200	200
	13	0.002556016	0.002569444	183	183	75+48+30+30
	14	0.002787761	0.002802222	200	200	200
	15	0.002555222	0.002568611	183	183	75+48+30+30
	16	0.002852973	0.002868611	205	205	165+40
	17	0.002555222	0.002568611	183	183	75+48+30+30
	18	0.002787761	0.002802222	200	200	200
	19	0.001569111	0.001576667	112	113	48+35+30
	20	0.001563556	0.001571111	112	113	48+35+30
	21	0.001569111	0.001576667	112	113	48+35+30
	22	0.001574667	0.001582222	113	113	48+35+30
	23	0.001638952	0.001646389	117	115	75+40
	24	0.001574667	0.001582222	113	113	48+35+30
	25	0.001569111	0.001576667	112	113	48+35+30
	26	0.001563556	0.001571111	112	113	48+35+30
	27	0.001569111	0.001576667	112	113	48+35+30
	28	0.001563556	0.001571111	112	113	48+35+30
	29	0.001569111	0.001576667	112	113	48+35+30
	30	0.001574667	0.001582222	113	113	48+35+30
	31	0.001638952	0.001646389	117	115	75+40
	32	0.001574667	0.001582222	113	113	48+35+30
	33	0.001569111	0.001576667	112	113	48+35+30
	34	0.001563556	0.001571111	112	113	48+35+30
Total	**-**	**0.066395541**	**0.066686111**	**4758**	**4758**	**4758**

Table LXXXIII – Complementary data of Scenario I using 11.31P_{tx} @ T = 60s.

	Mote m	Calculated e_m (in mAh)	Simulated e_m (in mAh)	Calculated battery (in mAh)	Assigned battery (in mAh)	Battery Set (in mAh)
	1	0.001875857	0.001875833	117	118	48+35+35
	2	0.001739614	0.001739722	109	110	55+55
	3	0.001739614	0.001739722	109	110	55+55
	4	0.001875857	0.001875833	117	118	48+35+35
	5	0.001739614	0.001739722	109	110	55+55
	6	0.001739614	0.001739722	109	110	55+55
	7	0.002847682	0.002861111	178	178	90+48+40
	8	0.003079428	0.003093889	192	192	48+48+48+48
	9	0.002846889	0.002860278	178	178	90+48+40
	10	0.00314464	0.003160278	196	195	165+30
	11	0.002846889	0.002860278	178	178	90+48+40
	12	0.003079428	0.003093889	192	192	48+48+48+48
	13	0.002847682	0.002861111	178	178	90+48+40
	14	0.003079428	0.003093889	192	192	48+48+48+48
	15	0.002846889	0.002860278	178	178	90+48+40
	16	0.00314464	0.003160278	196	195	165+30
	17	0.002846889	0.002860278	178	178	90+48+40
	18	0.003079428	0.003093889	192	192	48+48+48+48
	19	0.001860778	0.001868333	116	115	75+40
	20	0.001855222	0.001862778	116	115	75+40
	21	0.001860778	0.001868333	116	115	75+40
	22	0.001866333	0.001873889	116	115	75+40
	23	0.001930619	0.001938056	120	120	120
	24	0.001866333	0.001873889	116	115	75+40
	25	0.001860778	0.001868333	116	115	75+40
	26	0.001855222	0.001862778	116	115	75+40
	27	0.001860778	0.001868333	116	115	75+40
	28	0.001855222	0.001862778	116	115	75+40
	29	0.001860778	0.001868333	116	115	75+40
	30	0.001866333	0.001873889	116	115	75+40
	31	0.001930619	0.001938056	120	120	120
	32	0.001866333	0.001873889	116	115	75+40
	33	0.001860778	0.001868333	116	115	75+40
	34	0.001855222	0.001862778	116	115	75+40
Total	**-**	**0.076312208**	**0.076602778**	**4762**	**4752**	**4752**

Table LXXXIV – Complementary data of Scenario I using 11.31P_{tx} @ T = 600s.

	Mote m	**Calculated e_m (in mAh)**	**Simulated e_m (in mAh)**	**Calculated battery (in mAh)**	**Assigned battery (in mAh)**	**Battery Set (in mAh)**
	1	0.005025857	0.005025833	130	130	90+40
	2	0.004889614	0.004889722	127	126	48+48+30
	3	0.004889614	0.004889722	127	126	48+48+30
	4	0.005025857	0.005025833	130	130	90+40
	5	0.004889614	0.004889722	127	126	48+48+30
	6	0.004889614	0.004889722	127	126	48+48+30
	7	0.005997682	0.006011111	156	156	48+48+30+30
	8	0.006229428	0.006243889	162	163	75+48+40
	9	0.005996889	0.006010278	156	156	48+48+30+30
	10	0.00629464	0.006310278	163	163	75+48+40
	11	0.005996889	0.006010278	156	156	48+48+30+30
	12	0.006229428	0.006243889	162	163	75+48+40
	13	0.005997682	0.006011111	156	156	48+48+30+30
	14	0.006229428	0.006243889	162	163	75+48+40
	15	0.005996889	0.006010278	156	156	48+48+30+30
	16	0.00629464	0.006310278	163	163	75+48+40
	17	0.005996889	0.006010278	156	156	48+48+30+30
	18	0.006229428	0.006243889	162	163	75+48+40
	19	0.005010778	0.005018333	130	130	90+40
	20	0.005005222	0.005012778	130	130	90+40
	21	0.005010778	0.005018333	130	130	90+40
	22	0.005016333	0.005023889	130	130	90+40
	23	0.005080619	0.005088056	132	130	90+40
	24	0.005016333	0.005023889	130	130	90+40
	25	0.005010778	0.005018333	130	130	90+40
	26	0.005005222	0.005012778	130	130	90+40
	27	0.005010778	0.005018333	130	130	90+40
	28	0.005005222	0.005012778	130	130	90+40
	29	0.005010778	0.005018333	130	130	90+40
	30	0.005016333	0.005023889	130	130	90+40
	31	0.005080619	0.005088056	132	130	90+40
	32	0.005016333	0.005023889	130	130	90+40
	33	0.005010778	0.005018333	130	130	90+40
	34	0.005005222	0.005012778	130	130	90+40
Total	**-**	**0.183412208**	**0.183702778**	**4762**	**4758**	**4758**

Table LXXXV – Complementary data of Scenario I using 11.31P_{tx} @ T = 3600s.

	Mote m	**Calculated e_m (in mAh)**	**Simulated e_m (in mAh)**	**Calculated battery (in mAh)**	**Assigned battery (in mAh)**	**Battery Set (in mAh)**
	1	0.022525857	0.022525833	138	138	90+48
	2	0.022389614	0.022389722	137	136	48+48+40
	3	0.022389614	0.022389722	137	136	48+48+40
	4	0.022525857	0.022525833	138	138	90+48
	5	0.022389614	0.022389722	137	136	48+48+40
	6	0.022389614	0.022389722	137	136	48+48+40
	7	0.023497682	0.023511111	144	143	55+48+40
	8	0.023729428	0.023743889	145	145	120+25
	9	0.023496889	0.023510278	144	143	55+48+40
	10	0.02379464	0.023810278	146	145	120+25
	11	0.023496889	0.023510278	144	143	55+48+40
	12	0.023729428	0.023743889	145	145	120+25
	13	0.023497682	0.023511111	144	143	55+48+40
	14	0.023729428	0.023743889	145	145	120+25
	15	0.023496889	0.023510278	144	143	55+48+40
	16	0.02379464	0.023810278	146	145	120+25
	17	0.023496889	0.023510278	144	143	55+48+40
	18	0.023729428	0.023743889	145	145	120+25
	19	0.022510778	0.022518333	138	138	90+48
	20	0.022505222	0.022512778	138	138	90+48
	21	0.022510778	0.022518333	138	138	90+48
	22	0.022516333	0.022523889	138	138	90+48
	23	0.022580619	0.022588056	138	138	90+48
	24	0.022516333	0.022523889	138	138	90+48
	25	0.022510778	0.022518333	138	138	90+48
	26	0.022505222	0.022512778	138	138	90+48
	27	0.022510778	0.022518333	138	138	90+48
	28	0.022505222	0.022512778	138	138	90+48
	29	0.022510778	0.022518333	138	138	90+48
	30	0.022516333	0.022523889	138	138	90+48
	31	0.022580619	0.022588056	138	138	90+48
	32	0.022516333	0.022523889	138	138	90+48
	33	0.022510778	0.022518333	138	138	90+48
	34	0.022505222	0.022512778	138	138	90+48
Total	**-**	**0.778412208**	**0.778702778**	**4768**	**4756**	**4756**

Table LXXXVI – Complementary data of Scenario I using 11.31P_{tx} @ T = 86400s.

	Mote m	Calculated e_m (in mAh)	Simulated e_m (in mAh)	Calculated battery (in mAh)	Assigned battery (in mAh)	Battery Set (in mAh)
	1	0.505525857	0.511984722	139.9	139.9	–
	2	0.505389614	0.507151389	139.86	139.86	–
	3	0.505389614	0.507148056	139.86	139.86	–
	4	0.505525857	0.507148056	139.9	139.9	–
	5	0.505389614	0.511930556	139.86	139.86	–
	6	0.505389614	0.511930556	139.86	139.86	–
	7	0.506497682	0.511071944	140.17	140.17	–
	8	0.506729428	0.510831389	140.23	140.23	–
	9	0.506496889	0.506505278	140.17	140.17	–
	10	0.50679464	0.506551944	140.25	140.25	–
	11	0.506496889	0.505473056	140.17	140.17	–
	12	0.506729428	0.505520833	140.23	140.23	–
	13	0.506497682	0.506569722	140.17	140.17	–
	14	0.506729428	0.511468056	140.23	140.23	–
	15	0.506496889	0.511665	140.17	140.17	–
	16	0.50679464	0.509029167	140.25	140.25	–
	17	0.506496889	0.508991667	140.17	140.17	–
	18	0.506729428	0.509023333	140.23	140.23	–
	19	0.505510778	0.508799167	139.89	139.89	–
	20	0.505505222	0.510113889	139.89	139.89	–
	21	0.505510778	0.509362778	139.89	139.89	–
	22	0.505516333	0.505996667	139.9	139.9	–
	23	0.505580619	0.506044167	139.91	139.91	–
	24	0.505516333	0.505105278	139.9	139.9	–
	25	0.505510778	0.505151944	139.89	139.89	–
	26	0.505505222	0.506124167	139.89	139.89	–
	27	0.505510778	0.506378889	139.89	139.89	–
	28	0.505505222	0.510200556	139.89	139.89	–
	29	0.505510778	0.5086875	139.89	139.89	–
	30	0.505516333	0.508649722	139.9	139.9	–
	31	0.505580619	0.508725	139.91	139.91	–
	32	0.505516333	0.508636667	139.9	139.9	–
	33	0.505510778	0.5086825	139.89	139.89	–
	34	0.505505222	0.508741389	139.89	139.89	–
Total	**-**	**17.200412208**	**17.285395**	**4760**	**4760**	–

Appendix C

COMPLEMENTARY DATA OF CHAPTER V: SCENARIO I USING $46.76P_{TX}$

Table LXXXVII – Complementary data of Scenario I using 46.76P_{tx} @ T = 1s.

	Mote m	Calculated e_m (in mAh)	Simulated e_m (in mAh)	Calculated battery (in mAh)	Assigned battery (in mAh)	Battery Set (in mAh)
	1	0.001311056	0.001311111	61	60	30+30
	2	0.001311056	0.001311111	61	60	30+30
	3	0.001311056	0.001311111	61	60	30+30
	4	0.001311056	0.001311111	61	60	30+30
	5	0.001311056	0.001311111	61	60	30+30
	6	0.001311056	0.001311111	61	60	30+30
	7	0.001872167	0.001879722	87	88	48+40
	8	0.001938833	0.001946389	90	90	90
	9	0.0019055	0.001913056	89	88	48+40
	10	0.001938833	0.001946389	90	90	90
	11	0.0019055	0.001913056	89	88	48+40
	12	0.001938833	0.001946389	90	90	55+35
	13	0.001872167	0.001879722	87	88	48+40
	14	0.001938833	0.001946389	90	90	90
	15	0.0019055	0.001913056	89	88	48+40
	16	0.001938833	0.001946389	90	90	90
	17	0.0019055	0.001913056	89	88	48+40
	18	0.001938833	0.001946389	90	90	90
	19	0.004549944	0.004536944	212	213	165+48
	20	0.004483278	0.004470278	209	208	120+48+40
	21	0.004449944	0.004436944	207	208	120+48+40
	22	0.004416611	0.004403611	205	205	165+40
	23	0.004483278	0.004470278	209	208	120+48+40
	24	0.004416611	0.004403611	205	205	165+40
	25	0.004449944	0.004436944	207	208	120+48+40
	26	0.004483278	0.004470278	209	208	120+48+40
	27	0.004549944	0.004536944	212	213	165+48
	28	0.004483278	0.004470278	209	208	120+48+40
	29	0.004449944	0.004436944	207	208	120+48+40
	30	0.004416611	0.004403611	205	205	165+40
	31	0.004483278	0.004470278	209	208	120+48+40
	32	0.004416611	0.004403611	205	205	165+40
	33	0.004449944	0.004436944	207	208	120+48+40
	34	0.004483278	0.004470278	209	208	120+48+40
Total	**-**	**0.102331444**	**0.102214444**	**4762**	**4754**	**4754**

Table LXXXVIII – Complementary data of Scenario I using $46.76P_{tx}$ @ T = 10s.

	Mote m	Calculated e_m (in mAh)	Simulated e_m (in mAh)	Calculated battery (in mAh)	Assigned battery (in mAh)	Battery Set (in mAh)
	1	0.001363556	0.001363611	62	60	30+30
	2	0.001363556	0.001363611	62	60	30+30
	3	0.001363556	0.001363611	62	60	30+30
	4	0.001363556	0.001363611	62	60	30+30
	5	0.001363556	0.001363611	62	60	30+30
	6	0.001363556	0.001363611	62	60	30+30
	7	0.001924667	0.001932222	88	88	48+40
	8	0.001991333	0.001998889	91	90	90
	9	0.001958	0.001965556	90	90	90
	10	0.001991333	0.001998889	91	90	90
	11	0.001958	0.001965556	90	90	90
	12	0.001991333	0.001998889	91	90	90
	13	0.001924667	0.001932222	88	88	48+40
	14	0.001991333	0.001998889	91	90	90
	15	0.001958	0.001965556	90	90	90
	16	0.001991333	0.001998889	91	90	90
	17	0.001958	0.001965556	90	90	90
	18	0.001991333	0.001998889	91	90	90
	19	0.004602444	0.004589444	210	210	140+35+35
	20	0.004535778	0.004522778	207	208	120+48+40
	21	0.004502444	0.004489444	206	208	120+48+40
	22	0.004469111	0.004456111	204	205	165+40
	23	0.004535778	0.004522778	207	208	120+48+40
	24	0.004469111	0.004456111	204	205	165+40
	25	0.004502444	0.004489444	206	208	120+48+40
	26	0.004535778	0.004522778	207	208	120+48+40
	27	0.004602444	0.004589444	210	210	140+35+35
	28	0.004535778	0.004522778	207	208	120+48+40
	29	0.004502444	0.004489444	206	208	120+48+40
	30	0.004469111	0.004456111	204	205	165+40
	31	0.004535778	0.004522778	207	208	120+48+40
	32	0.004469111	0.004456111	204	205	165+40
	33	0.004502444	0.004489444	206	208	120+48+40
	34	0.004535778	0.004522778	207	208	120+48+40
Total	**-**	**0.104116444**	**0.103999444**	**4756**	**4756**	**4756**

Table LXXXIX – Complementary data of Scenario I using $46.76P_{tx}$ @ T = 60s.

	Mote m	Calculated e_m (in mAh)	Simulated e_m (in mAh)	Calculated battery (in mAh)	Assigned battery (in mAh)	Battery Set (in mAh)
	1	0.001655222	0.001655278	69	70	35+35
	2	0.001655222	0.001655278	69	70	35+35
	3	0.001655222	0.001655278	69	70	35+35
	4	0.001655222	0.001655278	69	70	35+35
	5	0.001655222	0.001655278	69	70	35+35
	6	0.001655222	0.001655278	69	70	35+35
	7	0.002216333	0.002223889	93	95	55+40
	8	0.002283	0.002290556	95	95	55+40
	9	0.002249667	0.002257222	94	95	55+40
	10	0.002283	0.002290556	95	95	55+40
	11	0.002249667	0.002257222	94	95	55+40
	12	0.002283	0.002290556	95	95	55+40
	13	0.002216333	0.002223889	93	95	55+40
	14	0.002283	0.002290556	95	95	55+40
	15	0.002249667	0.002257222	94	95	55+40
	16	0.002283	0.002290556	95	95	55+40
	17	0.002249667	0.002257222	94	95	55+40
	18	0.002283	0.002290556	95	95	55+40
	19	0.004894111	0.004881111	204	203	120+48+35
	20	0.004827444	0.004814444	202	200	200
	21	0.004794111	0.004781111	200	200	200
	22	0.004760778	0.004747778	199	198	120+48+30
	23	0.004827444	0.004814444	202	200	200
	24	0.004760778	0.004747778	199	198	120+48+30
	25	0.004794111	0.004781111	200	200	200
	26	0.004827444	0.004814444	202	200	200
	27	0.004894111	0.004881111	204	203	120+48+35
	28	0.004827444	0.004814444	202	200	200
	29	0.004794111	0.004781111	200	200	200
	30	0.004760778	0.004747778	199	198	120+48+30
	31	0.004827444	0.004814444	202	200	200
	32	0.004760778	0.004747778	199	198	120+48+30
	33	0.004794111	0.004781111	200	200	200
	34	0.004827444	0.004814444	202	200	200
Total	**-**	**0.114033111**	**0.113916111**	**4762**	**4758**	**4758**

Table XC – Complementary data of Scenario I using 46.76P_{tx} @ T = 600s.

	Mote m	Calculated e_m (in mAh)	Simulated e_m (in mAh)	Calculated battery (in mAh)	Assigned battery (in mAh)	Battery Set (in mAh)
	1	0.004805222	0.004805278	103	103	55+48
	2	0.004805222	0.004805278	103	103	55+48
	3	0.004805222	0.004805278	103	103	55+48
	4	0.004805222	0.004805278	103	103	55+48
	5	0.004805222	0.004805278	103	103	55+48
	6	0.004805222	0.004805278	103	103	55+48
	7	0.005366333	0.005373889	116	115	75+40
	8	0.005433	0.005440556	117	118	48+35+35
	9	0.005399667	0.005407222	116	115	75+40
	10	0.005433	0.005440556	117	118	48+35+35
	11	0.005399667	0.005407222	116	115	75+40
	12	0.005433	0.005440556	117	118	48+35+35
	13	0.005366333	0.005373889	116	115	75+40
	14	0.005433	0.005440556	117	118	48+35+35
	15	0.005399667	0.005407222	116	115	75+40
	16	0.005433	0.005440556	117	118	48+35+35
	17	0.005399667	0.005407222	116	115	75+40
	18	0.005433	0.005440556	117	118	48+35+35
	19	0.008044111	0.008031389	173	173	90+48+35
	20	0.007977444	0.007964722	172	173	90+48+35
	21	0.007944111	0.007931389	171	170	140+30
	22	0.007910778	0.007898056	170	170	140+30
	23	0.007977444	0.007964722	172	173	90+48+35
	24	0.007910778	0.007898056	170	170	140+30
	25	0.007944111	0.007931389	171	170	140+30
	26	0.007977444	0.007964722	172	173	90+48+35
	27	0.008044111	0.008031389	173	173	90+48+35
	28	0.007977444	0.007964722	172	173	90+48+35
	29	0.007944111	0.007931389	171	170	140+30
	30	0.007910778	0.007898056	170	170	140+30
	31	0.007977444	0.007964722	172	173	90+48+35
	32	0.007910778	0.007898056	170	170	140+30
	33	0.007944111	0.007931389	171	170	140+30
	34	0.007977444	0.007964722	172	173	90+48+35
Total	**-**	**0.221133111**	**0.221020556**	**4758**	**4760**	**4760**

Table XCI – Complementary data of Scenario I using $46.76P_{tx}$ @ T = 3600s.

	Mote m	**Calculated e_m (in mAh)**	**Simulated e_m (in mAh)**	**Calculated battery (in mAh)**	**Assigned battery (in mAh)**	**Battery Set (in mAh)**
	1	0.022305222	0.022305278	130	130	90+40
	2	0.022305222	0.022305278	130	130	90+40
	3	0.022305222	0.022305278	130	130	90+40
	4	0.022305222	0.022305278	130	130	90+40
	5	0.022305222	0.022305278	130	130	90+40
	6	0.022305222	0.022305278	130	130	90+40
	7	0.022866333	0.022873889	133	133	55+48+30
	8	0.022933	0.022940556	134	133	55+48+30
	9	0.022899667	0.022907222	134	133	55+48+30
	10	0.022933	0.022940556	134	133	55+48+30
	11	0.022899667	0.022907222	134	133	55+48+30
	12	0.022933	0.022940556	134	133	55+48+30
	13	0.022866333	0.022873889	133	133	55+48+30
	14	0.022933	0.022940556	134	133	55+48+30
	15	0.022899667	0.022907222	134	133	55+48+30
	16	0.022933	0.022940556	134	133	55+48+30
	17	0.022899667	0.022907222	134	133	55+48+30
	18	0.022933	0.022940556	134	133	55+48+30
	19	0.025544111	0.025531389	149	150	120+30
	20	0.025477444	0.025464722	149	150	120+30
	21	0.025444111	0.025431389	148	148	75+48+25
	22	0.025410778	0.025398056	148	148	75+48+25
	23	0.025477444	0.025464722	149	150	120+30
	24	0.025410778	0.025398056	148	148	75+48+25
	25	0.025444111	0.025431389	148	148	75+48+25
	26	0.025477444	0.025464722	149	150	120+30
	27	0.025544111	0.025531389	149	150	120+30
	28	0.025477444	0.025464722	149	148	75+48+25
	29	0.025444111	0.025431389	148	148	75+48+25
	30	0.025410778	0.025398056	148	148	75+48+25
	31	0.025477444	0.025464722	149	150	120+30
	32	0.025410778	0.025398056	148	148	75+48+25
	33	0.025444111	0.025431389	148	148	75+48+25
	34	0.025477444	0.025464722	149	150	120+30
Total	**-**	**0.816133111**	**0.816020556**	**4762**	**4758**	**4758**

Table XCII – Complementary data of Scenario I using $46.76P_{tx}$ @ $T = 86400$s.

	Mote m	Calculated e_m (in mAh)	Simulated e_m (in mAh)	Calculated battery (in mAh)	Assigned battery (in mAh)	Battery Set (in mAh)
	1	0.505305222	0.511984722	139.53	139.53	–
	2	0.505305222	0.507151389	139.53	139.53	–
	3	0.505305222	0.507148056	139.53	139.53	–
	4	0.505305222	0.507148056	139.53	139.53	–
	5	0.505305222	0.511930556	139.53	139.53	–
	6	0.505305222	0.511930556	139.53	139.53	–
	7	0.505866333	0.511071944	139.69	139.69	–
	8	0.505933	0.510831389	139.7	139.7	–
	9	0.505899667	0.506505278	139.7	139.7	–
	10	0.505933	0.506551944	139.7	139.7	–
	11	0.505899667	0.505473056	139.7	139.7	–
	12	0.505933	0.505520833	139.7	139.7	–
	13	0.505866333	0.506569722	139.69	139.69	–
	14	0.505933	0.511468056	139.7	139.7	–
	15	0.505899667	0.511665	139.7	139.7	–
	16	0.505933	0.509029167	139.7	139.7	–
	17	0.505899667	0.508991667	139.7	139.7	–
	18	0.505933	0.509023333	139.7	139.7	–
	19	0.508544111	0.508799167	140.43	140.43	–
	20	0.508477444	0.510113889	140.41	140.41	–
	21	0.508444111	0.509362778	140.4	140.4	–
	22	0.508410778	0.505996667	140.39	140.39	–
	23	0.508477444	0.506044167	140.41	140.41	–
	24	0.508410778	0.505105278	140.39	140.39	–
	25	0.508444111	0.505151944	140.4	140.4	–
	26	0.508477444	0.506124167	140.41	140.41	–
	27	0.508544111	0.506378889	140.43	140.43	–
	28	0.508477444	0.510200556	140.41	140.41	–
	29	0.508444111	0.5086875	140.4	140.4	–
	30	0.508410778	0.508649722	140.39	140.39	–
	31	0.508477444	0.508725	140.41	140.41	–
	32	0.508410778	0.508636667	140.39	140.39	–
	33	0.508444111	0.5086825	140.4	140.4	–
	34	0.508477444	0.508741389	140.41	140.41	–
Total	**-**	**17.238133111**	**17.285395**	**4760**	4760	–

Appendix D

COMPLEMENTARY DATA OF CHAPTER V: SCENARIO II USING P_{TX}

Table XCIII – Complementary data of Scenario II using P_{tx} @ T = 1s.

	Mote m	Calculated e_m (in mAh)	Simulated e_m (in mAh)	Calculated battery (in mAh)	Assigned battery (in mAh)	Battery Set (in mAh)
	1	0.001070778	0.001126389	119	118	48+40+30
	2	0.001588833	0.001710278	177	176	48+48+40+40
	3	0.0023555	0.002430278	262	260	200+30+30
	4	0.003123903	0.0033825	347	348	200+75+48+25
	5	0.002139528	0.002330556	238	238	165+48+25
	6	0.001154111	0.001209722	128	128	48+40+40
	7	0.000763833	0.000791667	85	85	55+30
	8	0.001084667	0.001133333	121	120	120
	9	0.001329806	0.001392222	148	148	75+48+25
	10	0.001885014	0.002004722	210	210	120+90
	11	0.003119736	0.003381111	347	348	200+75+48+25
	12	0.004416958	0.004905556	491	490	200+200+90
	13	0.002067653	0.00217	230	230	200+30
	14	0.001490222	0.001542222	166	166	48+48+35+35
	15	0.001016611	0.001051389	113	113	48+35+30
	16	0.001076333	0.001125	120	120	120
	17	0.000763833	0.000791667	85	85	55+30
	18	0.000788833	0.000816667	88	88	48+40
	19	0.000361056	0.000361111	40	40	40
	20	0.000549944	0.000563889	61	60	30+30
	21	0.000656889	0.000677778	73	73	48+25
	22	0.000683278	0.0007075	76	75	40+35
	23	0.001636403	0.001733611	182	180	120+30+30
	24	0.001166264	0.001228889	130	130	90+40
	25	0.001469389	0.001490278	163	163	55+30+30+48
	26	0.001167653	0.001181667	130	130	90+40
	27	0.000475639	0.000475556	53	55	55
	28	0.000679806	0.000700556	76	75	75
	29	0.000562444	0.000576389	63	65	35+30
	30	0.000386056	0.000386111	43	40	40
	31	0.000599944	0.000613889	67	65	35+30
	32	0.000361056	0.000361111	40	40	40
	33	0.000411056	0.000411111	46	48	48
	34	0.000411056	0.000411111	46	48	48
Total	**-**	**0.042814083**	**0.045175833**	**4764**	**4758**	**4758**

Table XCIV – Complementary data of Scenario II using P_{tx} @ T = 10s.

	Mote m	Calculated e_m (in mAh)	Simulated e_m (in mAh)	Calculated battery (in mAh)	Assigned battery (in mAh)	Battery Set (in mAh)
	1	0.001123278	0.001178889	120	120	120
	2	0.001641333	0.001763056	175	175	140+35
	3	0.002408	0.002482778	257	258	120+90+48
	4	0.003176403	0.003435278	339	340	200+140
	5	0.002192028	0.002383056	234	235	165+35+35
	6	0.001206611	0.001262222	129	128	48+40+40
	7	0.000816333	0.000844167	87	88	48+40
	8	0.001137167	0.001185833	121	120	120
	9	0.001382306	0.001445	148	148	75+48+25
	10	0.001937514	0.0020575	207	210	120+90
	11	0.003172236	0.003433611	339	340	200+140
	12	0.004469458	0.004958333	477	478	200+200+48+30
	13	0.002120153	0.002222778	226	225	200+25
	14	0.001542722	0.001595	165	165	165
	15	0.001069111	0.001103889	114	113	48+35+30
	16	0.001128833	0.0011775	120	120	120
	17	0.000816333	0.000844167	87	88	48+40
	18	0.000841333	0.000869167	90	90	90
	19	0.000413556	0.000413611	44	40	40
	20	0.000602444	0.000616389	64	65	40+25
	21	0.000709389	0.000730278	76	75	75
	22	0.000735778	0.00076	79	78	48+30
	23	0.001688903	0.001786111	180	180	140+40
	24	0.001218764	0.001281389	130	130	90+40
	25	0.001521889	0.001542778	162	160	120+40
	26	0.001220153	0.001234167	130	130	90+40
	27	0.000528139	0.000528056	56	55	55
	28	0.000732306	0.000753056	78	78	48+30
	29	0.000614944	0.000628889	66	65	35+30
	30	0.000438556	0.000438611	47	48	48
	31	0.000652444	0.000666389	70	70	35+35
	32	0.000413556	0.000413611	44	48	48
	33	0.000463556	0.000463611	49	48	48
	34	0.000463556	0.000463611	49	48	48
Total	**-**	**0.044599083**	**0.046962778**	**4759**	**4759**	**4759**

Table XCV – Complementary data of Scenario II using P_{tx} @ T = 60s.

	Mote m	**Calculated e_m (in mAh)**	**Simulated e_m (in mAh)**	**Calculated battery (in mAh)**	**Assigned battery (in mAh)**	**Battery Set (in mAh)**
	1	0.001414944	0.001470556	124	125	90+35
	2	0.001933	0.002054722	169	170	140+30
	3	0.002699667	0.002774444	236	236	140+48+48
	4	0.003468069	0.003726944	303	303	255+48
	5	0.002483694	0.002674722	217	218	140+48+30
	6	0.001498278	0.001553889	131	130	75+30+25
	7	0.001108	0.001135833	97	96	48+48
	8	0.001428833	0.0014775	125	125	75+25+25
	9	0.001673972	0.001736667	146	146	48+48+25+25
	10	0.002229181	0.002349167	195	195	140+55
	11	0.003463903	0.003725278	302	300	200+75+25
	12	0.004761125	0.00525	416	416	200+120+48+48
	13	0.002411819	0.002514444	211	210	120+90
	14	0.001834389	0.001886667	160	160	120+40
	15	0.001360778	0.001395556	119	120	120
	16	0.0014205	0.001469167	124	125	75+25+25
	17	0.001108	0.001135833	97	96	48+48
	18	0.001133	0.001160833	99	100	75+25
	19	0.000705222	0.000705278	62	60	30+30
	20	0.000894111	0.000908056	78	78	48+30
	21	0.001001056	0.001021944	87	88	48+40
	22	0.001027444	0.001051667	90	90	90
	23	0.001980569	0.002077778	173	173	90+48+35
	24	0.001510431	0.001573056	132	130	90+40
	25	0.001813556	0.001834444	158	158	75+48+35
	26	0.001511819	0.001525833	132	130	75+30+25
	27	0.000819806	0.000819722	72	70	35+35
	28	0.001023972	0.001044722	89	90	90
	29	0.000906611	0.000920556	79	80	40+40
	30	0.000730222	0.000730278	64	65	40+25
	31	0.000944111	0.000958056	82	80	40+40
	32	0.000705222	0.000705278	62	60	30+30
	33	0.000755222	0.000755278	66	65	40+25
	34	0.000755222	0.000755278	66	65	40+25
Total	**-**	**0.05451575**	**0.056879444**	**4763**	**4753**	**4753**

Table XCVI – Complementary data of Scenario II using P_{tx} @ T = 600s.

	Mote m	Calculated e_m (in mAh)	Simulated e_m (in mAh)	Calculated battery (in mAh)	Assigned battery (in mAh)	Battery Set (in mAh)
	1	0.004564944	0.004620556	134	135	75+35+25
	2	0.005083	0.005204444	150	150	120+30
	3	0.005849667	0.005924444	172	170	140+30
	4	0.006618069	0.006876667	195	195	165+30
	5	0.005633694	0.005824722	166	166	48+48+35+35
	6	0.004648278	0.004703889	137	136	48+48+40
	7	0.004258	0.004285833	125	125	90+35
	8	0.004578833	0.0046275	135	135	55+55+25
	9	0.004823972	0.004886389	142	140	140
	10	0.005379181	0.005498889	158	158	55+55+48
	11	0.006613903	0.006875278	195	195	140+55
	12	0.007911125	0.0084	233	233	120+48+35+30
	13	0.005561819	0.005664167	164	165	165
	14	0.004984389	0.005036389	147	145	120+25
	15	0.004510778	0.004545556	133	133	55+48+30
	16	0.0045705	0.004619167	135	135	75+35+25
	17	0.004258	0.004285833	125	125	90+35
	18	0.004283	0.004310833	126	125	90+35
	19	0.003855222	0.003855278	114	115	90+25
	20	0.004044111	0.004058056	119	120	120
	21	0.004151056	0.004171944	122	120	120
	22	0.004177444	0.004201667	123	125	90+35
	23	0.005130569	0.005227778	151	150	120+30
	24	0.004660431	0.004723056	137	138	90+48
	25	0.004963556	0.004984444	146	145	120+25
	26	0.004661819	0.004675833	137	138	90+48
	27	0.003969806	0.003969722	117	118	48+35+35
	28	0.004173972	0.004194722	123	123	75+48
	29	0.004056611	0.004070556	119	120	120
	30	0.003880222	0.003880278	114	115	90+25
	31	0.004094111	0.004108056	121	120	120
	32	0.003855222	0.003855278	114	115	90+25
	33	0.003905222	0.003905278	115	115	90+25
	34	0.003905222	0.003905278	115	115	90+25
Total	**-**	**0.16161575**	**0.163977778**	**4759**	**4758**	**4758**

Table XCVII – Complementary data of Scenario II using P_{tx} @ T = 3600s.

	Mote m	Calculated e_m (in mAh)	Simulated e_m (in mAh)	Calculated battery (in mAh)	Assigned battery (in mAh)	Battery Set (in mAh)
	1	0.022064944	0.022120556	139	140	140
	2	0.022583	0.022704722	142	140	140
	3	0.023349667	0.023424722	147	158	55+55+48
	4	0.024118069	0.024377222	152	150	120+30
	5	0.023133694	0.023325	146	145	120+25
	6	0.022148278	0.022203889	139	140	140
	7	0.021758	0.021785833	137	138	90+48
	8	0.022078833	0.0221275	139	140	140
	9	0.022323972	0.022386667	140	140	140
	10	0.022879181	0.022999167	144	145	120+25
	11	0.024113903	0.024375556	152	150	120+30
	12	0.025411125	0.025900556	160	160	120+40
	13	0.023061819	0.023164444	145	145	120+25
	14	0.022484389	0.022536667	141	140	140
	15	0.022010778	0.022045556	138	138	90+48
	16	0.0220705	0.022119167	139	138	90+48
	17	0.021758	0.021785833	137	138	90+48
	18	0.021783	0.021810833	137	138	90+48
	19	0.021355222	0.021355278	134	135	75+35+25
	20	0.021544111	0.021558056	136	135	75+35+25
	21	0.021651056	0.021671944	136	135	75+35+25
	22	0.021677444	0.021701944	136	135	75+35+25
	23	0.022630569	0.022728056	142	140	140
	24	0.022160431	0.022223056	139	138	90+48
	25	0.022463556	0.022484444	141	140	140
	26	0.022161819	0.022175833	139	138	90+48
	27	0.021469806	0.02147	135	135	75+35+25
	28	0.021673972	0.021695	136	135	75+35+25
	29	0.021556611	0.021570556	136	135	75+35+25
	30	0.021380222	0.021380278	135	135	75+35+25
	31	0.021594111	0.021608056	136	135	75+35+25
	32	0.021355222	0.021355278	134	135	75+35+25
	33	0.021405222	0.021405278	135	135	75+35+25
	34	0.021405222	0.021405278	135	135	75+35+25
Total	**-**	**0.75661575**	**0.758982222**	**4759**	**4759**	**4759**

Table XCVIII – Complementary data of Scenario II using P_{tx} @ T = 86400s.

	Mote m	Calculated e_m (in mAh)	Simulated e_m (in mAh)	Calculated battery (in mAh)	Assigned battery (in mAh)	Battery Set (in mAh)
	1	0.505064944	0.505124167	139.95	140	140
	2	0.505583	0.505710556	140.09	140	140
	3	0.506349667	0.506432778	140.3	140	140
	4	0.507118069	0.507388333	140.52	143	55+48+40
	5	0.506133694	0.506332778	140.24	140	140
	6	0.505148278	0.505207778	139.97	140	140
	7	0.504758	0.504788333	139.86	140	140
	8	0.505078833	0.505131111	139.95	140	140
	9	0.505323972	0.505391111	140.02	140	140
	10	0.505879181	0.506006111	140.17	140	140
	11	0.507113903	0.507386944	140.52	143	55+48+40
	12	0.508411125	0.508916111	140.87	143	55+48+40
	13	0.506061819	0.506170833	140.22	140	140
	14	0.505484389	0.505541111	140.06	140	140
	15	0.505010778	0.505048889	139.93	140	140
	16	0.5050705	0.505122778	139.95	140	140
	17	0.504758	0.504788333	139.86	140	140
	18	0.504783	0.504813333	139.87	140	140
	19	0.504355222	0.504356389	139.75	140	140
	20	0.504544111	0.504559722	139.8	140	140
	21	0.504651056	0.504674167	139.83	140	140
	22	0.504677444	0.504703611	139.84	140	140
	23	0.505630569	0.505732778	140.1	140	140
	24	0.505160431	0.505226111	139.97	140	140
	25	0.505463556	0.505489167	140.06	140	140
	26	0.505161819	0.505179444	139.97	140	140
	27	0.504469806	0.504471389	139.78	138	90+48
	28	0.504673972	0.504696944	139.84	140	140
	29	0.504556611	0.504572222	139.81	138	90+48
	30	0.504380222	0.504381389	139.76	138	90+48
	31	0.504594111	0.50461	139.82	140	140
	32	0.504355222	0.504356389	139.75	138	90+48
	33	0.504405222	0.504406667	139.76	138	90+48
	34	0.504405222	0.504406667	139.76	138	90+48
Total	**-**	**17.17861575**	**17.181124444**	**4760**	**4757**	**4757**

Appendix E

COMPLEMENTARY DATA OF CHAPTER V: SCENARIO II USING $11.31P_{TX}$

Table XCIX – Complementary data of Scenario II using $11.31P_{tx}$ @ T = 1s.

	Mote m	Calculated e_m (in mAh)	Simulated e_m (in mAh)	Calculated battery (in mAh)	Assigned battery (in mAh)	Battery Set (in mAh)
	1	0.007926975	0.007905556	252	253	165+48+40
	2	0.003123514	0.003136667	99	100	75+25
	3	0.003123514	0.003136667	99	100	75+25
	4	0.003123514	0.003136389	99	100	75+25
	5	0.007926975	0.007904444	252	253	165+48+40
	6	0.007926975	0.007904167	252	253	165+48+40
	7	0.007068499	0.007047778	225	225	200+25
	8	0.00682976	0.006810278	217	215	165+25+25
	9	0.002502088	0.002511667	80	80	40+40
	10	0.002548901	0.002558611	81	80	40+40
	11	0.001476646	0.001476667	47	48	48
	12	0.0015241	0.001524167	49	48	48
	13	0.002562283	0.002572778	82	80	40+40
	14	0.007503022	0.007481111	239	240	200+40
	15	0.00770198	0.007679167	245	245	200+45
	16	0.005037805	0.005024722	160	160	120+40
	17	0.005000153	0.004986944	159	160	120+40
	18	0.005031817	0.005018611	160	160	120+40
	19	0.004807345	0.004794167	153	155	120+35
	20	0.006160428	0.006142222	196	195	165+30
	21	0.005387121	0.005371667	172	170	140+30
	22	0.001990725	0.001999167	63	65	35+30
	23	0.002037501	0.002045278	65	65	35+30
	24	0.001108112	0.001108056	35	35	35
	25	0.001154926	0.001155	37	35	35
	26	0.002118593	0.002126944	67	65	35+30
	27	0.002377713	0.002387778	76	75	40+35
	28	0.006249686	0.006230556	199	200	200
	29	0.004696034	0.004683056	150	150	120+30
	30	0.004658382	0.004645278	148	150	120+30
	31	0.004733313	0.004720278	151	150	120+30
	32	0.004644148	0.004631111	148	150	120+30
	33	0.004690337	0.004677222	149	150	120+30
	34	0.004749539	0.004736389	151	150	120+30
Total	**-**	**0.149502426**	**0.149270556**	**4757**	**4760**	**4760**

Table C – Complementary data of Scenario II using 11.31P_{tx} @ T = 10s.

	Mote m	Calculated e_m (in mAh)	Simulated e_m (in mAh)	Calculated battery (in mAh)	Assigned battery (in mAh)	Battery Set (in mAh)
	1	0.007979475	0.007958333	251	250	200+25+25
	2	0.003176014	0.003189167	100	100	75+25
	3	0.003176014	0.003189167	100	100	75+25
	4	0.003176014	0.003189167	100	100	75+25
	5	0.007979475	0.007957222	251	250	200+25+25
	6	0.007979475	0.007957222	251	250	200+25+25
	7	0.007120999	0.007101111	224	225	200+25
	8	0.00688226	0.006863056	217	215	165+25+25
	9	0.002554588	0.002564444	80	80	40+40
	10	0.002601401	0.002611111	82	83	48+35
	11	0.001529146	0.001529167	48	48	48
	12	0.0015766	0.001576667	50	48	48
	13	0.002614783	0.002625278	82	80	40+40
	14	0.007555522	0.007533611	238	240	200+40
	15	0.00775448	0.007731667	244	245	200+45
	16	0.005090305	0.0050775	160	160	120+40
	17	0.005052653	0.005039722	159	160	120+40
	18	0.005084317	0.005071389	160	160	120+40
	19	0.004859845	0.004846944	153	155	120+35
	20	0.006212928	0.006194722	195	195	165+30
	21	0.005439621	0.005424167	171	170	140+30
	22	0.002043225	0.002051667	64	65	35+30
	23	0.002090001	0.002098056	66	65	35+30
	24	0.001160612	0.001160833	37	35	35
	25	0.001207426	0.0012075	38	40	40
	26	0.002171093	0.002179722	68	65	35+30
	27	0.002430213	0.002440278	76	75	40+35
	28	0.006302186	0.006283611	198	200	200
	29	0.004748534	0.004735556	149	150	120+30
	30	0.004710882	0.004698056	148	150	120+30
	31	0.004785813	0.004773056	151	150	120+30
	32	0.004696648	0.004683889	148	150	120+30
	33	0.004742837	0.00473	149	150	120+30
	34	0.004802039	0.004789167	151	150	120+30
Total	**-**	**0.151287426**	**0.151062222**	**4759**	**4759**	**4759**

Table CI – Complementary data of Scenario II using $11.31P_{tx}$ @ T = 60s.

	Mote m	Calculated e_m (in mAh)	Simulated e_m (in mAh)	Calculated battery (in mAh)	Assigned battery (in mAh)	Battery Set (in mAh)
	1	0.008271142	0.008250278	244	245	165+55+25
	2	0.003467681	0.003481111	102	100	75+25
	3	0.003467681	0.003481111	102	100	75+25
	4	0.003467681	0.003480833	102	100	75+25
	5	0.008271142	0.008248889	244	245	165+55+25
	6	0.008271142	0.008248889	244	245	165+55+25
	7	0.007412666	0.0073925	219	220	165+55
	8	0.007173926	0.007154722	212	213	165+48
	9	0.002846254	0.002856111	84	85	55+30
	10	0.002893068	0.002902778	85	85	55+30
	11	0.001820813	0.001820833	54	55	55
	12	0.001868266	0.001868333	55	55	55
	13	0.002906449	0.002916944	86	85	55+30
	14	0.007847189	0.007825556	232	230	200+30
	15	0.008046147	0.008023333	238	238	165+38+35
	16	0.005381971	0.005369167	159	160	120+40
	17	0.00534432	0.005331389	158	160	120+40
	18	0.005375983	0.005363056	159	160	120+40
	19	0.005151512	0.005138611	152	150	120+30
	20	0.006504595	0.006486111	192	190	165+25
	21	0.005731288	0.005715833	169	168	120+48
	22	0.002334891	0.002343333	69	70	40+30
	23	0.002381667	0.002389722	70	70	40+30
	24	0.001452279	0.0014525	43	45	45
	25	0.001499092	0.001499167	44	45	45
	26	0.00246276	0.002471389	73	73	48+25
	27	0.00272188	0.002731944	80	80	55+25
	28	0.006593853	0.006575278	195	195	165+30
	29	0.005040201	0.0050275	149	148	75+48+25
	30	0.005002549	0.004989722	148	148	75+48+25
	31	0.00507748	0.005064722	150	150	120+30
	32	0.004988315	0.004975556	147	148	75+48+25
	33	0.005034503	0.005021667	149	148	75+48+25
	34	0.005093705	0.005080833	150	150	120+30
Total	**-**	**0.161204092**	**0.160979722**	**4759**	**4759**	**4759**

Table CII – Complementary data of Scenario II using 11.31P_{tx} @ T = 600s.

	Mote m	**Calculated e_m (in mAh)**	**Simulated e_m (in mAh)**	**Calculated battery (in mAh)**	**Assigned battery (in mAh)**	**Battery Set (in mAh)**
	1	0.011421142	0.011401111	203	203	120+48+35
	2	0.006617681	0.006631111	117	118	48+35+35
	3	0.006617681	0.006631111	117	118	48+35+35
	4	0.006617681	0.006631111	117	118	48+35+35
	5	0.011421142	0.011400278	203	203	120+48+35
	6	0.011421142	0.011399167	203	203	120+48+35
	7	0.010562666	0.010542778	187	188	140+48
	8	0.010323926	0.010304722	183	183	55+48+40+40
	9	0.005996254	0.006006111	106	105	75+30
	10	0.006043068	0.006052778	107	105	75+30
	11	0.004970813	0.004970833	88	88	48+40
	12	0.005018266	0.005018333	89	88	48+40
	13	0.006056449	0.006066944	107	108	48+30+30
	14	0.010997189	0.010975278	195	195	140+55
	15	0.011196147	0.011173056	199	200	200
	16	0.008531971	0.008519167	151	150	120+30
	17	0.00849432	0.008481667	151	150	120+30
	18	0.008525983	0.008513333	151	150	120+30
	19	0.008301512	0.008288889	147	148	75+48+25
	20	0.009654595	0.009636389	171	170	140+30
	21	0.008881288	0.008865833	158	158	55+55+48
	22	0.005484891	0.005493333	97	96	48+48
	23	0.005531667	0.005539722	98	98	48+25+25
	24	0.004602279	0.0046025	82	83	48+35
	25	0.004649092	0.004649167	82	83	48+35
	26	0.00561276	0.005621389	100	100	75+25
	27	0.00587188	0.005881944	104	103	55+48
	28	0.009743853	0.009725278	173	173	75+48+25+25
	29	0.008190201	0.0081775	145	145	120+25
	30	0.008152549	0.00814	145	145	120+25
	31	0.00822748	0.008214722	146	146	48+48+25+25
	32	0.008138315	0.008125556	144	145	120+25
	33	0.008184503	0.008171944	145	145	120+25
	34	0.008243705	0.008231111	146	146	48+48+25+25
Total	**-**	**0.268304092**	**0.268084167**	**4757**	**4757**	**4757**

Table CIII – Complementary data of Scenario II using $11.31P_{tx}$ @ T = 3600s.

	Mote m	Calculated e_m (in mAh)	Simulated e_m (in mAh)	Calculated battery (in mAh)	Assigned battery (in mAh)	Battery Set (in mAh)
	1	0.028921142	0.028903056	159	160	120+40
	2	0.024117681	0.024131667	133	133	55+48+30
	3	0.024117681	0.024131667	133	133	55+48+30
	4	0.024117681	0.024131667	133	133	55+48+30
	5	0.028921142	0.028901389	159	160	120+40
	6	0.028921142	0.0289	159	160	120+40
	7	0.028062666	0.028043056	155	155	120+35
	8	0.027823926	0.027805	153	155	120+35
	9	0.023496254	0.023506389	130	130	90+40
	10	0.023543068	0.023553333	130	130	90+40
	11	0.022470813	0.022471111	124	125	90+35
	12	0.022518266	0.022518611	124	125	90+35
	13	0.023556449	0.0235675	130	130	90+40
	14	0.028497189	0.028476667	157	158	55+55+48
	15	0.028696147	0.028672778	158	158	55+55+48
	16	0.026031971	0.02602	144	145	90+55
	17	0.02599432	0.025982222	143	143	55+48+40
	18	0.026025983	0.026013889	143	143	55+48+40
	19	0.025801512	0.025789444	142	143	55+48+40
	20	0.027154595	0.0271375	150	150	120+30
	21	0.026381288	0.026366111	145	145	90+55
	22	0.022984891	0.022993611	127	128	48+40+40
	23	0.023031667	0.02304	127	128	48+40+40
	24	0.022102279	0.0221025	122	120	120
	25	0.022149092	0.022149444	122	120	120
	26	0.02311276	0.023121389	127	128	48+40+40
	27	0.02337188	0.023381944	129	128	48+40+40
	28	0.027243853	0.027225	150	150	120+30
	29	0.025690201	0.025678056	142	140	140
	30	0.025652549	0.025640556	141	140	140
	31	0.02572748	0.025715278	142	140	140
	32	0.025638315	0.025626111	141	140	140
	33	0.025684503	0.0256725	142	140	140
	34	0.025743705	0.025731667	142	140	140
Total	**-**	**0.863304092**	**0.863101111**	**4758**	**4758**	**4758**

Table CIV – Complementary data of Scenario II using 11.31P_{tx} @ T = 86400s.

	Mote m	**Calculated e_m (in mAh)**	**Simulated e_m (in mAh)**	**Calculated battery (in mAh)**	**Assigned battery (in mAh)**	**Battery Set (in mAh)**
	1	0.511921142	0.511984722	141	140	140
	2	0.507117681	0.507151389	140	140	140
	3	0.507117681	0.507148056	140	140	140
	4	0.507117681	0.507148056	140	140	140
	5	0.511921142	0.511930556	142	143	55+48+40
	6	0.511921142	0.511930556	142	143	55+48+40
	7	0.511062666	0.511071944	141	140	140
	8	0.510823926	0.510831389	141	140	140
	9	0.506496254	0.506505278	139	140	140
	10	0.506543068	0.506551944	139	140	140
	11	0.505470813	0.505473056	139	140	140
	12	0.505518266	0.505520833	139	140	140
	13	0.506556449	0.506569722	139	140	140
	14	0.511497189	0.511468056	141	140	140
	15	0.511696147	0.511665	141	140	140
	16	0.509031971	0.509029167	140	140	140
	17	0.50899432	0.508991667	140	140	140
	18	0.509025983	0.509023333	140	140	140
	19	0.508801512	0.508799167	140	140	140
	20	0.510154595	0.510113889	140	140	140
	21	0.509381288	0.509362778	140	140	140
	22	0.505984891	0.505996667	139	140	140
	23	0.506031667	0.506044167	139	140	140
	24	0.505102279	0.505105278	139	138	90+48
	25	0.505149092	0.505151944	139	138	90+48
	26	0.50611276	0.506124167	139	138	90+48
	27	0.50637188	0.506378889	139	138	90+48
	28	0.510243853	0.510200556	141	140	140
	29	0.508690201	0.5086875	140	140	140
	30	0.508652549	0.508649722	140	140	140
	31	0.50872748	0.508725	140	140	140
	32	0.508638315	0.508636667	140	140	140
	33	0.508684503	0.5086825	140	140	140
	34	0.508743705	0.508741389	140	140	140
Total	**-**	**17.285304092**	**17.285395**	**4759**	**4758**	**4758**

Appendix F

COMPLEMENTARY DATA OF CHAPTER V: SCENARIO II USING $46.76P_{TX}$

Table CV – Complementary data of Scenario II using $46.76P_{tx}$ @ T = 1s.

	Mote m	**Calculated e_m (in mAh)**	**Simulated e_m (in mAh)**	**Calculated battery (in mAh)**	**Assigned battery (in mAh)**	**Battery Set (in mAh)**
	1	0.007926975	0.007905556	252	253	165+48+40
	2	0.003123514	0.003136667	99	100	75+25
	3	0.003123514	0.003136667	99	100	75+25
	4	0.003123514	0.003136389	99	100	75+25
	5	0.007926975	0.007904444	252	253	165+48+40
	6	0.007926975	0.007904167	252	253	165+48+40
	7	0.007068499	0.007047778	225	225	200+25
	8	0.00682976	0.006810278	217	215	165+25+25
	9	0.002502088	0.002511667	80	80	40+40
	10	0.002548901	0.002558611	81	80	40+40
	11	0.001476646	0.001476667	47	48	48
	12	0.0015241	0.001524167	49	48	48
	13	0.002562283	0.002572778	82	80	40+40
	14	0.007503022	0.007481111	239	240	200+40
	15	0.00770198	0.007679167	245	245	200+45
	16	0.005037805	0.005024722	160	160	120+40
	17	0.005000153	0.004986944	159	160	120+40
	18	0.005031817	0.005018611	160	160	120+40
	19	0.004807345	0.004794167	153	155	120+35
	20	0.006160428	0.006142222	196	195	165+30
	21	0.005387121	0.005371667	172	170	140+30
	22	0.001990725	0.001999167	63	65	35+30
	23	0.002037501	0.002045278	65	65	35+30
	24	0.001108112	0.001108056	35	35	35
	25	0.001154926	0.001155	37	35	35
	26	0.002118593	0.002126944	67	65	35+30
	27	0.002377713	0.002387778	76	75	40+35
	28	0.006249686	0.006230556	199	200	200
	29	0.004696034	0.004683056	150	150	120+30
	30	0.004658382	0.004645278	148	150	120+30
	31	0.004733313	0.004720278	151	150	120+30
	32	0.004644148	0.004631111	148	150	120+30
	33	0.004690337	0.004677222	149	150	120+30
	34	0.004749539	0.004736389	151	150	120+30
Total	**-**	**0.149502426**	**0.149270556**	**4757**	**4760**	**4760**

Table CVI – Complementary data of Scenario II using $46.76P_{tx}$ @ T = 10s.

	Mote m	Calculated e_m (in mAh)	Simulated e_m (in mAh)	Calculated battery (in mAh)	Assigned battery (in mAh)	Battery Set (in mAh)
	1	0.007979475	0.007958333	251	250	200+25+25
	2	0.003176014	0.003189167	100	100	75+25
	3	0.003176014	0.003189167	100	100	75+25
	4	0.003176014	0.003189167	100	100	75+25
	5	0.007979475	0.007957222	251	250	200+25+25
	6	0.007979475	0.007957222	251	250	200+25+25
	7	0.007120999	0.007101111	224	225	200+25
	8	0.00688226	0.006863056	217	215	165+25+25
	9	0.002554588	0.002564444	80	80	40+40
	10	0.002601401	0.002611111	82	83	48+35
	11	0.001529146	0.001529167	48	48	48
	12	0.0015766	0.001576667	50	48	48
	13	0.002614783	0.002625278	82	80	40+40
	14	0.007555522	0.007533611	238	240	200+40
	15	0.00775448	0.007731667	244	245	200+45
	16	0.005090305	0.0050775	160	160	120+40
	17	0.005052653	0.005039722	159	160	120+40
	18	0.005084317	0.005071389	160	160	120+40
	19	0.004859845	0.004846944	153	155	120+35
	20	0.006212928	0.006194722	195	195	165+30
	21	0.005439621	0.005424167	171	170	140+30
	22	0.002043225	0.002051667	64	65	35+30
	23	0.002090001	0.002098056	66	65	35+30
	24	0.001160612	0.001160833	37	35	35
	25	0.001207426	0.0012075	38	40	40
	26	0.002171093	0.002179722	68	65	35+30
	27	0.002430213	0.002440278	76	75	40+35
	28	0.006302186	0.006283611	198	200	200
	29	0.004748534	0.004735556	149	150	120+30
	30	0.004710882	0.004698056	148	150	120+30
	31	0.004785813	0.004773056	151	150	120+30
	32	0.004696648	0.004683889	148	150	120+30
	33	0.004742837	0.00473	149	150	120+30
	34	0.004802039	0.004789167	151	150	120+30
Total	**-**	**0.151287426**	**0.151062222**	**4759**	**4759**	**4759**

Table CVII – Complementary data of Scenario II using 46.76P_{tx} @ T = 60s.

	Mote m	Calculated e_m (in mAh)	Simulated e_m (in mAh)	Calculated battery (in mAh)	Assigned battery (in mAh)	Battery Set (in mAh)
	1	0.008271142	0.008250278	244	245	165+55+25
	2	0.003467681	0.003481111	102	100	75+25
	3	0.003467681	0.003481111	102	100	75+25
	4	0.003467681	0.003480833	102	100	75+25
	5	0.008271142	0.008248889	244	245	165+55+25
	6	0.008271142	0.008248889	244	245	165+55+25
	7	0.007412666	0.0073925	219	220	165+55
	8	0.007173926	0.007154722	212	213	165+48
	9	0.002846254	0.002856111	84	85	55+30
	10	0.002893068	0.002902778	85	85	55+30
	11	0.001820813	0.001820833	54	55	55
	12	0.001868266	0.001868333	55	55	55
	13	0.002906449	0.002916944	86	85	55+30
	14	0.007847189	0.007825556	232	230	200+30
	15	0.008046147	0.008023333	238	238	165+38+35
	16	0.005381971	0.005369167	159	160	120+40
	17	0.00534432	0.005331389	158	160	120+40
	18	0.005375983	0.005363056	159	160	120+40
	19	0.005151512	0.005138611	152	150	120+30
	20	0.006504595	0.006486111	192	190	165+25
	21	0.005731288	0.005715833	169	168	120+48
	22	0.002334891	0.002343333	69	70	40+30
	23	0.002381667	0.002389722	70	70	40+30
	24	0.001452279	0.0014525	43	45	45
	25	0.001499092	0.001499167	44	45	45
	26	0.00246276	0.002471389	73	73	48+25
	27	0.00272188	0.002731944	80	80	55+25
	28	0.006593853	0.006575278	195	195	165+30
	29	0.005040201	0.0050275	149	148	75+48+25
	30	0.005002549	0.004989722	148	148	75+48+25
	31	0.00507748	0.005064722	150	150	120+30
	32	0.004988315	0.004975556	147	148	75+48+25
	33	0.005034503	0.005021667	149	148	75+48+25
	34	0.005093705	0.005080833	150	150	120+30
Total	**-**	**0.161204092**	**0.160979722**	**4759**	**4759**	**4759**

Table CVIII – Complementary data of Scenario II using $46.76P_{tx}$ @ T = 600s.

	Mote m	**Calculated e_m (in mAh)**	**Simulated e_m (in mAh)**	**Calculated battery (in mAh)**	**Assigned battery (in mAh)**	**Battery Set (in mAh)**
	1	0.011421142	0.011401111	203	203	120+48+35
	2	0.006617681	0.006631111	117	118	48+35+35
	3	0.006617681	0.006631111	117	118	48+35+35
	4	0.006617681	0.006631111	117	118	48+35+35
	5	0.011421142	0.011400278	203	203	120+48+35
	6	0.011421142	0.011399167	203	203	120+48+35
	7	0.010562666	0.010542778	187	188	140+48
	8	0.010323926	0.010304722	183	183	55+48+40+40
	9	0.005996254	0.006006111	106	105	75+30
	10	0.006043068	0.006052778	107	105	75+30
	11	0.004970813	0.004970833	88	88	48+40
	12	0.005018266	0.005018333	89	88	48+40
	13	0.006056449	0.006066944	107	108	48+30+30
	14	0.010997189	0.010975278	195	195	140+55
	15	0.011196147	0.011173056	199	200	200
	16	0.008531971	0.008519167	151	150	120+30
	17	0.00849432	0.008481667	151	150	120+30
	18	0.008525983	0.008513333	151	150	120+30
	19	0.008301512	0.008288889	147	148	75+48+25
	20	0.009654595	0.009636389	171	170	140+30
	21	0.008881288	0.008865833	158	158	55+55+48
	22	0.005484891	0.005493333	97	96	48+48
	23	0.005531667	0.005539722	98	98	48+25+25
	24	0.004602279	0.0046025	82	83	48+35
	25	0.004649092	0.004649167	82	83	48+35
	26	0.00561276	0.005621389	100	100	75+25
	27	0.00587188	0.005881944	104	103	55+48
	28	0.009743853	0.009725278	173	173	75+48+25+25
	29	0.008190201	0.0081775	145	145	120+25
	30	0.008152549	0.00814	145	145	120+25
	31	0.00822748	0.008214722	146	146	48+48+25+25
	32	0.008138315	0.008125556	144	145	120+25
	33	0.008184503	0.008171944	145	145	120+25
	34	0.008243705	0.008231111	146	146	48+48+25+25
Total	**-**	**0.268304092**	**0.268084167**	**4757**	**4757**	**4757**

Table CIX – Complementary data of Scenario II using $46.76P_{tx}$ @ T = 3600s.

	Mote m	Calculated e_m (in mAh)	Simulated e_m (in mAh)	Calculated battery (in mAh)	Assigned battery (in mAh)	Battery Set (in mAh)
	1	0.028921142	0.028903056	159	160	120+40
	2	0.024117681	0.024131667	133	133	55+48+30
	3	0.024117681	0.024131667	133	133	55+48+30
	4	0.024117681	0.024131667	133	133	55+48+30
	5	0.028921142	0.028901389	159	160	120+40
	6	0.028921142	0.0289	159	160	120+40
	7	0.028062666	0.028043056	155	155	120+35
	8	0.027823926	0.027805	153	155	120+35
	9	0.023496254	0.023506389	130	130	90+40
	10	0.023543068	0.023553333	130	130	90+40
	11	0.022470813	0.022471111	124	125	90+35
	12	0.022518266	0.022518611	124	125	90+35
	13	0.023556449	0.0235675	130	130	90+40
	14	0.028497189	0.028476667	157	158	55+55+48
	15	0.028696147	0.028672778	158	158	55+55+48
	16	0.026031971	0.02602	144	145	90+55
	17	0.02599432	0.025982222	143	143	55+48+40
	18	0.026025983	0.026013889	143	143	55+48+40
	19	0.025801512	0.025789444	142	143	55+48+40
	20	0.027154595	0.0271375	150	150	120+30
	21	0.026381288	0.026366111	145	145	90+55
	22	0.022984891	0.022993611	127	128	48+40+40
	23	0.023031667	0.02304	127	128	48+40+40
	24	0.022102279	0.0221025	122	120	120
	25	0.022149092	0.022149444	122	120	120
	26	0.02311276	0.023121389	127	128	48+40+40
	27	0.02337188	0.023381944	129	128	48+40+40
	28	0.027243853	0.027225	150	150	120+30
	29	0.025690201	0.025678056	142	140	140
	30	0.025652549	0.025640556	141	140	140
	31	0.02572748	0.025715278	142	140	140
	32	0.025638315	0.025626111	141	140	140
	33	0.025684503	0.0256725	142	140	140
	34	0.025743705	0.025731667	142	140	140
Total	**-**	**0.863304092**	**0.863101111**	**4758**	**4756**	**4756**

Table CX – Complementary data of Scenario II using $46.76P_{tx}$ @ T = 86400s.

	Mote m	Calculated e_m (in mAh)	Simulated e_m (in mAh)	Calculated battery (in mAh)	Assigned battery (in mAh)	Battery Set (in mAh)
	1	0.511921142	0.511984722	141	140	140
	2	0.507117681	0.507151389	140	140	140
	3	0.507117681	0.507148056	140	140	140
	4	0.507117681	0.507148056	140	140	140
	5	0.511921142	0.511930556	142	143	55+48+40
	6	0.511921142	0.511930556	142	143	55+48+40
	7	0.511062666	0.511071944	141	140	140
	8	0.510823926	0.510831389	141	140	140
	9	0.506496254	0.506505278	139	140	140
	10	0.506543068	0.506551944	139	140	140
	11	0.505470813	0.505473056	139	140	140
	12	0.505518266	0.505520833	139	140	140
	13	0.506556449	0.506569722	139	140	140
	14	0.511497189	0.511468056	141	140	140
	15	0.511696147	0.511665	141	140	140
	16	0.509031971	0.509029167	140	140	140
	17	0.50899432	0.508991667	140	140	140
	18	0.509025983	0.509023333	140	140	140
	19	0.508801512	0.508799167	140	140	140
	20	0.510154595	0.510113889	140	140	140
	21	0.509381288	0.509362778	140	140	140
	22	0.505984891	0.505996667	139	140	140
	23	0.506031667	0.506044167	139	140	140
	24	0.505102279	0.505105278	139	138	90+48
	25	0.505149092	0.505151944	139	138	90+48
	26	0.50611276	0.506124167	139	138	90+48
	27	0.50637188	0.506378889	139	138	90+48
	28	0.510243853	0.510200556	141	140	140
	29	0.508690201	0.5086875	140	140	140
	30	0.508652549	0.508649722	140	140	140
	31	0.50872748	0.508725	140	140	140
	32	0.508638315	0.508636667	140	140	140
	33	0.508684503	0.5086825	140	140	140
	34	0.508743705	0.508741389	140	140	140
Total	**-**	**17.285304092**	**17.285395**	**4759**	4758	4758

Appendix G

COMPLEMENTARY DATA OF CHAPTER V: SCENARIO III USING P_{TX}

Table CXI – Complementary data of Scenario III using P_{tx} @ T = 1s.

	Mote m	**Calculated e_m (in mAh)**	**Simulated e_m (in mAh)**	**Calculated battery (in mAh)**	**Assigned battery (in mAh)**	**Battery Set (in mAh)**
	1	0.000796241	0.000796389	78	78	48+30
	2	0.000966148	0.000966111	95	95	55+40
	3	0.00129111	0.001291111	127	128	48+40+40
	4	0.002725986	0.002726111	269	268	165+55+48
	5	0.002017306	0.002017222	199	200	200
	6	0.00098837	0.000988333	97	96	48+48
	7	0.000945315	0.000945278	93	95	55+40
	8	0.001579111	0.001579167	156	146	48+48+25+25
	9	0.002240531	0.002240556	221	220	165+55
	10	0.001171086	0.001171111	115	115	90+25
	11	0.002566804	0.002566944	253	253	165+48+40
	12	0.003792807	0.003792778	374	375	255+120
	13	0.001759435	0.001759444	173	173	75+48+25+25
	14	0.001411056	0.001411111	139	138	90+48
	15	0.000997167	0.000997222	98	98	48+25+25
	16	0.001025407	0.001025556	101	100	75+25
	17	0.000695315	0.000695278	69	70	35+35
	18	0.000645315	0.000645278	64	65	35+30
	19	0.000399944	0.0004	39	40	40
	20	0.000666611	0.000666667	66	65	35+30
	21	0.00090087	0.000900833	89	88	48+40
	22	0.001074481	0.001074444	106	105	55+25+25
	23	0.003022167	0.003022222	298	298	200+48+25+25
	24	0.003645932	0.003645833	359	358	200+55+55+48
	25	0.004752105	0.004752222	468	468	200+120+75+48+25
	26	0.002124597	0.002124722	209	210	140+35+35
	27	0.000686403	0.000686389	68	70	35+35
	28	0.000663139	0.000663056	65	65	35+30
	29	0.000562444	0.0005625	55	55	55
	30	0.000386056	0.000386111	38	40	40
	31	0.000591611	0.000591667	58	60	30+30
	32	0.0003555	0.000355556	35	35	35
	33	0.000394389	0.000394444	39	40	40
	34	0.00047587	0.000475833	47	48	48
Total	**-**	**0.048316629**	**0.0483175**	**4760**	**4758**	**4758**

Table CXII – Complementary data of Scenario III using P_{tx} @ T = 10s.

	Mote m	Calculated e_m (in mAh)	Simulated e_m (in mAh)	Calculated battery (in mAh)	Assigned battery (in mAh)	Battery Set (in mAh)
	1	0.000848741	0.000848889	81	80	40+40
	2	0.001018648	0.001018611	97	98	48+25+25
	3	0.00134361	0.001343611	128	128	48+40+40
	4	0.002778486	0.002778611	264	265	200+35+30
	5	0.002069806	0.00207	197	198	120+48+30
	6	0.00104087	0.001040833	99	100	75+25
	7	0.000997815	0.000997778	95	95	55+40
	8	0.001631611	0.001631667	155	155	120+35
	9	0.002293031	0.002293056	218	218	140+48+30
	10	0.001223586	0.001223611	116	115	90+25
	11	0.002619304	0.002619444	249	248	200+48
	12	0.003845307	0.003845556	365	365	200+165
	13	0.001811935	0.001811944	172	170	140+30
	14	0.001463556	0.001463611	139	140	140
	15	0.001049667	0.001049722	100	100	75+25
	16	0.001077907	0.001078056	102	103	55+48
	17	0.000747815	0.000747778	71	70	35+35
	18	0.000697815	0.000697778	66	65	35+30
	19	0.000452444	0.0004525	43	40	40
	20	0.000719111	0.000719167	68	70	35+35
	21	0.00095337	0.000953333	91	90	90
	22	0.001126981	0.001126944	107	108	48+30+30
	23	0.003074667	0.003074722	292	290	200+90
	24	0.003698432	0.003698611	351	350	200+75+75
	25	0.004804605	0.004804722	456	455	255+200
	26	0.002177097	0.002177222	207	206	55+55+48+48
	27	0.000738903	0.000738889	70	70	35+35
	28	0.000715639	0.000715556	68	70	35+35
	29	0.000614944	0.000615	58	60	30+30
	30	0.000438556	0.000438611	42	40	40
	31	0.000644111	0.000644167	61	60	30+30
	32	0.000408	0.000408056	39	40	40
	33	0.000446889	0.000446944	42	40	40
	34	0.00052837	0.000528333	50	50	25+25
Total	**-**	**0.050101629**	**0.050103333**	**4759**	**4752**	**4752**

Table CXIII – Complementary data of Scenario III using P_{tx} @ T = 60s.

	Mote m	Calculated e_m (in mAh)	Simulated e_m (in mAh)	Calculated battery (in mAh)	Assigned battery (in mAh)	Battery Set (in mAh)
	1	0.001140407	0.001140556	90	90	90
	2	0.001310315	0.001310278	104	105	75+30
	3	0.001635276	0.001635278	130	130	90+40
	4	0.003070153	0.003070278	243	243	140+55+48
	5	0.002361472	0.002361389	187	186	90+48+48
	6	0.001332537	0.0013325	106	105	75+30
	7	0.001289481	0.001289444	102	103	55+48
	8	0.001923278	0.001923333	153	153	75+48+30
	9	0.002584698	0.002584722	205	205	165+40
	10	0.001515253	0.001515278	120	120	120
	11	0.002910971	0.002911111	231	230	200+30
	12	0.004136974	0.004136944	328	328	255+48+25
	13	0.002103602	0.002103611	167	166	48+48+35+35
	14	0.001755222	0.001755278	139	140	140
	15	0.001341333	0.001341389	106	105	75+30
	16	0.001369574	0.001369722	109	110	55+55
	17	0.001039481	0.001039444	82	80	55+25
	18	0.000989481	0.000989444	78	78	48+30
	19	0.000744111	0.000744167	59	60	30+30
	20	0.001010778	0.001010833	80	80	55+25
	21	0.001245037	0.001245	99	100	75+25
	22	0.001418648	0.001418611	113	113	48+35+30
	23	0.003366333	0.003366389	267	268	165+55+48
	24	0.003990099	0.003990278	316	315	255+30+30
	25	0.005096272	0.005096389	404	405	255+120+30
	26	0.002468764	0.002468889	196	195	165+30
	27	0.001030569	0.001030556	82	80	40+40
	28	0.001007306	0.001007222	80	80	40+40
	29	0.000906611	0.000906667	72	70	35+35
	30	0.000730222	0.000730278	58	60	30+30
	31	0.000935778	0.000935833	74	75	40+35
	32	0.000699667	0.000699722	55	55	55
	33	0.000738556	0.000738611	59	60	30+30
	34	0.000820037	0.00082	65	65	35+30
Total	**-**	**0.060018296**	**0.060019444**	**4759**	**4758**	**4758**

Table CXIV – Complementary data of Scenario III using P_{tx} @ T = 600s.

	Mote m	**Calculated e_m (in mAh)**	**Simulated e_m (in mAh)**	**Calculated battery (in mAh)**	**Assigned battery (in mAh)**	**Battery Set (in mAh)**
	1	0.004290407	0.004290556	122	120	120
	2	0.004460315	0.004460278	127	128	48+40+40
	3	0.004785276	0.004785278	136	136	48+48+40
	4	0.006220153	0.006220278	177	176	48+48+40+40
	5	0.005511472	0.005511667	157	158	55+55+48
	6	0.004482537	0.0044825	128	128	48+40+40
	7	0.004439481	0.004439444	126	126	48+48+30
	8	0.005073278	0.005073333	145	145	120+25
	9	0.005734698	0.005734722	163	163	55+48+30+30
	10	0.004665253	0.004665278	133	133	55+48+30
	11	0.006060971	0.006061111	173	173	90+48+35
	12	0.007286974	0.007287222	208	208	120+48+40
	13	0.005253602	0.005253611	150	150	120+30
	14	0.004905222	0.004905278	140	140	140
	15	0.004491333	0.004491389	128	128	48+40+40
	16	0.004519574	0.004519722	129	128	48+40+40
	17	0.004189481	0.004189444	119	120	120
	18	0.004139481	0.004139444	118	118	48+35+35
	19	0.003894111	0.003894167	111	110	55+55
	20	0.004160778	0.004160833	119	120	120
	21	0.004395037	0.004395	125	125	90+35
	22	0.004568648	0.004568611	130	130	90+40
	23	0.006516333	0.006516389	186	186	90+48+48
	24	0.007140099	0.007140278	203	203	155+48
	25	0.008246272	0.008246667	235	235	200+35
	26	0.005618764	0.005618889	160	160	120+40
	27	0.004180569	0.004180556	119	120	120
	28	0.004157306	0.004157222	118	118	48+35+35
	29	0.004056611	0.004056667	116	115	75+40
	30	0.003880222	0.003880278	111	110	55+55
	31	0.004085778	0.004085833	116	115	75+40
	32	0.003849667	0.003849722	110	110	55+55
	33	0.003888556	0.003888611	111	110	55+55
	34	0.003970037	0.00397	113	113	48+35+30
Total	**-**	**0.167118296**	**0.167120278**	**4762**	**4758**	**4758**

Table CXV – Complementary data of Scenario III using P_{tx} @ T = 3600s.

	Mote m	Calculated e_m (in mAh)	Simulated e_m (in mAh)	Calculated battery (in mAh)	Assigned battery (in mAh)	Battery Set (in mAh)
	1	0.021790407	0.021790556	136	136	48+48+40
	2	0.021960315	0.021960556	137	136	48+48+40
	3	0.022285276	0.022285556	139	138	90+48
	4	0.023720153	0.023720278	148	148	75+48+25
	5	0.023011472	0.023011667	144	143	55+48+40
	6	0.021982537	0.0219825	137	136	48+48+40
	7	0.021939481	0.021939444	137	136	48+48+40
	8	0.022573278	0.022573333	141	140	140
	9	0.023234698	0.023235	145	145	120+25
	10	0.022165253	0.022165278	138	138	90+48
	11	0.023560971	0.023561111	147	148	75+48+25
	12	0.024786974	0.024787222	155	155	120+35
	13	0.022753602	0.022753611	142	143	55+48+40
	14	0.022405222	0.022405278	140	140	140
	15	0.021991333	0.021991389	137	136	48+48+40
	16	0.022019574	0.022019722	138	138	90+48
	17	0.021689481	0.021689444	135	135	55+40+40
	18	0.021639481	0.021639444	135	135	55+40+40
	19	0.021394111	0.021394167	134	135	55+40+40
	20	0.021660778	0.021660833	135	135	55+40+40
	21	0.021895037	0.021895	137	136	48+48+40
	22	0.022068648	0.022068611	138	138	90+48
	23	0.024016333	0.024016667	150	150	120+30
	24	0.024640099	0.024640278	154	155	120+35
	25	0.025746272	0.025746667	161	160	120+40
	26	0.023118764	0.023118889	144	143	55+48+40
	27	0.021680569	0.021680556	135	135	55+40+40
	28	0.021657306	0.021657222	135	135	55+40+40
	29	0.021556611	0.021556667	135	135	55+40+40
	30	0.021380222	0.021380278	134	135	55+40+40
	31	0.021585778	0.021585833	135	135	55+40+40
	32	0.021349667	0.021349722	133	133	55+48+30
	33	0.021388556	0.021388611	134	135	55+40+40
	34	0.021470037	0.02147	134	135	55+40+40
Total	**-**	**0.762118296**	**0.762121389**	**4759**	**4756**	**4756**

Table CXVI – Complementary data of Scenario III using P_{tx} @ T = 86400s.

	Mote m	Calculated e_m (in mAh)	Simulated e_m (in mAh)	Calculated battery (in mAh)	Assigned battery (in mAh)	Battery Set (in mAh)
	1	0.504790407	0.504792778	140	140	140
	2	0.504960315	0.504963333	140	140	140
	3	0.505285276	0.505289444	140	140	140
	4	0.506720153	0.506728889	140	140	140
	5	0.506011472	0.506017778	140	140	140
	6	0.504982537	0.504985556	140	140	140
	7	0.504939481	0.504942222	140	140	140
	8	0.505573278	0.505578056	140	140	140
	9	0.506234698	0.506241667	140	140	140
	10	0.505165253	0.505168611	140	140	140
	11	0.506560971	0.506568889	140	140	140
	12	0.507786974	0.507798333	142	143	55-48+40
	13	0.505753602	0.505758611	140	140	140
	14	0.505405222	0.505409167	140	140	140
	15	0.504991333	0.504994444	140	140	140
	16	0.505019574	0.505022778	140	140	140
	17	0.504689481	0.504691667	140	140	140
	18	0.504639481	0.504641389	140	140	140
	19	0.504394111	0.504395278	140	140	140
	20	0.504660778	0.504662778	140	140	140
	21	0.504895037	0.504897778	140	140	140
	22	0.505068648	0.505071667	140	140	140
	23	0.507016333	0.507025556	140	140	140
	24	0.507640099	0.507651389	142	143	55-48+40
	25	0.508746272	0.50876	142	143	55-48+40
	26	0.506118764	0.506124444	140	140	140
	27	0.504680569	0.504682222	140	140	140
	28	0.504657306	0.504659167	140	140	140
	29	0.504556611	0.504558333	139	138	90+48
	30	0.504380222	0.504381389	139	138	90+48
	31	0.504585778	0.5045875	139	138	90+48
	32	0.504349667	0.504350833	139	138	90+48
	33	0.504388556	0.504389722	139	138	90+48
	34	0.504470037	0.504471389	139	138	90+48
Total	**-**	**17.184118296**	**17.184263056**	**4760**	**4757**	**4757**

Appendix H

COMPLEMENTARY DATA OF CHAPTER V: SCENARIO III USING $11.31P_{TX}$

Table CXVII – Complementary data of Scenario III using 11.31P_{tx} @ T = 1s.

	Mote m	**Calculated e_m (in mAh)**	**Simulated e_m (in mAh)**	**Calculated battery (in mAh)**	**Assigned battery (in mAh)**	**Battery Set (in mAh)**
	1	0.005178885	0.005206111	236	236	140+48+48
	2	0.003254707	0.003266944	148	148	75+48+25
	3	0.003146333	0.003155556	143	143	55+48+40
	4	0.003947873	0.003963889	180	180	140+40
	5	0.005207021	0.0052375	237	236	140+48+48
	6	0.002001889	0.002009444	91	90	55+35
	7	0.001731889	0.001739444	79	80	40+40
	8	0.003002936	0.0030175	137	136	48+48+40
	9	0.00255253	0.002560833	116	115	90+25
	10	0.008027157	0.0080775	366	366	200+48+48+35+35
	11	0.005977586	0.006012222	272	271	140+48+48+35
	12	0.011649723	0.0117275	531	530	500+30
	13	0.002774059	0.002785	126	126	48+48+30
	14	0.003993275	0.004013889	182	180	120+30+30
	15	0.001796889	0.001804444	82	83	48+35
	16	0.001814944	0.0018225	83	83	48+35
	17	0.001759389	0.001766944	80	80	40+40
	18	0.001846056	0.001853611	84	83	48+35
	19	0.001516611	0.001524167	69	70	35+35
	20	0.002295361	0.002308889	105	105	75+30
	21	0.002093729	0.002103611	95	95	55+40
	22	0.001862999	0.001870556	85	85	55+30
	23	0.004377679	0.004401944	199	200	200
	24	0.001618553	0.001618611	74	75	75
	25	0.001707073	0.001706944	78	78	48+30
	26	0.005486685	0.005520556	250	250	200+25+25
	27	0.002225594	0.002234167	101	100	75+25
	28	0.002685637	0.002697778	122	120	120
	29	0.001581889	0.001589444	72	70	35+35
	30	0.001523556	0.001531111	69	70	70
	31	0.001534667	0.001542222	70	70	70
	32	0.001441611	0.001449167	66	65	35+30
	33	0.001426056	0.001433611	65	65	35+30
	34	0.001485222	0.001492778	68	70	70
Total	**-**	**0.104526062**	**0.105046389**	**4761**	**4754**	**4754**

Table CXVIII – Complementary data of Scenario III using 11.31P_{tx} @ T = 10s.

	Mote m	Calculated e_m (in mAh)	Simulated e_m (in mAh)	Calculated battery (in mAh)	Assigned battery (in mAh)	Battery Set (in mAh)
	1	0.005231385	0.005258889	234	235	200+35
	2	0.003307207	0.003319722	148	148	75+48+25
	3	0.003198833	0.003208333	143	143	55+48+40
	4	0.004000373	0.004016667	179	180	140+40
	5	0.005259521	0.005290556	235	235	200+35
	6	0.002054389	0.002061944	92	90	55+35
	7	0.001784389	0.001791944	80	80	40+40
	8	0.003055436	0.003070278	137	138	48+55+35
	9	0.00260503	0.002613611	117	118	48+35+35
	10	0.008079657	0.008130556	362	363	255+48+30+30
	11	0.006030086	0.006065	270	270	200+35+35
	12	0.011702223	0.011780833	524	525	500+25
	13	0.002826559	0.0028375	127	128	48+40+40
	14	0.004045775	0.004066944	181	180	140+40
	15	0.001849389	0.001856944	83	83	48+35
	16	0.001867444	0.001875	84	85	30+30+25
	17	0.001811889	0.001819444	81	80	40+40
	18	0.001898556	0.001906111	85	85	55+30
	19	0.001569111	0.001576667	70	70	35+35
	20	0.002347861	0.002361389	105	105	75+30
	21	0.002146229	0.002156111	96	96	48+48
	22	0.001915499	0.001923056	86	85	55+30
	23	0.004430179	0.004455	198	198	120+48+30
	24	0.001671053	0.001671111	75	75	75
	25	0.001759573	0.001759722	79	80	55+25
	26	0.005539185	0.005573611	248	248	200+48
	27	0.002278094	0.002286944	102	100	75+25
	28	0.002738137	0.002750556	123	123	75+48
	29	0.001634389	0.001641944	73	73	48+25
	30	0.001576056	0.001583611	71	70	35+35
	31	0.001587167	0.001594722	71	70	35+35
	32	0.001494111	0.001501667	67	65	35+30
	33	0.001478556	0.001486111	66	65	35+30
	34	0.001537722	0.001545278	69	70	35+35
Total	**-**	**0.106311062**	**0.106837778**	**4761**	**4759**	**4759**

Table CXIX – Complementary data of Scenario III using $11.31P_{tx}$ @ T = 60s.

	Mote m	Calculated e_m (in mAh)	Simulated e_m (in mAh)	Calculated battery (in mAh)	Assigned battery (in mAh)	Battery Set (in mAh)
	1	0.005523052	0.005550556	226	225	200+25
	2	0.003598873	0.003611389	147	148	75+48+25
	3	0.0034905	0.003500278	143	143	55+48+40
	4	0.00429204	0.004308333	176	176	48+48+40+40
	5	0.005551188	0.005581944	227	228	140+48+40
	6	0.002346056	0.002353611	96	96	48+48
	7	0.002076056	0.002083611	85	85	55+30
	8	0.003347103	0.003361944	137	138	48+55+35
	9	0.002896697	0.002905278	119	118	48+40+30
	10	0.008371324	0.0084225	343	343	255+48+40
	11	0.006321752	0.006356944	259	260	200+30+30
	12	0.01199389	0.0120725	491	490	200+200+55+35
	13	0.003118226	0.003129167	128	128	48+40+40
	14	0.004337442	0.004358333	178	178	90+48+40
	15	0.002141056	0.002148611	88	88	48+40
	16	0.002159111	0.002166667	88	88	48+40
	17	0.002103556	0.002111111	86	85	55+30
	18	0.002190222	0.002197778	90	90	90
	19	0.001860778	0.001868333	76	75	75
	20	0.002639528	0.002653333	108	108	48+30+30
	21	0.002437895	0.002447778	100	100	75+25
	22	0.002207166	0.002214722	90	90	90
	23	0.004721845	0.004746667	193	193	120+48+25
	24	0.00196272	0.001962778	80	80	40+40
	25	0.00205124	0.002051389	84	85	55+30
	26	0.005830852	0.005865278	239	240	200+40
	27	0.00256976	0.002578611	105	105	75+30
	28	0.003029803	0.0030425	124	125	75+25+25
	29	0.001926056	0.001933611	79	80	40+40
	30	0.001867722	0.001875278	76	75	75
	31	0.001878833	0.001886389	77	75	75
	32	0.001785778	0.001793333	73	73	48+25
	33	0.001770222	0.001777778	72	73	48+25
	34	0.001829389	0.001836944	75	75	75
Total	**-**	**0.116227729**	**0.116755278**	**4758**	**4759**	**4759**

Table CXX – Complementary data of Scenario III using 11.31P_{tx} @ T = 600s.

	Mote m	Calculated e_m (in mAh)	Simulated e_m (in mAh)	Calculated battery (in mAh)	Assigned battery (in mAh)	Battery Set (in mAh)
	1	0.008673052	0.008700833	185	185	120+35+30
	2	0.006748873	0.006761389	144	145	120+25
	3	0.0066405	0.006650278	142	140	140
	4	0.00744204	0.007458333	159	160	120+40
	5	0.008701188	0.008732222	185	185	120+35+30
	6	0.005496056	0.005503611	117	118	48+35+35
	7	0.005226056	0.005233611	111	110	55+55
	8	0.006497103	0.006512222	138	138	90+48
	9	0.006046697	0.006055278	129	130	90+40
	10	0.011521324	0.011572778	246	248	200+48
	11	0.009471752	0.009507222	202	200	200
	12	0.01514389	0.015222778	323	323	200+75+48
	13	0.006268226	0.006279444	134	133	48+55+30
	14	0.007487442	0.007508611	160	160	120+40
	15	0.005291056	0.005298611	113	113	48+35+30
	16	0.005309111	0.005316667	113	113	48+35+30
	17	0.005253556	0.005261111	112	113	48+35+30
	18	0.005340222	0.005347778	114	113	48+35+30
	19	0.005010778	0.005018333	107	108	48+30+30
	20	0.005789528	0.005803333	123	123	48+40+35
	21	0.005587895	0.005597778	119	118	48+35+35
	22	0.005357166	0.005364722	114	113	48+35+30
	23	0.007871845	0.007896667	168	168	120+48
	24	0.00511272	0.005112778	109	108	48+30+30
	25	0.00520124	0.005201389	111	110	55+55
	26	0.008980852	0.009015278	191	190	165+25
	27	0.00571976	0.005728611	122	120	120
	28	0.006179803	0.0061925	132	130	90+40
	29	0.005076056	0.005083611	108	108	48+30+30
	30	0.005017722	0.005025278	107	108	48+30+30
	31	0.005028833	0.005036389	107	108	48+30+30
	32	0.004935778	0.004943333	105	105	75+30
	33	0.004920222	0.004927778	105	105	75+30
	34	0.004979389	0.004986944	106	105	75+30
Total	**-**	**0.223327729**	**0.2238575**	**4761**	**4754**	**4754**

Table CXXI – Complementary data of Scenario III using $11.31P_{tx}$ @ T = 3600s.

	Mote m	Calculated e_m (in mAh)	Simulated e_m (in mAh)	Calculated battery (in mAh)	Assigned battery (in mAh)	Battery Set (in mAh)
	1	0.026173052	0.026201667	152	153	55+48+25+25
	2	0.024248873	0.024261667	141	140	140
	3	0.0241405	0.024150556	140	140	140
	4	0.02494204	0.024958889	145	145	120+25
	5	0.026201188	0.026232778	152	150	120+30
	6	0.022996056	0.023003889	134	135	75+35+25
	7	0.022726056	0.022733889	132	130	90+40
	8	0.023997103	0.024012222	140	140	140
	9	0.023546697	0.023555556	137	138	90+48
	10	0.029021324	0.029073889	169	168	120+48
	11	0.026971752	0.027007778	157	158	55+55+48
	12	0.03264389	0.032723889	190	190	165+25
	13	0.023768226	0.023779444	138	138	90+48
	14	0.024987442	0.025008056	145	145	120+25
	15	0.022791056	0.022798889	133	133	55+48+30
	16	0.022809111	0.022816944	133	133	55+48+30
	17	0.022753556	0.022761389	132	133	55+48+30
	18	0.022840222	0.022848056	133	133	55+48+30
	19	0.022510778	0.022518611	131	130	90+40
	20	0.023289528	0.023303611	135	135	75+30+30
	21	0.023087895	0.023097778	134	135	75+30+30
	22	0.022857166	0.022865	133	133	55+48+30
	23	0.025371845	0.025396944	148	148	75+48+25
	24	0.02261272	0.022613056	132	133	55+48+30
	25	0.02270124	0.022701667	132	133	55+48+30
	26	0.026480852	0.026515278	154	153	55+48+25+25
	27	0.02321976	0.023228889	135	135	75+30+30
	28	0.023679803	0.0236925	138	138	90+48
	29	0.022576056	0.022583889	131	130	90+40
	30	0.022517722	0.022525556	131	130	90+40
	31	0.022528833	0.022536667	131	130	90+40
	32	0.022435778	0.022443611	131	130	90+40
	33	0.022420222	0.022428056	130	130	90+40
	34	0.022479389	0.022487222	131	130	90+40
Total	**-**	**0.818327729**	**0.818867778**	**4760**	**4755**	**4755**

Table CXXII – Complementary data of Scenario III using $11.31P_{tx}$ @ T = 86400s.

	Mote m	Calculated e_m (in mAh)	Simulated e_m (in mAh)	Calculated battery (in mAh)	Assigned battery (in mAh)	Battery Set (in mAh)
	1	0.509173052	0.509219444	140	140	140
	2	0.507248873	0.507272778	140	140	140
	3	0.5071405	0.507156667	140	140	140
	4	0.50794204	0.507969722	140	140	140
	5	0.509201188	0.509243611	140	140	140
	6	0.505996056	0.506008056	139	138	90+48
	7	0.505726056	0.505737222	139	138	90+48
	8	0.506997103	0.507017222	139	138	90+48
	9	0.506546697	0.506561111	139	138	90+48
	10	0.512021324	0.512096389	141	143	55-48+40
	11	0.509971752	0.510025	140	140	140
	12	0.51564389	0.515748333	142	143	55-48+40
	13	0.506768226	0.506782222	140	140	140
	14	0.507987442	0.508015	140	140	140
	15	0.505791056	0.505802222	140	140	140
	16	0.505809111	0.505820556	140	140	140
	17	0.505753556	0.505765	140	140	140
	18	0.505840222	0.505851667	140	140	140
	19	0.505510778	0.505521389	140	140	140
	20	0.506289528	0.506303056	140	140	140
	21	0.506087895	0.506101111	140	140	140
	22	0.505857166	0.505868611	140	140	140
	23	0.508371845	0.508403333	140	140	140
	24	0.50561272	0.505615833	140	140	140
	25	0.50570124	0.505704722	140	140	140
	26	0.509480852	0.509513611	141	143	55-48+40
	27	0.50621976	0.506231389	140	140	140
	28	0.506679803	0.5066925	140	140	140
	29	0.505576056	0.505586667	140	140	140
	30	0.505517722	0.505528056	140	140	140
	31	0.505528833	0.505539444	140	140	140
	32	0.505435778	0.505446111	140	140	140
	33	0.505420222	0.505430833	139	138	90+48
	34	0.505479389	0.50549	140	140	140
Total	**-**	**17.240327729**	**17.241068889**	**4759**	**4759**	**4759**

Appendix I

COMPLEMENTARY DATA OF CHAPTER V: SCENARIO III USING $46.76P_{TX}$

Table CXXIII – Complementary data of Scenario III using 46.76P_{tx} @ T = 1s.

	Mote m	**Calculated e_m (in mAh)**	**Simulated e_m (in mAh)**	**Calculated battery (in mAh)**	**Assigned battery (in mAh)**	**Battery Set (in mAh)**
	1	0.005549944	0.005536944	126	126	48+48+30
	2	0.015659936	0.015705556	355	355	255+75+25
	3	0.015659936	0.015704722	355	355	255+75+25
	4	0.015659936	0.015704444	355	355	255+75+25
	5	0.005549944	0.005536944	126	126	48+48+30
	6	0.005549944	0.005536944	126	126	48+48+30
	7	0.00521712	0.005204167	118	128	48+55+25
	8	0.005342669	0.005329722	121	120	120
	9	0.010303797	0.010319722	234	235	200+35
	10	0.004055132	0.004125278	92	90	90
	11	0.003834021	0.003896111	87	88	48+40
	12	0.004040601	0.00411	92	90	90
	13	0.010927959	0.010944722	248	248	200+48
	14	0.005330345	0.005317222	121	120	120
	15	0.005265376	0.005252222	119	118	48+40+30
	16	0.005298709	0.005285556	120	120	120
	17	0.005238129	0.005225	119	118	48+40+30
	18	0.005259172	0.005246111	119	118	48+40+30
	19	0.00501559	0.0050025	114	115	90+25
	20	0.004999873	0.004986944	113	113	48+35+30
	21	0.004998176	0.004985	113	113	48+35+30
	22	0.008122307	0.008126111	184	185	120+35+30
	23	0.003065471	0.003102778	70	70	35+35
	24	0.001579601	0.001595278	36	35	35
	25	0.001612934	0.001628611	37	35	35
	26	0.003111295	0.003151389	71	70	35+35
	27	0.009716137	0.009725	220	220	140+40+40
	28	0.005036765	0.005023611	114	115	90+25
	29	0.004891348	0.004878333	111	110	75+35
	30	0.004830768	0.004817778	110	110	75+35
	31	0.004846484	0.004833333	110	110	75+35
	32	0.004688629	0.004675556	106	105	75+30
	33	0.004721962	0.004708889	107	105	75+30
	34	0.004851191	0.004838333	110	110	75+35
Total	**-**	**0.209831201**	**0.210060833**	**4759**	**4757**	**4757**

Table CXXIV – Complementary data of Scenario III using 46.76P_{tx} @ T = 10s.

	Mote m	Calculated e_m (in mAh)	Simulated e_m (in mAh)	Calculated battery (in mAh)	Assigned battery (in mAh)	Battery Set (in mAh)
	1	0.005602444	0.00559	126	126	48+48+30
	2	0.015712436	0.015668889	353	353	255+48+25+25
	3	0.015712436	0.015668056	353	353	255+48+25+25
	4	0.015712436	0.015666667	353	353	255+48+25+25
	5	0.005602444	0.00559	126	126	48+48+30
	6	0.005602444	0.00559	126	126	48+48+30
	7	0.00526962	0.005257222	119	128	48+55+25
	8	0.005395169	0.0053825	121	120	120
	9	0.010356297	0.010328611	233	233	120+48+35+30
	10	0.004107632	0.004127222	92	90	90
	11	0.003886521	0.003904444	87	88	48+40
	12	0.004093101	0.004112222	92	90	90
	13	0.010980459	0.010947222	247	248	200+48
	14	0.005382845	0.005370278	121	120	120
	15	0.005317876	0.005305278	120	120	120
	16	0.005351209	0.005338611	120	120	120
	17	0.005290629	0.005278056	119	120	120
	18	0.005311672	0.005299167	119	120	120
	19	0.00506809	0.005055556	114	115	90+25
	20	0.005052373	0.005039722	114	115	90+25
	21	0.005050676	0.005038056	114	115	90+25
	22	0.008174807	0.008150278	184	185	120+35+30
	23	0.003117971	0.003130833	70	70	35+35
	24	0.001632101	0.001632222	37	35	35
	25	0.001665434	0.001665556	37	35	35
	26	0.003163795	0.003177222	71	70	35+35
	27	0.009768637	0.009738333	220	220	140+40+40
	28	0.005089265	0.005076667	114	115	90+25
	29	0.004943848	0.004931389	111	110	75+35
	30	0.004883268	0.004870556	110	110	75+35
	31	0.004898984	0.004886389	110	110	75+35
	32	0.004741129	0.004728611	107	105	75+30
	33	0.004774462	0.004761944	107	105	75+30
	34	0.004903691	0.004891111	110	110	75+35
Total	**-**	**0.211616201**	**0.211198889**	**4757**	**4759**	**4759**

Table CXXV – Complementary data of Scenario III using $46.76P_{tx}$ @ T = 60s.

	Mote m	Calculated e_m (in mAh)	Simulated e_m (in mAh)	Calculated battery (in mAh)	Assigned battery (in mAh)	Battery Set (in mAh)
	1	0.005894111	0.005881667	127	126	48+48+30
	2	0.016004102	0.015961389	344	343	255+48+40
	3	0.016004102	0.015959444	344	343	255+48+40
	4	0.016004102	0.015959167	344	343	255+48+40
	5	0.005894111	0.005881667	127	126	48+48+30
	6	0.005894111	0.005881667	127	126	48+48+30
	7	0.005561287	0.005548889	119	120	120
	8	0.005686836	0.005674444	122	120	120
	9	0.010647963	0.010618889	229	228	140+48+40
	10	0.004399299	0.004418889	95	95	55+40
	11	0.004178188	0.004196111	90	90	90
	12	0.004384768	0.004404167	94	95	55+40
	13	0.011272126	0.011239444	242	240	200+40
	14	0.005674512	0.005661944	122	120	120
	15	0.005609543	0.005596944	121	120	120
	16	0.005642876	0.005630556	121	120	120
	17	0.005582296	0.005569722	120	120	120
	18	0.005603339	0.005590833	120	120	120
	19	0.005359756	0.005347222	115	115	90+25
	20	0.00534404	0.005331667	115	115	90+25
	21	0.005342343	0.005329722	115	115	90+25
	22	0.008466474	0.008442222	182	180	140+40
	23	0.003409638	0.0034225	73	73	48+25
	24	0.001923767	0.001923889	41	40	40
	25	0.001957101	0.001957222	42	40	40
	26	0.003455462	0.003468889	74	75	75
	27	0.010060304	0.010030278	216	216	120+48+48
	28	0.005380931	0.005368333	116	115	90+25
	29	0.005235514	0.005223056	112	110	75+35
	30	0.005174934	0.0051625	111	110	75+35
	31	0.005190651	0.005178056	112	110	75+35
	32	0.005032795	0.005020278	108	108	48+30+30
	33	0.005066129	0.005053611	109	110	75+35
	34	0.005195358	0.005182778	112	110	75+35
Total	**-**	**0.221532868**	**0.221118056**	**4761**	**4736**	**4736**

Table CXXVI – Complementary data of Scenario III using $46.76P_{tx}$ @ T = 600s.

	Mote m	Calculated e_m (in mAh)	Simulated e_m (in mAh)	Calculated battery (in mAh)	Assigned battery (in mAh)	Battery Set (in mAh)
	1	0.009044111	0.009031667	131	130	90+40
	2	0.019154102	0.019113056	277	276	140+48+48+40
	3	0.019154102	0.019109722	277	276	140+48+48+40
	4	0.019154102	0.019108611	277	276	140+48+48+40
	5	0.009044111	0.009031667	131	130	90+40
	6	0.009044111	0.009031667	131	130	90+40
	7	0.008711287	0.008698889	126	126	48+48+30
	8	0.008836836	0.008824444	128	128	48+40+40
	9	0.013797963	0.013770278	200	200	200
	10	0.007549299	0.007569167	109	110	55+55
	11	0.007328188	0.007346389	106	105	75+30
	12	0.007534768	0.007554167	109	110	55+55
	13	0.014422126	0.014389167	209	210	120+90
	14	0.008824512	0.008812222	128	128	48+40+40
	15	0.008759543	0.008747222	127	128	48+40+40
	16	0.008792876	0.008780556	127	128	48+40+40
	17	0.008732296	0.00872	126	126	48+48+30
	18	0.008753339	0.008741111	127	126	48+48+30
	19	0.008509756	0.0084975	123	123	48+40+35
	20	0.00849404	0.008481667	123	123	48+40+35
	21	0.008492343	0.00848	123	123	48+40+35
	22	0.011616474	0.011592222	168	168	120+48
	23	0.006559638	0.0065725	95	95	55+40
	24	0.005073767	0.005073889	73	73	48+25
	25	0.005107101	0.005107222	74	75	75
	26	0.006605462	0.006618889	96	96	48+48
	27	0.013210304	0.01318	191	190	165+25
	28	0.008530931	0.008518611	124	125	90+35
	29	0.008385514	0.008373056	121	120	120
	30	0.008324934	0.0083125	121	120	120
	31	0.008340651	0.008328333	121	120	120
	32	0.008182795	0.008170556	119	120	120
	33	0.008216129	0.008203889	119	120	120
	34	0.008345358	0.008333056	121	120	120
Total	**-**	**0.328632868**	**0.328223889**	**4758**	**4754**	**4754**

Table CXXVII – Complementary data of Scenario III using $46.76P_{tx}$ @ T = 3600s.

	Mote m	Calculated e_m (in mAh)	Simulated e_m (in mAh)	Calculated battery (in mAh)	Assigned battery (in mAh)	Battery Set (in mAh)
	1	0.026544111	0.026531944	137	136	48+48+40
	2	0.036654102	0.036616389	189	190	165+25
	3	0.036654102	0.036616389	189	190	165+25
	4	0.036654102	0.036608889	189	190	165+25
	5	0.026544111	0.026531944	137	136	48+48+40
	6	0.026544111	0.026531944	137	136	48+48+40
	7	0.026211287	0.026199167	135	135	55+55+25
	8	0.026336836	0.026324722	136	136	48+48+40
	9	0.031297963	0.031271111	161	160	120+40
	10	0.025049299	0.025068611	129	130	90+40
	11	0.024828188	0.024845833	128	128	48+40+40
	12	0.025034768	0.025053611	129	130	90+40
	13	0.031922126	0.031889444	165	165	165
	14	0.026324512	0.026312222	136	136	48+48+40
	15	0.026259543	0.026247222	135	135	55+55+25
	16	0.026292876	0.026280556	136	136	48+48+40
	17	0.026232296	0.02622	135	135	55+55+25
	18	0.026253339	0.026241111	135	135	55+55+25
	19	0.026009756	0.0259975	134	133	55+48+30
	20	0.02599404	0.025981944	134	133	55+48+30
	21	0.025992343	0.02598	134	133	55+48+30
	22	0.029116474	0.029091944	150	150	120+30
	23	0.024059638	0.0240725	124	125	90+35
	24	0.022573767	0.022573889	116	115	90+25
	25	0.022607101	0.022607222	117	115	90+25
	26	0.024105462	0.024118889	124	125	90+35
	27	0.030710304	0.030678333	158	158	55+55+48
	28	0.026030931	0.026018611	134	133	55+48+30
	29	0.025885514	0.025873333	133	133	55+48+30
	30	0.025824934	0.025812778	133	133	55+48+30
	31	0.025840651	0.025828333	133	133	55+48+30
	32	0.025682795	0.025670556	132	133	55+48+30
	33	0.025716129	0.025703889	133	133	55+48+30
	34	0.025845358	0.025833056	133	133	55+48+30
Total	**-**	**0.923632868**	**0.923233889**	**4760**	**4757**	**4757**

Table CXXVIII – Complementary data of Scenario III using 46.76P_{tx} @ T = 86400s.

	Mote m	**Calculated e_m (in mAh)**	**Simulated e_m (in mAh)**	**Calculated battery (in mAh)**	**Assigned battery (in mAh)**	**Battery Set (in mAh)**
	1	0.509544111	0.511984722	140	140	140
	2	0.519654102	0.507151389	143	143	55+48+40
	3	0.519654102	0.507148056	143	143	55+48+40
	4	0.519654102	0.507148056	143	143	55+48+40
	5	0.509544111	0.511930556	140	140	140
	6	0.509544111	0.511930556	140	140	140
	7	0.509211287	0.511071944	140	140	140
	8	0.509336836	0.510831389	140	140	140
	9	0.514297963	0.506505278	141	140	140
	10	0.508049299	0.506551944	139	138	90+48
	11	0.507828188	0.505473056	139	138	90+48
	12	0.508034768	0.505520833	139	138	90+48
	13	0.514922126	0.506569722	141	140	140
	14	0.509324512	0.511468056	140	140	140
	15	0.509259543	0.511665	140	140	140
	16	0.509292876	0.509029167	140	140	140
	17	0.509232296	0.508991667	140	140	140
	18	0.509253339	0.509023333	140	140	140
	19	0.509009756	0.508799167	140	140	140
	20	0.50899404	0.510113889	140	140	140
	21	0.508992343	0.509362778	140	140	140
	22	0.512116474	0.505996667	141	140	140
	23	0.507059638	0.506044167	139	140	140
	24	0.505573767	0.505105278	139	140	140
	25	0.505607101	0.505151944	139	138	90+48
	26	0.507105462	0.506124167	139	138	90+48
	27	0.513710304	0.506378889	141	140	140
	28	0.509030931	0.510200556	140	140	140
	29	0.508885514	0.5086875	140	140	140
	30	0.508824934	0.508649722	140	140	140
	31	0.508840651	0.508725	140	140	140
	32	0.508682795	0.508636667	140	140	140
	33	0.508716129	0.5086825	140	140	140
	34	0.508845358	0.508741389	140	140	140
Total	**-**	**17.345632868**	**17.285395**	**4766**	**4759**	**4759**

Appendix J

COMPLEMENTARY DATA OF CHAPTER V: TRANSMISSION POWER LEVELS OF SCENARIO I, II AND III

Table CXXIX – Transmission power levels of Scenario I.

	P_{tx}	**11.31**P_{tx}	**46.76**P_{tx}
Mote m	**Transmission Power**	**Transmission Power**	**Transmission Power**
1	P_{tx}	P_{tx}	P_{tx}
2	P_{tx}	P_{tx}	P_{tx}
3	P_{tx}	P_{tx}	P_{tx}
4	P_{tx}	P_{tx}	P_{tx}
5	P_{tx}	P_{tx}	P_{tx}
6	P_{tx}	P_{tx}	P_{tx}
7	P_{tx}	$11.31P_{tx}$	$11.31P_{tx}$
8	P_{tx}	$11.31P_{tx}$	$11.31P_{tx}$
9	P_{tx}	$11.31P_{tx}$	$11.31P_{tx}$
10	P_{tx}	$11.31P_{tx}$	$11.31P_{tx}$
11	P_{tx}	$11.31P_{tx}$	$11.31P_{tx}$
12	P_{tx}	$11.31P_{tx}$	$11.31P_{tx}$
13	P_{tx}	$11.31P_{tx}$	$11.31P_{tx}$
14	P_{tx}	$11.31P_{tx}$	$11.31P_{tx}$
15	P_{tx}	$11.31P_{tx}$	$11.31P_{tx}$
16	P_{tx}	$11.31P_{tx}$	$11.31P_{tx}$
17	P_{tx}	$11.31P_{tx}$	$11.31P_{tx}$
18	P_{tx}	$11.31P_{tx}$	$11.31P_{tx}$
19	P_{tx}	$11.31P_{tx}$	$46.76P_{tx}$
20	P_{tx}	$11.31P_{tx}$	$46.76P_{tx}$
21	P_{tx}	$11.31P_{tx}$	$46.76P_{tx}$
22	P_{tx}	$11.31P_{tx}$	$46.76P_{tx}$
23	P_{tx}	$11.31P_{tx}$	$46.76P_{tx}$
24	P_{tx}	$11.31P_{tx}$	$46.76P_{tx}$
25	P_{tx}	$11.31P_{tx}$	$46.76P_{tx}$
26	P_{tx}	$11.31P_{tx}$	$46.76P_{tx}$
27	P_{tx}	$11.31P_{tx}$	$46.76P_{tx}$
28	P_{tx}	$11.31P_{tx}$	$46.76P_{tx}$
29	P_{tx}	$11.31P_{tx}$	$46.76P_{tx}$
30	P_{tx}	$11.31P_{tx}$	$46.76P_{tx}$
31	P_{tx}	$11.31P_{tx}$	$46.76P_{tx}$
32	P_{tx}	$11.31P_{tx}$	$46.76P_{tx}$
33	P_{tx}	$11.31P_{tx}$	$46.76P_{tx}$
34	P_{tx}	$11.31P_{tx}$	$46.76P_{tx}$

Table CXXX – Transmission power levels of Scenario II.

	P_{tx}	**11.31 P_{tx}**	**46.76 P_{tx}**
Mote m	**Transmission Power**	**Transmission Power**	**Transmission Power**
1	P_{tx}	11.31 P_{tx}	46.76 P_{tx}
2	P_{tx}	11.31 P_{tx}	11.31 P_{tx}
3	P_{tx}	11.31 P_{tx}	11.31 P_{tx}
4	P_{tx}	11.31 P_{tx}	11.31 P_{tx}
5	P_{tx}	11.31 P_{tx}	46.76 P_{tx}
6	P_{tx}	11.31 P_{tx}	46.76 P_{tx}
7	P_{tx}	11.31 P_{tx}	46.76 P_{tx}
8	P_{tx}	11.31 P_{tx}	46.76 P_{tx}
9	P_{tx}	11.31 P_{tx}	11.31 P_{tx}
10	P_{tx}	11.31 P_{tx}	11.31 P_{tx}
11	P_{tx}	P_{tx}	P_{tx}
12	P_{tx}	P_{tx}	P_{tx}
13	P_{tx}	11.31 P_{tx}	11.31 P_{tx}
14	P_{tx}	11.31 P_{tx}	46.76 P_{tx}
15	P_{tx}	11.31 P_{tx}	46.76 P_{tx}
16	P_{tx}	11.31 P_{tx}	46.76 P_{tx}
17	P_{tx}	11.31 P_{tx}	46.76 P_{tx}
18	P_{tx}	11.31 P_{tx}	46.76 P_{tx}
19	P_{tx}	11.31 P_{tx}	46.76 P_{tx}
20	P_{tx}	11.31 P_{tx}	46.76 P_{tx}
21	P_{tx}	11.31 P_{tx}	46.76 P_{tx}
22	P_{tx}	11.31 P_{tx}	11.31 P_{tx}
23	P_{tx}	11.31 P_{tx}	11.31 P_{tx}
24	P_{tx}	P_{tx}	P_{tx}
25	P_{tx}	P_{tx}	P_{tx}
26	P_{tx}	11.31 P_{tx}	11.31 P_{tx}
27	P_{tx}	11.31 P_{tx}	11.31 P_{tx}
28	P_{tx}	11.31 P_{tx}	46.76 P_{tx}
29	P_{tx}	11.31 P_{tx}	46.76 P_{tx}
30	P_{tx}	11.31 P_{tx}	46.76 P_{tx}
31	P_{tx}	11.31 P_{tx}	46.76 P_{tx}
32	P_{tx}	11.31 P_{tx}	46.76 P_{tx}
33	P_{tx}	11.31 P_{tx}	46.76 P_{tx}
34	P_{tx}	11.31 P_{tx}	46.76 P_{tx}

Table CXXXI – Transmission power levels of Scenario III.

	P_{tx}	**11.31 P_{tx}**	**46.76 P_{tx}**
Mote m	**Transmission Power**	**Transmission Power**	**Transmission Power**
1	P_{tx}	11.31 P_{tx}	46.76 P_{tx}
2	P_{tx}	11.31 P_{tx}	46.76 P_{tx}
3	P_{tx}	11.31 P_{tx}	46.76 P_{tx}
4	P_{tx}	11.31 P_{tx}	46.76 P_{tx}
5	P_{tx}	11.31 P_{tx}	46.76 P_{tx}
6	P_{tx}	11.31 P_{tx}	46.76 P_{tx}
7	P_{tx}	11.31 P_{tx}	46.76 P_{tx}
8	P_{tx}	11.31 P_{tx}	46.76 P_{tx}
9	P_{tx}	11.31 P_{tx}	46.76 P_{tx}
10	P_{tx}	11.31 P_{tx}	11.31 P_{tx}
11	P_{tx}	11.31 P_{tx}	11.31 P_{tx}
12	P_{tx}	11.31 P_{tx}	11.31 P_{tx}
13	P_{tx}	11.31 P_{tx}	46.76 P_{tx}
14	P_{tx}	11.31 P_{tx}	46.76 P_{tx}
15	P_{tx}	11.31 P_{tx}	46.76 P_{tx}
16	P_{tx}	11.31 P_{tx}	46.76 P_{tx}
17	P_{tx}	11.31 P_{tx}	46.76 P_{tx}
18	P_{tx}	11.31 P_{tx}	46.76 P_{tx}
19	P_{tx}	11.31 P_{tx}	46.76 P_{tx}
20	P_{tx}	11.31 P_{tx}	46.76 P_{tx}
21	P_{tx}	11.31 P_{tx}	46.76 P_{tx}
22	P_{tx}	11.31 P_{tx}	46.76 P_{tx}
23	P_{tx}	11.31 P_{tx}	11.31 P_{tx}
24	P_{tx}	P_{tx}	P_{tx}
25	P_{tx}	P_{tx}	P_{tx}
26	P_{tx}	11.31 P_{tx}	11.31 P_{tx}
27	P_{tx}	11.31 P_{tx}	46.76 P_{tx}
28	P_{tx}	11.31 P_{tx}	46.76 P_{tx}
29	P_{tx}	11.31 P_{tx}	46.76 P_{tx}
30	P_{tx}	11.31 P_{tx}	46.76 P_{tx}
31	P_{tx}	11.31 P_{tx}	46.76 P_{tx}
32	P_{tx}	11.31 P_{tx}	46.76 P_{tx}
33	P_{tx}	11.31 P_{tx}	46.76 P_{tx}
34	P_{tx}	11.31 P_{tx}	46.76 P_{tx}